A *sec61* Mutant Defective In 19S Regulatory Particle Binding

Dissertation

zur Erlangung des akademischen Grades
des Doktors der Naturwissenschaften
der Naturwissenschaftlich-Technischen Fakultät III
Chemie, Pharmazie, Bio- und Werkstoffwissenschaften der
Universität des Saarlandes

vorgelegt von

Marie-Luise Kaiser

Saarbrücken
2014

Tag des Kolloquiums: 24.03.2015

Dekan: Prof. Dr. Dirk Bähre

Prüfungsausschuss:	Prof. Dr. Karin B. Römisch	(1. Berichterstatter)
	Prof. Dr. Manfred J. Schmitt	(2. Berichterstatter)
	Prof. Dr. Uli Müller	(Vorsitzender)
	Dr. Frank Hannemann	(Akademischer Beisitzer)

Ever Tried.

Ever Failed.

No Matter.

Try Again.

Fail Again.

Fail Better.

- S. Beckett -

Try not.

Do.

Or do not !

- Yoda -

TABLE OF CONTENTS

LIST OF FIGURES 9

LIST OF TABLES 10

DECLARATION 11

ABSTRACT 12

ZUSAMMENFASSUNG 13

1 INTRODUCTION 14

1.1 THE SECRETORY PATHWAY 14

1.1.1 CELLULAR COMPARTMENTALIZATION 14

1.1.2 TARGETING SEQUENCES 14

1.1.3 THE ROUTE OF SECRETORY PROTEINS THROUGH THE SECRETORY PATHWAY 16

1.2 PROTEIN TRANSLOCATION INTO THE ENDOPLASMIC RETICULUM 20

1.2.1 THE ER AS CENTRAL COMPARTMENT DURING PROTEIN SECRETION 20

1.2.2 COTRANSLATIONAL PROTEIN TRANSLOCATION INTO THE ER 21

1.2.3 POSTTRANSLATIONAL PROTEIN TRANSLOCATION INTO THE ER 25

1.2.4 THE ER PROTEIN TRANSLOCATION CHANNEL 27

1.2.4.1 CO-AND POSTTRANSLATIONAL PROTEIN IMPORT INTO THE ER CONVERGE AT THE TRANSLOCON 27

1.2.4.2 THE SEC61 COMPLEX 28

1.2.4.2.1 THE SEC61P SUBUNIT 28

1.2.4.2.2 THE SBH1P SUBUNIT 32

1.2.4.2.3 THE SSS1P SUBUNIT 32

1.2.4.2.4 THE TRANSLOCATION MODEL 33

1.2.4.3 THE SSSH1 COMPLEX 34

1.2.4.4 THE SEC COMPLEX 36

1.3 PROTEIN FOLDING/MODIFICATIONS AND THE ER QUALITY CONTROL 37

1.3.1 PROTEIN FOLDING AND MODIFICATIONS IN THE ER 37

1.3.2 ER QUALITY CONTROL 38

1.3.2.1 ER QUALITY CONTROL OF GLYCOPROTEINS 39

1.4 THE UNFOLDED PROTEIN RESPONSE **42**

1.5 THE UBIQUITIN PROTEASOME SYSTEM **46**

1.5.1 UBIQUITIN AND UBIQUITINATION 46

1.5.2 THE 26S PROTEASOME 48

1.5.2.1 THE 20S CORE PARTICLE 51

1.5.2.2 THE 19S REGULATORY PARTICLE 51

1.6 ER-ASSOCIATED DEGRADATION **54**

1.6.1 THE DISLOCON 58

1.7 AIM OF THIS STUDY **65**

2 MATERIALS AND METHODS **66**

2.1 MATERIALS AND GENERAL PROCEDURES **66**

2.1.1 LABORATORY EQUIPMENT, REAGENTS, CHEMICALS AND THEIR SUPPLIERS 66

2.1.2 BACTERIAL AND *S. CEREVISIAE* STRAINS 69

2.1.3 PLASMIDS 73

2.1.4 PRIMERS 77

2.1.5 ANTIBODIES 78

2.1.6 ENZYMES 79

2.1.7 MEDIA AND BUFFERS 79

2.2 METHODS **81**

2.2.1 STERILIZATION 81

2.2.2 GROWTH OF *S. CEREVISIAE* 81

2.2.3 GROWTH OF *E. COLI* 81

2.2.4 POLYMERASE CHAIN REACTION 81

2.2.4.1 SPLICE OVERLAP EXTENSION (SOE) PCR 82

2.2.5 LARGE SCALE EXTRACTION OF PLASMID DNA 85

2.2.6 SMALL SCALE EXTRACTION OF PLASMID DNA: ALKALINE LYSIS MINIPREPS 86

2.2.7 ETHANOL PRECIPITATION 86

2.2.8 AGAROSE GEL ELECTROPHORESIS 87

2.2.9 RECOVERY OF DNA FRAGMENTS 87

2.2.10 RESTRICTION DIGESTION OF PCR PRODUCTS AND PLASMID DNA 87

2.2.11 Dephosphorylation of Vector DNA 88
2.2.12 Ligation of Vector DNA and Insert DNA 88
2.2.13 Microdialysis 89
2.2.14 Transformation of *E. coli* Cells with Plasmid DNA 89
2.2.14.1 Preparation of Electrocompetent Cells 89
2.2.14.2 Transformation of electrocompetent Cells 89
2.2.14.3 Transformation of Chemically Competent Cells 90
2.2.15 DNA Sequencing 90
2.2.16 Preparation of Lyticase 90
2.2.17 Transformation of *S. cerevisiae* 91
2.2.18 Verification of *S. cerevisiae* Transformations 92
2.2.19 *S. cerevisiae* Growth on Plates (Drop Test) 93
2.2.20 *S. cerevisiae* Translocation Assay 93
2.2.21 Isolation of *S. cerevisiae* RNA 93
2.2.22 Isolation of *S. cerevisiae* Chromosomal DNA 94
2.2.23 Preparation of Cell Extracts 94
2.2.24 Protein Gel Electrophoresis and Western Blot Analysis 95
2.2.24.1 Protein Gel Electrophoresis 95
2.2.24.2 Coomassie Staining and Drying of Protein Gels 95
2.2.24.3 Western Blot Analysis 96
2.2.25 Preparation of Rough Microsomal Membranes 96
2.2.26 Preparation of Ribosome- and Proteasome-Stripped Membranes 97
2.2.27 Preparation of Reconstituted Proteoliposomes 98
2.2.28 Preparation of Phosphatidylchoine/Phosphatidylethanolamine 99
2.2.29 Preparation of *S. cerevisiae* Cytosol for Proteasome Purification 99
2.2.30 Purification of *S. cerevisiae* Proteasome 26S Holoemzyme and 19S RP Subcomplex 100
2.2.30.1 Peptidase Activity Assay 101
2.2.31 Proteasome Binding assay 101
2.2.32 Unfolded Protein Response Assays 102
2.2.32.1 Quantitative Liquid β-Galactosidase Assay 102
2.2.32.2 Growth Defects on Tunicamycin Plates (Drop Test) 103
2.2.32.3 *HAC1* mRNA Splice Assay 103
2.2.33 Pulse-Chase Experiments 104

2.2.33.1 PULSE LABELING 104
2.2.33.2 CHASE 105
2.2.33.3 IMMUNOPRECIPITATION 106
2.2.34 *IN VITRO* TRANSCRIPTION, TRANSLATION, TRANSLOCATION AND RETROTRANSLOCATION 107
2.2.34.1 PREPARATION OF *S. CEREVISIAE* CYTOSOL FOR *IN VITRO* ASSAYS 107
2.2.34.2 PREPARATION OF *S. CEREVISIAE* TRANSLATION EXTRACT 107
2.2.34.3 LINEARIZATION AND RE-ISOLATION OF PLASMID DNA 109
2.2.34.4 *IN VITRO* TRANSCRIPTION REACTION 109
2.2.34.5 *IN VITRO* TRANSLATION REACTION 110
2.2.34.6 *IN VITRO* TRANSLOCATION ASSAY 111
2.2.34.7 *IN VITRO* RETROTRANSLOCATION ASSAY 112
2.2.35 PEGYLATION ASSAY 113

3 RESULTS 115
3.1 OVERVIEW 115
3.2 GENERATION OF *S. CEREVISIAE SEC61* MUTANTS 117
3.2.1 GENERATION AND VERIFICATION OF THE *SEC61* MUTANTS *SEC61-S179P*, *SEC61-S353C* AND *SEC61-S179P/S353C* 117
3.2.2 GENERATION AND VERIFICATION OF THE *SEC61* INTEGRATION MUTANTS *SEC61-S179P*, *SEC61-S353C*, *SEC61-S179P/S353C*, *SEC61-302* AND *SEC61-303* 120
3.3 GROWTH ANALYSIS OF THE *SEC61* MUTANTS 124
3.4 TESTING FOR TRANSLOCATION DEFECTS USING *URA3*-REPORTER FUSION PROTEINS 128
3.5 PROTEASOME BINDING ASSAY 131
3.5.1 PURIFICATION OF 19S REGULATORY PARTICLE 131
3.5.2 PROTEASOME BINDING ASSAYS 134
3.6 ANALYSIS OF UPR IN THE *SEC61* MUTANTS 138
3.6.1 DETECTION OF UPR INDUCTION IN THE *SEC61* MUTANTS USING THE QUANTITATIVE LIQUID β-GALACTOSIDASE ASSAY 138
3.6.2 DETECTION OF THE UPR INDUCTION IN THE *SEC61* MUTANTS ON THE RNA LEVEL 141
3.6.3 GROWTH ANALYSES OF THE *SEC61* MUTANTS IN THE *ΔIRE* BACKGROUND 143

3.7 ERAD IN THE *SEC61* MUTANTS **146**
3.7.1 CPY*$_{HA}$ ERAD IN THE *SEC61* MUTANTS 146
3.7.2 MUTANT ALPHA FACTOR PRECURSOR ERAD IN THE *SEC61* MUTANTS 150
3.7.3 KWW ERAD IN THE *SEC61* MUTANTS 154
3.7.4 STE6-166P ERAD IN THE *SEC61* MUTANTS 157
3.8 ANALYSIS OF *IN VITRO* TRANSLOCATION AND ERAD IN THE *SEC61* MUTANTS **160**
3.8.1 *IN VITRO* TRANSLOCATION OF PPαF INTO *SEC61* MICROSOMES 160
3.8.2 *IN VITRO* ERAD OF ΔGPαF IN THE *SEC61* MUTANTS 163
3.9 DETECTION OF CONFORMATIONAL CHANGES IN MUTANT SEC61P **168**

4 DISCUSSION **174**
4.1 TEMPERATURE- AND STRESS-SENSITIVITY OF THE *SEC61* MUTANTS **175**
4.2 PROTEIN TRANSLOCATION INTO THE ER IN THE *SEC61* MUTANTS **176**
4.3 PROTEASOME BINDING IN THE *SEC61* MUTANTS **178**
4.4 CHARACTERIZATION OF UPR-ACTIVATION IN THE *SEC61* MUTANTS **182**
4.5 ERAD OF SOLUBLE AND TRANSMEMBRANE SUBSTRATES IN THE *SEC61* MUTANTS **184**
4.6 ERAD OF ΔGPαF IN A CELL-FREE SYSTEM **186**
4.7 CONCLUSION **188**

5 REFERENCES **190**
6 ABBREVIATIONS **242**
7 PUBLICATIONS **248**
8 ACKNOWLEDGEMENTS **249**

LIST OF FIGURES

Figure 1.1.2.1	Signal sequences of secretory proteins	16
Figure 1.1.3.1	The secretory pathway	19
Figure 1.2.1.1	Translocation complexes in *S. cerevisiae*	21
Figure 1.2.2.1	Cotranslational protein translocation into the ER of *S. cerevisiae*	25
Figure 1.2.3.1	Posttranslational protein translocation into the ER of *S. cerevisiae*	27
Figure 1.2.4.2.1.1	The Sec61p subunit	31
Figure 1.3.2.1.1	N-glycan processing in the ER	42
Figure 1.4.1	The *S. cerevisiae* Unfolded Protein Response	45
Figure 1.5.2.1	The 26S proteasome	50
Figure 1.6.1	ERAD pathways in *S. cerevisiae*	57
Figure 2.1.3.1	Simplified vector maps of pRS306 and pRS315	75
Figure 2.1.3.2	Simplified plasmid maps of the pRS306-*truncsec61* and pRS315 -*sec61* constructs	76
Figure 2.2.4.1.1	SOE-PCR	83
Figure 3.1.1	Topology model of Sec61p	116
Figure 3.2.1.1	Generation and verification of *sec61* mutants in the JDY638 background	119
Figure 3.2.2.1	Generation and verification of *sec61* integration mutants	123
Figure 3.3.1	Growth analyses of the *sec61* mutants	127
Figure 3.4.1	Detection of translocation defects using a reporter translocation assay	130
Figure 3.5.1.1	Affinity purification of 19S RPs	133
Figure 3.5.2.1	Proteasome binding assay	137
Figure 3.6.1.1	Analysis of UPR induction in the *sec61* mutants using the liquid quantitative β-galactosidase assay	140
Figure 3.6.2.1	Analysis of UPR induction in the *sec61* mutants using the *HAC1* pre-mRNA splicing assay	142
Figure 3.6.3.1	Growth analyses of the *sec61* mutants in the *IRE1* and *Δire1* bakground	145
Figure 3.7.1.1	Degradation of mutant Carboxypeptidase Y (CPY*) in the *sec61* mutants	149
Figure 3.7.2.1	Degradation of mutant alpha factor precursor (Δgpαf) in the *sec61* mutants	153
Figure 3.7.3.1	Degradation of KWW in the *sec61* mutants	156
Figure 3.7.3.1	Degradation of Ste6-166p in the *sec61* mutants	159
Figure 3.8.1.1	*In vitro* import of ppαf into *sec61* microsomes	162
Figure 3.8.2.1	*In vitro* ERAD of Δgpαf in *SEC61*	164
Figure 3.8.2.2	*In vitro* ERAD of Δgpαf in the *sec61* mutants (I)	166
Figure 3.8.2.3	*In vitro* ERAD of Δgpαf in the *sec61* mutants (II)	167
Figure 3.9.1	Topology model of Sec61p (modified)	169
Figure 3.9.2	Analysis of a conformational change in mutant Sec61p	173

LIST OF TABLES

Table 2.1	Laboratory equipment used in this study	66
Table 2.2	Chemicals, reagents and consumables used in this study	67
Table 2.3	*E. coli* strains used in this study	69
Table 2.4	*S. cerevisiae* strains used in this study	71
Table 2.5	Plasmids used in this study	73
Table 2.6	Oligonucleotides used in this study	77
Table 2.7	Primary and secondary antibodies used in this study	78
Table 2.8	Enzymes used in this study and their sources	79
Table 2.9	*S. cerevisiae* media used routinely in this study	79
Table 2.10	Composition of Synthetic Complete Amino Acid Drop-Out Mixture* for *S. cerevisiae*	80
Table 2.11	*E. coli* media used routinely in this study	80
Table 2.12	Standard reaction mixture for PCRs	82
Table 2.13	Standard thermal cycler program for PCRs	82
Table 2.14	SOE-PCR setups for the generation of *sec61* mutants	84
Table 2.15	Standard reaction mixture for the restriction digestion of DNA	88
Table 2.16	Reaction mixture for the dephosphorylation of digested vector DNA	88
Table 2.17	Standard reaction mixture for the ligation of vector and insert DNA	88
Table 2.18	Calculation of lyticase activity (example: $OD_{600\ START}$ = 1.85)	91
Table 2.19	Reverse transcription reaction mixture	104
Table 2.20	*In vitro* transcription reaction setup	110
Table 2.21	Standard *in vitro* translation reaction setup	111
Table 2.22	Standard translocation reaction setup	112
Table 2.23	Composition of 18 % denaturing polyacrylamide 4 M urea gels	112

DECLARATION

Hiermit versichere ich an Eides statt, dass ich die vorliegende Arbeit selbstständig und ohne Benutzung anderer als die angegebenen Hilfsmittel angefertigt habe. Die aus anderen Quellen oder indirekt übernommenen Daten und Konzepte sind unter Angabe der Quelle gekennzeichnet. Die Arbeit wurde bisher weder im In- noch im Ausland in gleicher oder ähnlicher Form in einem Verfahren zur Erlangung eines akademischen Grades vorgelegt.

_____

Ort, Datum, Unterschrift

ABSTRACT

In eukaryotes, the biogenesis of secretory proteins requires their translocation into the endoplasmic reticulum (ER) through the Sec61 channel. Proteins passing through the secretory pathway are under the control of the ER quality control (ERQC). Proteins that fail to fold are recognized and dislocated from the ER back into the cytosol for proteasomal degradation, a process known as ER-associated degradation (ERAD). The composition of the retrotranslocation channel is controversial, but dislocation of many soluble substrates is dependent on the Sec61 channel. The proteasome 19S regulatory particle (RP), which binds and unfolds substrates destined for proteasomal degradation, binds directly to the Sec61 channel via its base and is required and sufficient for the retrotranslocation of specific misfolded proteins.

This thesis describes the identification of a *sec61* mutant, carrying a point mutation in the ER-lumenal loop 7 of Sec61p, displaying reduced affinity of the Sec61 channel for the 19S RP in a proteasome binding assay using ER-derived reconstituted proteoliposomes. The *sec61-S353C* mutant neither displayed defective protein import into the ER nor elevated ER stress levels in intact cells. In a cell-free assay a reduction in retrotranslocation of a 19S RP-dependent ERAD substrate in the presence of limiting concentrations of proteasomes was detected for *sec61-S353C*. This suggests that conformational changes in Sec61p hinging on the large ER-lumenal loop 7 are prerequisites for 19S RP binding to the channel. The data indicate that the interaction between the Sec61 channel and the 19S RP is pivotal for the export of specific substrates from the ER to the cytosol for degradation by the 26S proteasome.

ZUSAMMENFASSUNG

In Eukaryoten erfordert die Biogenese sekretorischer Proteine deren Translokation in das Endoplasmatische Retikulum (ER) durch den Sec61-Kanal. Proteine des sekretorischen Weges unterliegen der ER-Qualitätskontrolle (ERQC). Fehlgefaltete Proteine werden erkannt und zur proteasomalen Degradation zurück ins Cytosol dislozierT; ein Prozess, der als ER-assoziierte Proteindegradation (ERAD) bezeichnet wird. Die Zusammensetzung des Retrotranslokationskanals ist strittig, jedoch erfordert die Dislokation vieler löslicher Substrates den Sec61-Kanal. Das 19S Regulatorische Partikel (RP), das proteasomal zu degradierende Substrate erkennt und entfaltet, bindet direkt an den Sec61-Kanal mittels seines Basis-Komplexes und ist weiterhin nötig und ausreichend für die Retrotranslokation bestimmter fehlgefalteter Proteine.

Die vorliegende Arbeit beschreibt die Identifizierung einer *sec61* Mutante, die eine Punktmutation im ER-lumenalen Loop 7 von Sec61p besitzt, die zu einer reduzierten Affinität des Kanals für das 19S RP führt. Die Mutante *sec61-S353* weist weder Defekte in der Proteintranslokation in das ER, noch erhöhte ER-Stresslevel in intakten Zellen auf. In einem zellfreien System konnte für *sec61-S353C* eine Reduzierung der Retrotranslokation eines 19S RP-abhängigen ERAD Substrates in der Anwesenheit limitierender Proteasomen-Konzentrationen detektiert werden. Die Resultate deuten darauf hin, dass Konformationsänderungen in Sec61p um den ER-lumenalen Loop 7 Voraussetzung für die 19S RP Bindung an den Sec61-Kanal sind, und dass die Interaktion des Sec61-Kanals mit dem 19S RP von Bedeutung für den Export bestimmter Substrate vom ER ins Cytosol zur Degradation durch das Proteasom ist.

1 INTRODUCTION

1.1 THE SECRETORY PATHWAY

1.1.1 CELLULAR COMPARTMENTALIZATION

One fundamental principle found in eukaryotes as well as in prokaryotes is the compartmentalization of cells (Martin, 2010). The separation into cellular spaces allows otherwise incompatible processes to occur simultaneously inside one cell by providing the cell with different environments that facilitate specific metabolic functions. This results in the high specificity and regulation of cellular processes by e.g. locating enzymes that catalyze consecutive reactions in close proximity to each other (Chen *et al.*, 2005; Herrmann & Spang, 2008). Eukaryotic cells contain various organelles, such as mitochondria, the endoplasmic reticulum (ER) and the Golgi apparatus (Weeden, 1981; Allen, 2003; Carrie *et al.*, 2009; Zimmer, 2009; Martin 2010). Prokaryotic cells, which do not contain membrane-bound compartments per se, have developed a different form of compartmentalization, also referred to as self- or autocompartmentalization (Lupas *et al.*, 1997b). In prokaryotes, compartmentalization is only comparable to that of eukaryotes to a certain extend, as seen in the separation between cytoplasm, inner and outer membrane as well as the periplasm in Gram-negative bacteria (Lupas *et al.*, 1997b; Kerfeld *et al.*, 2005; Martin, 2010). In both, prokaryotes and eukaryotes, however, proteins are synthesized in the cytoplasm; the only exception being a subset of proteins synthesized by mitochondria and plastids which are coded for by the genomes of these semiautonomous organelles (Palade, 1975; Blobel, 1980; Warren & Wickner, 1996). Due to the existence of specific compartments, delivery of many proteins to these various locations is a prerequisite for proper cellular function (Wickner & Schekman, 2005).

1.1.2 TARGETING SEQUENCES

Protein transport to the correct compartment within the cell is determined by targeting sequences, specific amino acid sequences present at the N-terminus or C-terminus of proteins destined for locations other than the cytosol (Breitfeld *et al.*, 1989; von Heijne, 1990; Kim & Hwang, 2013). Depending on the nature of these sorting signals (secretory signal peptides, nuclear localization signals, mitochondrial targeting peptides, peroxisomal targeting sequences etc.), proteins are directed to their final destination, such as the secretory pathway, the nucleus, the mitochondria and the peroxisome, accordingly (Blobel & Sabatini, 1971; Schechter *et al.*, 1975; Dobberstein *et al.*, 1977; Maccecchini *et al.*, 1979). Targeting sequences are recognized by receptors found in the cytoplasm or at the cytoplasmic face of the appropriate organelle and are removed in many cases

once the protein has been targeted correctly (Blobel & Dobberstein, 1975a, 1975b; McGeoch, 1985; Chou & Elrod, 1999).

First introduced by Blobel and Sabatini, followed by the experimental verification by Milstein and colleagues, the existence of N-terminal targeting peptides for secretory proteins (= signal peptides) led to the development of the signal hypothesis (Blobel & Sabatini, 1971, Milstein *et al.*, 1972; improved by Blobel & Dobberstein, 1975a, 1975b). Once it became clear that the secretion of proteins depends on N-terminal signal sequences, which lead to their translocation across the ER membrane, it soon became obvious that the nature of signal sequences is mainly hydrophobic (von Heijne, 1984). The signal peptides that target secretory proteins to the ER were the first targeting sequences to be investigated (von Heine & Abrahmsén, 1989). Eukaryotic and bacterial signal peptides all share a similar structure: an N-terminal net-positively charged region (n-region), a central hydrophobic region (h-region) and a slightly polar C-terminal region (c-region) (ref. Figure 1.1.2.1; von Heijne, 1990). The c-region is the most conserved part of the signal peptides containing the cleavage site for signal peptidase (von Heijne, 1983, 1985; Gierasch, 1989; Hegde & Bernstein, 2006). The consensus cleavage site is determined by small residues at positions -1 and -3 relative to the cleavage site (von Heijne, 1986). The specific residues at position -1 and -3 relative to the cleavage site have been suggested to contact the signal peptidase near its active site (von Heijne, 1985; Gierasch, 1989; von Heijne & Abrahmsén, 1989; Hegde & Bernstein, 2006). The c-region has also been suggested to form a β-strand that binds to the signal peptidase (SP) (Paetzel *et al.*, 1998). The h-region is thought to form an α-helix when bound to signal recognition particle (SRP; ref. 1.2.2), whereas the n-region might bind SRP (Batey *et al.*, 2000).

Proteins that are transported into the ER but are not destined for secretion contain retention sequences: the C-terminal retention sequence KDEL (mammalian cells; yeast: HDEL; for soluble proteins) and the K(X)KXX peptides (X = any amino acid; for membrane proteins) (Munro & Pelham, 1987; Cosson & Letourneur, 1994; Pelham, 1995; Barlowe *et al.*, 2000). Soluble proteins destined to reside in the ER, which are accidentally incorporated into COPII-coated vesicles, are recognized by Golgi-resident KDEL-receptors (Aoe *et al.*, 1998). The resulting complex is then returned to the ER via COPI vesicles (Munro & Pelham, 1987; Pelham, 2000). Escaped ER membrane proteins are recycled back to the ER by the K(X)KXX peptides at the cytosolic C-terminus of the proteins (type I transmembrane ER proteins, in yeast and mammalian cells) which directly bind to the COPI coat in the Golgi and are transported back to the ER (Jackson *et al.*, 1993; Cosson & Letourneur, 1997; Gaynor *et al.*, 1994; Pelham, 1995; Ma & Goldberg, 2013). A retrieval signal found in type II transmembrane proteins is the N-terminal XXRR motif that is found in mammalian cells (Jackson *et al.*, 1990; Schutze *et al.*, 1994).

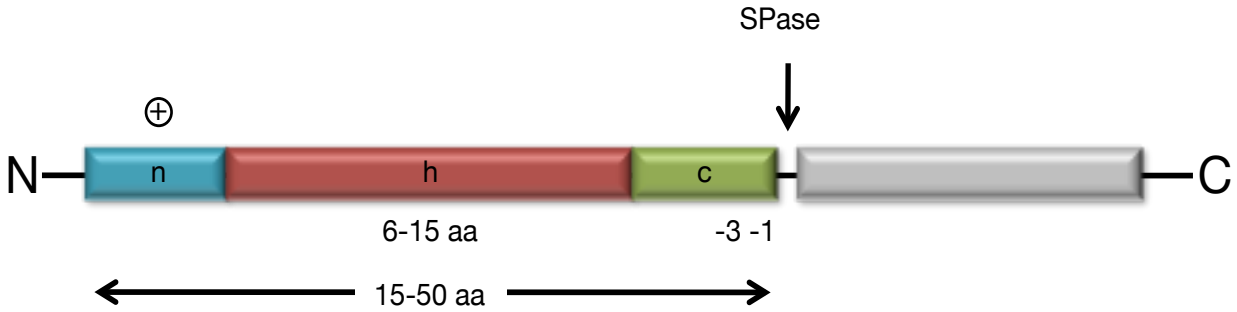

Figure 1.1.2.1. Signal sequences of secretory proteins. Schematic representation of the tripartite composition of the N-terminal protein targeting sequence of secretory proteins. The sequence consists of a net-positively charged n-domain at the N-terminus, a central hydrophobic h-domain and a slightly polar c-domain, which contains the signal peptidase (SP) consensus cleavage site defined by small residues at position -1 and -3 relative to the cleavage site. The mature protein part is depicted in grey (adapted from Martoglio & Dobberstein, 1998).

1.1.3 THE ROUTE OF SECRETORY PROTEINS THROUGH THE SECRETORY PATHWAY

In eukaryotes, nuclear-encoded proteins can be divided according to their location within the cell into cytosolic, mitochondrial, chloroplast, peroxisomal, nuclear and secretory proteins. Secretory proteins and transmembrane proteins of the secretory pathway, account for about 30 % of the eukaryotic proteome (Ghaemmaghami *et al.*, 2003). Their synthesis and maturation route is called the secretory pathway, which comprises the ER, Golgi apparatus, vacuoles (lysosomes), endosomes and the plasma membrane (ref. Figure 1.1.3.1). Not only proteins destined for secretion by the cell enter the secretory pathway, but also transmembrane proteins and proteins resident in exocytic and endocytic compartments (Mellman & Warren, 2000; Vazquez-Martinez *et al.*, 2012).

The secretory pathway, which is essential and highly conserved in eukaryotes, transports newly synthesized proteins, following their import into the ER, via the Golgi apparatus to their final destinations and, on their way along the pathway, ensures their maturation by folding and covalent modifications (Rapoport, 2007). One specific feature of the secretory pathway is the vesicular transport by which the compartments that form the endomembrane system communicate with one another as well as the extracellular environment (Rothman & Wieland, 1996; Schekman & Orci, 1996). Regardless of their final destination, all secretory proteins first enter the ER on their way along the secretory pathway through the Sec61 translocation channel (Rapoport, 2007).

The ER is the major site of protein maturation and biosynthesis. Here, proteins fold, oligomerize, acquire disulfide (S-S) bonds and N-linked oligosaccharide chains as soon as they are translocated into the lumen of the organelle (Dill, 1985; Braakman *et al.*, 1992; Zapun *et al.*, 1999). At the same time the ER is the site of protein quality control (ER Quality Control (ERQC); ref. 1.3.2), an essential mechanism, which ensures that only properly folded, modified and assembled proteins leave the ER

via ER-derived transport vesicles (Ellgaard & Helenius, 2003; Sitia & Braakman, 2003; Määttänen *et al.*, 2010). Proteins, which are improperly folded and are therefore likely to form toxic aggregates, are recognized and degraded via the ER-associated Degradation (ERAD; ref. 1.6) pathway (Lippincott-Schwartz *et al.*, 1988; Dobson, 2004; Tyedmers *et al.*, 2010). During ERAD, misfolded proteins are recognized and retrotranslocated via the retrotranslocon into the cytosol, where they are degraded by the 26S proteasome (ref. 1.5.2) (Sommer & Jentsch, 1993; Kostova & Wolf, 2003; Römisch, 2005; Vembar & Brodsky, 2008). Misfolded proteins that are not properly recognized and degraded as such accumulate in the ER lumen, thereby inducing the Unfolded Protein Response (UPR; ref. 1.4), a signaling pathway which leads to the activation of genes involved in ERAD as well as others that help clear the high load of misfolded proteins in the ER (Travers *et al.*, 2000; Korennykh & Walter, 2012).

Proteins that pass the ERQC are transported further through the secretory pathway. They are packaged into ER-derived COPII vesicles, which bud from so-called ER exit sites - ribosome-free subdomains of the ER, which have been suggested to form spontaneously (Bannykh & Balch, 1997; Barlowe, 2000; Hammond & Glick, 2000). Upon budding from the ER the COPII vesicles presumably fuse to form the ER-Golgi intermediate compartment (ERGIC) (Lee *et al.*, 2004c). The ERGIC is an early site of protein sorting which is mediated by COPI vesicles (Bannykh & Balch, 1997; Barlowe, 2000; Klumpermann, 2000). Proteins destined for further transport remain in the ERGIC whereas some proteins, such as cargo receptors, are recycled back to the ER for reuse (Orci *et al.*, 2000; Appenzeller-Herzog & Hauri, 2006). From the ERGIC proteins move through the various Golgi compartments (*cis* Golgi network (CGN), *cis* cisternae, *medial* cisternae, *trans* cisternae, trans Golgi network (TGN)), each containing a compartment-specific set of enzymes (Becker & Melkonian, 1996; Rossanese *et al.*, 1999; Mellman & Warren, 2000; Bard & Malhotra, 2006). Whereas COPII-coated vesicles mediate anterograde transport to the Golgi, COPI vesicles mediate retrograde transport from the Golgi apparatus to the ER and between Golgi cisternae (Klumpermann, 2000; Orci *et al.*, 2000; Duden, 2003). New findings, however, suggest that COPI-coated vesicles might be involved in anterograde transport as well, although this mechanism has not yet been fully elucidated (Moelleken *et al.*, 2007). Two models have been suggested by which secretory proteins move through the Golgi apparatus (Glick, 2000). The first model proposes that transport involves the formation of transport vesicles and their movement through the various Golgi compartments. In this model, the Golgi compartments remain stable entities, which are maintained by vesicular transport-mediated import and export of material (Rothman & Wieland, 1996; Farquhar & Palade, 1998; Glick, 2000; Pelham & Rothman, 2000). In the second model, the cisternal maturation model, *cis* cisternae are formed *de novo* and gradually mature to become *medial* and then *trans* cisternae by accumulating medial and trans enzymes, a process that is mediated by retrograde traffic of vesicles from later cisternae containing the appropriate enzymes (Glick & Malhotra, 1998; Losev *et al.*, 2006; Emr *et al.*, 2009). Proteins that are destined for post-Golgi destination are packaged into clathrin-

coated vesicles. These vesicles move from the Golgi to the plasma membrane as well as to the endosome or vacuole (lysosome) and from the plasma membrane to the endosome (Schmid, 1997; Lemmon, 2001).

During vesicular traffic, vesicles bud from donor compartments, move to and eventually fuse with acceptor compartments. These budding- and fusion-events are mediated largely by SNARE (soluble N-ethylmaleimide-sensitive-factor attachment receptor) proteins and Rab-GTPases (Novick & Brennwald, 1993; Pfeffer, 1994; Zerial & McBride, 2001).

Rab GTPases are a family of Ras-like enzymes that play important roles in the secretory and endocytic pathways (Allan *et al.*, 2000; Zerial & McBride, 2001; Pfeffer & Aivazian. 2004; Hutagalung & Novick, 2011). They have been suggested to be involved in processes that mediate recognition of fusion partners during vesicular traffic (Allan *et al.*, 2000). Thus, Rabs act to facilitate SNARE complex formation but are not core elements of such complexes (Fasshauer *et al.*, 1997, 1998; Otto *et al.*, 1997, Mayer, 1999). SNARE proteins are found on vesicles (v-SNAREs) and target membranes (t-SNAREs) and together with Rab proteins they mediate fusion of vesicles with the target membrane (Rothman *et al.*, 1994; Jahn & Südhof, 1999; Swanton *et al.*, 2000; Duman & Forte, 2003; Ohya *et al.*, 2009).

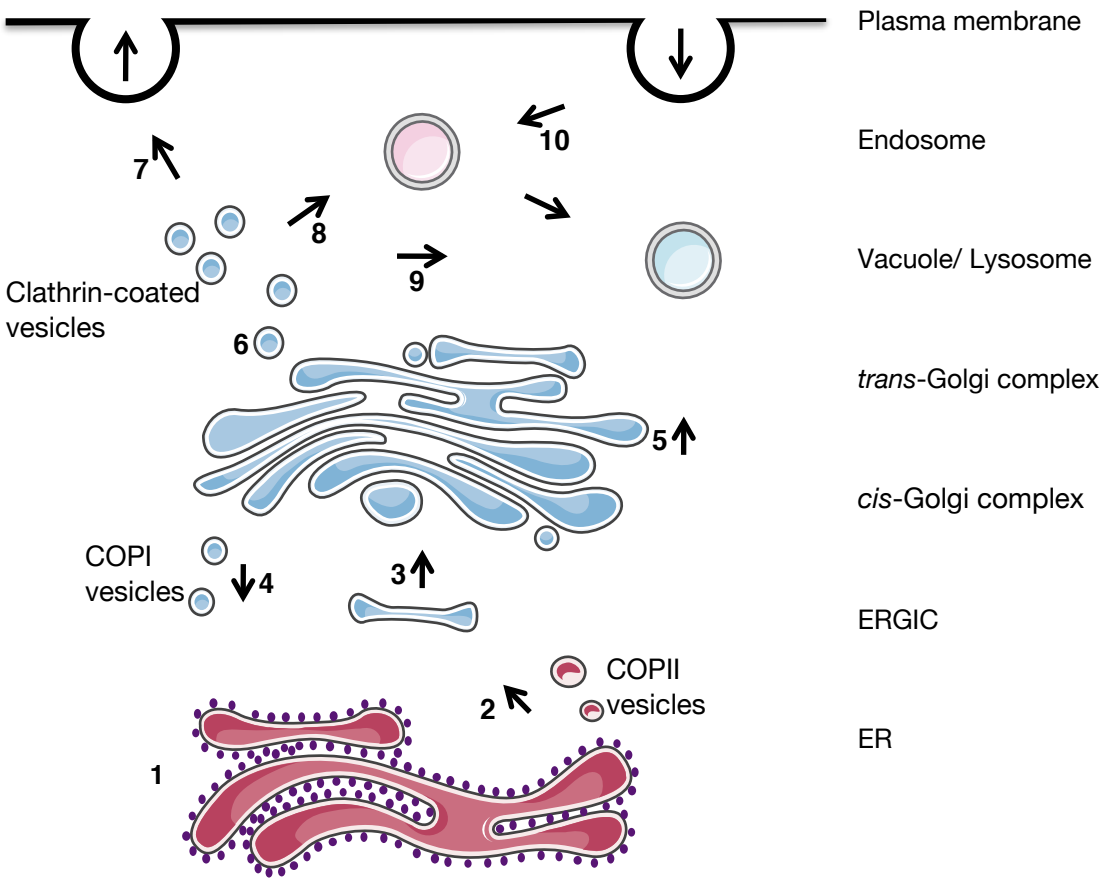

Figure 1.1.3.1. The secretory pathway. (1) Secretory proteins are translocated into the ER either cotranslationally or posttranslationally. Upon import into the ER the proteins' signal sequences are cleaved-off by signal peptidase. Newly synthesized poypeptide chains are inserted into the ER membranes or cross it into the ER lumen. In the ER secretory proteins are modified (e.g. glycosylated in the case of glycoproteins) and fold. Folding in the ER is assisted by chaperones in the ER lumen. Secretory proteins that fail to fold properly are recognized by the ERQC and are retrotranslocated into the cytosol where they are degraded by 26S proteasomes (not shown). (2) Some proteins, e.g. ER enzymes, stay in the ER. The remaining proteins move further along the secretory pathway. They are packaged into COPII-coated vesicles and transported to the *cis*-Golgi complex via the ERGIC (3). (4) Missorted ER-resident proteins containing a sorting signal for ER retrieval (as well as vesicle membrane proteins needed for reuse) are transported back to the ER in COPI-coated vesicles. (5) Secretory proteins destined for secretion or other locations within the cell are transported from the *cis*-Golgi complex to the *trans*-Golgi complex. (6) In the *trans*-Golgi complex proteins destined for post-Golgi destinations are packaged into clathrin-coated vesicles and are either transported to the plasma membrane for secretion into the extracellular space (7) or move in clathrin-coated vesicles from the Golgi to endosomes (clathrin-coated vesicles containing AP-1 adaptor protein complex) (8) or directly to lysosomes (vacuoles in yeast and plants) (clathrin-coated vesicles containing AP-3 adaptor complex) (9). (10) During endocytosis extracellular and membrane proteins are taken up in vesicles budding from the plasma membrane. These vesicles can move proteins to endosomes and vacuoles (adapted from Grant & Sato, 2006; Miller & Krijsne-Locker, 2008).

1.2 PROTEIN TRANSLOCATION INTO THE ENDOPLASMIC RETICULUM

1.2.1 THE ER AS CENTRAL COMPARTMENT DURING PROTEIN SECRETION

The ER is the organelle within the cell that coordinates the biosynthesis, maturation, quality control and degradation of secretory and membrane proteins via multiple pathways. Thus, the ER plays a crucial role in the cell, enabling it to cope with the large diversity of proteins that enter the ER on their way through the secretory pathway (Farquhar & Hauri, 1997; Powell & Latterich, 2000).

Secretory proteins enter the ER via the Sec61 translocon, which forms a protein-conducting channel in the ER membrane (ref. 1.2.4), either as they are still being synthesized on the ribosome (cotranslational protein import; ref. 1.2.2) or after they have been fully synthesized (posttranslational protein import; ref. 1.2.3) (Johnson & van Waes, 1999; Zimmermann *et al.*, 2011; Park & Rapoport, 2012). Protein complexes mediating co- and posttranslational import differ in their composition (ref. Figure 1.2.1.1). In yeast cells, proteins are imported both cotranslationally and posttranslationally, whereas in mammalian cells the vast majority of proteins enter the ER cotranslationally (Gilmore *et al.*, 1982; Bird *et al.*, 1987; Panzner *et al.*, 1995; Ng *et al.*, 1996; Lakkaraju *et al.*, 2012; Lang *et al.*, 2012). Both modes of protein translocation share the removal of the N-terminal ER targeting sequence of the secretory protein by the multi-subunit enzyme SP located on the ER membrane (Dalbey & von Heijne, 1992; Weihofen *et al.*, 2002). Following signal sequence cleavage, oligosaccharyltransferase (OST) glycosylates proteins containing the recognition sequence Asn-X-Ser/Thr (Johnson & van Waes, 1999). ER-specific modifications are the addition of glycosylphophatidylinositol anchors (GPI-anchor) and N-linked glycans, both of which are synthesized as lipid-linked precursors at the ER membrane (Tatu *et al.*, 1993; Spurway *et al.*, 2001).

The functionally diverse group of tail-anchored (TA) proteins takes in a specific role (Borgese *et al.*, 2003a, 2003b). TA proteins are targeted posttranslationally for insertion into the ER membrane, using C-terminal anchors, in yeast and mammals but use a different pathway, the TRC40/GET pathway (TRC = transmembrane recognition complex; GET = guided entry of TA proteins) (Kutay *et al.*, 1995). Factors involved in TA membrane protein integration into the ER membrane are the SRP, cytosolic chaperones or the TRC (Abell *et al.*, 2004, 2007; Rabu *et al.*, 2008; Stefanovic & Hegde, 2007). Various studies have suggested that TA membrane protein integration into the ER membrane is not Sec61-dependent (Kutay *et al.*, 1995, Steel *et al.*, 2002, Yabal *et al.*, 2003; Brambillasca *et al.*, 2005; Stefanovic & Hegde, 2007; Lang *et al.*, 2012). While, some TA membrane proteins can enter the ER membrane unassisted, others require the SR or TRC receptor in the ER membrane (Abell *et al.*, 2004; Brambillasca *et al.*, 2005, 2006; Vilardi *et al.*, 2011). Once inserted into the ER, TA proteins are sorted to their respective resident organelles via vesicular transport (Beilharz *et al.*, 2003).

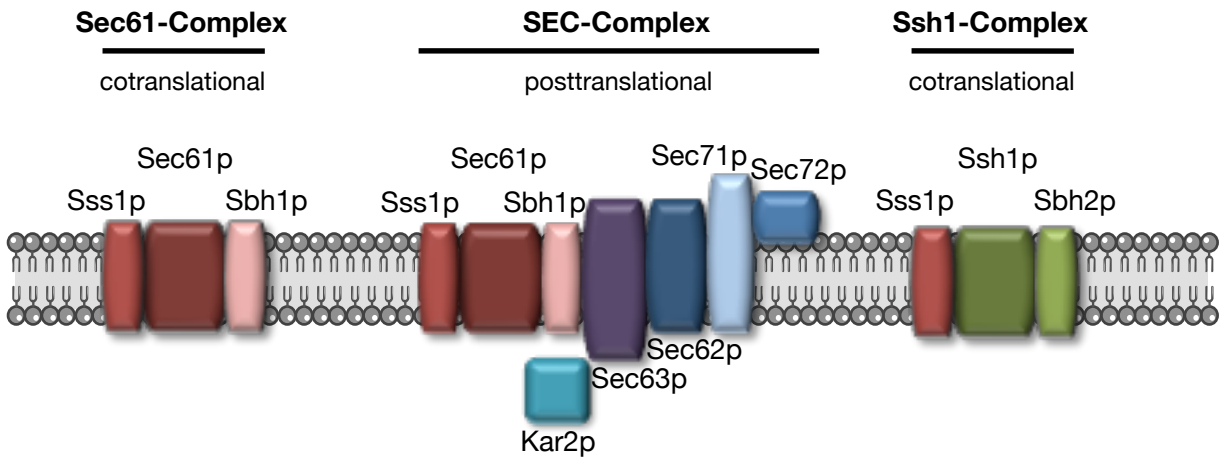

Figure 1.2.1.1. Translocation complexes in *S. cerevisiae*. In yeast, depending on the mode of translocation into the ER, different proteins in or at the ER membrane associate to form complexes, which mediate co- or posttranslational import as indicated. During cotranslational import the translocation channel forming protein Sec61p associates with Sss1p and Sbh1p to form the Sec61 complex, which is the minimal complex during cotranslational protein import. Sec63p is also involved in cotranslational protein translocation (not depicted here) The Ssh1 complex is an alternative cotranslational translocation complex. Here, the central component is Ssh1p, which is associated with Sss1p and Sbh2p, a homologue of Sbh1p. This complex is not essential. During posttranslational import the Sec61 complex associates with the tetrameric Sec63 complex forming the heptameric SEC complex. The ER-lumenal Hsp70-chaperone Kar2p is involved in posttranslational import. (adapted from Finke, 1999; Unger, 2000).

1.2.2 COTRANSLATIONAL PROTEIN TRANSLOCATION INTO THE ER

During cotranslational protein import into the ER, secretory and membrane proteins are recognized and translocated across the ER membrane through the Sec61 translocon as soon as they emerge from the ribosome (Andrews & Johnson, 1996; Hanein *et al.*, 1996; Menetret *et al.*, 2000; Park & Rapoport, 2012). This mode of translocation has been shown to be essential in mammalian cells but not in *S. cerevisiae* (Hann & Walter, 1991; Mutka & Walter, 2001).

Cotranslational protein import involves binding of the signal recognition particle (SRP) to the hydrophobic domain of the signal sequence or a transmembrane domain (TMD) in the nascent polypeptide, which leads to the formation of the so-called ribosome-nascent chain-SRP complex (RNC-SRP complex) (ref. Figure 1.2.2.1; Walter & Blobel, 1980, 1981a; Walter *et al.*, 1981; Anderson *et al.*, 1982). The RNC-SRP complex is targeted to the ER membrane via the SRP receptor (SR) (Gilmore *et al.*, 1982a, 1982b; Walter & Johnson, 1994). Upon interaction of SRP with its receptor SRP is released from the signal sequence and the secretory protein is transferred to the translocon (Rapiejko & Gilmore, 1997; Matlack *et al.*, 1998; Johnson & van Waes, 1999). The secretory protein is then translocated through the translocon into the ER (Walter & Lingappa, 1986,

Beckman *et al.*, 1997; Park & Rapoport, 2012). Membrane proteins are laterally released into the lipid bilayer by the Sec61 complex (Menetret *et al.*, 2000; van den Berg *et al.*, 2004; Trueman *et al.*, 2011; Park & Rapoport, 2012).

Eukaryotic SRP is an evolutionarily conserved ribonucleoprotein particle (RNP) that consists of one RNA molecule and six polypeptides (Walter & Blobel, 1980, 1982). SRP is an essential component during cotranslational targeting to the ER in mammals (Walter & Blobel, 1980, 1982). Mammalian SRP consists of the 7SL RNA and the two monomeric protein subunits SRP19 and SRP54 as well as the two heterodimers SRP68/72 and SRP9/14 (Walter & Blobel, 1980, 1982). In yeast, SRP consists of the scR1 RNA and the subunits Srp72p, 68p, 54p, 21p, Sec65p (Srp19p) and Srp14p (Hann & Walter, 1991). Five of these subunits are homologous to the respective mammalian subunits (Amaya *et al.*, 1990; Stirling & Hewett, 1992). Instead of the SRP9/14 heterodimer, yeast SRP contains the Srp14p-homodimer (Strub *et al.* 1999; Mason *et al.* 2000). It further contains the Srp9p-related protein Srp21p and scR1 RNA (Brown *et al.* 1994). The yeast scR1 RNA (522 nucleotides) consists of four domains (I – IV), which bind to the SRP protein subunits (Felici *et al.*, 1989).

Eukaryotic SRP can be divided into an Alu and an S domain (Ullu *et al.* 1982; Lakkaraju *et al.*, 2008). The 7SL RNA contains an Alu sequence, which forms the Alu domain with the SRP9/14 heterodimer, as well as an S segment (van Nues & Brown, 2004; Lakkaraju *et al.*, 2008). The Alu domain causes an elongation arrest or retardation until targeting of the RNC-SRP complex to the translocon is complete (Siegel & Walter, 1985; Mason *et al.*, 2000). The SRP S domain consists of the SRP-RNA-specific S segment of the RNA, SRP54, SRP68/SRP72 und SRP19 (Gundelfinger *et al.*, 1983; Siegel & Walter, 1988). The S domain mediates signal sequence binding and targeting (Siegel & Walter, 1988). The SRP68/SRP72 dimer in particular is involved in the interaction of SRP with the SR, rendering it essential for translocation (Siegel & Walter, 1988). SRP19 binds to the tips of the 7S RNA's domains III and IV aligning them in parallel, which is prerequisite for binding of SRP54 to domain IV (Hainzl *et al.* 2002; Kuglstatter *et al.* 2002; Oubridge *et al.* 2002). In mammalian cells the heterodimer SRP68/72 binds to distinct positions in domains II-IV, which comprise the nuclease-resistent S domain of SRP (Gundelfinger *et al.*, 1983; Siegel and Walter, 1986; Zopf *et al.*, 1990; van Nues & Brown, 2004).

The conserved SRP54 (54 kDa) subunit of SRP, which harbors GTPase activity, mediates binding to the signal sequence at the N-terminus of secretory or membrane proteins thereby increasing the affinity of GTP for SRP (Siegel & Walter, 1988; Lütcke *et al.*, 1992). SRP54 not only interacts with the signal sequence but also with the SRP-RNA and the SRP receptor (SR) (Krieg *et al.*, 1986; Kurzchalia *et al.*, 1986; Siegel & Walter, 1988; Römisch *et al.*, 1989; Bernstein *et al.*, 1989; Zopf *et al.*, 1990).

The eukaryotic SR is a heterodimeric complex consisting of SRα (69 kDa) and SRβ (30 kDa) (Tajima *et al.*, 1986; Miller *et al.*, 1995). The SR is located on the surface of the ER and is anchored to the ER membrane via the N-terminal TMD of SRβ (Miller *et al.*, 1995).

SRα mediates the interaction between SRP and the ER by binding to SRβ via its N-terminus (Miller *et al.*, 1995; Young *et al.*, 1995; Ogg *et al.*, 1998; Andrews *et al.*, 1989). Assembly of the SRα-SRβ heterodimer depends on GTP-binding to SRβ, which displays GTPase activity (Miller *et al.*, 1995). The GTPase domain of SRβ is essential for SR function (Ogg *et al.*, 1998). It is involved in mediating the binding of RNC to the translocon (Miller *et al.*, 1995). Yeast SRα and SRβ are both necessary for cotranslational protein import (Fulga *et al.*, 2001; Helmers *et al.*, 2003).

During SRP-dependent translocation the RNC is transported to the protein translocation channel very efficiently (ref. Figure 1.2.2.1; Lütcke *et al.*, 1992). Binding of SRP to the secretory protein happens early during translocation as SRP is associated with ribosomes close to the ribosomal polypeptide exit tunnel. This enables SRP to screen the nascent polypeptide chain for the presence of a signal sequence (Walter & Blobel, 1980; Walter & Johnson, 1994). Thus, the SRP-RNC complex is formed as soon as the signal sequence of the nascent polypeptide chain emerges from the exit site of the large ribosomal subunit. Subsequently, binding of the SRP to the RNC remains stable until the RNC reaches the SR complex in the ER membrane (Walter & Johnson, 1994; Keenan *et al.*, 2001).

The signal sequence is bound by the SRP54 subunit of SRP increasing its affinity for the ribosome. At this point the translation is stalled (Walter *et al.*, 1980, 1981b; Mason *et al.*, 2000). The formation of the RNC-SRP complex also increases the affinity of SRP54 for GTP, thereby increasing the affinity of SRP for SR (Gilmore *et al.*, 1982a; Meyer *et al.*, 1982; Bacher *et al.*, 1996). Through binding of SRP to SR, the affinity of SRα for GTP is increased (Bacher *et al.*, 1996). Binding of SRα and SRP to GTP stabilizes the RNC-SR-SRP complex (Rapiejko & Gilmore, 1997). As the RNC-SRP complex is targeted to the SR, SRα binding to SRP leads to GTP hydrolysis (SRP54-SRα GTPase cycle; Rapiejko & Gilmore, 1992, 1997; Bacher *et al.*, 1996; Halic *et al.*, 2006). This results in the dissociation of the SRP54 from the signal sequence and eventually SRP is released into the cytosol (Rapiejko & Gilmore, 1997). At the same time the RNC is transferred to the Sec61 complex (Song *et al.*, 2000). The ribosome associates with the translocon, which destabilizes the interaction between SRβ and the ribosome, and the ribosome stays associated with the Sec61 channel until it translates a non-secretory protein (Potter & Nicchitta, 2000, 2002; Fulga *et al.*, 2001). SRβ regulates the transfer of the nascent polypeptide chain from SRP to the translocon (Bacher *et al.*, 1999).

Dissociation of SRP needs to happen prior to the association of the RNC with the translocon as the binding sites on the ribosome's large subunit for SRP54 and Sec61 overlap (Halic *et al.*, 2006).

The SRP9/14-mediated elongation arrest is abolished after transfer of the signal sequence into the translocon and dissociation of the SRP from the ribosome and SR subunits from the translocon

(Neuhof *et al.*, 1998). Elongation arrest probably serves to ensure efficient translocation by keeping the polypeptide chain in a translocation competent state (Siegel & Walter, 1985, 1986; Thomas *et al.*, 1997; Mason *et al.*, 2000; Nagai *et al.*, 2003).

The protein-conducting channel in the ER membrane is the Sec61 complex consisting of the three subunits Sec61p, Sbh1p and Sss1p in yeast (mammalian cells: Sec61α, β and γ) (van den Berg *et al.*, 2004; Park & Rapoport, 2012). Also required for protein import into the ER is the ER-lumenal chaperone Kar2p (yeast; mammalian cells: BiP = Immunoglobulin heavy chain binding protein; also known as GRP78: glucose-regulated protein of 78 kDa), a member of the Hsp70 family (heat shock protein of about 70 kDa) and one of the most abundant chaperones in the ER lumen (Vogel *et al.*, 1990; Brodsky *et al.*, 1995; Young *et al.*, 2001). Members of the Hsp70-family function in an ATP-dependent manner and with the aid of Hsp40 co-chaperones and so-called nucleotide exchange factors (NEF) (Bukau & Horwich, 1998; Sousa & Lafer, 2006; Kampinga & Craig, 2010). BiP (Kar2p) is involved in protein import into the ER as well as in protein folding (ref. 1.3) and degradation (ref. 1.6) as well as in the regulation of the UPR (ref. 1.4) (Haas & Wabl, 1983; Munro & Pelham, 1986; Flaherty *et al.*, 1990; Bukau & Horwich, 1998; Alder *et al.*, 2005; Schäuble *et al.*, 2012).

For the ER membrane protein Sec63p a role in co-translational protein import into the ER has been suggested in mammals and yeast (Brodsky *et al.*, 1995; Young *et al.*, 2001; Lang *et al.*, 2012; Schäuble *et al.*, 2012). The driving force during cotranslational protein import into the ER has been suggested to be the elongation of the nascent polypeptide chain on the translating ribosome (Hamman *et al.*, 1998; Pilon *et al.*, 1998). During protein import, SP cleaves off the signal sequence (Weihofen *et al.*, 2002, Zimmermann *et al.*, 2011).

Components involved in cotranslational import into the ER of mammalian cells only are TRAM (translocation-associated membrane protein) and the TRAP complex (translocon-associated protein) (Fons *et al.*, 2003; Zimmermann *et al.*, 2011). TRAM seems to be needed for the translocation of specific secretory proteins (Görlich & Rapoport, 1993). It has also been suggested to be involved in cotranslational integration of membrane proteins (Do *et al.*, 1996; Knight & High, 1998; Hegde *et al.*, 1998). TRAP has been suggested to be involved in the translocation of another subset of secretory proteins (Fons *et al.*, 2003).

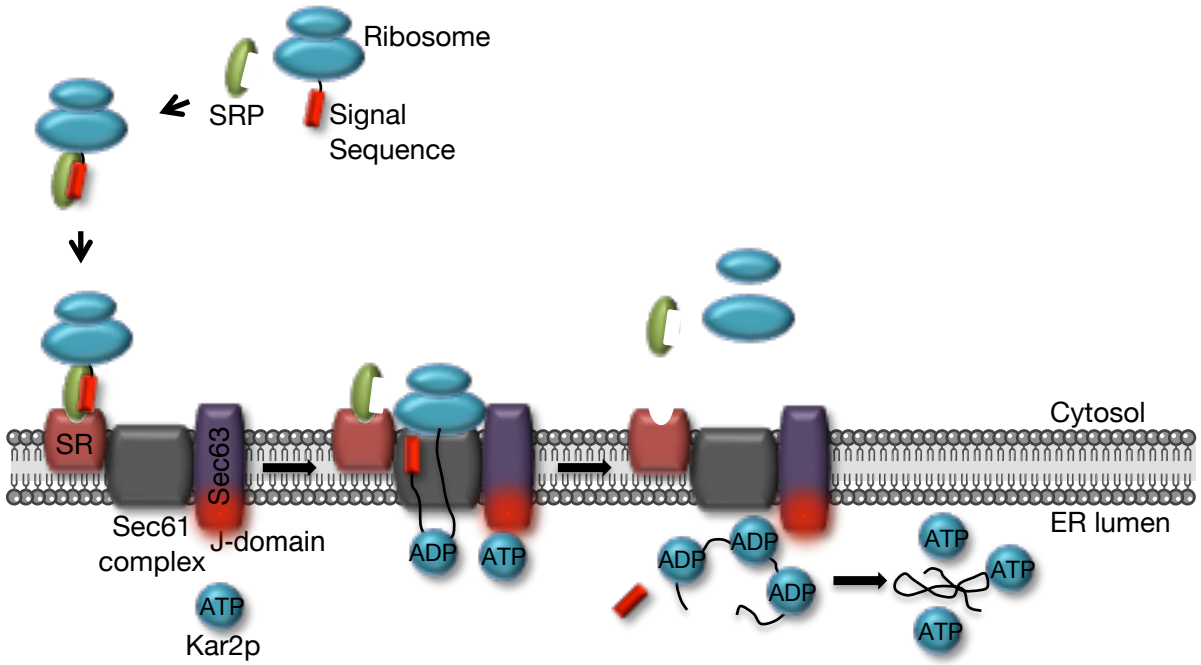

Figure 1.2.2.1 Cotranslational protein translocation into the ER of *S. cerevisiae*. Start = TOP LEFT: As presecretory proteins are synthesized by ribosomes in the cytosol, SRP binds their signal sequences. Binding of SRP leads to an elongation arrest of the nascent protein. The RNC-SRP complex binds to the SR (consisting of SRα and SRβ) in the ER membrane thus targeting the ribosome to the translocon. The signal sequence is inserted into the translocon and SRP dissociates from the SR into the cytosol. SR dissociates from the translocon. The ER-lumenal chaperone Kar2p (BiP) is recruited by Sec63p and assists in folding of the nascent polypeptide chain. As soon as the cleavage site is accessible SP cleaves off the signal sequence (not shown). Secretory glycoproteins are modified by OST with N-linked glycans during and after import (not shown). After termination of translation ribosomes only dissociate from the translocons when they translate non-secretory proteins (adapted from Park & Rapoport, 2012).

1.2.3 POSTTRANSLATIONAL PROTEIN TRANSLOCATION INTO THE ER

Although not as well understood as cotranslational translocation (especially in higher eukaryotes), posttranslational protein import in *S. cerevisiae* has been shown to be an essential translocation mode (ref. Figure 1.2.3.1; Corsi & Schekman, 1996; Kalies & Hartmann, 1998). During posttranslational protein import into the ER, precursor proteins are fully synthesized on cytosolic ribosomes and released before they are translocated into the ER (Plath *et al.*, 1998; Plath & Rapoport, 2000). Proteins are bound by cytosolic chaperones of the Hsp70 family, which keep them in a translocation-competent state (Chirico *et al.*, 1988; Deshaies *et al.*, 1988; Caplan & Douglas, 1992). Whether there is a mechanism similar to the one during cotranslational import, which recognizes signal sequences and targets proteins to the ER membrane is, as of yet, not fully understood. In *S. cerevisiae*, however, the components in the ER membrane that mediate

posttranslational translocation are known (Rapoport *et al.*, 1999; Zimmermann *et al.*, 2011). In yeast, the trimeric Sec61 complex (Sec61p, Sbh1p and Sss1p) associates with the tetrameric Sec63 complex (Sec63p, Sec62p, Sec71p and Sec72p) to form the heptameric SEC complex (ref. Figure 1.2.1.1; Deshaies *et al.*, 1991; Panzner *et al.*, 1995). This complex together with ATP and the ER-lumenal protein Kar2p (BiP) has been shown to be sufficient *in vitro* for posttranslational protein import (Brodsky & Schekman, 1993; Panzner *et al.* 1995).

Crosslinking studies have indicated that Sec61p interacts with signal sequences in an ATP- and Kar2p (BiP)-independent manner (Plath *et al.*, 1998). The binding site for the signal sequence is located between TMD 2 and 7 of Sec61p. The signal sequence forms a helix that is close to Sec62p and Sec71p (Plath *et al.*, 1998). The C-terminus of the protein could be crosslinked to Sec72p but not to Sec63p, Sbh1p and Sss1p (Plath *et al.*, 1998; Matlack *et al.*, 1998; van den Berg *et al.*, 2004).

Posttranslational protein import into the ER is driven by protein folding and ~ modifications, and is assisted by the Hsp70 protein Kar2p (BiP) (Brodsky & Schekman, 1993; Scidmore *et al.*, 1993). Kar2p (BiP) binds to the DnaJ homology domain of Sec63p, which recruits the chaperone to the ER membrane, mediating binding to the imported protein (Lyman & Schekman, 1995; Corsi & Schekman, 1997; Matlack *et al.*, 1999; Misselwitz *et al.*, 1999; Tyedmer *et al.*, 2003). It has been suggested that ATP hydrolysis by Kar2p (BiP) provides the energy required for the interaction of Kar2p (BiP) and the ER-lumenal DnaJ-domain of Sec63p, which is important for the transit of the precursor through the ER membrane and the release of the protein into the ER lumen (ref. 1.2.4.4; Lyman & Schekman 1995, 1997; Corsi & Schekman, 1997; Matlack *et al.*, 1999; Misselwitz *et al.*, 1999; Tyedmers *et al.*, 2003).

There are two models for the pulling-in of the protein by Kar2p (BiP). The “Brownian ratchet” model, which is the preferred model, proposes that BiP binds to segments of the translocating protein thereby preventing sliding back towards the cytosol (Matlack *et al.*, 1997, 1998). Here, the translocation rate is limited by the rate at which translocating preproteins spontaneously unfold (Sanders *et al.*, 1992; Matlack *et al.*, 1999). The “translocation motor” model suggests that Kar2p (BiP) binds to the translocating chain and actively pulls the protein through the channel by an ATP-driven conformational change (Schatz and Dobberstein, 1996). Both scenarios seem possible and might depend on the folding state of the precursor protein (Simon *et al.*, 1992; Glick, 1995; Schatz and Dobberstein, 1996; Matlack *et al.*, 1998).

As for cotranslational import, during posttranslational import into the ER, the signal sequence is cleaved off by SP and OST modifies glycoproteins by adding N-linked glycans to the Asn-X-Ser/Thr glycosylation site all of which promotes folding and hence import (Rapoport *et al.*, 1999; Zimmermann *et al.*, 2011).

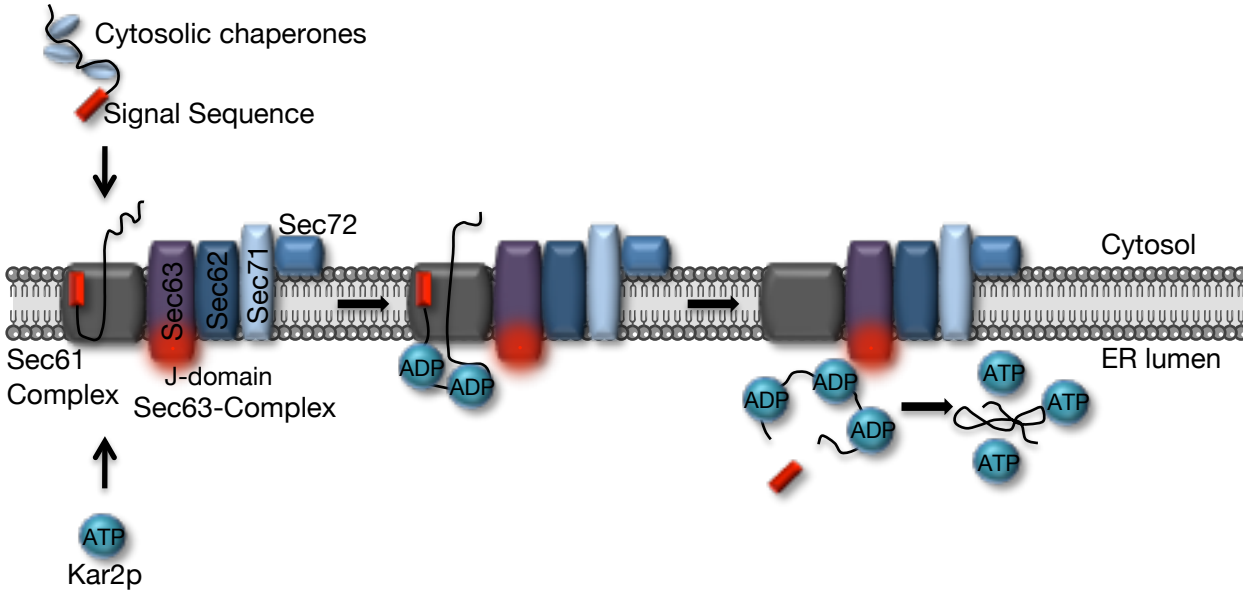

Figure 1.2.3.1. Posttranslational protein translocation into the ER of *S. cerevisiae*. Start = TOP LEFT: Following its synthesis in the cytosol the unfolded secretory polypeptide containing an N-terminal signal sequence is kept in solution by cytosolic chaperones. The completed polypeptide chain is targeted to the SEC complex where it binds with its signal sequence to the Sec63 complex (i.e. to Sec62p, Sec71p, Sec72p; not shown) and is then transferred to Sec61p in the core complex of the translocon. Cytosolic chaperones are released from the polypeptide upon entry into the translocon. Protein import is assisted by the ER-lumenal chaperone Kar2p (BiP). Kar2p is recruited and activated by Sec63p. Sec63p containing a DnaJ domain interacts with Kar2p in its ATP-bound state thereby stimulating ATP hydrolysis. In its ADP-bound state Kar2p binds polypeptides emerging from the translocation channel. As soon as the polypeptide has passed through the channel another Kar2p molecule binds. This process is repeated until the polypeptide is fully translocated. Kar2p is then released upon exchange of ADP to ATP (opens the binding pocket of Kar2p). During protein import SP cleaves the signal sequence and in the case of secretory glycoproteins OST modifies proteins by adding N-linked glycans (not shown) (adapted from Park & Rapoport, 2012).

1.2.4 THE ER PROTEIN TRANSLOCATION CHANNEL

1.2.4.1 CO- AND POSTTRANSLATIONAL PROTEIN IMPORT INTO THE ER CONVERGE AT THE TRANSLOCON

The eukaryotic translocation channel is formed by the Sec61 complex. In *S. cerevisiae* this evolutionarily conserved heterotrimeric complex consists of the three membrane protein subunits Sec61p, Sss1p and Sbh1p (ref. Figure 1.2.1.1; Panzner *et al.*, 1995; Hanein *et al.*, 1996; Beckmann *et al.*, 1997). The Sec61 complex is the essential membrane component for protein translocation (Deshaies & Schekman, 1987). Depending on the mode of translocation, the translocation channel needs to associate with other components in order to gain its full translocation capacity (Görlich &

Rapoport, 1993). The ribosome is the main driving force during cotranslational translocation, when the newly synthesized polypeptide moves directly from the translating ribosome into the translocation channel, a process that is fueled by the energy gained from ribosomal GTP hydrolysis during translation (Connolly & Gilmore, 1986; Görlich *et al.*, 1992; Bange *et al.*, 2007). Posttranslationally translocated proteins that are first fully synthesized in the cytosol before they are translocated across the ER membrane require the association of the Sec61 complex with the tetrameric Sec63p complex and the ER-lumenal chaperone Kar2p (BiP) (Matlack *et al.*, 1999; Rapoport, 2007; Zimmermann *et al.*, 2011; Park & Rapoport, 2012).

1.2.4.2 THE SEC61 COMPLEX

The Sec61 complex is the central component during protein import of secretory and membrane proteins (Wilkinson *et al.*, 1996). It not only forms the translocation channel, it also serves as the ribosome receptor and recognizes signal sequences (Park & Rapoport, 2012). The translocation channel is remarkable as it transports a large variety of secretory and membrane proteins across the ER membrane which is an essential step during biosynthesis of these proteins. Secretory proteins and membrane proteins are targeted to the membrane by the hydrophobic signal sequence or a hydrophobic transmembrane (TM) segment, respectively (Görlich *et al.*, 1992; Hartmann *et al.*, 1994; Panzner *et al.*, 1995). While soluble proteins are transported across the membrane through the protein-conducting channel, membrane proteins are released into the lipid bilayer through a lateral opening in the channel, called the lateral gate, as soon as the hydrophobic TM segment traverses the channel (Trueman *et al.*, 2011). The fact that the translocation channel is able to distinguish such a variety of proteins gives it a special role in the secretory pathway. Trimeric complexes homologous to the mammalian complex have been identified in various eukaryotic and prokaryotic organisms (Schatz & Beckwith, 1990; Görlich *et al.*, 1992; Panzner *et al.*, 1995; Finke *et al.*, 1996). The mammalian Sec61 complex consists of Secα, Secβ and Secγ, which are homologous to the *S. cerevisiae* subunits Sec61p, Sbh1p and Sss1p, respectively (Görlich *et al.*, 1992; Hartmann *et al.*, 1994, Panzner *et al.*, 1995; van den Berg *et al.*, 2004). Protein translocation in prokaryotes is mediated by the SecYEG complex, consisting of the subunits SecY, SecE and SecG (Stirling *et al.*, 1992; Görlich *et al.*, 1992; Hartmann *et al.*, 1994; Breyton *et al.*, 2002).

1.2.4.2.1 THE SEC61P SUBUNIT

Sec61p, with its highly conserved sequence is essential in *S. cerevisiae* and *Escherichia coli* (*E. coli*) (Mothes *et al.*, 1994; van den Berg *et al.*, 2004). It not only functions as the ribosome receptor in the ER membrane during cotranslational translocation, but it is also the subunit that forms the active translocation pore interacting with the translocating polypeptides (Görlich *et al.*, 1992; Sanders *et al.*,

1992; Kalies *et al.*, 1994: Mothes *et al.*, 1994; Prinz *et al.*, 2000; Levy *et al.*, 2001). Moreover, Sec61p has been suggested to be the central component during ERAD involved in the formation of the retrotranslocation channel and as the proteasome binding site during ERAD (ref. 1.6.1; McCracken & Brodsky, 1996; Wiertz *et al.*, 1996b; Pilon *et al.*, 1997, 1998; Schmitz *et al.*, 2000, 2005). Although the nature of the retrotranslocon is still under debate, retrotranslocation of many soluble substrates depends on the Sec61 channel (Pilon *et al.*, 1997, 1998; Kalies *et al.*, 2005; Römisch, 2005; Ng *et al.*, 2007; Schäfer & Wolf, 2009). The role of Sec61p in ERAD is supported by studies in *S. cerevisiae*, which have revealed that mutations in TMD 3 and TMD 4 as well as in loop (L) 4 cause defects in retrotranslocation (Pilon *et al.*, 1997; Wilkinson *et al.*, 2000).

The Sec61p subunit (*S. cerevisiae*; mammals: Secα; archea and bacteria: SecY) of the Sec61 complex displays a highly conserved structure consisting of ten TMDs (TMD 1-10) with the C- and N-termini as well as L 2, 4, 6 and 8 in the cytosol and L 1, 3, 5 and 7 facing the ER-lumenal side (ref. Figure 1.2.4.2.1.1; Akiyama & Ito, 1987; Görlich *et al.*, 1992; Stirling, 1993; Hartmann *et al.*, 1994; Wilkinson *et al.*, 1996; Johnson & van Waes, 1999; Raden *et al.*, 2000).

The crystal structure of the *M. jannaschii* protein-conducting channel has revealed that the α-subunit (Sec61p in *S. cerevisiae*; Secα in mammals; SecY in archea and bacteria) is open on one side (viewed from the top) and surrounded by the γ-subunit (Sss1p in S. cereviaise; Secγ in mammals; SecE in archea and bacteria) on two sides which makes limited contact with TMD 1, TMD 5, TMD 6 and TMD 10, thereby acting as a clamp holding the two halves of the α-subunit together (van den Berg *et al.*, 2004). The β-subunit (Sbh1p in *S. cerevisiae*; Secβ in mammals and archaea; SecG in bacteria) is only peripherally associated with the α-subunit (van den Berg *et al.*, 2004). The whole Sec61p structure can be divided into two halves (TMD 1-5 and TMD 6-10), which are connected by a loop between TMD 5 and TMD 6 (van den Berg *et al.*, 2004). The crystal structure also shows that some of the ten TMDs are not perpendicular to the plane of the ER membrane (TMD 2, TMD 5, TMD 7) and some do not span the membrane entirely (TMD 9, TMD 10) (van den Berg *et al.*, 2004). A quite remarkable feature in the Sec61p/Secα structure is the segment between TMD 1 and TMD 2a. This segment forms a long loop that ends in a short helix (= TMD 2a), the so-called plug (ref. Figure 1.2.4.2.1.1; van den Berg *et al.*, 2004). TMD 2a is connected to TMD 2b by a segment that resembles a β-hairpin loop (ref. Figure 1.2.4.2.1.1; van den Berg *et al.*, 2004). One model suggests that the membrane barrier is maintained by the plug and the so-called pore ring during the Sec61 channel's resting state as well as during translocation (van den Berg *et al.*, 2004; Li *et al.*, 2007; Saparov *et al.*, 2007; Zimmer *et al.*, 2008; Park & Rapoport, 2011). The pore ring consists of six hydrophobic residues and interacts with the plug in the resting channel (van den Berg *et al.*, 2004; Li *et al.*, 2007). During translocation the plug is displaced and the pore ring forms a seal around the translocating polypeptide thereby maintaining a barrier for small molecules during translocation (ref. 1.2.4.5; van den Berg *et al.*, 2004; *Li et al.*, 2007; Saparov *et al.*, 2007; Junne *et al.*, 2010; Park & Rapoport, 2011). The crystal structure of the Sec61 complex has also shown that L 6 and 8 and the

C-terminal tail of Sec61p are accessible for cytosolic binding partners, supporting data from *sec61* mutants defective in ribosome binding and cotranslational import, that suggest that those domains are important for the binding of ribosomes and respective binding partners (Pool *et al.*, 2002; Raden *et al.*, 2000; Song *et al.*, 2000; van den Berg *et al.*, 2004). It has been demonstrated that ribosomes and proteasomes compete for binding to the translocation channel, but bind to different sites in Sec61p (Lee *et al.*, 2004b; Kalies *et al.*, 2005; Ng *et al.*, 2007). While the binding site for 26S proteasomes still needs to be elucidated, for ribosomes L 8 has been identified to be the binding site. A *sec61* mutant (*sec61R406E*) with a point mutation in a conserved part of L 8 has shown reduced affinity for ribosomes but not for proteasomes (Cheng *et al.*, 2005; Kalies *et al.*, 2005; Ng *et al.*, 2007).

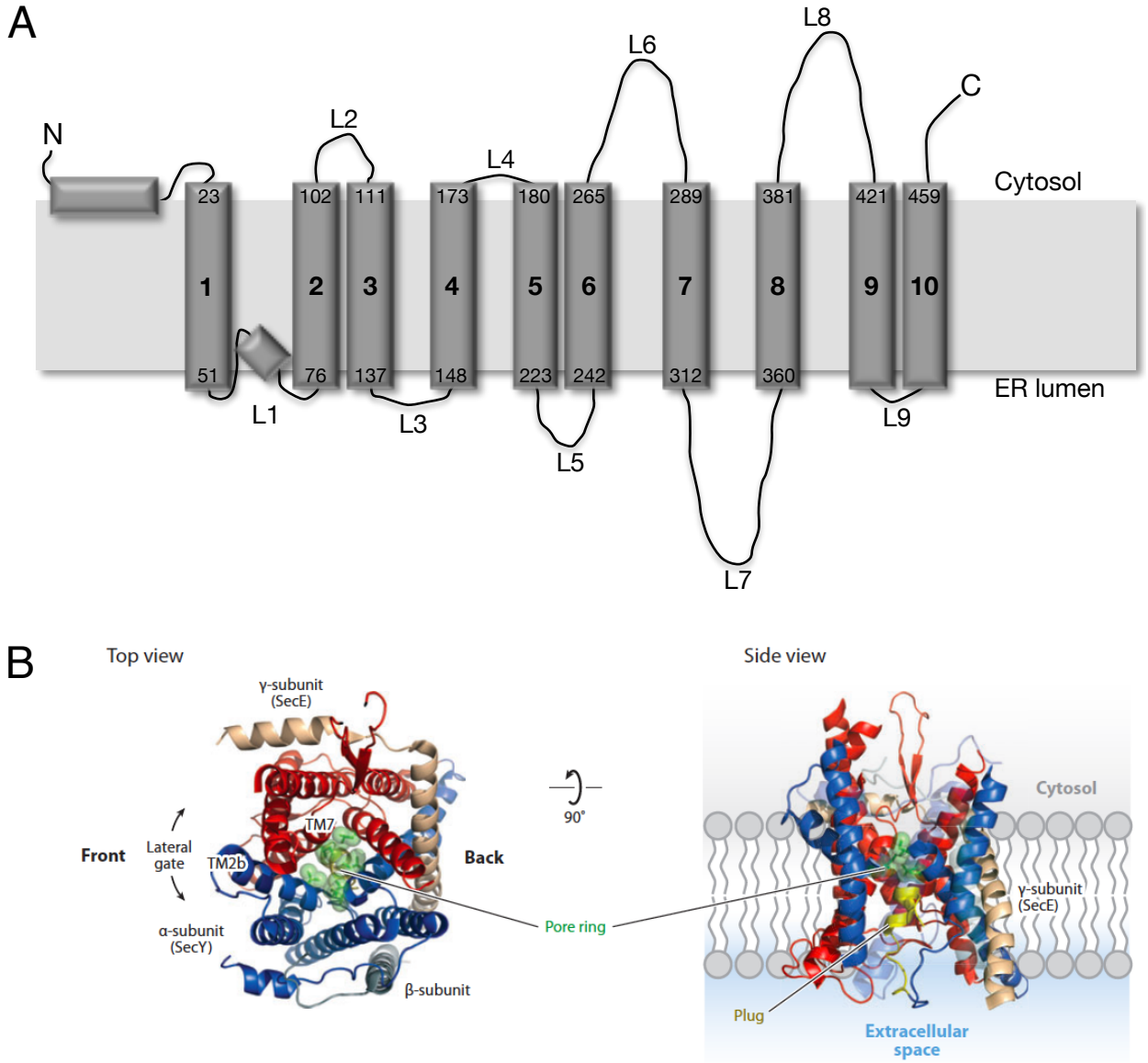

Figure 1.2.4.2.1.1. The Sec61p subunit. (A) The predicted topology model of Sec61p shows that the protein (480 amino acids) consists of ten TMDs. Both, the N- and C-termini are located towards the cytosol. The dimensions of the TMDs have been modified according to van den Berg *et al.*, 2004: TMD1: P^{23}-L^{51}; TMD2: T^{76}-Q^{102}; TMD3: R^{111}-G^{137}; TMD4: P^{148}-K^{173}; TMD5: G^{180}-A^{223}; TMD6: P^{242}-Y^{265}; TMD7: S^{289}-Q^{312}; TMD8: I^{360}-I^{381}; TMD9: A^{421}-G^{443}, TMD10: S^{444}-Y^{459} (adapted from Wilkinson *et al.*, 1996; Raden *et al.*, 2000; van den Berg *et al.*, 2004). (B) Crystal structure of the *M. jannaschii* SecY complex (3.2 Å). Shown is the closed SecY channel viewed from the cytosol (LEFT) and from the side extending through the plasma membrane (RIGHT). The positions of the α-, β- and γ-subunit are indicated. Highlighted are the two halves of SecY surrounding the translocation pore, the C-terminal domain (red; TMD 6-10) and the N-terminal domain (blue; TMD 1-5). The plug (yellow), the pore ring (green) and the lateral gate (LEFT), all of which play important roles during translocation, are indicated (van den Berg *et al.*, 2004; taken from Park & Rapoport, 2012).

1.2.4.2.2 THE SBH1P SUBUNIT

Sbh1p (Sec61β homologue; *S. cerevisiae*: Sbh1p; mammals: Sec61ß, archaea: Secß; bacteria: SecG) is a tail-anchored protein with one transmembrane span and the N-terminus in the cytosol (Panzner *et al.*, 1995; Toikkanen *et al.*, 1996). *S. cerevisiae* contains a second gene, *SBH2*, which is homologous to *SBH1* and encodes the β-subunit of the Ssh1 complex (Ssh1p, Sbh2p, Sss1p) (ref. 1.2.4.3 and Figure 1.2.1.1; Finke *et al.*, 1996; Toikkanen *et al.*, 1996). Sbh1p and Sbh2p are not essential in yeast but deletion of both genes makes cells temperature-sensitive (Stirling *et al.*, 1993; Hartmann *et al.*, 1994; Finke *et al.*, 1996; Toikkanen *et al.*, 1996; Kalies *et al.*, 1998). The *M. jannaschii* crystal structure shows that the helical transmembrane span of the β-subunit is preceded by a cytosolic segment that is disordered, and hence not visible in the crystal, and that contact of the β-subunit with the α-subunit is only limited (ref. Figure 1.2.4.2.1.1.B; van den Berg *et al.*, 2004; Park & Rapoport, 2012). The TMD of Sbh1p has been shown to be sufficient to suppress temperature-sensitive growth of *Δsbh1 Δsbh1* yeast and also for interaction with Sec61p (Feng *et al.,* 2007). Sbh1p has been suggested to be involved in the insertion of secretory proteins into the channel and also has been shown to interact with the SP complex and the OST complex (Kalies *et al.*, 1998; Chavan *et al.*, 2005; Feng *et al.*, 2007). Biochemical studies with Sbh2p revealed that its cytosolic domain mediates interaction of SR with the Ssh1 complex (Jiang *et al.*, 2008).

1.2.4.2.3 THE SSS1P SUBUNIT

The Sss1p (Sec sixty-one suppressor; *S. cerevisiae*: Sss1p; mammals: Sec61γ; archaea and bacteria: SecE) subunit is a tail-anchored protein consisting of two α-helices with the N-terminal helix lying on the cytosolic surface of the membrane and the C-terminal helix traversing the ER membrane at an angle, such that the protein surrounds the Sec61p TMDs like a clamp (ref. Figure 1.2.4.2.1.1; Esnault *et al.*, 1993, 1994; Hartmann *et al.*, 1994; van den Berg *et al.* 2004; Osborne *et al.*, 2005). The subunit is conserved and essential for protein import (Esnault *et al.*, 1994; Hartmann *et al.*, 1994; Finke *et al.*, 1995; Wilkinson *et al.*, 2010). In *S. cereviaise*, *sss1* null mutants could be complemented using the human homologue (Hartmann *et al.*, 1994). Just like Sec61p, Sss1p is essential in *S. cerevisiae* and SecE in *E. coli* (Mothes *et al.*, 1994). The N-terminal helix of Sss1p displays an amphipathic character with the hydrophobic part facing the membrane where it contacts the C-terminal part of Sec61p (ref. Figure 1.2.4.2.1.1; Murphy & Beckwith, 1994; Satoh *et al.*, 2003; van den Berg *et al.*, 2004). A short β-strand follows this helix, which forms a sheet with a part of a β-hairpin that is formed between TMD 6 and TMD 7 of Sec61p (ref. Figure 1.2.4.2.1.1; van den Berg *et al.*, 2004). The TMD of Sss1p seems to act as a clamp holding the two halves of Sec61p together (ref. Figure 1.2.4.2.1.1; van den Berg *et al.*, 2004). Data from the crystal structure of the *M. jannaschii* SecY complex have shown that the TMD is a long helix that makes contact with the TMD 1, 5, 6 and 10 of the α-subunit (van den Berg *et al.*, 2004). Moreover, data from crosslinking

experiments also revealed that Sss1p interacts with TMD 8 as well as TMD 6 and TMD 7 of Sec61p (ref. Figure 1.2.4.2.1.1). This interaction has been suggested to have a stabilizing effect on the channel (Esnault *et al.*, 1994; Wilkinson *et al.*, 1997). During its interaction with Sec61p, Sss1p might play a crucial role during plug removal for channel opening. It has also been suggested to act as a surrogate signal sequence (Plath *et al.*, 1998; van den Berg *et al.*, 2004). Sss1p not only interacts with Sec61p, it has also been suggested to bind to Ssh1p (in the Ssh1 complex; ref. 1.2.4.3) and interact with the OST complex. Interaction with the latter has been suggested to be important for efficient N-linked glycosylation of glycoproteins as it might mediate binding of OST to the translocation channel (Scheper *et al.*, 2003; Chavan *et al.*, 2005).

1.2.4.2.4 THE TRANSLOCATION MODEL

Data from biochemical studies and from structural analyses of the translocon have led to the development of a translocation model (Deshaies *et al.*, 1991; Görlich & Rapoport, 1993; Panzner *et al.*, 1995; van den Berg *et al.*, 2004):

During translocation the Sec61 complex has been suggested to form oligomers consisting of two to four complexes (Beckman *et al.*, 1997; Manting *et al.*, 2000; Menetret *et al.*, 2000; Beckmann *et al.*, 2001; Breyton *et al.*, 2002; Morgan *et al.*, 2002; Duong, 2003; Mori *et al.* 2003; van den Berg *et al.*, 2004). It has been proposed, however, that a single Sec61 complex is sufficient to form a functional translocation channel, although it might exist as a dimer or tetramer (i.e. a dimer of dimers) (Veenendaal *et al.*, 2001; Mori *et al.*, 2003; Snapp *et al.*, 2004; Cannon *et al.*, 2005; Devile *et al.*, 2011). Oligomerization might be necessary in order to recruit various accessory components of the import machinery (e.g. SP, OST, TRAM, TRAP) (Yahr & Wickner, 2000; Duong *et al.*, 2003; van den Berg *et al.*, 2004).

The X-ray structure of the *M. jannaschii* protein-conducting channel has helped immensely in understanding the basic mechanism underlying translocation (ref. Figure 1.2.4.2.1.1; van den Berg *et al.*, 2004). While the closed versus the translocating channel have been proposed to be 9-15 Å and 40-60 Å respectively, data from the *M. jannaschii* structure suggest the size of the closed channel entrance to be 20-25 Å (Hamman *et al.*, 1997, 1998; van den Berg *et al.*, 2004). The translocation pore formed by one copy of the Sec61 complex is sealed by the so-called pore ring and the plug (TMD 2a) before translocation occurs (Beckmann *et al.*, 1997; Menetret *et al.*, 2000; Beckmann *et al.*, 2001; Morgan *et al.*, 2002; Manting *et al.*, 2000). Depending on the mode of translocation the channel partners (i.e. ribosomes or the Sec62/63p complex in eukaryotes) bind, which partially opens the lateral gate (Zimmer *et al.*, 2008; Tzukasaki *et al.*, 2008). Binding of channel partners alone, however, is insufficient to open the channel (Simon & Blobel, 1991; Matlack *et al.*, 1998; van den Berg *et al.*, 2004). Opening of the protein-conducting channel is triggered by binding of the signal sequence, which intercalates between TMD 2b and TMD 7 of Sec61p such that

the substrate is inserted into the channel in a loop (Jungnickel & Rapoport, 1995; Plath *et al.*, 1998; van den Berg *et al.*, 2004; Zimmer *et al.*, 2008). It has been suggested that signal sequence binding destabilizes those interactions of the plug that keep it in the centre of the pore (van den Berg *et al.*, 2004). In order for the channel to open and to be translocation-competent, the plug needs to be displaced (Becker *et al.*, 2009; Zimmer *et al.*, 2008; du Plessis *et al.*, 2009). It has been suggested that signal sequence binding further promotes separation of TMD 2b and TMD 7 resulting in the displacement of the plug to its open state position, which is close to the γ-subunit (van den Berg *et al.*, 2004). More recent studies, however, indicate that signal sequence insertion only partially opens the channel (Wilkinson *et al.*, 2010; Trueman *et al.*, 2011). It has been suggested that Sss1p may play a role during translocation by completing channel opening and thus activating the translocon (Wilkinson *et al.*, 2010). The clamp domain of Sss1p has been proposed to undergo a rearrangement relative to the hinge domain of Sec61p, which would eventually promote lateral gate opening (Wilkinson *et al.*, 2010). As a result, the polypeptide chain would be able to fully access the channel (van den Berg *et al.*, 2004; Wilkinson *et al.*, 2010). Once the channel is open, the mature region of the polypeptide is properly inserted into the channel with the pore ring forming a seal around the translocating polypeptide chain (van den Berg *et al.*, 2004; Park & Rapoport, 2012). The signal sequence is finally cleaved-off by SP as soon as the cleavage site is accessible at the lumenal end of the channel (Böhni *et al.*, 1988; Dalbey & von Heijne, 1992; Paetzel *et al.*, 1998; Chen *et al.*, 2001). The channel returns to its closed state when the polypeptide has been fully translocated, with the plug moving back to its closed state position (van den Berg *et al.*, 2004).

Although the biosynthesis of membrane proteins is less well understood, the scenario could be similar. TMDs might move into the lipid bilayer through the so-called lateral gate (van den Berg *et al.*, 2004; Trueman *et al.*, 2011). It has been shown that during lateral gate opening TMD 7, 8 and 9 of Sec61p move outwards, resulting in TMD 9 being close to the cytosolic domain of Sss1p (van den Berg *et al.*, 2004; Wilkinson *et al.*, 2010). This indicates that both TMD 9 of Sec61p and Sss1p mediate complete channel opening and translocon activation (Zimmer *et al.*, 2008; Wilkinson *et al.*, 2010; Trueman *et al.,* 2011).

1.2.4.3. THE SSH1 COMPLEX

In *S. cerevisiae*, there is another trimeric complex homologous to the Sec61 complex suggested to be involved in cotranslational import (Finke *et al.*, 1996). The Ssh1 complex consists of Ssh1p (Sec sixty-one homologue; about 34 % homology), Sbh2p (Sec sixty-one β homologue) and Sss1p (Finke *et al.*, 1996; Prinz *et al.*, 2000; Wittke *et al.*, 2002). This complex is likely to be involved in cotranslational import, which is supported by studies that have shown that Ssh1p can interact with ribosomes and signal sequences of a subset of proteins and that growth of *Δssh1* cells is

compromised when the gene encoding a subunit of SRP is disrupted (Finke *et al.*, 1996; Prinz *et al.*, 2000; Wilkinson *et al.*, 2001; Wittke *et al.*, 2002).

The central component of the complex, Ssh1p, is nonessential as deduced as *Δssh1* mutants are alive (Finke *et al.*, 1996; Plemper *et al.*, 1997; Gillece *et al.*, 2000; Wilkinson *et al.*, 2001). Although homologous to Sec61p, Ssh1p does not seem to be functionally interchangeable with Sec61p, as it does not complement lethal *sec61* mutations (Wilkinson *et al.*, 2001).

Initial studies on Ssh1p have shown that *Δssh1* mutants are proficient in protein translocation into the ER as well as in retrotranslocation of misfolded glycoproteins from the ER lumen to the cytosol (Finke *et al.*, 1996, Plemper *et al.*, 1997; Gillece *et al.*, 2000). A *Δssh1* mutant containing the *sec61-2* temperature-sensitive allele is not viable at the permissive temperature for the *sec61-2* allele (Finke *et al.*, 1996).

Ssh1p binds ribosomes with the same affinity as Sec61p (Finke *et al.*, 1996; Prinz *et al.*, 2000). More recent data from Wilkinson *et al.* (2001) support the existence of two separate, functionally nonequivalent translocons in the yeast ER, containing Sec61p and Ssh1p, respectively, both of which mediate translocation and dislocation. In a set of elegant experiments the authors showed that Ssh1p is involved in SRP-dependent translocation (Wilkinson *et al.*, 2001). *Δssh1* cells are defective in co- and posttranslational import and show defects in the retrotranslocation of CPY* and an induction of the UPR (Wilkinson *et al.*, 2001). Thus, during fast growth, Sec61 channels probably provide insufficient translocation capacity on their own. Under normal growth conditions the demand for proper secretory pathway function is crucial. In the absence of Sec61p, however, protein translocation into the ER through the Ssh1p channel is not sufficient for cells to survive, i.e. as Ssh1p channels cannot import posttranslationally, at least one posttranslational substrate must be essential (Wilkinson *et al.*, 2001). It is, however, likely that Ssh1p serves as a “back-up” or reserve translocon, which, under certain growth conditions, provides the cell with physiological flexibility (Wilkinson *et al.*, 2001).

Recent analyses using an SRP-dependent substrate revealed that this substrate was targeted preferably to Ssh1p suggesting that Ssh1p might act as a protein-conducting channel comparable to Sec61p (Spiller & Stirling, 2011). Moreover, Ssh1p-mediated translocation using the model substrates also involved Sec63p, revealing an interaction between Ssh1p and Sec63p in cotranslational translocation (Spiller & Stirling, 2011).

In yeast, a GEF-role for the β-subunits of the translocon (Sbh1p and Sbh2p) during SR-heterodimerization has been shown (Toikkanen *et al.*, 1996; Legate *et al.*, 2000; Schwartz & Blobel, 2003). The interaction between the subunits and the GTPase domain of SRβ mediates dissociation of GDP from SRβ (Helmers *et al.*, 2003). Sbh2p has also been suggested to recognize a substrate-specific feature of the RNC and to mediate differential targeting of a model substrate to the Ssh1 complex, which is in line with indications that Sbh1/Sbh2 mediate interaction between the translocon and SR (Spiller *et al.*, 2011; Jiang *et al.*, 2008).

1.2.4.4 THE SEC COMPLEX

In *S. cerevisiae* there are distinct multi-subunit complexes for cotranslational and posttranslational protein translocation (ref. Figure 1.2.1.1; Park & Rapoport, 2012). During posttranslational import the Sec61 complex (Sec61p, Sbh1p, Sss1p) associates with the tetrameric Sec63 complex (Sec62p, Sec63p, Sec71p, Sec72p) forming the heptameric SEC complex (Deshaies *et al.*, 1991; Panzner *et al.*, 1995; Wittke *et al.*, 1999). This complex does not bind to ribosomes supporting its role during posttranslational translocation for which it is essential (Brodsky & Schekman, 1993; Panzner *et al.*, 1995). The function of its individual components, however, is not yet fully understood.

The essential subunit Sec62p (yeast: 32 kDa) is a transmembrane protein with two TMDs and its C- and N-termini facing the cytosol (Deshaies & Schekman, 1989, 1990). Mammalian Sec62p has been shown to associate with ribosomes suggesting a role during cotranslational import (Müller *et al.*, 2010). Sec62p has been suggested not to be involved in ERAD, as a *sec62* mutant does not display defective ERAD for the ERAD substrates CPY* and Δgpαf, and Sec62p is not found in proteasome-associated Sec61 complexes (Pilon *et al.*, 1997; Plemper *et al.*, 1997; Ng *et al.*, 2007).

Sec63p (75 kDa) has three transmembrane domains, with its N-terminus located towards the ER-lumen and the C-terminus towards the cytosol (Feldheim *et al.*, 1992; Brodsky & Schekman, 1993). Further, it contains a DnaJ domain in the ER-lumenal loop between TMD 2 and TMD 3 (Feldheim *et al.*, 1992; Scidmore *et al.*, 1993). Sec63p interacts via its DnaJ domain with the ER-lumenal Hsp70 chaperone Kar2p (BiP), recruiting it for co- and posttranslational import (Brodsky *et al.*, 1995; Misselwitz *et al.*, 1999; Tyedmers *et al.*, 2000; Hendershot, 2004). This interaction is a prerequisite for posttranslational translocation (Matlack *et al.*, 1997, 1999; Scidmore *et al.*, 1999). In yeast, however, it has been suggested to play a role in cotranslational import depending on the nature of the signal sequence (Spiller & Stirling, 2011; Lang *et al.*, 2012; Mades *et al.*, 2012). Studies using human cell lines have indicated that here Sec63p is not essential for cotranslational import but is involved in the biogenesis of polytopic transmembrane proteins. It has been shown that overexpression of *SEC63* in mammalian cells reduces the levels of certain multi-spanning membrane proteins and vice versa assigning Sec63p a nonessential regulator role in cotranslational insertion of certain transmembrane proteins (Mades *et al.*, 2012). Further, as Sec63p in mammalian cells is close to Sec61p, a role as a gatekeeper during expansion of the translocon during membrane insertion of proteins is possible (Lang *et al.*, 2012; Mades *et al.*, 2012). Data from experiments in human cells have further indicated that the role of Sec63p in polytopic membrane protein biogenesis is independent of Sec62p (Mades *et al.*, 2012). Studies in yeast and mammalian cells have shown that Sec62p and Sec63p interact with each other (Meyer *et al.*, 2000; Müller *et al.*, 2010; Harada *et al.*, 2011). In yeast, Sec63p has been described to play a role during ERAD (Pilon *et al.*, 1997; Plemper *et al.*, 1997, Ng *et al.*, 2007). A *sec63* mutant in the J-domain shows a delayed degradation of ERAD substrates, therefore Sec63p is possibly part of the dislocation channel (Pilon *et al.*, 1997; Plemper *et al.*, 1997; Gillece *et al.*, 2000).

Sec71p (yeast: 24 kDa) is a membrane protein with one transmembrane domain (N-terminus towards the ER lumen; two glycosylation sites), which associates with Sec72p (yeast: 21 kDa), a soluble protein located on the cytosolic side of the ER (Brodsky & Schekman, 1993; Feldheim *et al.*, 1993; Feldheim & Schekman, 1994; Panzner *et al.*, 1995). Both proteins are nonessential but deletion of both genes causes temperature sensitivity in yeast (Feldheim & Schekman, 1994; Plath *et al.*, 1998). Together with Sec62p they have been suggested to act in signal sequence recognition during posttranslational import (Lyman & Schekman, 1997). Neither Sec71p nor Sec72p are required for ERAD (Fang & Green; 1994; Plemper *et al.*, 1997).

1.3 PROTEIN FOLDING/MODIFICATIONS AND THE ER QUALITY CONTROL

1.3.1 PROTEIN FOLDING AND MODIFICATIONS IN THE ER

The first compartment of the secretory pathway is the ER, which plays an essential role in the biogenesis of secretory proteins (Ghaemmaghami *et al.*, 2003; Kanapin *et al.*, 2003; Vazquez-Martinez *et al.*, 2012).

Upon their import into the ER (ref. 1.2.2 and 1.2.3) through the Sec61 translocon (ref. 1.2.4) proteins destined for secretion or membranes of the secretory pathway meet with the elaborate folding and modification machinery of the ER (Deshaies *et al.*, 1991; Gething, 1999; Johnson & Waes, 1999; Rapoport, 2007; Braakman & Bulleid, 2011). The unique environment of the ER favours protein folding and modifications that would not be possible in the cytosol (Dill *et al.*, 2008). The ER is equipped with a high concentration of molecular chaperones that maintain protein solubility and assist in protein folding, enzymes that catalyze posttranslational modifications as well as other factors that directly mediate protein folding (Jahn & Radford, 2005; McClellan *et al.*, 2005; Bukau *et al.*, 2006). The large variety of chaperones, co-chaperones, prolyl-isomerases, glycan-modifiying enzymes and other enzymes assist folding and are important for proteins to gain their final structure (van Anken & Braakman, 2005). The ER is also the major calcium-storage organelle of the cell and proper folding and chaperone function is often dependent on calcium (Wada *et al.*, 1991; Meldolesi & Pozzan, 1998).

Following signal sequence cleavage by SP, OST glycosylates proteins at asparagine (Asn) in the recognition site Asn-X-Ser/Thr (Tatu *et al.*, 1993; Johnson & van Waes, 1999; Spurway *et al.*, 2001). The aforementioned ER-lumenal chaperone Kar2p (BiP) promotes folding by binding to folding intermediates thereby stabilizing the protein and preventing the formation of toxic aggregates (ref. 1.2.2 and 1.2.3; Hendershot *et al.*, 1995, 1996, 2004). BiP is also involved in the regulation of the UPR (ref. 1.4) and targeting of proteins for ERAD (ref. 1.6) (Plemper *et al.*, 1997; Brodsky *et al.*, 1999; Bertolotti *et al.*, 2000; Kabani *et al.*, 2003; Kimata *et al.*, 2003).

Lectin-like chaperones, such as calnexin (CNX) and calreticulin (CRT) are another protein family important during protein folding (ref. 1.3.2; Helenius & Aebi, 2004; Vembar & Brodsky, 2008; Braakman & Bulleid, 2011). These proteins are able to bind to glycan structures of glycoproteins, thereby deciding, depending on the composition of the glycan structure, whether the protein is terminally folded or misfolded or whether it needs to undergo another folding cycle (Caramelo & Parodi, 2007). Hence, lectin-like chaperones are important components of the ERQC (Bhamidipati *et al.*, 2005; Benitez *et al.*, 2011). In addition, glucosidases and mannosidases modify N-linked glycans (Zapun *et al.*, 1999). All of these modifications are important for proper protein folding.

The oxidation, reduction and isomerisation of disulfide bonds are catalyzed by ER-lumenal protein disulfide isomerases (PDIs; yeast: Pdip, 4 homoloques), which possess isomerase and thiol oxidoreductase activity (Freedman *et al.*, 1994; Laboissiere *et al.*, 1995; Norgaard *et al.*, 2001; Tu & Weismman, 2004; Appenzeller-Herzog & Ellgaard, 2008). PDIs are also involved in multi-subunit protein assembly, as they bind proteins, thereby stabilizing intermediates (Wilson *et al.*, 1998). PDIs have also been suggested to be involved in the prevention of aggregate formation and in ERAD of several subsrates (Koivu *et al.*, 1987; Gillece *et al.*, 1999; Wahlman *et al.*, 2007; Gauss *et al.*, 2011). Peptidyl prolyl isomerases (PPIases) catalyze formation of cis-trans-isomerization of peptidyl-prolyl bonds (Kruse *et al.*, 1995; Schmid, 1995)

Only if secretory proteins are modified and folded accordingly can they leave the ER and be transported to their final destination.

1.3.2 ER QUALITY CONTROL

The ERQC is important for the preservation of ER function as the ER has to deal with a big load of newly synthesized protein that need to be properly modified and folded prior to reaching their final destination (Pryer *et al.*, 1992; Bonifacino & Klausner, 1994; Hammond & Helenius, 1995; Kostova & Wolf, 2003; Römisch, 2005). Not all proteins, i.e. an estimated 30 % do not reach their final structure and therefore do not move further along the secretory pathway but are retained in the ER before they are targeted to ERAD (Schubert *et al.*, 2000; Ellgaard & Helenius, 2003, Sitia & Braakman, 2003).

Post-translational modifications as well as proper protein folding and assembly in the ER are essential for protein function. Proteins that do not fold properly can interfere with the functions of their properly folded counterparts and are prone to form aggregates, which are toxic to the cell (Tyedmers *et al.*, 2010). Secretory and membrane proteins are therefore subject to ERQC (Ellgaard & Helenius, 2003). During ERQC the protein folding status of a protein is evaluated. If molecular chaperones are able to assist in proper folding, the protein can enter ER-to-Golgi transport vesicles and is delivered to its final destination. If, however, the protein is not properly folded, it is retained in the ER to allow it to undergo further cycles of folding (McCracken & Brodsky, 1996; Ellgaard &

Helenius, 2003). Terminally misfolded proteins are subjected to the ERAD (ref. 1.6) pathway during which misfolded proteins are transported from the ER to the cytosol and degraded by the cytosolic 26S proteasome (Brodsky & McCracken, 1999; Römisch, 2005; Sayeed & Ng, 2005; Nakatsukata & Brodsky, 2008). If the load of misfolded, aggregated proteins in the ER is bigger than the clearing rate, other pathways are induced, such as the UPR (ref. 1.4) or autophagy (Klionsky, 2007; Ron & Walter, 2007).

ERAD is closely linked to the ubiquitin proteasome system (UPS; ref. 1.5) as many ERAD substrates are polyubiquitinated and degraded by the 26S proteasome (Chandu & Nandi, 2002, 2004; Varshavsky 2005). ERAD substrates are soluble and membane proteins that fail to fold or assemble properly or are not posttranslationally modified or damaged (Bonifacino & Klausner, 1994; Hammond & Helenius, 1995). The recognition of some soluble ERAD substrates might involve the recognition of exposed hydrophobic patches by members of the Hsp70 family, like BiP (Kar2p), and co-chaperones of the Hsp40 family as well as NEFs (nucleotide exchange factors) (Brodsky *et al.*, 1999; Gething, 1999; Kabani *et al.*, 2003; Hendershot, 2004; Hegde *et al.*, 2006). BiP (Kar2p) at least is part of the multiprotein complex involved in ERAD-L of glycoproteins (Plemper *et al.*, 1997). It has been proposed that BiP (Kar2p) is involved in early ERAD substrate recognition (Knittler *et al.*, 1995; Schmitz *et al.*, 1995; Plemper *et al.*, 1997; Nishikawa *et al.*, 2001; Zhang *et al.*, 2001).

1.3.2.1 ER QUALITY CONTROL OF GLYCOPROTEINS

The attachment of carbohydrate moieties to proteins plays an essential role in a lot of biological processes in eukaryotes (Varki, 1993; Haltiwanger & Lowe, 2004; Lehle *et al.*, 2006). The importance of glycoproteins is emphasized by the fact that about 50 % of all cellular proteins are glycoproteins (Apweiler *et al.*, 1999; Zhou *et al.*, 2007).

The majority of proteins (~ 2/3) that are targeted to the secretory pathway are N-linked glycoproteins (Knop *et al.*, 1996b; Jakob *et al.*, 1998). During N-linked glycosylation, the oligosaccharide $GlcNAc_2Man_9Glc_3$ (GlcNAc = N-acetylglucosamine; Man = mannose; Glc = Glucose; G3M9) is linked to the amino group of the asparagine residue in the consensus sequence Asn-X-Ser/Thr (X = any amino acid except proline) of a glycoprotein (Helenius & Aebi, 2004). Upon protein import into the ER the OST complex catalysis the attachment of the carbohydrate moiety to proteins (Lehle *et al.*, 2006). Carbohydrates attached to proteins do not only have an impact on protein conformation, they also contribute to protein stability and serve as a signal during ERQC (Knop *et al.*, 1996b; Helenius & Aebi, 2004; Hitt & Wolf, 2004; Lehle *et al.*, 2006).

The mechanism by which N-glycosylated misfolded proteins are targeted to the ERQC is better understood than that for unglycosylated proteins. The proposed model suggests that whether a protein is degraded or secreted depends on both its structure and the time a protein remains in the ER (Jakob *et al.*, 1998). The $GlcNAc_2Man_9Glc_3$ structure is added during protein import in both yeast

and mammalian cells (Ellgaard *et al.*, 1999; Liu *et al.*, 1999). During early folding steps in the mammalian ER glucosidase I and II remove the terminal two glucose molecules on the A branch of the oligosaccharide moiety leading to $GlcNAc_2Man_9Glc$ (ref. Figure 1.3.2.1.1; Helenius & Aebi, 2004; Aebi *et al.*, 2010). Next, one of the two homologous lectins CNX (membrane protein) or CRT (ER-lumenal protein) binds to the mono-glucosylated glycan structure (Hammond *et al.*, 1994; Helenius *et al.*, 1997; Aebi *et al.*, 2010; Pearse *et al.*, 2010; Stolz et al., 2010). Mammalian ERp57, a member of the PDI family, is then recruited to the lectin-bound glycan in a transient interaction (Freedman *et al.*, 1994; Holtzman, 1997; Oliver *et al.*, 1999). ERp57 promotes further folding and formation of disulfide bonds (Oliver *et al.*, 1999). In yeast, Pdi1p might fulfill ERp57's task (Buck *et al.*, 2007; Gauss *et al.*, 2011). Fully folded proteins are released from the CNX/CRT cycle and glucosidase II removes the third terminal glucose of the A branch (Aebi *et al.*, 2010). A correctly folded protein with a $GlcNAc_2Man_9$ signature can be demannosylated by Golgi-resident mannosidase I and II and move further along the secretory pathway (Gabel & Bergmann, 1985; Moremen, 2002;Vembar & Brodsky, 2008; Aebi *et al.*, 2010). If the protein cannot reach its final conformation, however, it is recognized and reglucosylated by UDP-glucose:glycoprotein glucosyltransferase (UGGT) which adds a glucose molecule from UDP-glucose to $GlcNAc_2Man_9$ (Caramelo *et al.*, 2003; Taylor *et al.*, 2003). The protein then re-enters the CNX/(CRT)-ERp57 folding cycle (Helenius & Aebi, 2004). Upon correct folding, the glycoprotein is not recognized by UGGT anymore and can be packaged into ER-to-Golgi transport vesicles to leave the ER (Helenius, 1994; Caramelo *et al.*, 2004; Warren & Mellman, 1999). Terminally misfolded proteins on the other hand are recognized and targeted to ERAD (Vembar & Brodsky, 2008). There is no UGGT in *S. cerevisiae* (Xu *et al.*, 2004; Meaden et al., 2008; Braakman & Bulleid, 2011).

After removal of the third terminal glucose by glucosidase II, ER mannosidase I can access the α1,2-linked mannose of the glycan's B branch and removes it (ref. Figure 1.3.2.1.1; Fagioli & Sitia, 2001). ER mannosidase I is a slow-acting enzyme, which supports the mannose timer hypothesis (Su *et al.*, 1993; Helenius *et al.*, 1997). Initially, the resulting $GlcNAc_2Man_8$ B-glycan was thought to serve as the signal for degradation in both yeast and mammalian cells (Knop *et al.*, 1996b; Liu *et al.*, 1997; Jakob *et al.*, 1998; 2001). Early studies proposed that lectins or lectin-like proteins recognize this glycan structure on misfolded glycoproteins (Lui *et al.*, 1997; Jabkob *et al.*, 1998; Yang *et al.*, 1998). Htm1p/EDEM (EDEM = ER degradation-enhancing α-mannosidase-like protein), which shows homology to class I mannosidases, has been suggested to act as a lectin (Jakob *et al.*, 2001; Hosokawa *et al.*, 2001; Mast *et al.*, 2005; Clerc *et al.*, 2009). In mammals three α1,2-mannosidases (EDEM1-3; EDEM1 and EDEM3 are homologous to Htm1p) have been identified (Kanehara *et al.*, 2007; Olivari & Molinari, 2007). EDEMs are soluble ER-lumenal proteins that show mannosidase activity, i.e at least EDEM1 and 3 (Hirao *et al.*, 2006; Olivari *et al.*, 2006). The removal of the terminal α1,2-linked mannose of the A branch enables the protein to exit the CNX/CRT cycle and the additional trimming of the C branch down to $GlcNAc_2Man_6$ and $GlcNAc_2Man_5$ structures generates

the final ERAD signal (Moremen & Molinari, 2006; Molinari, 2007). The signal leads to retrotranslocation, ubiquitination and proteasomal degradation of the protein.

In *S. cerevisiae*, there is no mechanism comparable to the CNX/CRT cycle known to date (Fernandez *et al.*, 1994; Vembar & Brodsky, 2008; Clerc *et al.*, 2009). There is, however, a homologue to CNX, Cne1p, whose exact role in ERAD is unclear (Parlati *et al.*, 1995; Knop *et al.*, 1996b; Xu *et al.*, 2004a, 2004b; Kimura *et al.*, 2005; Kostova & Wolf, 2005; Clerc *et al.*, 2009). For Cne1p binding of monoglucoyted oligosaccharaides (G1M9) was demonstrated using lectin site mutants (Xu *et al.*, 2004a; Hosokawa *et al.*, 2010). For a subset of glycosylated and nonglycosylated substrates Cne1p exhibits chaperone activity (Parlati *et al.*, 1995; Xu *et al.*, 2004a, 2004b). It was also found to be involved in the quality control of some underglycosylated forms of CPY* where the role of Cne1p was antagonistic to Htm1p: When Htm1p was absent the substrate was stabilized and when Cne1p was absent degradation was accelerated (Kostova & Wolf, 2005). Under heat stress conditions Cne1p interacts with Kar2p (BiP) and Pdi1p which have been suggested to partly recover the function of Cne1p in Cne1p-disrupted cells (Brodsky *et al.*, 1999; Zhang *et al.*, 2008a, 2008b).

The yeast α1,2-mannosidase homologue Htm1p/Mnl1p (Htm1 = homologous to mannosidase 1; Mnl1 = mannosidase-like protein 1) removes the terminal α1,2-mannose molecules from the C branch of the $GlcNAc_2Man_8$-glycan generated by mannosidase I (α1,2-exomannosidase) (Hosokawa *et al.*, 2001; Jakob *et al.*, 2001; Mast *et al.*, 2005; Hirao *et al.*, 2006; Clerc *et al.*, 2009). The resulting $GlcNAc_2Man_7$ C-glycan has been proposed to serve as the degradation signal (Clerc *et al.*, 2009).

Studies in yeast have shown that whereas ER mannosidase I works on the B branch and produces a terminal α1,3-linked mannose, Htm1p works on the C branch leading to an α1,6-linked mannose (Clerc *et al.*, 2009). Mammalian EDEM1 and EDEM3 also seem to work on the α1,2-linked mannose of the A branch (Hirao *et al.*, 2004, Olivari *et al.*, 2006; Clerc *et al.*, 2009). Htm1p has been shown to be involved in ERAD-L (Vashist & Ng, 2004). Htm1p also interacts with Pdip, which has been shown to recognize misfolded proteins and target them to the retrotranslocon (Gillece *et al.*, 1999; Krogan *et al.*, 2006; Clerc *et al.*, 2009).

Another α1,2-mannosidase has been identified, Mnl2, trimming the glycan structure on the A branch, resulting in a $GlcNAc_2Man_5$ species, which has been suggested to be recognized by the lectin Yos9p (ref. Figure 1.3.2.1.1; Aebi *et al.*, 2010; Benitez *et al.*, 2011).

The mannose 6-phosphate homology domain of Yos9p is essential for ERAD-L of glycoproteins (Buschhorn *et al.*, 2004; Bhamidipati *et al.*, 2005; Kim *et al.*, 2005). Yos9p acts downstream of Htm1p binding to α1,6-linked C-glycans generated by Htm1p (Quan *et al.*, 2008; Clerc *et al.*, 2009). It is part of the Hrd1 complex (ref. 1.4), which is formed around the Hrd1p E3 ligase (Gardner *et al.*, 2000; Carvalho *et al.*, 2006). Misfolded proteins complexed to chaperones or lectins interact with Hrd3p (of the Hrd1 complex), which seems to initiate export and degradation (Plemper *et al.*, 1999a; Gardner *et al.*, 2000). Yos9p is one of the targeting lectins which ferries misfolded proteins to the Hrd1 complex (Vashist & Ng, 2004; Denic *et al.*, 2006; Gauss *et al.*, 2006; Quan *et al.*, 2008).

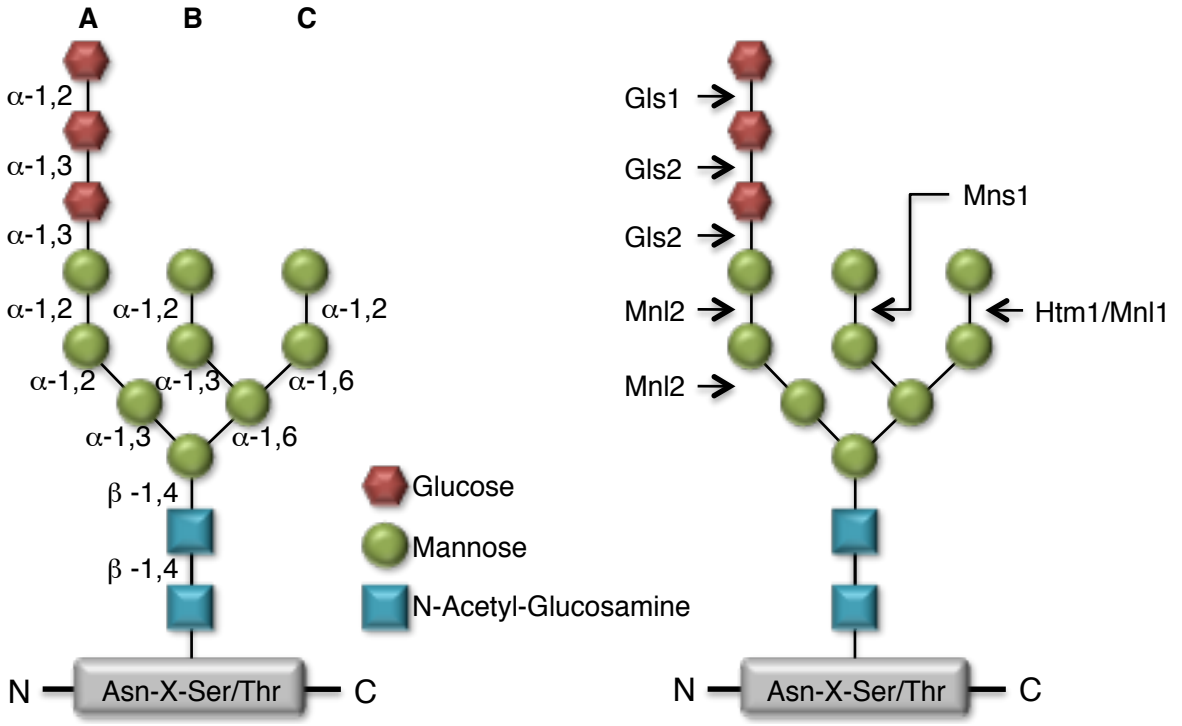

Figure 1.3.2.1.1. N-glycan processing in the ER. In *S.cerevisiae* N-glycan processing and recognition starts with the attachment of the $GlcNAc_2Man_9Glc_3$ oligosaccaride to asparagines in the consensus motif Asn-X-Ser/Thr by OST. The glucose residues are sequentially processed by glucosidase I an II. Monoglucosylated N-linked oligosaccharides are recognized by the yeast CNX homologue Cne1p (not shown; Xu *et al.*, 2004a). The terminal α1,2-linked mannose on the B branch of the glycan is processed by ER α1,2-mannosidase (Mns1) resulting in the B-glycan $GlcNAc_2Man_8$. Htm1p trims the α1,2-linked mannose on the C branch generating $GlcNAc_2Man_7$. This structure (or a Man_5-structure generated by Mnl2), containing a terminal α1,6-linked mannose, can then be recognized by the lectin Yos9p (not shown) as the degradation signal and the glycoprotein is subjected to the ERAD pathway (adapted from Benitez *et al.*, 2011).

1.4 THE UNFOLDED PROTEIN RESPONSE

The UPR is an ER-to-nucleus signal transduction pathway that is tightly linked to the ERAD pathway (Casagrande *et al.*, 2000; Friedlander *et al.*, 2000; Travers *et al.*, 2000; Spear & Ng, 2001; Korennykh & Walter, 2012). This cellular protection mechanism, which is triggered by the accumulation of unfolded or incompletely folded secretory or membrane proteins in the ER, is vital for maintaining cellular function under ER stress conditions (Korennykh & Walter, 2012). The primary function of the UPR is to sense accumulation of misfolded proteins in the ER and to trigger a cellular response that enables the cell to cope with the protein overload. As a result, the folding capacity of

the ER as well as the degradation capacity for misfolded proteins is increased while the amount of newly translated proteins entering the ER is reduced (Ng *et al.*, 2000; Spear & Ng, 2003).

In *S. cerevisiae* the key components of the UPR are the ER membrane protein Ire1p (inositol-requiring protein 1) and the transcription factor (TF) Hac1p that mediate the signal transmission from the ER to the nucleus (Cox *et al.*, 1993; Mori *et al.*, 1993; Cox & Walter, 1996; Mori *et al.*, 1996; Nikawa *et al.*, 1996; Travers *et al.*, 2000; Ma & Hendershot, 2001).

Ire1p consists of an N-terminal sensor domain located in the ER lumen and a C-terminal CDK2-like serine/threonine kinase domain fused to a ribonuclease domain (RNase) in the cytosol (ref. Figure 1.4.1; Welihinda & Kaufman, 1996; Sidrauski & Walter, 1997). Detection of misfolded proteins by the sensor domain leads to Ire1p oligomerization resulting in RNase activation (Shamu & Walter, 1996; Credle *et al.*, 2005; Aragon *et al.*, 2009; Korennykh *et al.*, 2009, 2011). Two models have been suggested explaining the sensor mechanism: The first model involves competitive binding of misfolded proteins and the Ire1p sensor domain to the ER chaperone BiP (Bertolotti *et al.*, 2000; Zhou *et al.*, 2006). In a normally growing cell with the ER in homeostasis BiP is associated with Ire1p (Bertolotti *et al.*, 2000; Kimata *et al.*, 2003, 2004). When misfolded proteins accumulate in the ER, BiP is recruited and dissociates from the sensor domain (Dorner *et al.*, 1992; Ng *et al.*, 1992; Beh & Rose, 1995). As a result, Ire1p oligomerizes and undergoes trans-autophosphorylation and thus gets activated (Shamu & Walter, 1996; Bertolotti *et al.*, 2000; Kimata *et al.*, 2003; Zhou *et al.*, 2006). The second model suggests that misfolded proteins directly bind to the sensor domain of Ire1p also leading to the activation of Ire1p (Credle *et al.*, 2005; Gardner & Walter, 2011). This model further implies that BiP acts as a mediator that keeps Ire1p monomer concentrations at a distinct level, which is needed for sufficient sensing of misfolded proteins (Pincus *et al.*, 2010).

High-order oligomerization of Ire1p in the plane of the ER membrane is needed for activation of its kinase and RNase domains (Credle *et al.*, 2005; Aragon *et al.*, 2009; Korennykh *et al.*, 2009, 2011). The Ire1p kinase domain serves as a scaffold for RNase domain oligomerization (Korennykh *et al.*, 2009). It has been suggested that four signals are mandatory for successful oligomerization: The first two involve the binding of BiP and association of unfolded proteins to the lumenal domain of Ire1p. The third is the binding of cofactors to the ATP pocket of the kinase domain of Ire1p and finally, the fourth, is the trans-autophosphorylation of the kinase domain (Bertolotti *et al.*, 2000; Kimata *et al.*, 2003; Korennykh *et al.*, 2009, 2011; Korennykh & Walter, 2012).

Nevertheless, it has been shown that the kinase activity of Ire1p is not essential for UPR activation (Papa *et al.*, 2003; Chawla *et al.*, 2011; Rubio *et al.*, 2011). It is, however, involved in the regulation of RNase domain oligomerization (Korennykh *et al.*, 2009). The autophosphorylation of the Ire1p kinase domain results in a stronger Ire1p association and additionally it is also responsible for faster shutdown as soon as the ER has adjusted to ER stress (Korennykh *et al.*, 2009; Chawla *et al.*, 2011; Rubio *et al.*, 2011).

The activated Ire1p RNase excises a translation-inhibitory intron from the 3' end of the uninduced form of the transcription factor *HAC1* mRNA (*HAC1*^{u}; u = uninduced) followed by religation of the two exons by tRNA ligase (Sidrauski & Walter, 1997; Kawahara *et al.*, 1998). The resulting *HAC*^{i} mRNA (i = induced) encodes the active transcription factor Hac1p (a bZIP transcritption factor) (Shamu & Walter, 1996; Sidrauski *et al.*, 1996; Chapman & Walter, 1997; Rügsegger *et al.*, 2001). Hac1p enters the nucleus where it binds to the UPR regulatory element (UPRE) in the promoter region of the respective UPR target genes, thereby inducing their expression (Mori *et al.*, 1992; Kohno *et al.*, 1993; Cox & Walter, 1996). Among the UPR target genes are genes encoding proteins involved in translocation (translocon subunits), folding (ER-resident chaperones), glycosylation, ER-to-Golgi transport and retrieval, lipid biosynthesis, cell wall biosynthesis, vacuolar sorting as well as components of the ERAD pathway (Mori *et al.*, 1992; 1998; Cox & Walter, 1996; Sidrauski *et al.*, 1996; Casagrande *et al.*, 2000; Friedlander *et al.*, 2000; Ng *et al.*, 2000; Tavers *et al.*, 2000; Fewell *et al.*, 2001; Patil & Walter, 2001; Higashio & Kohno, 2002). Upon decrease of ER stress the cell returns to normal physiological conditions and expression of UPR target genes is reduced (Merksamer *et al.*, 2008; Papa, 2012). If the UPR fails to achieve cellular homeostasis, prolonged UPR induction leads to apoptosis (Jäger *et al.*, 2012). While in *S. cerevisiae* only the Ire1p pathway is known, in mammalian cells three arms of the UPR mediated by IRE1 (yeast Ire1p homologue), ATF6 (activating transcription factor-6) and PERK (protein kinase RNA (PKR)-like ER kinase), respectively, have been identified (Niwa *et al.*, 1999; Lee *et al.*, 2002; Schröder & Kaufmann, 2005; Bernales *et al.*, 2006).

The UPR and ERAD are interconnected processes (Casagrande *et al.*, 2000; Friedlander *et al.*, 2000; Ng *et al.*, 2000; Travers *et al.*, 2000). While the induction of the UPR is required for efficient ERAD, defects or reduction in ERAD induce the UPR to ensure cell viability (Casagrande *et al.*, 2000; Ng *et al.*, 2000; Spear & Ng, 2003). Furthermore, defects in both processes are synthetically lethal, although neither of them is essential (Zhou & Schekman, 1999; Travers *et al.*, 2000)

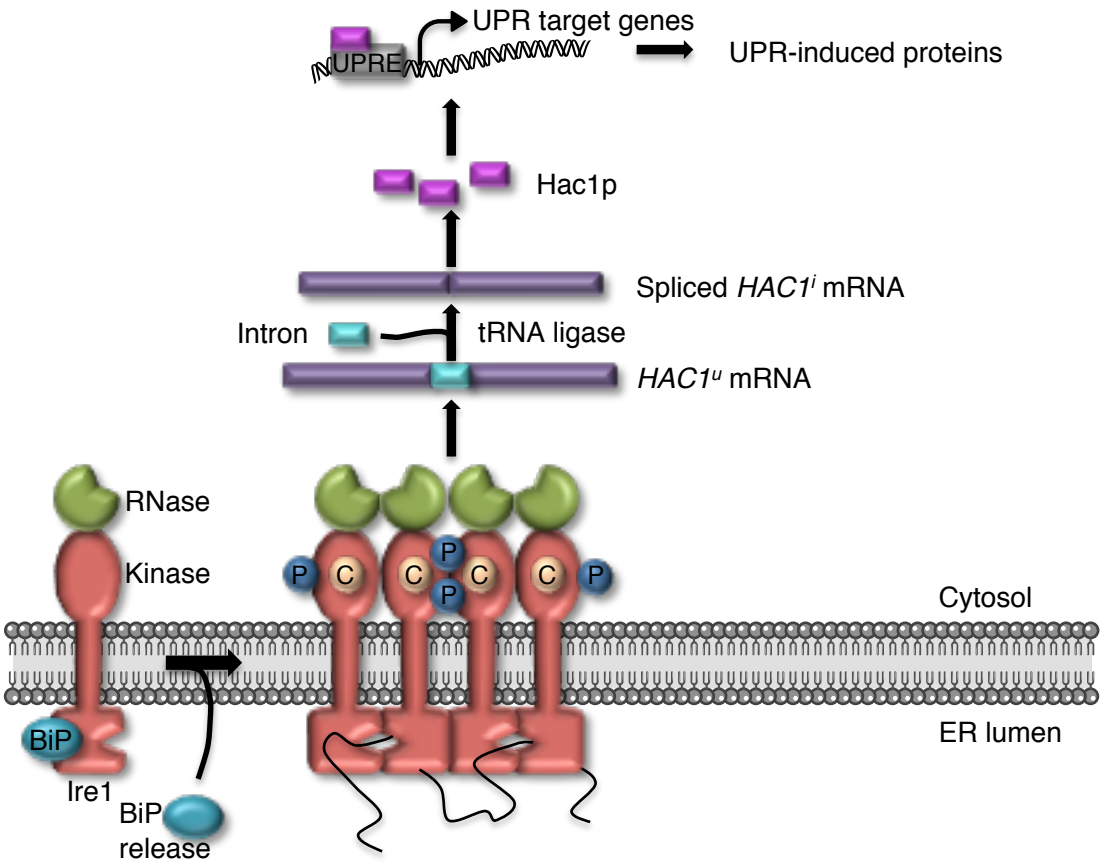

Figure 1.4.1. The *S. cerevisiae* Unfolded Protein Response. Start = LEFT**:** The ER-membrane protein Ire1p remains as inactive monomers under normal physiological conditions due to binding of the ER chaperone BiP (Kar2p). The UPR is induced under ER-stress conditions (i.e. when misfolded proteins accumulate in the ER). This leads to the titration of BiP off Ire1p (or direct binding of the misfolded protein species to Ire1p). This enables Ire1p monomers to form dimers and higher-order oligomers, which then undergo trans-autophosphorylation. Thus activated Ire1p together with tRNA ligase is involved in the translation of the transcription factor Hac1p by excising a translation inhibitory intron from the *HAC1* mRNA (*HAC1*^{u}). Splicing of *HAC1* mRNA leads to the formation of two exons, which are ligated by tRNA ligase. Translation of the resulting *HAC1*^{i} mRNA leads to the translation of the TF Hac1p. Hac1p enters the nucleus where it binds to the UPRE in the promoter region of UPR target genes thereby up-regulating their expression. Translation of UPR-induced proteins increases the folding capacity of the ER by remodeling the secretory pathway in such a way that it enables the cell to cope with the misfolded protein overload. The normal physiological conditions of the cell are regained by the reduction of misfolded proteins in the ER. (P: phosphorylation of the kinase domains; C: kase-binding cofactors; adapted from Ron & Walter, 2007; Korennykh & Walter, 2012).

1.5 THE UBIQUITIN PROTEASOME SYSTEM

In eukaryotes, the ubiquitin proteasome system (UPS) is the key mechanism for the regulated intracellular degradation of proteins (Wang & Maldonado, 2006). The UPS is a complex system that is interconnected with a broad range of cellular processes such as cell cycle control, DNA repair, transcription, signal transduction etc. (Ciechanover, 1998; Hicke, 2001; Weissman, 2001). It is essential as it helps maintaining cellular protein homeostasis, which, if disturbed, can lead to a variety of disorders such as neurodegenerative, cardiovascular and oncogenic disorders (Hershko & Ciechanover, 1998; Nandi *et al.*, 2006). Tight regulation of the UPS is vital for cellular maintenance (Varshavsky, 2005). As part of the protein quality control, the UPS is especially important for the regulated degradation of defective proteins, including proteins that are misfolded, denatured, incomplete or oxidized. Those or otherwise damaged proteins tend to accumulate and form aggregates which are toxic to the cell (Ciechanover & Brundin, 2003; Chandu & Nandi, 2002, 2004).
The two major players of the UPS are ubiquitin (ref. 1.5.1) and the 26S proteasome (ref 1.5.2). In eukaryotes, both are abundant in the nucleus as well as in the cytosplasm (Glickman *et al.*, 1998a; Pickart, 2001; Weissman, 2001; Pickart & Cohen, 2004). The degradation of proteins by the UPS involves two tightly regulated, consecutive steps: During the first step, the ubiquitination, ubiquitin molecules are covalently attached to a UPS substrate. The second step involves the recognition and degradation of the substrate by the 26S proteasome (Hershko & Ciechanover, 1998; Chandu & Nandi, 2002, 2004; Ciechanover & Brundin, 2003).

1.5.1 UBIQUITIN AND UBIQUITINATION

In eukaryotes, some proteins destined for proteasomal degradation are ubiquitinated (Rock *et al.*, 1994). During ubiquitination, the small protein modifier ubiquitin (Ub) is covalentely conjugated to a lysine residue in the substrate (Glickman & Ciechanover, 2002; Pickart, 2004). The addition of further Ub moieties leads to the formation of polyubiquitin chains (Hartmann-Petersen & Gordon, 2004; Pickart & Eddins, 2004; Kerscher *et al.*, 2006). Substrates containing a chain of at least four Ubs are recognized by the 26S proteasome for degradation (Elsasser & Finley, 2005).
Ubiquitin is a highly conserved protein of about 76 residues ubiquitously expressed in eukaryotes (Ciechanover *et al.*, 1978; Wilkinson *et al.*, 1980; Pickart, 2000; Wolf, 2011). It belongs to the ubiquitin protein family, a family of structurally conserved protein modifiers which all regulate essential functions (Petroski, 2008; Wickliffe *et al.*, 2009). Although different in sequence all members of this protein family share one structural feature, the so-called ubiquitin fold (β-grasp fold), and the same biochemical mechanism, i.e. the formation of an isopeptide bond between the terminal glycine of the protein modifier and an amino group of the target protein (Burroughs *et al.*, 2007). Other ubiquitin-like modifiers (UBL), found in all eukaryotes, are NEDD8 (neuronal-precursor-cell-

expressed developmentally down-regulated protein-8; Rub1 in *S. cerevisiae*) and SUMO (small ubiquitin-like modifier) (Kumar *et al.*, 1993; Rao-Naik *et al.*, 1998; Bayer *et al.*, 1998; Whithy *et al.*, 1998; Kerscher *et al.*, 2006).

During ubiquitination mono- or polyubiquitin chains are covalently attached to the target protein. This process is ATP-dependent (Ciechanover *et al.*, 1980; Pickart, 2001; Weissman 2001; Ciechanover & Iwai, 2004). There are various possible linkages in a polyubiquitin chain. Of the 7 lysines in ubiquitin (K6, K11, K27, K29, K33, K48, K63), K11, K29, K48 and K63 have been shown to form polyubiquitin chains *in vivo*, with G76-K48 linked polyubiquitin chains of at least four ubiquitins being the best understood type of chain serving as the predominant signal for proteasomal degradation (Chau *et al.*, 1989; Dubiel & Gordon, 1999; Thrower *et al.*, 2000; Weissman, 2001; Pickart & Fushman, 2004; Windheim *et al.*, 2008; Keating & Bowie, 2009). K29, K11 and even K63 linkages, however, have also been suggested to be competent for proteasomal degradation (Baboshina & Haas, 1996; Koegl *et al.*, 1999; Jin *et al.*, 2008; Hofman & Pickart, 2001; Kim *et al.*, 2007; Saeki *et al.*, 2009). Less is known about the function of otherwise linked polyubiquitin chains.

Ubiquitination involves three steps, which are mediated by three sets of enzymes: ubiquitin-activating (E1), ubiquitin-conjugating (E2) and ubiquitin-ligating (E3) enzymes (Hershko *et al.*, 1983). During the first step, an E1 enzyme activates the C-terminal glycine (G76) of ubiquitin in an ATP-dependent manner, resulting in the formation of a ubiquitin-adenylate intermediate (Haas & Rose, 1982). A thioester linkage is formed between the C-terminal carboxyl group of ubiquitin and the sulfhydryl group of the E1 active site cysteine (Jentsch, 1992). The second step is mediated by an E2, catalyzing the transfer of ubiquitin from the E1 to the E2 active site cysteine. This leads to the formation of a thioester between the E2 and ubiquitin (E2-Ub) (Jentsch, 1992). Finally, upon interaction with E2-Ub, an E3 ubiquitin ligase mediates the transfer of ubiquitin to the target protein. During this last step, an isopeptide bond is formed between a lysine (ε-amino group) in the target protein and the C-terminal glycine of ubiquitin (Hershko *et al.*, 1983; Pickart 2001).

There are two main types of E3 ubiquitin ligases in eukaryotes: RING (really interesting new gene) ubiquitin ligases and HECT (homologous to E6-associated protein carboxy terminus) ubiquitin ligases, containing the C-terminal RING or the HECT domain, respectively (Freemont *et al.*, 1991; Wang & Pickart, 2006; Deshaies & Joazeiro, 2009). HECT E3s use a cysteine residue within the HECT domain as acceptor for ubiquitin from the E2, leading to the formation of a thioester between ubiquitin and the HECT E3. The ubiquitin is then transferred to the substrate (Huibregtse *et al.*, 1995; Scheffner *et al.*, 1995; Wang & Pickart, 2005). RING E3 enzymes contain the RING domain (conserved cysteine- and histine-rich motif), which coordinates zinc ions (Freemont *et al.*, 1991; Lorick *et al.*, 1999). Unlike HECT E3s, RING E3s do not form thioesters with ubiquitin; they bring ubiquitin-associated E2s close to the substrate and thus mediate the ubiquitin transfer (Deshaies & Joazeiro, 2009). The ERAD E3 ligases Hrd1p and Doa10p belong to the family of RING E3 ligases (Bordallo *et al.*, 1998; Bays *et al.*, 2001, Ravid *et al.*, 2006; Sato *et al.*, 2009; Carvalho *et al.*, 2010).

For RING E3 ligases there are two modes by which polyubiquitination of substrates can be mediated: Polyubiquitin chains either form sequentially or are added en bloc to the substrate (Deshaies & Joazeiro, 2009; Pierce *et al.*, 2009). During the first mode, single ubiquitin molecules associated with an E2 are added sequentially to the substrate (Eletr *et al.*, 2005; Deshaies & Joazeiro, 2009). After the transfer the E2 dissociates from the E3 enabling another E2-Ub moiety to associate with the E3, enabling the transfer of the next Ub to the substrate (Deshaies & Joazeiro, 2009). In the second mode polyubiquitin chains preassemble on the E2 and are then tranferred to the target protein (Hershko, 1983; Komitzer & Ciechanover, 2000; Li *et al.*, 2007; Ravid & Hochstrasser, 2007). An additional class of enzymes, the E4s, has been described to be involved in polyubiquitin chain elongation (Hoppe, 2005).

Deubiquitination is a highly regulated process also involved in many cellular processes such as DNA repair and proteasomal protein degradation. Deubiquitinating enzymes (DUBs), which are cysteine proteases or metalloproteases, catalyze the removal of ubiquitin from proteins (Nijman *et al.*, 2005; Reyes-Turcu *et al.*, 2009). During the UPS, DUBs are essential for ubiquitin recycling, generation of monoubiquitin from polyubiquitin chains, activation of ubiquitin precursors as well as reversal of ubiquitination (Deshaies & Joazeiro, 2009).

1.5.2 THE 26S PROTEASOME

The most downstream executive component of the UPS is the 26S proteasome, a multi-protein complex of about 2.5 MDa in eukaryotes, highly conserved from archaea to eukaryotes (Hershko & Ciechanover, 1998; Wolf & Hilt, 2004; Hanna & Finley, 2007; Tomko & Hochstrasser, 2011). In *S.cerevisiae* the majority of 26S proteasomes are associated with the ER and the nuclear envelope whereas the remaining pool is free in the cytosol and nucleoplasm (Enenkel *et al.*, 1998). As the central protease in the cell the 26S proteasome is confronted with a large number of substrates that are destined for degradation (Voges *et al.*, 1999). The assembly of this multi-protein enzyme needs to be tightly controlled in order to maintain its sophisticated structure and function (Bedford *et al.*, 2010). The 26S proteasome plays a vital role during the degradation of ER-dislocated misfolded proteins (Voges *et al.*, 1999; Finley, 2009; Murata *et al.*, 2009). The 26S proteasome not only degrades polyubiquitinated misfolded proteins, but also proteins with a short half-life and otherwise defective proteins (Hershko *et al.*, 2000). Substrates can be delivered to the 26S proteasome via different pathways using different types of ubiquitin chains and other modifications (ref. 1.5.1; Rock & Goldberg, 1999: Voges *et al.*, 1999; Elsasser & Finley, 2005; Finley, 2009). In eukaryotes, the proteasome consists of at least 33 subunits (*S. cerevisiae*), which assemble into two subcomplexes, the 19S regulatory particle (RP) and the 20S core particle (CP) (ref. Figure 1.5.2.1; Peters *et al.*, 1993; Wolf & Hilt, 2004; Hanna & Finley, 2007; Murata *et al.*, 2009; Bedford *et al.*, 2010). The 20S CP is the 670 kDa barrel-shaped subcomplex, which harbours the proteolytically active sites inside

its cavity (ref. 1.5.2.1; Larsen & Finley, 1997; Glickman *et al.*, 1998a; Kunjappa & Hochstrasse, 2014). The 900 kDa 19S RP plays important roles during the recognition of ubiquitinated proteins (ref. 1.5.2.2). It also directs them into the 20S CP central channel for degradation (Groll *et al.*, 2000; Verma *et al.*, 2000; Finley *et al.*, 2002; Liu *et al.*, 2002). The 26S holoenzyme consists of one 20S CP and either one or two 19S RP at either side of the 20S CP (Peters *et al.*, 1993; Groll *et al.*, 1997; Tomko & Hochstrasser, 2011). The 26S proteasomes are highly dynamic structures that undergo various conformational changes during the degradation process (Bedford *et al.*, 2010). The 19S RP AAA-ATPases have been suggested to undergo conformational changes during ATP binding and hydrolysis which are crucial for substrate unfolding and translocation into the 20S CP (ref. 1.5.2.2; Babbitt *et al.*, 2005; Horwitz *et al.*, 2007; Kriegenburg *et al.*, 2008; Finley, 2009). The 19S RP may act in a similar way during the extraction of misfolded proteins from the ER (Lee *et al.*, 2004a, 2004b; Ng *et al.*, 2007).

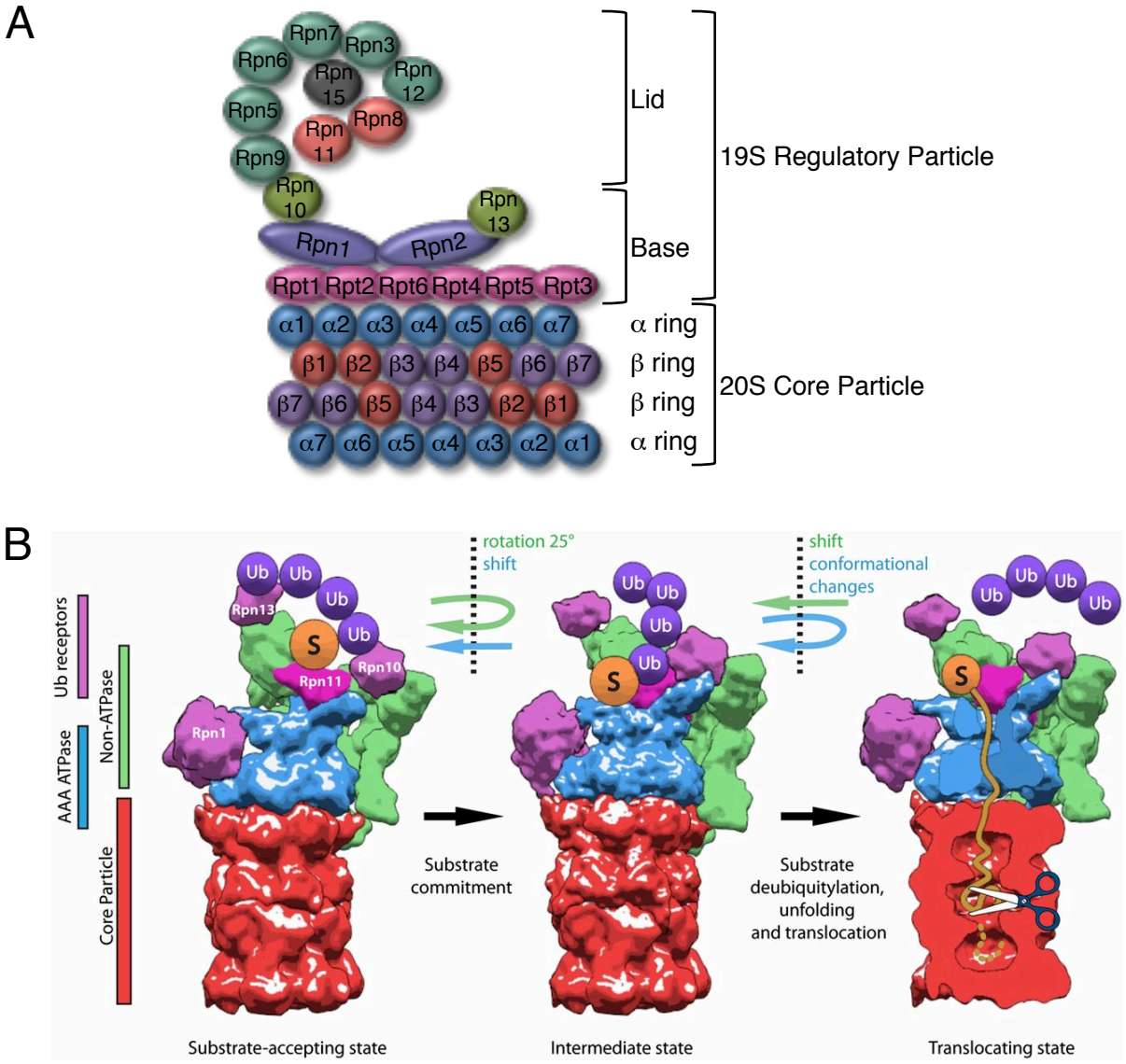

Figure 1.5.2.1. The 26S proteasome. (A) Schematic representation of the 26S proteasome, consisting of the 20S CP and one or two (not shown) 19S RP. The 20S CP consists of two outer hetero-heptameric alpha-rings and two inner hetero-heptamieric beta-rings. The subunits β1, β2 and β5 (red) harbour the proteolytic avtivity. The 19S RP can be further divided into the base (Rpt1-6, Rpn1, 2, 10 and 13) and the lid (Rpn3, 5-9, 11, 12 and 15). Proteasome cyclosome (PC) repeat containing subunits (purple), Mpr1 and Pad1 in the N terminus (MPN) domain containing subunits (red), proteasome-COP9-eIf3 (PCI) domain containing subunits (dark green) and Ub receptros (light green) are indicated (adapted from Ichihara, 2010). (B) Substrate degradation model. (I) Polyubiquitylated substrates (S) are recruited to the Ub receptors Rpn10 and Rpn13 (LEFT). (II) During the commitment step substrates are bound more tightly to the 26S proteasome by the AAA-ATPases (CENTER). (III) Substrates are further transferred to Rpn11 where deubiquitylation occurs prior to protein unfolding in the upper AAA-ATPase cavity. Unfolded substrates are translocated into the 20S CP cavity for degradation (Lasker *et al.*, 2012; taken from Unverdorben *et al.*, 2014).

1.5.2.1 THE 20S CORE PARTICLE

The 20S proteasome CP is highly conserved among various organisms (Groll *et al.*, 1997; Dahlmann *et al.*, 1999; Unno *et al.*, 2002; Groll *et al.*, 2005). It is composed of a stack of four heteroheptameric rings, two outer α-rings and two inner β-rings (Groll *et al.*, 1997). Each type of ring is formed by seven related α- or β-subunits, respectively (stack arrangement: α1-7; β1-7; β1-7; α1-7; ref. Figure 1.6.2.1; Baumeister *et al.*, 1998). While the α-rings serve as docking domains for the 19S RP, the β-rings harbour the proteolytically active sites β1, β2 and β5 (Baumeister *et al.*, 1998; Smith *et al.*, 2007). The three subunits display caspase-like (cleaving after acidic residues), trypsin-like (cleaving after basic residues) and chymotrypsin-like (cleaving after hydrophobic residues) activity, respectively (Groll *et al.*, 1997; Baumeister *et al.*, 1998; Voges *et al.*, 1999; Kisselev *et al.*, 2006; Sharon *et al.*, 2006). The catalytic sites, located inside the 20S cavity to prevent unspecific degradation, degrade substrates into short peptides that range from 4 to 25 amino acids in length (Chen & Hochstrasser, 1996; Heinemeyer *et al.*, 1997). These peptides are further processed by cellular peptidases into amino acids, which are then recycled by the cell (Lowe *et al.*, 1995; Groll *et al.*, 1997; Kisselev *et al.*, 1999; Unno *et al.*, 2002). Substrates enter the 20S cavity through the so-called gate, which is composed of the N-termini of the α-subunits close to the ends of the barrel (Groll *et al.*, 2000). In yeast, engagement of the proteolytic sites stabilizes the whole 26S complex (Ferrell *et al.*, 2000; Groll *et al.*, 2000). In yeast as well as in humans, the assembly of the 20S CP is a largely conserved process and can take place independently of the 19S RP, or associated with other regulators (Velichutina *et al.*, 2004; Hirano *et al.*, 2006, 2008; Kusmierczyk *et al.*, 2008; Yashiroda *et al.*, 2008; Murata *et al.*, 2009; Bedford *et al.*, 2010).

1.5.2.2 THE 19S REGULATORY PARTICLE

The 19S RP consists of 19 proteins and plays a vital role not only for substrate recognition but also for gate opening so that the interior of the 20S CP is accessible for degradation (Glickman *et al.*, 1998a; Braun *et al.*, 1999; Liu *et al.*, 2002, 2003; Jung & Grune, 2007). The 19S RP is crucial for accepting ubiquitinated substrates, as well as for the deubiquitination and unfolding of degradation substrates (Hershko *et al.*, 1984; Hough *et al.*, 1986; Braun *et al.*, 1999; Liu *et al.*, 2002). The 19S RP can be further divided into two subcomplexes, the lid and the base (ref. Figure 1.5.2.1; Glickman *et al.*, 1998a, 1998b). The base subcomplex consists of six AAA-type ATPases (ATPases Associated with a variety of cellular Activities), Rpt1-6 (Rpt: Regulatory Particle AAA-ATPase), the only ATP-hydrolyzing proteins in the 19S RP, and the four non-ATPase proteins Rpn1, Rpn2, Rpn10 and Rpn13 (Rpn: Regulatory Particle Non-AAA-ATPase) (Lucero *et al.*, 1995; Fujimuro *et al.*, 1998; Glickman *et al.*, 1998a, 1999). The lid subcomplex contains the rest of the Rpn subunits (Rpn3,

Rpn5, Rpn6, Rpn7, Rpn8, Rpn9, Rpn11, Rpn12 and Rpn15) (Beyer, 1997; Finley *et al.*, 1998; Patel & Latterich, 1998; Liu *et al.*, 2002; Lasker *et al.*, 2012).

The six AAA-ATPases (order: Rpt1, Rpt2, Rpt6, Rpt3, Rpt4, Rpt5) in the 19S RP base belong to the Walker family of ATPases containing the A (ATP binding) and B motif, two conserved elements (Walker *et al.*, 1982). These proteins within the 19S RP form a hexameric ring stacked on top of the heptameric ring in the 20S CP (Nandi *et al.*, 2006; Finley *et al.*, 2009; Förster *et al.*, 2009; Zhang *et al.*, 2009). The Rpt subunits are important for substrate unfolding, 20S CP gate opening and substrate translocation to the 20S CP (Djuranovic *et al.*, 2009; Zhang *et al.*, 2009; Tomko *et al.*, 2010). Gate opening is mediated by the docking of the C-termini of the AAA-ATPases into the pockets created between the α-subunits of the 20S CP (Smith *et al.*, 2007). Rpt 2, Rpt3, and Rpt5 are especially interesting, as their C-termini have been suggested to open the gate of the 20 CP (Smith *et al.*, 2007). For Rpt2 and Rpt3 it has been shown that their C-termini, containing an HbYX (hydrophobic-tyrosine-X*)* motif, are located in the pockets between the 20S CP subunits α3/α4 and α1/α2, respectively (Lasker *et al.*, 2012). The HbYX motif has been shown to induce opening of the gate (Smith *et al.*, 2007; Tian *et al.*, 2011; Lasker *et al.*, 2012). Rpt5 also contains the HbYX motif, but its C-terminus is more flexible and able to occupy pockets α5/α6 or α6/α7 (Lakser *et al.*, 2012).

The Rpn subunits located in the 19S RP lid and base mediate substrate recognition and transfer to the 20S CP (Deveraux *et al.*, 1994; Lam *et al.*, 1997; Lasker *et al.*, 2012). In general, the Rpn subunits can be divided into four groups: (1) proteasome cyclosome (PC) repeat-containing subunits (Rpn1 and Rpn2), (2) Mpr1 and Pad1 in the N-terminus (MPN) domain.containing subunits (Rpn8 and Rpn11), (3) proteasome-COP9-eIf (PCI) domain-containing subunits (Rpn3, Rpn5, Rpn6, Rpn7, Rpn9 and Rpn12) and (4) Ub receptors (Rpn10 and Rpn13) (Frank, 2006; Förster *et al.*, 2010; Lasker *et al.*, 2012). The Ub receptors Rpn10 and Rpn13 (non-essential in yeast) in the base have been described to be peripherally located in the 26S proteasome (van Nocker *et al.*, 1996; Seeger *et al.*, 2003; Husnjak *et al.*, 2008). Apart from the 19S RP Ub receptors, polyubiquitinated substrates can be recognized by shuttling Ub receptors like Dsk2 and Rad23 (Wilkinson *et al.*, 2001). They recognize polyubiquitinated substrates and bind them via their ubiquitin-associated domain (UBA) and bind to Rpn1, Rpn10 or Rpn13 at their ubiquitin-like domain (UBL) (Wilkinson *et al.*, 2001; Finley *et al.*, 2009). Rpn10 and Rpn13 are unrelated in structure and are only 90 Å apart, which is the size of a tetraubiquitin chain (Zhang *et al.*, 2009; Sakata *et al.*, 2011). This might explain why polyubiquitin chains have been suggested to be at least four ubiquitins long for the degradation signal to be fully active (Deveraux *et al.*, 1994; Piotrowski *et al.*, 1997; Lasker *et al.*, 2012). After the initial binding, the polyubiquitinated substrate is more tightly bound to the proteasome and via the coiled coils of the Rpt4/Rpt5 and Rpt1/Rpt2 dimers, located under Rpn10 and Rpn13 respectively, the substrate is further transferred within the proteasome for degradation (Perham, 2000; Peth *et al.*, 2010). It has been suggested that these coiled coils are flexible structures that undergo a swinging motion thereby scanning the space above for prospective substrates, binding them and eventually

exposing them to Rpn11 (Smith *et al.*, 2007; Sakata *et al.*, 2011). The movement might even mediate gate opening as the coiled coils are located above the Rpt subunits (Rpt2, Rpt3, Rpt5) whose C-termini open the gate (Lasker *et al.*, 2012). Rpn11 is located above the gate formed by the Rpt subunits and deubiquitinates degradation substrates before they are unfolded in the upper AAA-ATPase cavity and further translocated into the 20S CP where they are degraded (Smith *et al.*, 2007; Bohn *et al.*, 2010; Lasker *et al.*, 2012).

The non-ATPase subunits Rpn1 and Rpn2, also located in the 19S RP base, are homologous proteins displaying a toroid structure (Kajava, 2002; Effantin *et al.*, 2009; Lakser *et al.*, 2012). They have been suggested to act as a scaffold binding some proteasomal subunits as well as proteasome-associated proteins (Lupas *et al.*, 1997a; Elsasser *et al.*, 2002; Effantin *et al.*, 2009; Gomez *et al.*, 2011). Rpn1 is close to the Rpt1/Rpt2 dimer and has been suggested to be a very flexible structure, which recruits shuttling ubiquitin receptors and the deubiquitinating enzyme (DUB) Ubp6 which docks to the Leucine-rich repeats (LRRs) of Rpn1 (Wilkinson *et al.*, 2001; Elsasser *et al.*, 2002; Gomez *et al.*, 2011; Lasker *et al.*, 2012). Rpn2 makes contact with Rpt3/Rpt6 via its domain close to the 20S CP and also interacts with the Rpn8/Rpn11 dimer via a toroidal segment and Rpn13, Rpn12 and Rpn3 with its distal end (Kajava, 2002). Although the lid had been thought to be distal to the 20S CP, structural studies suggest that it flanks the side of the Rpt hexamer and even contact the 20S CP via the N-termini of Rpn6 and Rpn5 (ref. Figure 1.5.2.1; Glickman *et al.*, 1998b; Lakser *et al.*, 2012). The lid displays deubiquitination activity (Glickman *et al.*, 1998b; Verma *et al.*, 2002; Yao & Cohen, 2002). All six PCI-domain-containing subunits can be found in the 19S RP lid. They have been suggested to display a solenoid structure consisting of several bihelical repeats upstream of the PCI domain, which has been shown for Rpn6 (Fukunaga *et al.*, 2010; Lander *et al.*, 2012; Lasker *et al.*, 2012). All six subunits can be found in the same region of the 19S RP where they are arranged in a horseshoe-like manner (order: Rpn9/Rpn5/Rpn6/Rpn7/Rpn3/ Rpn12). The horseshoe covers a large part of the Rpt-ring and interacts with the Rpn8/Rpn11 dimer as well as Rpn2 and Rpn10 via its ends (Förster *et al.*, 2010; Pathare *et al.*, 2011; Lasker *et al.*, 2012). The PCI hexamer has been suggested to act as a scaffold for the AAA-ATPase ring, which is highly flexible in structure especially during the degradation process, as well as for Rpn11, which is held in position close to the opening of the AAA-ATPase ring (ref. Figure 1.5.2.1; Glynn *et al.*, 2009; Smith *et al.*, 2011; Lasker *et al.*, 2012). Another function proposed for the PCI hexamer is that of a shield against the AAA-ATPases in order to prevent uncontrolled degradation (Smith *et al.*, 2011; Lasker *et al.*, 2012).

In the 19S RP lid Rpn8 and Rpn11 form a heterodimer closely above the opening of the AAA-ATPase ring (Lasker *et al.*, 2012). Rpn11 displays deubiquitination activity, which can be attributed to the zinc-binding JAMM (JAB1/ MPN/Mov34 metalloenzyme) motif found within its MPN domain (Verma *et al.*, 2002; Yao & Cohen, 2002). Rpn11 acts in an ATP-dependent manner and is only active when the 19S RP is fully assembled (Verma *et al.*, 2002; Förster *et al.*, 2010). The functions

of some of the other lid subunits are yet to be elucidated (Glickman *et al.*, 1998b; Verma *et al.*, 2002; Hanna & Finley, 20008; Lakser *et al.*, 2012)

The 19S RP assembly is highly elaborate process involving four chaperones: Nas2 (human: p27), Nas6 (human: gankyrin/p28), Rpn14 (Human PAAF1) and Hsm3 (human S5b), which all differ in structure and do not display distinct enzyme activity (Schultz *et al.*, 1998, Verma *et al.*, 2000; Park *et al.*, 2005; Dawson *et al.*, 2006; Letunic *et al.*, 2009). It is very likely that chaperones involved in 19S RP assembly prevent premature interactions of the subunits, e.g. binding of Rpt subunits to the 20S CP (Kaneko *et al.*, 2009; Roelofs *et al.*, 2009; Saeki *et al.*, 2009; Tomko & Hochstrasser, 2011). In concert with the 20S CP, acting as a scaffold during 19S RP assembly, chaperones might regulate 20S CP-Rpt interaction (Park *et al.*, 2009; Roelofs *et al.*, 2009; Bedford *et al.*, 2010). The role of the chaperones during this process requires further investigation, especially as there might be more than one pathway possible for 26S assembly (Hendil *et al.*, 2009; Kaneko *et al.*, 2009; Roelofs *et al.*, 2009; Saeki *et al.*, 2009; Thompson *et al.*, 2009).

1.6 ER-ASSOCIATED DEGRADATION

As misfolded secretory proteins are toxic it is essential for proper cellular function that these are recognized by the ERQC (ref. 1.3.2) and degraded by the UPS (ref. 1.5) (Kostova & Wolf, 2003; Aebi *et al.*, 2010; Stolz & Wolf, 2010). ERAD, apart from vacuolar (lysosomal) degradation, is the major degradation pathway for secretory proteins (Hiller *et al.*, 1996; Sommer & Wolf, 1997; Brodsky & McCracken, 1999). ERAD involves the recognition of misfolded proteins by the ERQC, their retrotranslocation into the cytosol, ubiquitination and degradation by the 26S proteasome (Hiller *et al.*, 1996; Sommer & Wolf, 1997; Brodsky & McCracken, 1999). Through extensive studies, especially in yeast, a lot of components of ERAD have been identified (Pilon *et al.*, 1997, 1998; Plemper *et al.*, 1997, 1998, 1999a, 1999b; Römisch, 2005). In yeast there are three ERAD pathways, depending on the location of the lesion within the protein: ERAD-C (lesion in cytoplasmic domain), ERAD-L (lesion in luminal domain, either of soluble or membrane protein) and ERAD-M (lesion in membrane-spanning domain) (Vashist & Ng, 2004; Carvalho *et al.*, 2006; Denic *et al.*, 2006). Either one of two multi-protein complexes, built around ER-resident E3 ligases, the Doa10p complex or Hrd1p/Der3p complex, are involved in the three pathways (ref. Figure 1.6.1; Deshaies & Joazeiro, 2009). Both ligases, Hrd1p and Doa10p, belong to the RING domain E3 ubiquitin ligases (ref. 1.5.1; Bordallo *et al.*, 1998; Carvalho *et al.*, 2006; Kreft *et al.*, 2006; Deshaies & Joazeiro, 2009). The ERAD-C pathway is mediated by the Doa10p complex (Bordallo *et al.*, 1998; Bays *et al.*, 2001; Deak & Wolf, 2001). ERAD-C substrates are first recognized by the Hsp70/Hsp40 chaperones Ssa1p, Ydj1p and Hlj1p in the cytosol, followed by their degradation by the Doa10p complex (Bukau & Horwich, 1998; Zhang *et al.*, 2001, Huyer *et al.*, 2004b). Associated with the Doa10p complex are the E2 enzymes (ref. 1.5.1) Ubc7p and Ubc6p (Biederer *et al.*, 1997; Hampton, 2002; Vashist & Ng,

2004). While Ubc6p is anchored to the ER membrane, Ubc7p is soluble and requires Cue1p as binding partner to recruit Ubc7p to the ER-membrane (Biederer *et al.*, 1997). ERAD-C substrate ubiquitination is then mediated by the E3 ligase Doa10p (Vashist & Ng, 2004; Carvalho *et al.*, 2006).
Substrate ubiquitination of the ERAD-L and ERAD-M pathway is mediated by the Hrd1p ligase of the Hrd1p complex (Bays *et al.*, 2001; Deak & Wolf, 2001). The ERAD-L pathway has been proposed to be less complex compared to ERAD-C (Carvalho *et al.*, 2006; Willer *et al.*, 2008; Eisele *et al.*, 2010). ERAD-L substrates are recognized by ER Hsp70/Hsp40 chaperones Kar2p, Jem1p, Scj1p (Brodsky *et al.*, 1999; Youker *et al.*, 2004; Nishikawa *et al.*, 2005; Eisele *et al.*, 2010). Also involved in ERAD-L substrate recognition are Pdi1p, which also has chaperone-like activity, the lectin Yos9p as well as the ER-lumenal domain of the membrane-anchored protein Hrd3p (ref. 1.3.2.1; Plemper *et al.*, 1999a; Gardner *et al.*, 2000; Clerc *et al.*, 2009). Apart from interacting with ERAD substrates, Hrd3p is necessary to stabilize the E3 ligase Hrd1p (Gardner *et al.*, 2000). Other components of the Hrd1p complex during ERAD-L are the E2 enzyme Ubc7p bound to Cue1p, and the membrane proteins Usa1p and Der1p (Biederer et al., 1997; Hampton, 2002; Vashist & Ng, 2004). Usa1p has been shown to be involved in the oligomerization of the Hrd1p complex and to mediate the link between Der1p and the complex (Carvalho *et al.*, 2006; Denic *et al.*, 2006). The precise role of Der1p is still unknown (Knop *et al.*, 1996a; Hitt & Wolf, 2004; Horn *et al.*, 2009).
ERAD-M is less well understood than the other two pathways, but substrates of this pathway use the Hrd1p complex as well (Vembar & Brodsky, 2008; Ruggiano *et al.*, 2014). No chaperone involvement in ERAD-M is known, which might be possible as misfolded proteins could be recognized directly by the E3 ligase in the ER membrane (Sato *et al.*, 2009; Ruggiano *et al.*, 2014). ERAD-M, however, shares most Hrd1p complex components with the ERAD-L pathway, apart from Usa1p and Der1p (Carvalho *et al.*, 2006).
The Cdc48p complex, consisting of Cdc48p, Npl4p and Ufd1p, acts in all three ERAD pathways (Rape *et al.*, 2001; Braun *et al.*, 2002; Rabinovich *et al.*, 2002; Ye *et al.*, 2001, 2003). The cofactor Ubx2p recruits the Cdc48p complex to the E3 ligases (Schuberth *et al.*, 2004). For the Cdc48 complex two roles have been proposed: as a segregase the Cdc48p complex recognizes and binds to ubiquitinated proteins at the ER membrane making them available for degradation by the 26S protasome by separating them from associated nonubiquitinated proteins (Rape *et al.*, 2001; Braun *et al.*, 2002). As a dislocase the Cdc48p complex has been proposed to extract ERAD substrates from the dislocon providing the energy required for the process (Ye *et al.*, 2001, 2003).
The central component of the Cdc48p complex is Cdc48p (yeast; mammals: p97) (Moir *et al.*, 1982). Cdc48p, a member of the AAA-ATPase family, is essential in eukaryotes (Moir *et al.*, 1982; Frohlich *et al.*, 1991; Wolf & Stolz, 2011). While for Cdc48p a role has been described in protein degradation, it is also involved in many cellular processes such as homotypic membrane fusion, cell cycle, transcriptional regulation and cell death (Woodman, 2003; Jentsch & Rumpf, 2007; Braun & Zischka, 2008; Meyer & Popp, 2008; Deichsel *et al.*, 2009; Wilcox & Laney, 2009; Barbin *et al.*, 2010).

Cdc48p is a homohexameric complex consisting of six protomers which are arranged around a central pore (Pye *et al.*, 2006). Each protomer contains one flexible N-terminal domain, two conserved AAA domains (D1 and D2) and one disordered C-terminal domain (Pye *et al.*, 2006). The AAA domains contain a Walker A and a Walker B motif each, which are necessary for nucleotide binding and hydrolysis, respectively (Briggs *et al.*, 2008). Although the exact function of Cdc48p remains unclear it has been suggested that nucleotide binding and hydrolysis results in a conformational change in the complex, which might be required for Cdc48p's function as a segregase (Dai & Li, 2001; Rape *et al.*, 2001; Braun *et al.*, 2002; Davies *et al.*, 2008).

Substrate-recruiting factors, which mainly bind to the N-terminal domain of Cdc48p, are thought to recognize Cdc48p substrates (Jentsch & Rumpf, 2007; Madsen *et al.*, 2009; Buchberger, 2010). The N-terminal domain of Cdc48p binds ubiquitin, with a preference for polyubiquitin with a K48 linkage, but it also was found to be involved in ubiquitin-independent pathways (Krick *et al.*, 2010). Cdc48p also associates with DUBs (deubiquitinating enzymes) such as Otu1, which (like Rpn11) mediate deubiquitination at the 26S proteasome (Rumpf & Jentsch, 2005).

Experimentally, it is, however, complicated to distinguish between a function of the Cdc48p complex as a dislocase or a segregase (Rape *et al.*, 2001; Braun *et al.*, 2002; Ye *et al.*, 2001, 2003). It is for instance not clear whether the substrates, which remain membrane-associated in Cdc48p complex mutants, are associated with the cytoplasmic face of the ER or reside in the ER lumen (Rape *et al.*, 2001). It is also not clear whether *in vitro* retrotranslocation assays, using permeabilized mammalian cells, indeed monitor extraction of the respective substrate from the ER membrane by Cdc48p and not its disaggregation on the cytoplasmic face of the ER by Cdc48p, as the half-life of the substrate is very short compared to the experimental conditions, complicating the interpretation of results (Wiertz *et al.*, 1996a; Shamu *et al.*, 1999; Ye *et al.*, 2001, 2003).

While Cdc48p has been suggested to bind to retrotranslocation intermediates in the dislocon, direct ERAD susbtrates to proteasomes and thus couple substrate extraction from the ER and degradation, the 19S RP proteasomal subunit is the only ERAD component for which an active role in ERAD substrate extraction has been demonstrated (Wiertz *et al.*, 1996a; Glickman *et al.*, 1998a; Rubin *et al.*, 1998; Braun *et al.*, 2002; Lee *et al.*, 2004a; Verma *et al.*, 2004). In *S. cerevisiae* the 19S RP is the only required cytosolic factor for the extraction of an ERAD-L substrate *in vitro* (ref. 1.5.2.2; Lee *et al.*, 2004a). Also, an association of the 19S RP and Sec61p has been demonstrated (Kalies *et al.*, 2005; Ng *et al.*, 2007).

Extracted ERAD substrates are deglycosylated by the N-glycanase Png1p (Suzuki *et al.*, 1998; Wang *et al.*, 2009). Ufd2p (E4 ligase activity) is involved in polyubiquitination, while adaptor proteins Rad23p and Dsk2p (UBA-UBL domain containing proteins) recognize proteins and shuttle them to the 26S proteasome (Koegl *et al.*, 1999; Funakoshi *et al.*, 2002; Rao & Sasaki, 2002; Medicherla *et al.*, 2004).

It has been suggested that all three ERAD pathways exist in mammals as homologues to all yeast

ERAD components have been identified (Lilley & Ploegh, 2004; Ye *et al.*, 2004; Carvalho *et al.*, 2006). There is also evidence that in mammalian cells additional pathways might operate since there are many more ER-resident E3 ligases (Carvahlo *et al.*, 2006; Deshaies & Joazeiro, 2009).

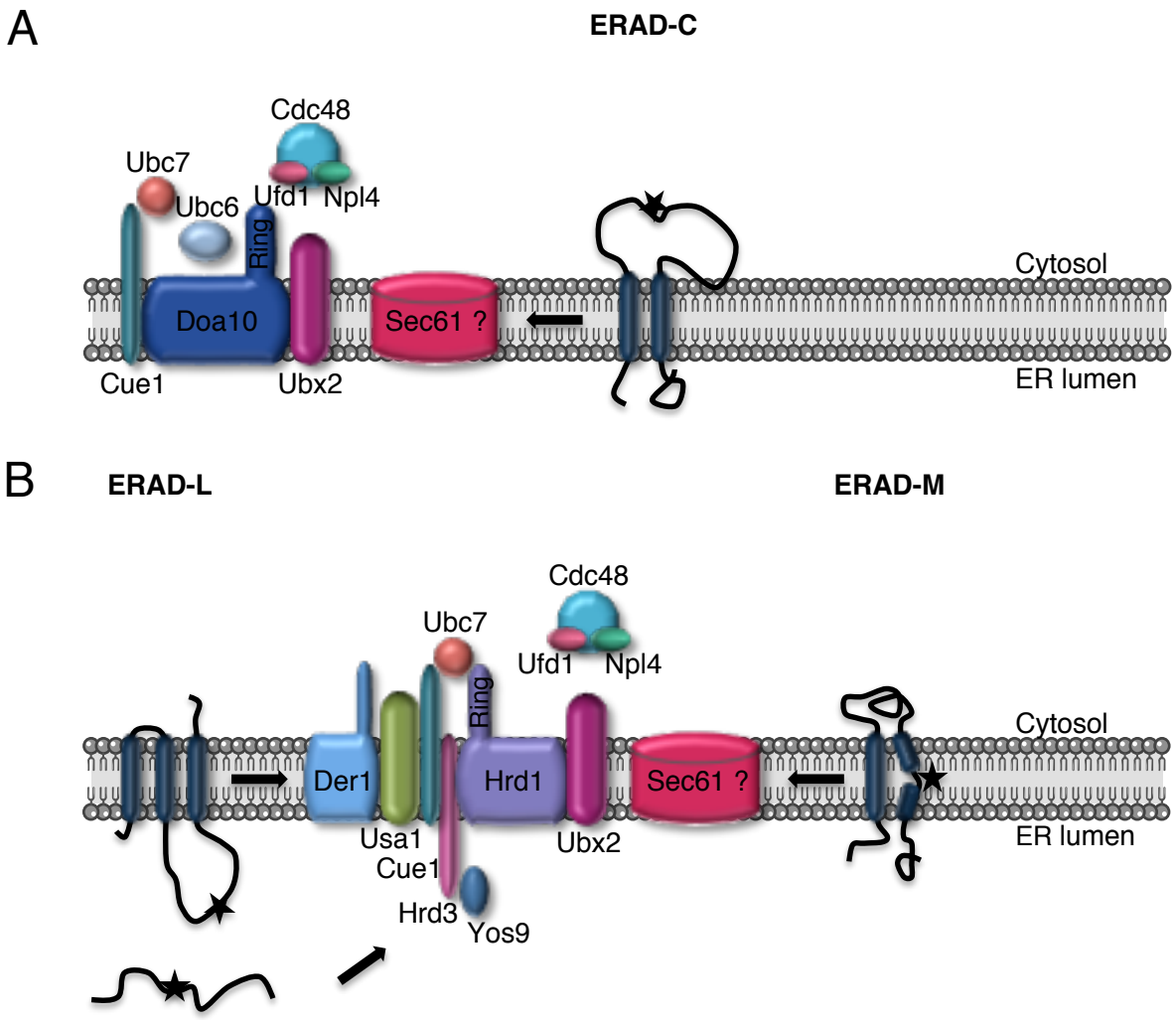

Figure 1.6.1. ERAD pathways in *S. cerevisiae*. (A) During ERAD-C membrane proteins with misfolded cytosolic regions are degraded via the Doa10p complex. Ubx2p, Cue1p, Ubc6p and Ubc7p as well as the Cdc48p/Npl4p/Ufd1p complex are further components during ERAD-C. Whether Sec61p forms the retrotranslocon during ERAD-C is still unclear. (B) Proteins with lumenal misfolded domains are degraded via the ERAD-L pathway. The Hrd1p/Hr3p complex formed by the Hrd1p E3 ligase and Hrd3p is the central component of ERAD-L. Also in the complex are Ubc7p and Cue1p as well as Der1p, Ubx2p and Usa1p. The lectin Yos9p interacts with Hrd3p and Kar2p (not shown) recruiting proteins destined for degradation by the Hrd1p/Hrd3p complex. Sec61p is believed to be part of the ERAD-L machinery. The Cdc48p/Npl4p/Ufd1p complex is also required for ERAD-L. Less is known about the ERAD-M pathway. Proteins with lesions within the membrane are degraded via this pathway,.which also conatins the Hrd1p/Hrd3p complex (adapted from Carvalho *et al.*, 2006)

1.6.1. THE DISLOCON

Since the components of the UPS are located in the cytosol, ERAD substrates need to be retrotranslocated from the ER into the cytosol through the so-called retrotranslocon (dislocon) prior to degradation (Jensen *et al.*, 1995; Ward *et al.*, 1995; McCracken & Brodsky, 1996; Wiertz *et al.*, 1996a). The nature of the retrotranslocon is still under debate, but several studies have suggested components of the protein import and ERAD machinery form the retrotranslocation channel (see below; Römisch, 2005; Nakatsukasa & Brodsky, 2008; Hampton & Sommer, 2012).

One candidate for the retrotranslocon is Sec61p, the same protein forming the protein import channel in the ER membrane (Rapoport *et al.*, 1996; Pilon *et al.*, 1997, 1998; Johnson & Haigh, 2000; van den Berg *et al.*, 2004; Römisch, 2005; Rapoport, 2007). Employment of the same channel for protein import as well as for protein export not only would mean an economical solution for the cell, several genetic and biochemical studies have given strong evidence that Sec61p forms or is part of the retrotranslocon (Wiertz *et al.*, 1996b; Pilon *et al.*, 1997, 1998; Plemper *et al.*, 1997; Johnson & van Waes, 1999, Wilkinson *et al.*, 2000; Schäfer & Wolf, 2009). For Sec61p a switch from import to export mode has been suggested, the respective binding partner triggering this switch, however, have not been elucidated so far (Wiertz *et al.*, 1996b; Johnson & Haigh, 2000). Further, due to the fact that Sec61p is encoded by an essential gene (*SEC61*) studies using a *Δsec61* null mutant cannot be performed (Stirling *et al.*, 1992). Moreover, the central role of Sec61p during the initial translocation of ERAD substrates into the ER (i.e. *sec61* mutants defective in ERAD also display defects in protein import into the ER) complicates the analysis/interpretation of degradation kinetics (Rapoport *et al.*, 1996; Pilon *et al.*, 1997; 1998; Wilkinson *et al.*, 2000). Nevertheless, due to the line of strong evidence a role of Sec61p during retrotranslocation cannot be denied at least for ERAD-L substrates (see below; Pilon *et al.*, 1997, 1998; Römisch, 2005; Schäfer & Wolf, 2009).

Early studies in mammalian cells have shown that the major histocompatibility complex (MHC) class I heavy chain (HC) is rapidly degraded in cells expressing the human cytomegalovirus (HCMV) protein US11, suggesting that degradation is triggered by the viral protein (Wiertz *et al.*, 1996a). Another study from the same group demonstrated that the cytomegalovirus (CMV) protein US2 also triggers dislocation of MHC class I HC (Wiertz *et al.*, 1996b). In mammalian cells infected with HCMV, a MHC class I HC degradation intermediate, in a complex with US2, was found to associate with the Sec61 complex prior to degradation suggesting that retrotranslocation was through the same channel that also mediates protein import into the ER (Rapoport *et al.*, 1996; Wiertz *et al.*, 1996b). The two transmembrane ERAD substrates US2 and MHC class I HC were rapidly degraded in pulse-chase studies (Wiertz *et al.*, 1996b). Upon addition of a proteasome inhibitor in those experiments, a degradation intermediate of MHC class I HC accumulated in the cells and could be coimmunoprecipitated with Sec61p (Wiertz *et al.*, 1996b). The MHC class I HC degradation intermediate was also found to be associated with the proteasome, indicating that the Sec61 complex and the proteasome are closely linked (Wiertz *et al.*, 1996b). This study also demonstrated

that MHC class I HC are degraded even in normal cells when the protein fails to fold properly, i.e. upon the addition of DTT, and that unfolded HC reassociates with the Sec61 complex (Wiertz *et al.*, 1996b).

Other early studies revealed that in wild-type cells not the whole Sec61p population is associated with the protein import machinery (Panzner *et al.*, 1995; Plemper *et al.*, 1997; Pilon *et al.*, 1998). It was stated that 30-50 % of Sec61p, although associated with the trimeric Sec61 complex, are not involved in protein import (Panzner *et al.*, 1995; Plemper *et al.*, 1997). Thus, a recruitment of this Sec61p pool fraction to ERAD has been suggested (Panzner *et al.*, 1995; Plemper *et al.*, 1997; Pilon *et al.*, 1998).

Genetic and biochemical studies using *sec61* mutants with mutation in TMD 3, TMD 4 and loop 7 of Sec16p, i.e. *sec61-41*, *sec61-32* and *sec61-3*, respectively, showed defects in secretory precursor import as well as in the degradation of the soluble misfolded protein Δgpαf in a cell-free system using yeast microsomes (Stirling *et al.*, 1992; Sommer & Jentsch, 1993; Pilon *et al.*, 1997, 1998). Crosslinking experiments revealed that the fully translocated ERAD substrate Δgpαf was associated with Sec61p prior to export and released upon initiation of export *in vitro*, supporting data that suggest Sec61p as the retrotranslocon and at the same time excluding an indirect effect due to Sec61p's role in import (Pilon *et al.*, 1997). Also, these mutants were conditional for protein import into the ER but defective for export at all temperatures tested (Pilon *et al.*, 1997).

Pulse-chase studies monitoring the degradation of the ERAD substrates CPY* and Pdr5* (C1427Y), the mutant plasma membrane ATP-binding cassette (ABC) transporter, in a *sec61-2* mutant demonstrated that retrotranslocation of the substrate was dependent on a functional Sec61p (Finger *et al.*, 1993; Biederer *et al.*, 1996; Plemper *et al.*, 1997; 1998). The *sec61-2* mutant is defective in the formation of retrotranslocons (Plemper *et al.*, 1997, 1998). Further, it has been shown that another components of the import machinery, Sec63p, is involved in ERAD of CPY* (Servas & Römisch, 2013).

In another genetic study by the same group, Sec61p was shown to functionally interact with Hrd3p, an ER membrane glycoprotein essential for ERAD, and the E3 ligase Hrd1p (Hampton *et al.*, 1996; Bordallo *et al.*, 1998; Plemper *et al.*, 1999a). Initially, pulse-chase and cycloheximide-chase analyses in a *Δhrd3* background revealed that the degradation of CPY* was slowed down and Hrd1p was rapidly degraded, respectively (Finger *et al.*, 1993; Plemper *et al.*, 1999a). It was therefore suggested that Hrd3p is needed for ERAD complex stability as in its absence Hrd1p is readily degraded via the UPS (Plemper *et al.*, 1999a). Further, suppression of Hrd1p degradation was observed in a *Δhrd3 sec61-2* double mutant supporting the idea that Sec61p is involved in retrotranslocation and degradation of Hrd1p (Plemper *et al.*, 1997; 1999a).

Crosslinking experiments using the export-deficient mutants *sec61-32* and *sec61-41* demonstrated that the misfolded secretory protein Δgpαf remained associated with PDI, a chaperone involved in ERQC (Gilbert, 1997; Gillece *et al.*, 1999). At the same time, *pdi1* mutants were deficient in export of

Δgpαf from yeast microsomes, indicating that PDI recognizes misfolded proteins and targets them to Sec61p (Gillece *et al.*, 1999).

Gillece and colleagues also could show that glycopeptide export requires Sec61p in a cell-free assay using yeast microsomes (Gillece *et al.*, 2000). Employing a cell-free assay using yeast microsomes, glycopeptide export was inhibited when Sec61 channels were blocked with ribosomes (Gillece *et al.*, 2000). Moreover, specific *sec61* alleles were defective in glycopeptide export. While mutants with strong import and ERAD defects for misfolded proteins, *sec61-32* and *sec61-41*, were only moderately defective in glycopeptide export, in *sec61* mutants, such as *sec61-2* and *sec61-8*, that only show minor defects in ERAD of misfolded proteins, glycopeptide export was severely impaired (Pilon *et al.*, 1997, 1998; Gillece *et al.*, 2000).

Experiments using mammalian microsomes saturated with RNC complexes, which block the Sec61 channel, have shown that these membranes are incompetent for the retrotranslocation of amyloid beta-peptide and cholera toxin from the ER into the cytosol, further supporting a role of Sec61p (Sec61α) during ERAD (Schmitz *et al.*, 2000; 2004).

An involvement of Sec61p especially in ERAD-L has been shown in several studies (Huyer *et al.*, 2004b; Sato *et al.*, 2006; Willer *et al.*, 2008; Schäfer & Wolf, 2009). In a series of pulse-chase studies it was shown that while CPY* degradation was slowed down in the *sec61-2* mutant, ERAD of Ste6p* (Q1249X), an integral membrane ERAD substrate depending on the E3 ligase Doa10p, was with wild-type kinetics (Huyer *et al.*, 2004b). While ERAD of Ste6p* did not depend on Sec61p it seemd to require its homologue Ssh1p (Huyer *et al.*, 2004b). ERAD of the mutant ABC transporter Pdr5*, which is structurally related to Ste6p*, however, depends on Sec61p (Plemper *et al.*, 1998). It therefore has to be taken into account that these results might result from different strain backgrounds or expression levels of the substrates. Degradation of another transmembrane ERAD substrate, Hmg2p, in *sec61-2* was with wild-type kinetics also suggesting that Sec61p is involved in ERAD-L rather than in the other ERAD pathways (Huyer *et al.*, 2004b; Sato *et al.*, 2006).

Another study demonstrated that antigen processing and antigen presentation by MHC class I molecules in dendritic cells, which has as a prerequisite the access of antigens to the ER and subsequently transport to the cytosol where degradation occurs, was drastically decreased when Sec61α levels were reduced by RNAi (Imai *et al.*, 2005). This finding strongly suggested that Sec61α is involved in retrotranslocation of antigens to the cytosol (Imai *et al.*, 2005).

Data from several studies also indicate that retrotranslocation and degradation by the proteasome act in concert, suggesting an association of Sec61p with the 26S proteasome (Wiertz *et al.*, 1996b; Bordallo *et al.*, 1998; de Virgilio *et al.*, 1998; Mayer *et al.*, 1998; Plemper *et al.*, 1998; Ng *et al.*, 2007). Studies from our lab, in collaboration with Jeff Brodsky, have shown that *in vitro* the 19S RP is sufficient for export of Δgpαf (Lee *et al.*, 2004b). Additional studies in collaboration with Kai Kalies have demonstrated direct binding of the 19S RP to the Sec61 channel and that proteasomes and ribosomes bind competitively to different sites on Sec61p (Lee *et al.*, 2004b; Kalies *et al.*, 2005; Ng

et al., 2007). Dependence of *in* vitro retrotranslocation of fluorescently labeled ΔgpαF on ATP and the proteasome has also been demonstrated using mammalian microsomes (Wahlman *et al.*, 2007).

A switch in transport directionality of Sec61p has been suggested for the retrotranslocaion of misfolded ERAD substrates (Plemper *et al.*, 1997, 1998, 1999a; Pilon *et al.*, 1998; Romisch, 1999; Meusser *et al.*, 2005). Such a change in transport directionality has also been suggested for the proteasomal degradation of apoliprotein B under ER stress, where the switch from import to export is triggered upon association with cytosolic chaperones (Pariyarath *et al.*, 2001; Fisher and Ginsberg, 2002; Oyadomari *et al.*, 2006).

Further evidence for Sec61p as a bi-directional translocation channel came form a study showing that Sec61p is required for ERAD of the two CPY* derivatives DPY* and OPY* and that degradation of those ERAD substrates is independent of import into the ER (Willer *et al.*, 2008). This study employed the degradation-defective *sec61-3* mutant. Cells of *sec61-3* were loaded with the two ERAD-L substrates at the permissive temperature, at which protein import and export were comparable to the wild-type (Willer *et al.*, 2008). ERAD was then monitored upon shifting the cells to 17 °C (Willer *et al.*, 2008). Defects in ERAD could thus not be attributed to any indirect effect due to disturbed import (Willer *et al.*, 2008).

In a more recent study in yeast, a physical contact between Sec61p and known ERAD components was investigated to support data from genetic and biochemical studies indicating interaction of Sec61p with those components (Hampton *et al.*, 1996; Plemper *et al.*, 1999a; Schäfer & Wolf, 2009). In order to circumvent the issues that coincide with the role of Sec61p as the biosynthetic translocon and to analyze only proteins that have been completely imported into the ER, immunoprecipitation experiments were performed with cells were treated with cycloheximide preventing the synthesis of new proteins (Schäfer & Wolf 2009). Sec61p could be immunoprecipitated with the Hrd1p-Der1p ligase complex (Schäfer & Wolf, 2009). Moreover, Sec61p was isolated with the ERAD-L substrate CPY* and it was further suggested that binding of CPY* to Sec61p is independent of the Hrd1p-Der1p ligase complex (Schäfer & Wolf, 2009).

Taken together, the data strongly suggest that Sec61p forms the dislocon or is at least part of the retrotanslocation channel. Several other studies, however, argue that Sec61p cannot be the retrotranslocon for all ERAD substrates, which is supported by studies that show an involvement in ERAD-L only (Huyer *et al.*, 2004b; Sato *et al.*, 2006; Willer *et al.*, 2008; Schäfer & Wolf, 2009).

While fluorescence quenching experiments have proposed that the ribosome-engaged translocon has a pore diameter of 40-60 Å, the crystal structure of the archaeal Sec61 complex homologue SecYEG has indicated a diameter of 10-12 Å (Hamman *et al.*, 1997; van den Berg et al., 2004; Osborne & Rapoport, 2007). Due to the latter finding some groups argue that the retrotranslocon would be too small to accommodate ERAD substrates (Fiebiger *et al.*, 2002; Tirosh *et al.*, 2003; Lilley & Ploegh, 2004). The crystal structure, however, does not provide data on flexibility of the translocon (Hamman *et al.*, 1997; Johnson & van Waes, 1999; Wirth *et al.*, 2003).

Although some studies suggest Ssh1p as an alternative retrotranslocon, data are inconclusive (Wilkinson *et al.*, 2001; Huyer *et al.*, 2004b). In yeast, Ssh1p is not required for export of glycopeptides and CPY*, at least in thie strain background used (Gillece *et al.*, 2000; Plemper *et al.*, 1997).

Data from *in vitro* studies have demonstrated that *sbh1* and *sbh2* mutants, which are not essential in yeast, are defective for import when both are deleted only at high temperature (Finke *et al.*, 1996). Export in a cell-free system has shown that *sbh1 sbh2* mutants are competent for ERAD (Römisch, 2005, unpublished data). Deletion of *SBH1* and *SBH2* did not affect CPY* steady-state levels (Plemper *et al.*, 1997).

Doa10p and Hrd1p are ER membrane resident E3 ligases involved in ERAD (ref. 1.5.1; Vashist & Ng, 2004; Carvalho *et al.*, 2006). Doa10p has 6 TMDs and is responsible for degradation of ERAD-C substrates (Bays *et al.*, 2001; Swanson *et al.*, 2001; Kreft *et al.*, 2006). Hrd1p has 4 TMDs and is involved in degradation of ERAD-L and ERAD-M substrates (Hampton *et al.*, 1996; Deak & Wolf, 2001). Especially for Hrd1p a role as the dislocon has been proposed due to the large number of hydrophilic residues in its transmembrane domains, leading to the idea that the E3 ligase, apart from its ubiquitination function, might be able to recognize mislocalized TMDs by their hydrophilic amino acids (Sato *et al.*, 2009). Also, interaction of multiple Hrd1p molecules, mediated by Usa1p, has been demonstrated, leading to the idea that a channel could be formed, which would be sufficient for retrotranslocation of ERAD substrates (Hom *et al.*, 2009). Pore formation, however, has not been demonstrated so far. Other studies have demonstrated that Hrd1p is sufficient for mediation of ERAD even in the absence of other ERAD components, such as Der1p, Hrd3p and Usa1p (Gardner *et al.*, 2000; Sato *et al.*, 2009; Carvalho *et al.*, 2010). These studies, however do not rule out a role of Sec61p by the use of e.g. ERAD-deficient *sec61* mutants (Gardner *et al.*, 2000; Carvalho *et al.*, 2010; Sato *et al.*, 2009). Crosslinking experiments using Hrd1p, which was modified with photocrosslinking residues at various positions in the protein, and a derivative of the ERAD-L substrate CPY*, have shown that the substrate contacts the E3 ligase at specific residues located in the ER membrane which was interpreted as retrotranslocation of the ERAD substrate through a channel formed by Hrd1p (Carvalho *et al.*, 2010; Stanley *et al.*, 2011). As ERAD substrate ubiquitination is a prerequisite for proteasomal degradation of many substrates one would, however, expect an interaction of the E3 ligase with ERAD substrates. Thus, the above study could “merely” be another indication for the mediation of substrate recognition by the transmembrane region of Hrd1p (Sato *et al.*, 2009; Carvalho *et al.*, 2010). An earlier study investigated the role of Hrd1p as the retrotranslocation channel using the Hmg1p-Hrd1p (fusion of RING-H2 domain of Hrd1p and HMGR (TMD of Hmg1 isozyme of yeast)) fusion protein which self-ubiquitinates independently of Hrd1p and undergoes proteasomal degradation (Garza *et al.*, 2009). *In vitro* retrotranslocation of the Hmg1p-Hrd1p fusion protein was shown even in microsomes derived from a *Δhrd1* null strain (Garza *et al.*, 2009). Further, cycloheximide chases demonstrated that the fusion protein was rapidly

degraded in a *Δhrd1* null mutant as well as in a *Δhrd1 Δdoa10* double mutant questioning a role of both E3 ligases as the retrotranslocation channel (Garza *et al.*, 2009).

Der1p (yeast), a protein in the ER membrane with four TMDs, has been suggested as another retrotranslocon candidate (Knop *et al.*, 1996a; Wahlman *et al.*, 2007). Yeast Der1p, the first protein found to be required for ERAD of soluble substrates CPY* and PrA*, has since been demonstrated to act during ERAD-L (Knop *et al.*, 1996a; Taxis *et al.*, 2003; Hitt & Wolf, 2004). In yeast, a *Δder1* null mutant displays more or less severe defects in the degradation of various ERAD-L substrates, suggesting a central role of Der1p during the degradation of misfolded soluble proteins (Hill & Cooper, 2000; Walter *et al.*, 2001; Taxis *et al.*, 2003; Vashist & Ng, 2004; Willer *et al.*, 2008). ERAD-M substrates do not seem to require Der1p for degradation, as seen in a study using Hmg2p, ERAD of which does not require Der1p, it homologue Dfm1p or even Sec61p (Sato *et al.*, 2006; Garza *et al.*, 2009). Further, due to its composition of four TMDs it cannot form the retrotranslocation channel alone (Knop *et al.*, 1996a; Hitt & Wolf, 2004). Der1p, however, has been shown to form homooligomers, which might be sufficient to form the retrotranslocation channel, but the fact that Der1p is not required for ERAD of all substrate also suggests that Der1p cannot be the only retrotranslocation channel (Knop *et al.*, 1996a; Vashist & Ng, 2004; Ye *et al.*, 2004, 2005). Its important role during ERAD-L is also demonstrated by the fact that in *Δder1* cells ER stress is increased leading to the induction of the UPR, during which Der1p itself is strongly up-regulated (Knop *et al.*, 1996; Travers *et al.*, 2000; Ye *et al.*, 2004). In a more recent study Der1p could be crosslinked to ERAD substrates as well as to the substrate receptor Hrd3p suggesting that it plays a role in the initiation of protein export from the ER by threading substrates into the ER membrane and directing them to Hrd1p (Mehnert *et al.*, 2014). For the mammalian homoloque Derlin-1, one of three homologues in mammals (Derlin-1, Derlin-2 and Derlin-3), a central role during ERAD has also been demonstrated. Studies in mammalian cells suggest that Derlin-1 rather than Sec61p forms the retrotranslocation channel (Lilley & Ploegh, 2004; Ye *et al.*, 2004). In cells expressing the CMV protein US11, the degradation of a MHC class I HC retrotranslocation intermediate is triggered by the viral protein, and US11 also recruits MHC class I HC to DERLIN-1 (Lilley & Ploegh, 2004). For a mutant form of US11, rendering the protein capable of complex formation with MHC class I HC, retrotranslocation is disturbed (Lilley & Ploegh, 2004). As wild-type ($US11_{WT}$-HC) but not mutant MHC class I HC-US11 ($US11_{Q192L}$-HC) complexes contained Derlin-1, it was suggested that dislocation requires Derlin-1 (Lilley & Ploegh, 2004). A dominant-negative version of Derlin-1 (Derlin-1^{GFP}) further revealed that Derlin-1 interferes with US11-mediated MHC class I dislocation (Lilley & Ploegh, 2004). The authors favour Derlin-1 as part of the retrotranslocon and at the same time question Sec61p as the export channel, as, to them, the diameter of the SecY (~ 15-20 Å) complex is not sufficient enough to mediate dislocation especially of more complex substrates (Lilley & Ploegh, 2004; van den Berg *et al.*, 2004). Ye and colleagues demonstrated in a similar study using canine microsomes that the AAA-ATPase p97 associates with Derlin-1 and VCP-interacting

membrane protein (VIMP). RNAi studies in the nematode *C. elegans* have shown that depletion of Derlin-1 results in ER stress (Ye *et al.*, 2004). This is in concordance with studies in yeast, which have shown that the UPR is induced in the absence of Der1p (Knop *et al.*, 1996a).

It has been indicated that Derlins are involved in the dislocation of cholera toxin from the ER into the cytosol and in the liberation of polyomavirus-encoded proteins from the ER, further implicating that the role of the Derlins is multifaceted (Lilley *et al.*, 2006; Bernardi *et al.*, 2007).

An involvement of Derlin-1 in ERAD has been further suggested in various studies in which the protein could be coimmunoprecipitated with ERAD components, such as HRD1 and p97, as well as with ERAD substrates (Katiyar *et al.*, 2005; Schulze *et al.*, 2005; Lilley & Ploegh, 2005; Ye *et al.*, 2005; Younger *et al.*, 2006; Okuda-Shimizu & Hendershot, 2007).

In a more recent study, Derlin-1 and not Sec61α, was implicated as the putative dislocon (Wahlman *et al.*, 2007). Here, fluorescently labeled Δgpαf (Δgpαf-BOF) was retrotranslocated in a cell-free assay using canine microsomes and mammalian cytosol (Wahlman *et al.*, 2007). This study demonstrated that in the presence of the irreversible proteasome inhibitor lactacystine retrotranslocation did not occur, showing that the proteasome is required for retrotranslocation (Wahlman *et al.*, 2007). In this study blocking the translocation pore by adding RNCs or antibodies against Sec61α (αSec61α) did not affect retrotranslocation of the fluorescently labeled ERAD substrates, while antibodies against Derlin-1 drastically reduced retrotranslocation, questioning the idea of ERAD substrate retrotranslocation through the protein conducting channel (Crowley *et al.*, 1994; Hamman *et al.*, 1998; Gillece *et al.*, 2000; Schmitz *et al.*, 2000; Wahlman *et al.*, 2007). The authors did, however, not show that the Sec61α-antibodies were able to block ribosome binding to the microsomes, or that their epitope was accessible in intact microsomes (Wahlman *et al.*, 2007). Photocosslinking of Δgpαf to Derlin-1 but not to Sec61α was also demonstrated, but export substrates were not stalled (Wahlman *et al.*, 2007).

Channel formation of Der1p is unlikely due its structure and further has not been shown so far (Hitt & Wolf, 2004). It has been suggested, however, that it might form a part of the retrotranslocation channel (Lilley & Ploegh, 2004; Ye *et al.*, 2004, Hampton & Sommer, 2012). Data, which could demonstrate this, are still missing.

1.7 AIM OF THIS STUDY

The aim of this study was to get a deeper insight into the role of the Sec61 channel during ERAD. More specifically, I tried to elucidate which domain(s) of Sec61p (yeast; Sec61α in mammals), the pore-forming component of the Sec61 complex, mediate(s) the interaction between the 19S RP of the 26S proteasome and the protein translocation channel and whether a disturbed Sec61p-19S RP interaction leads to defects in ERAD (Andrews & Johnson, 1996; Hanein *et al.*, 1996; Wiertz *et al.*, 1996b; Pilon *et al.*, 1997).

In a previous study, two *sec61* mutants, *sec61-302* (D168G, S179P, F263L, S353C) and *sec61-303* (D168G, F263L), sharing two of the same point mutations, were isolated which both displayed defective cotranslational import into the ER (Ng *et al.*, 2007). In a binding assay using 19S RP and reconstituted proteoliposomes derived from ER membranes of each mutant, however, only *sec61-302* displayed a reduction in proteasome affinity (Ng *et al.*, 2007). These results suggested that one of the two point mutations in *sec61-302*, S179P and/or S353C, which do not occur in *sec61-303* was responsible for the observed reduction in proteasome binding (Ng *et al.*, 2007).

My initial aim was to generate *sec61* mutants which contained the amino acid substitution S179P, S353C or both and to elucidate which of the two point mutations mediate the observed defect in proteasome binding (Ng *et al.*, 2007). In addition, I wanted to investigate ERAD defects using specific substrates, UPR induction and synthetic effects with *Δire1*.

The purpose of my work was to further understand the role of Sec61p and 19S RP during misfolded protein dislocation from the ER.

2 MATERIALS AND METHODS

2.1 MATERIALS AND GENERAL PROCEDURES

2.1.1 LABORATORY EQUIPMENT, REAGENTS, CHEMICALS AND THEIR SUPPLIERS

Laboratory equipment used in this study is listed in Table 2.1. Reagents, chemicals and consumables are listed in Table 2.2.

Table 2.1. Laboratory equipment used in this study.

Company	Products
Beckman Coulter Inc.	Optima™ MAX-XP Benchtop Ultracentrifuge Optima™ L-90 K Ultracentrifuge Adapter for Microfuge® Tubes 1.5 ml
Bio-Rad Laboratories Inc.	PowerPac™ HC Power Supply Trans-Blot® Electrophoretic Transfer Cell (with plate electrodes and super cooling coil) Model 583 Gel Dryer (with vacuum pump) ChemiDoc™ XRS Image Lab™ Software MicroPulser™ Electroporator
Bio Spec Products Inc.	Mini-Beadbeater-24
Carl Roth® GmbH & Co. KG	Hemocytometer Neubauer Improved
Cawo Solutions	CAWOMAT 2000 IR (X-ray film processor)
Eppendorf AG	Concentrator Plus (vacuum concentrator, evaporator) Thermomixer® Comfort (24 x 1.5 ml) MiniSpin® Centrifuge Microcentrifuge 5415R
GE Healthcare	Typhoon™ Trio Variable Mode Imager (Phosphorimager) Storage Phosphor Screens (with exposure cassettes) Ultrospec 2100 pro UV/Visible Spectrophotometer (Amersham Biosciences) Amersham Hypercassette Autoradiography Cassettes ImageQuant™ TL Software
Hamilton Beach® Brands Inc.	Rio™ Commercial Bar Blender (stainless steel blender)
Hellma® Analytics	Quartz Glass Cuvettes (QS; pathlength: 10 mm)
IKA®-Werke GmbH & Co. KG	RH basic2 IKAMAG® EUROSTAR Power Basic (laboratory overhead stirrer)
Infors AG	Multitron Standard Incubation Shaker
Invitrogen™ (Life Technologies part of Thermo Fisher Scientific Inc.)	XCell SureLock™ Mini-Cell (Novex®)
KGW Isotherm	Dewar Carrying Flask 4 L
Leica Microsystems	Microscope
Merck Millipore (part of Merck KGaA)	Milli-Q® Integral Water Purification System
neoLab® Migge Laborbedarf.Vertrieb s GmbH	Overhead Rotator (20 tubes) neoLab-Rocking Shaker
PEQLAB Biotechnologie GmbH (part of VWR)	E-Box VX2 Gel Documentation System peqSTAR 2 X Gradient Thermocycler PerfectBlue Gel System Mini S/M
Scientific Industries Inc.	Vortex-Genie® 2
Sigma Laborzentrifugen GmbH	SIGMA 4K15 Refrigerated Centrifuge
Thermo Scientific (Thermo Fisher Scientific Inc.)	Sorvall Evolution® RC Centrifuge

Wheaton®	Potter-Elvehjem Style Tissue Grinder with PTFE Pestle, 55 ml

Table 2.2. Chemicals, reagents and consumables used in this study.

Company	Products
AGFA HealthCare GmbH	Agfa Developer G153 Agfa Fixer G354
Applichem GmbH	Ampicillin Sodium Salt (BioChemica) DEPC (BioChemica) Kanamycin Sulfate (BioChemica) Tunicamycin HEPES – Sodium Salt Sodium Chloride Magnesium Chloride Sodium Acetate Magnesium Acetate Ammonium Acetate
Avanti® Polar Lipids, Inc	L-α-Phosphatidylcholine (Liver, Bovine), Chloroform L-α-Phosphatidylethanolamine (Liver, Bovine), Chloroform
BD (Becton, Dickinson & Company)	Bacto™ Casamino Acids Bacto™ Peptone Bacto™ Yeast Extract Difco™ Yeast Nitrogen Base without Amino Acids & Ammonium Sulfate Difco™ Yeast Nitrogen Base without Amino Acids
Beckman Coulter GmbH	Polycarbonate Bottles, thick-walled, 70 ml (rotor type 45 Ti) Polyallomer Tubes, thin-walled, 4.4 ml (rotor type SW 60 Ti) Polycarbonate Tubes, thick-walled, 1.0/1.4 ml (TLS-55) Polycarbonate Tubes, thick-walled, 3.0/3.5 ml (TLA-100.3) Microfuge® Tubes, Polyallomer, 1.5 ml
Bioline (part of Meridian Life Science® Company)	Alpha-Select Silver Efficiency (chemically competent cells) Quick-Stick Ligase
Bio-Rad Laboratories Inc.	Nitrocellulose Membrane (0.2 µM, 0.45 µM pore size) Bio-Beads® SM Adsorbents Precision Plus Protein™ All Blue Standards Electroporation Cuvettes, 0.2 µm gap
Biozym Scientific GmbH	Fast-Link™ DNA Ligation Kit (Epicentre®)
Carl Roth® GmbH & Co. KG	PMSF (≥99 %) Roti®-Aqua-Phenol (RNA extraction) Rotiphorese® Gel 30 (37,5:1) β-Mercaptoethanol (99 %, p.a.) TEMED (99 %, p.a.) Roti®-Phenol/Chloroform/Isoamyl-Alcohol (Nucleic acid extraction) Peptone (from Casein) Yeast Extract Glycine (PUFFERAN®, ≥99 %, p.a.) Agar-Agar, Kobe I Ammonium Peroxydisulfate (≥98 %, p.a.) SDS Pellets (≥99 %) RNase AWAY® Glycerol (≥98 %) Triton X 100, pure 2-Nitrophenyl-β-D-Galactopyranoside
Fermentas (part of Thermo Fisher Scientific Inc.)	Conventional and FastDigest® Restriction Enzymes T4 DNA Ligase FastAP™ Thermosensitive Alkaline Phosphatase GeneRuler™ 1 kb DNA Ladder

	GeneRuler™ 1 kb Plus DNA Ladder PageRuler™ Prestained Protein Ladder PageRuler™ Plus Prestained Protein Ladder ATP, 100 mm Solution GTP, 100 mM Solution RNase A, DNase and Protease-free (10 mg/ml) 5-Fluoroorotic Acid
Formedium™	Synthetic Complete Drop-Out Mixture, (SC) (-Ade, -His, -Leu, -Lys, -Trp, -Ura), (Kaiser Mixture)
FujiFilm	Medical X-ray Film (Super HR-E30)
GE Healthcare Life Sciences (part of GE Healthcare)	Protein A Sepharose™ CL-4B Disposable PD-10 Desalting Columns (empty)
Invitrogen™ (Life Technologies part of Thermo Fisher Scientific Inc.)	TOPO® TA Cloning® Kit for Sub-cloning NuPAGE® Novex® 4-12 % Bis-Tris Gel 1.5 mm, 10 Well (Novex®) NuPAGE® MOPS SDS Running Buffer (20X) (Novex®) UltraPure™ Agarose
Merck Millipore (part of Merck KGaA)	AEBSF, Hydrochloride (Calbiochem®) Cycloheximide (Calbiochem®) MF-Millipore™ Membrane Filters (0.025 µm pore size, Microdialysis of DNA) Centricon® YM-100 Centrifugal Filter Devices
New England BioLabs® (NEB) GmbH	Micrococcal Nuclease, 2000000 gel units/ ml Conventional Restriction Enzymes
PEQLAB Biotechnologie GmbH (part of VWR)	KAPA HiFi™ PCR Kit Electroporation Cuvettes (#71-2020)
Perkin Elmer Inc.	EXPRE^{35}S^{35}S Protein Labeling Mix, [^{35}S]-, 50mM Tricine (pH 7.4), 10 mM 2-Mercaptoethanol L-[^{35}S]-Methionine (Activity > 1000 Ci) [Methyl-^{14}C] Methylated Protein Molecular Weight Marker
Promega GmbH	Recombinant RNasin® Ribonuclease Inhibitor SP6 RNA Polymerase Ribo m7G Cap Analog rATP, rCTP, rUTP, rGTP, 100 mM
Roche Life Science (Roche Diagnostics)	Complete™, Mini, EDTA-free Protease Inhibitor Cocktail Tablets Creatine Phosphate, > 97 %
Rockland™ Immunochemicals Inc.	Anti-HA Antibody (Biomol)
Sartorius AG	Minisart® Plus Syringe Filters (0.2, 0.45 µm pore size)
Sigma-Aldrich® Co. LLC.	Adenine (≥99 %) (Sigma) L-Cysteine (≥98 %) (Sigma) L-Histidine (Sigma) Uracil (≥99 %) (Sigma) L-Leucine (≥98.5 %) (Sigma) L-Tryptophan (≥98 %) (Sigma) L-Methionine (≥99 %) (Sigma) L-Cysteine (≥99 %) (Sigma) ANTI-FLAG® M2 Affinity Agarose Gel (Sigma) ANTI-FLAG® Antibody, produced in rabbit (Sigma) FLAG® Peptide, lyophilized powder (Sigma) DL-Dithiothreitol, BioUltra, ≥99.0 % (Sigma) Sucrose BioXtra, ≥99.5 % (Sigma) Tryptone, enzymatic digest from casein (Fluka) D-(+)-Glucose (≥99.5 %) (Sigma) Deoxyribonucleic Acid Sodium Salt, from salmon testes (Sigma) Absolute Ethanol ACS Reagent, ≥99.5 % (Sigma-Aldrich) Bromophenol Blue Sodium Salt (Sigma)

	Trizma® Base, BioUltra, for molecular biology, ≥99.8 % (Sigma) Urea (Sigma) MES, low moisture content, ≥99 % (Sigma) Sodium Azide, BioUltra, ≥99.5 % Tween® 29 (Sigma) DMSO Glass Beads, acid-washed 425-600 µm (Sigma) EDTA, anhydrous, ≥99 % (Sigma-Aldrich) EGTA (≥97 %) (Sigma) Lithium Acetate Dihydrate, BioXtra (Sigma) Polyethylene Glycol, BioXtra, average mol wt 3,350 (Sigma-Aldrich) D-(+)-Galactose (≥99 %) (Sigma-Aldrich) D-(+)-Raffinose Pentahydrate (≥98 %) (Sigma) Sodium Chloride, for molecular biology (≥98 %) GenElute™ PCR Clean-Up Kit (Sigma) GenElute™ HP Plasmid Maxiprep Kit (Sigma) GenElute™ Gel Extraction Kit (Sigma) Puromycin Dihydrochloride (10 mg/ml) (Sigma) Corning® Cryogenic Vials, internal thread (2.0 mL) Creatine Phosphokinase, from rabbit muscle
Sucofin	Skimmed Milk Powder
Thermo Fisher Scientific Inc.	Pierce 660 nm Protein Assay Reagent SuperSignal West Dura Extended Duration Chemiluminescent Substrate (ECL) Filter Units – 115/250/500 ml capacity, MF75™ Series, 0.45 µm pore size DMSO MS(PEG_8) (Methyl-PEG-NHS-Ester reagent) (Pierce)
VWR® International	Essigsäure 99 % GPR RECTAPUR® Ethanol Absolut AnalaR NORMAPUR®
ZChL	* All other chemicals not mentioned above but mentioned in the respective sections of this chapter

2.1.2 BACTERIAL AND *S. CEREVISIAE* STRAINS

Origin and genotype for bacterial and *S. cerevisiae* strains are listed in Tables 2.3 and 2.4 respectively.

Table 2.3. *E. coli* strains used in this study.

Strain	Genotype	Source
DH5α	*F⁻ endA1 glnV44 thi-1 recA1 relA1 gyrA96 deoR nupG Φ80dlacZΔM15 Δ(lacZYA-argF)U169, hsdR17(r_K^- m_K^+), λ–*	Hanahan, 1983
Top10	*F- mcrA Δ(mrr-hsdRMS-mcrBC) ϕ80lacZΔM15 ΔlacX74 nupG recA1 araD139 Δ(ara-leu)7697 galE15 galK16 rpsL(Str^R) endA1 λ^-*	Invitrogen®
Alpha-Select Silver Efficiency Competent Cells	*F⁻ deoR endA1 recA1 relA1 gyrA96 hsdR17(r_k^-, m_k^+) supE44 thi-1 phoA Δ(lacZYA-argF)U169 Φ80lacZΔM15 λ^-*	Bioline
KRB3	Lyticase expressing *E. coli* (in DH5α)	Shen *et al.*, 1991

KRB38	pDJ100 (ppαf cloned into pSP65, behind SP6 promoter) (in HB101)	R. Schekman Hansen *et al.*, 1986
KRB41	pαF3Q (pΔgpαf in MC1600)	Mayinger & Meyer *et al.*, 1993
KRB257	pGEM2αF	Mayinger & Meyer *et al.*, 1993
KRB319	pDN431 (*CPY*$_{HA}$*; *URA3*)	Ng *et al.*, 2000
KRB351	p416 pΔgpαf (in DH5α)	Mumberg *et al.*, 1994
KRB356	pBW11 (*SEC61* WT in pRS315)	Stirling *et al.*, 1992
KRB733	pJC30 (*UPRE-LacZ* reporter construct; pRS314 backbone)	D. Ng
KRB734	pJC31 (*CYC1* TATA box fused to *LacZ* control for KRB733; pRS314 backbone)	D. Ng
KRB842	pRS315 in DH5α	M. Schmitt Sikorski & Hieter, 1989
KRB855	pRS313-*CPY-URA3*	Ng *et al.*, 1996
KRB856	pRS313-*PHO8-URA3* (in DH5α)	Ng *et al.*, 1996
KRB857	pRS313 (in DH5α)	J. Brown Sikorski & Hieter, 1989
KRB862	pRS315-*sec61-S179P* (in DH5α)	This study
KRB863	pRS315-*sec61-S353C* (in DH5α)	This study
KRB864	pRS315-*sec61-S179P/S353C* (in DH5α)	This study
KRB865	pRS306-*truncsec61-S179P* (in DH5α)	This study
KRB866	pRS306-*truncsec61-S353C* (in DH5α)	This study
KRB867	pRS306-*truncsec61-S179P/S353C* (in DH5α)	This study
KRB882	pSM70 KHN-HA (*URA3*)	D. Ng Vashist *et al.*, 2001 Vashist *et al.*, 2004
KRB883	pSM101 KWW-HA (*URA3*)	D. Ng Vashist & Ng, 2004
KRB884	pSM1083 *ste6-166-HA* (*URA3*)	D. Ng (S. Michaelis) Vashist *et al.*, 2004 Loayza *et al.*, 1998
KRB899	pRS306-*truncsec61-302* (in DH5α)	This study
KRB900	pRS306-*truncsec61-303* (in DH5α)	This study

Table 2.4. *S. cerevisiae* strains used in this study*.

Name	Genotype	Use	Source/Reference
KRY40/ GPY60	*MATα leu2-3,112 ura3-52 his4-579 trp1-289 prb1 pep4::URA3 gal2*	Translation extract	Baker *et al.*, 1988
KRY47	*MATα leu2-3,112 ura3-52*	WT strain (microsome preparation, integration of truncated *sec61* genes into genome	Pilon *et al.* 1997
KRY92	*ade2-1 ura3-1 his3-11,15 leu2-3,112 trp1-1 can1-100*	*DER1* (W303-1B)	Knop *et al.*, 1996 (Dieter Wolf)
KRY93	*ade2-1 ura3-1 his3-11,15 leu2-3,112 trp1-1 can1-100 Δder1*	*Δder1* (W303-1B Δder1)	Knop *et al.*, 1996 (Dieter Wolf)
KRY159	*MATa leu2-3, 112 his3-11,15 trp1-1 ura3-1 ade2-1 can1-100 leu2-3,112::LEU+UPRE-lacZ MET+*	*IRE1*	Sidrauski/Peter Walter Shamu & Walter, 1996
KRY160	*MATa eu2-3,112 his3-11,15 trp1-1 ura3-1 ade2-1 can1-100 leu2-3,112::LEU+ UPRE-lacZ MET+ ire1::TRP1 pRS304* (entire Ire1p coding sequence deleted)	*Δire1*	Sidrauski/Peter Walter Shamu & Walter, 1996
KRY161	*MATα ade2-1 ura3-1 his3-11,15 leu2-3,112 trp1-1* can1-100 prc1-	W303-1C	D. Wolf Knop *et al.*, 1996
KRY200	*MATα can1-100 leu2-3,112 his3-11,15 trp1-1 ura3-1 ade2-1 sec61::HIS3* [*pDQ sec61-32*]	*sec61-32*	R. Schekman Pilon *et al.*, 1998
KRY201	*MATα can1-100 leu2-3,112 his3-11,15 trp1-1 ura3-1 ade2-1 sec61::HIS3 pDQ1[sec61-41]*	*sec61-41*	R. Schekman Pilon *et al.*, 1998
KRY221	*MATα sec61-3 trp1-1 leu2-3,112 ura3-52*	*sec61-3*	C. Stirling
KRY275	*leu2-3,112 ura3 his3-11,15*	Cytosol preparation	Hiller *et al.* 1996
KRY333	*his3Δ200 leu2-3.112 lya2-801 trp1Δ63 ura3-52 RPT1^{FH}::Ylplac211(URA3)*	26S, 19S RP preparation	Verma *et al.*, 2000
KRY461	*MATα sec61::HIS3 leu2 trp1 prc1-1 his3 ura3 [pGAL-SEC61-URA3]*	pGAL-*SEC61* cross of RSY764 with W303-1C	KB Römisch (Römisch Lab)
KRY706	BMA38a, *kanr-pGAL-SEC61, his3-Δ200 leu2-3.112 trp1-Δ1 ura3-1 ade2-1 can1-100* [*pRS313-SEC61(HIS-CEN)*]	*SEC61*	Ng *et al.*, 2006
KRY712	BMA38a, *kanr-pGAL-SEC61, his3-Δ200 leu2-3.112 trp1-Δ1 ura3-1 ade2-1 can1-100* [*pCEN-LEU-sec61-D168G/ S179P/F263L/S353C*] [*pRS313 (HIS-CEN)*]	*sec61-302*	Ng *et al.*, 2006
KRY715	BMA38a, *kanr-pGAL-SEC61, his3-Δ200 leu2-3.112 trp1-Δ1 ura3-1 ade2-1 can1-100* [*pCEN-LEU-sec61-D168G, F163L*] [pRS313 (*HIS-CEN*)]	*sec61-303*	Ng *et al.*, 2006
KRY849	BMA38a, *kanr-pGAL-SEC61, his3-Δ200 leu2-3.112 trp1-Δ1 ura3-1 ade2-1 can1-100* [*pCEN-LEU-sec61-S179P*]	*sec61-S179P* (transformation of KRB862 into KRY858)	This study

KRY850	BMA38a, *kanr-pGAL-SEC61, his3-Δ200 leu2-3.112 trp1-Δ1 ura3-1 ade2-1 can1-100* [*pCEN-LEU-sec61-S353C*]	*sec61-S353C* (transformation of KRB863 into KRY858)	This study
KRY851	BMA38a, *kanr-pGAL-SEC61, his3-Δ200 leu2-3.112 trp1-Δ1 ura3-1 ade2-1 can1-100* [*pCEN-LEU-sec61-S179P/S353C*]	*sec61-S179P/S353C* (transformation of KRB864 into KRY858)	This study
KRY852	*MATα leu2-3,112 ura3-52* [*pRS306-truncsec61-S179P*]	Truncated version of *sec61-S179P* (KRB865) integrated into KRY47 (for *in vitro* studies)	This study
KRY853	*MATα leu2-3,112 ura3-52* [*pRS306-truncsec61-S353C*]	Truncated version of *sec61-S353C* (KRB866) integrated into KRY47 (for *in vitro* studies)	This study
KRY854	*MATα leu2-3,112 ura3-52* [*pRS306-truncsec61-S179P/S353C*]	Truncated version of *sec61-S179P/S353C* (KRB867) integrated into KRY47 (for *in vitro* studies)	This study
KRY858/ JDY638	BMA38a, *kanr-pGAL-Sec61, his3-Δ200 leu2-3.112 trp1-Δ1 ura3-1 ade2-1 can1-100*	WT *SEC61* under Gal promoter	J. Brown
KRY878	*MATα ire1::KANMX, leu2-3, his3-11,trp1-1, ura3-1, can1-100, ade2-1*	*Δire1*	C. Servas (Römisch Lab)
KRY879	*MATα ade2-1 ura3-1 his3-11,15 leu2-3,112 trp1-1 can1-100 der1::natNT2*	*Δder1* in W303-1B background	C. Servas (Römisch Lab)
KRY880	*MATα ade2-1 ura3-1 his3-11,15 leu2-3,112 trp1-1 can1-100 prc1-1 der1::natNT2*	W303-1C (*prc1-1*) *Δder1*	C. Servas (Römisch Lab)
KRY901	*IRE1* [*pRS306-truncsec61-S179P*]	Truncated version of *sec61-S179P* (KRB865) integrated into KRY159	This study
KRY902	*IRE1* [*pRS306-truncsec61-S353C*]	Truncated version of *sec61-S353C* (KRB866) integrated into KRY159	This study
KRY903	*IRE1* [*pRS306-truncsec61-S179P/S353C*]	Truncated version of *sec61-S179P/S353C* (KRB867) integrated into KRY159	This study
KRY904	*IRE1* [*pRS306-truncsec61-302*]	Truncated version of *sec61-302* (KRB899) integrated into KRY159	This study
KRY905	*IRE1* [*pRS306-truncsec61-303*]	Truncated version of *sec61-303* (KRB900) integrated into KRY159	This study
KRY906	*Δire1* [*pRS306-truncsec61-S179P*]	Truncated version of *sec61-S179P* (KRB865) integrated into KRY160	This study
KRY907	*Δire1* [*pRS306-truncsec61-S353C]*	Truncated version of *sec61-S353C*	This study

		(KRB866) integrated into KRY160	
KRY908	*Δire1* [*pRS306-truncsec61-S179P/S353C*]	Truncated version of *sec61-S179P* (KRB867) integrated into KRY160	This study
KRY909	*Δire1* [*pRS306-truncsec61-302*]	Truncated version of *sec61-302* (KRB899) integrated into KRY160	This study
KRY910	*Δire1* [*pRS306-truncsec61-303*]	Truncated version of *sec61-303* (KRB900) integrated into KRY160	This study

* Long-time storage of the microorganisms was in sterile glycerol. In brief, a fresh overnight culture of each strain was mixed with sterile glycerol (final concentration: 50 % (v/v)) and stored in cryogenic tubes at – 80 °C.

Table 2.4 contains all *S. cerevisiae* strains that were added to the strain-catalogue and stored at – 80 °C. Strains that were generated by transformation with CEN plasmids to use in the respective assays (eg. liquid β-Galactosidase assay, reporter plasmid translocation assay) were not stored. Here, the respective plasmid (transformed into *E. coli*) was stored at – 80 °C (ref. Table 2.5).

2.1.3 PLASMIDS

The plasmids used and created in this study were taken from the strain collection of the Department of Microbiology (Saarland University, Germany) and are listed in Table 2.5.

Figure 2.1.3.1 shows the simplified vector maps of pRS306 and pRS315 both of which were used to create the appropriate *sec61* constructs. Simplified plasmid maps of the resulting *sec61* constructs are shown in Figure 2.1.3.2.

Table 2.5. Plasmids used in this study.

Plasmid (Strain cat. #)	Characteristics	Use	Reference/Source
p416pΔgpαf (KRB351)	Overexpression of pΔgpαf (*URA3)* Contains: MET25 promoter	Pulse-chase experiments (pΔgpαf expression)	Mumberg *et al.*, 1994
pαF3Q (KRB41)	Gene for pΔgpαf in MC1600. Linearization with *Sal*I for transcription.	*In vitro* transcription and translation of pΔgpαf	Mayinger & Meyer, 1993
pBW11 (KRB356)	WT SEC61 in pRS315	Template for SOE-PCR	Stirling *et al.*, 1992 Wilkinson *et al.*, 1996
pDJ100 (KRB38)	(ppαf cloned into pSP65, behind SP6 promoter) (in HB101) Linearization with *Xba*I for transcription.	*In vitro* transcription and translation of ppαf	Schekman Hansen *et al.*, 1986
pDN106 (KRB855)	CPY-Ura3p fusion protein (pRS313-*CPY-URA3*; *HIS3*)	Import analysis (post-translational import)	D. Ng Ng *et al.*, 1996
pDN431	CPY^*_{HA} in YCP50 (*URA3*)	Pulse-chase	D. Ng

(KRB319)		experiments	Ng *et al.*, 2000
pGEM2αF (KRB257)	Gene for ppαf (wild type; serine variant) in pGEM. SP6 promoter. Linearization with *Sal*I to transcribe.	*In vitro* transcription and translation of ppαF.	Mayinger & Meyer, 1993
pJC30 (KRB733)	(*UPRE-LacZ* reporter construct; pRS314 backbone)	Liquid β-Galactosidase assay	D. Ng
pJC31 (KRB734)	(CYC1 TATA box fused to *LacZ*; pRS314 backbone)	Liquid β-Galactosidase assay (control for pJC30)	D. Ng
pJEY203 (KRB856)	Pho8p-Ura3p fusion protein (pRS313-*PHO8-URA3*; *HIS3*)	Import analysis (co-translational import)	D. Ng Ng *et al.*, 1996
pRS306 (KRB368)	Yeast integration vector (*URA3*)	Cloning of mutant *sec61* into pRS306; integration of *sec61* into yeast genome	R. Duden Sikorski & Hieter *et al.*, 1989
pRS306-*truncsec61-302* (KRB899)	Truncated version of *sec61-302* (generated from C. Ng's plasmid # 14*)	Integration plasmid	This study
pRS306-*truncsec61-303* (KRB900)	Truncated version of *sec61-303* (generated from C. Ng's plasmid # 18*)	Integration plasmid	This study
pRS306-*truncsec61-S179P* (KRB865)	Truncated version of sec*61-S179P* cloned into pRS306	Integration plasmid	This study
pRS306-*truncsec61-S179P/S353C* (KRB867)	Truncated version of *sec61-S179P/S353C* cloned into pRS306	Integration plasmid	This study
pRS306-*truncsec61-S353C* (KRB866)	Truncated version of *sec61-S353C* cloned into pRS306	Integration plasmid	This study
pRS313 (KRB857)	Empty vector	Control for import analysis (co- and posttranslational import)	J. Brown
pRS315 (KRB842)	CEN vector (*LEU2*)	Cloning of mutant *sec61* into pRS315	Sikorski & Hieter, 1989
pRS315-*sec61-S179P* (KRB862)	*sec61-S179P* cloned into pRS315	CEN plasmid	This study
pRS315-*sec61-S179P/S353C* (KRB864)	*sec61-S179P/S353C* cloned into pRS315	CEN plasmid	This study
pRS315-*sec61-S353C* (KRB863)	*sec61-S353C* cloned into pRS315	CEN plasmid	This study
pSM101 (KRB883)	KWW-HA (*URA3*)	Pulse-chase experiments	D. Ng Vashist & Ng, 2004
pSM1083 (KRB884)	Ste6-166p-HA (*URA3*) (in pRS316)	Pulse-chase experiments	D. Ng (S. Michaelis) Loayza *et al.*, 1998

* Plasmids were stored at – 20 °C by C. Ng.

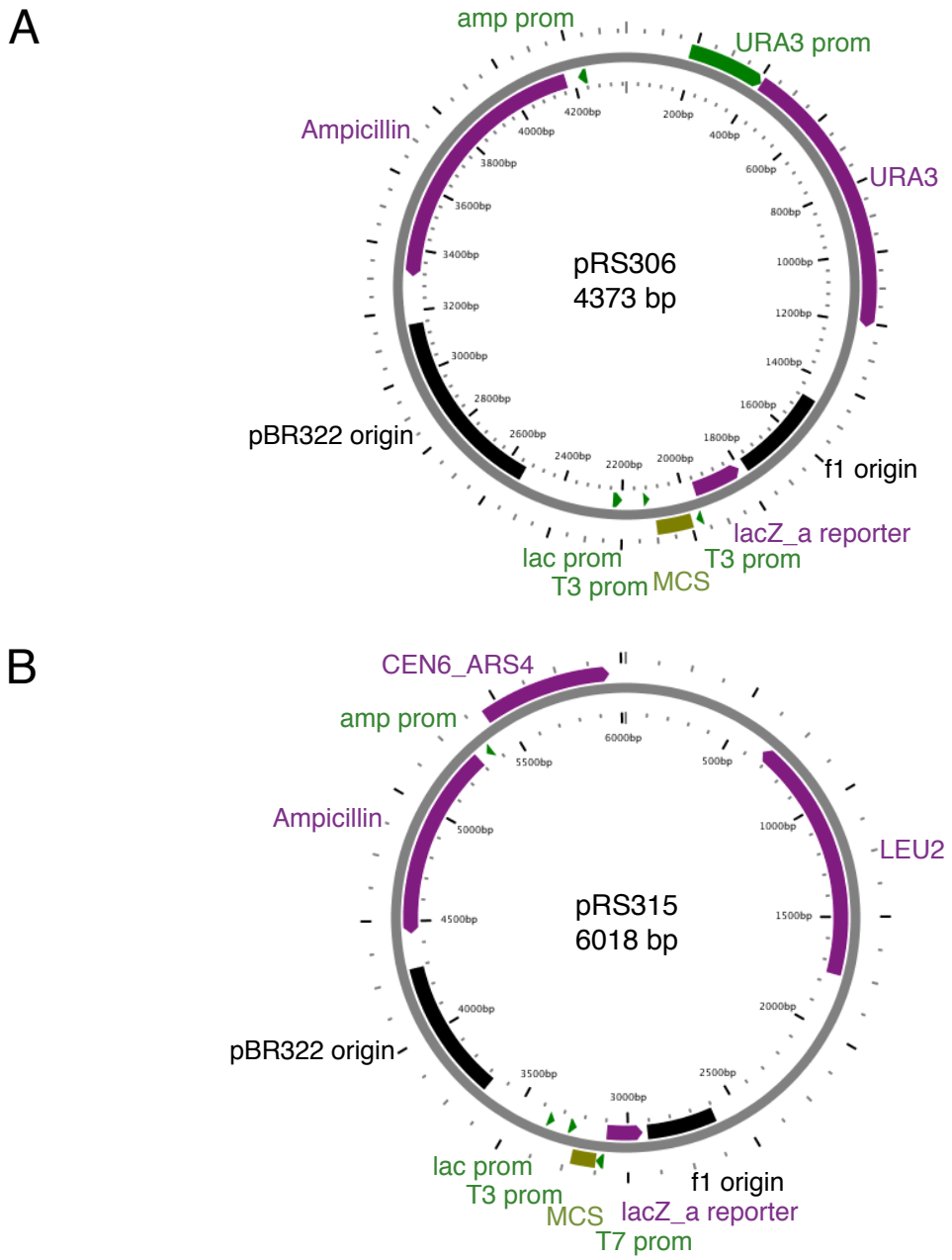

Figure 2.1.3.1. Simplified vector maps of pRS306 and pRS315. (A) The yeast integrative vector pRS306 does not replicate autonomously, but integrates into the yeast genome by homologous recombination. It contains the auxotrophic marker *URA3* and an ampicillin resistance gene for selection in *E. coli*. In this study pRS306 was used to create the desired pRS306-*truncsec61** constructs for the integration into the yeast genome (ref. Figure 2.1.3.2.A). Strains transformed with integration plasmids are extremely stable. (B) The yeast centromer vector pRS315 is an autonomously replicating vector, containing a centromer sequence (CEN) and an autonomously replicating sequence (ARS). It further contains the auxotrophic marker *LEU2* and an ampicillin resistance gene for selection in *E. coli*. In this study pRS315 was used for the expression of the desired *sec61* mutants. The full-length *sec61* mutants were cloned into pRS315. The resulting constructs are shown in Figure 2.1.3.2.B.

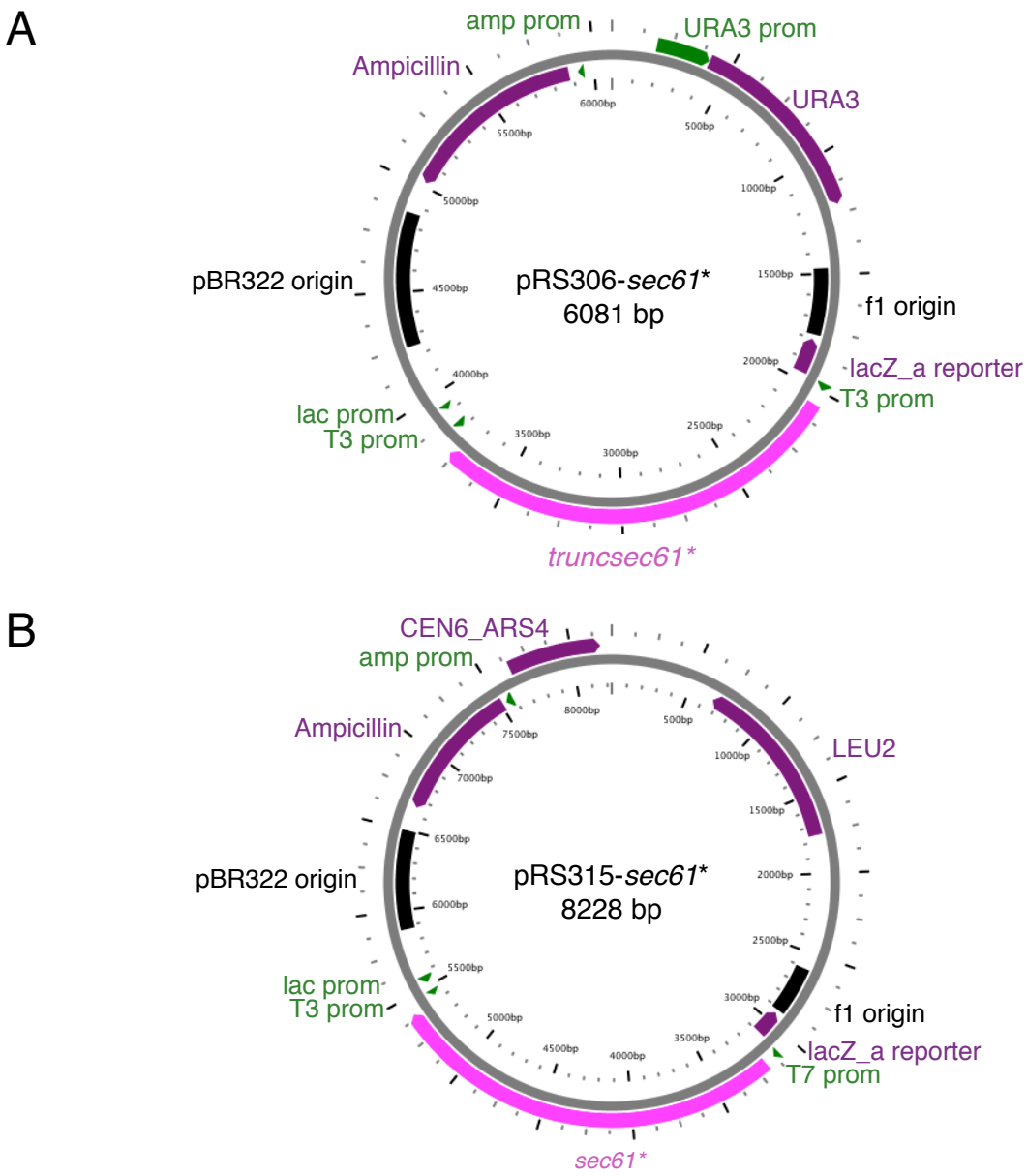

Figure 2.1.3.2. Simplified plasmid maps of the pRS306-*truncsec61 and pRS315 -*sec61** constructs.** The mutated versions of *SEC61* were generated by SOE-PCR (ref. 2.2.4.1, Table 2.14). (A) Truncated versions of the respective *sec61* mutants were cloned into the *Hind*III site (*truncsec61-S179P, truncsec61-S353C, truncsec61-S179P/ S353C*) or the *Eco*RI/*Xho*I site (*truncsec61-302, truncsec61-303*) of pRS306. The constructs were used to transform KRY47 (+ KRY159, KRY160). An *Sfi*I restriction site (nucleotide exchange: T201G → resulting aa substitution: R67R) was introduced into the truncated *sec61* mutants by SOE-PCR. Linearization of the pRS306-*truncsec61** constructs with *Sfi*I prior to transformation creates linear ends that are recombinogenic which directs integration to the site in the genome that is homologous to these ends. The yeast strains constructed with the pRS306-*truncsec61** plasmids were examined by PCR analysis to confirm the correct site of integration. (B) Full-length versions of the respective *sec61* mutants were cloned into the *Hind*III site of pRS315 to create the desired pRS315-*sec61** constructs. The *sec61* mutants were generated by SOE-PCR (ref. 2.2.4.1, Table 2.14). The constructs were used to transform KRY858 (JDY638).
(* designates *(trunc)sec61-S179P, (trunc)sec61-S353C, (trunc)sec61-S179P/S353C, truncsec61-302 and truncsec61-303*).

2.1.4 PRIMERS

Primers used in this study (e.g. in order to create the appropriate *sec61* constructs (ref. Figure 2.1.3.1 and 2.1.3.2)) are listed in Table 2.6.

Table 2.6. Oligonucleotides used in this study.

Name	Sequence (5' → 3')	Length (Tm [°C]*)	Application
5' *Hin*dIII SEC61 5'UTR #-445 (445 bp upstream of ATG)	aagcttAAGCTTGCTATAAGC TAGAATGTATTGAATGTAT TC	36 (59)	SOE-PCR full length *sec61* mutants (#-445=bp upstream of ATG)
5' *Eco*RI SEC61#57 (57 bp downstream of ATG)	gaattcAGTGATTGCTCCAG AAAGGAAGGTTCC	27 (60)	Truncated *sec61-302*, *sec61-303*
5' *Hin*dIII SEC61#57 (57 bp downstream of ATG)	aagcttAGTGATTGCTCCAG AAAGGAAGGTTCC	27 (60)	SOE-PCR (truncated *sec61* mutants; #57=bp downstream of ATG)
5' SOE SEC61 T201G (R67R)	CTGTACTGGCTACGGGCC ATGCTGGC	26 (66)	SOE-PCR (truncated *sec61* mutants; T201G, silent mutation→*Sfi*I site creation)
3' SOE SEC61 T201G (R67R)	GCCAGCATGGCCCGTAGC CAGTACAG	26 (66)	SOE-PCR (truncated *sec61* mutants; T201G, silent mutation→*Sfi*I site creation)
5' SOE SEC61 T535C (S179P)	GTTACGGCTTGGGTCCCG GTATTTCTCTG	29 (64)	SOE-PCR (*sec61-S179P*; T535C)
3' SOE SEC61 T535C (S179P)	CAGAGAAATACCGGGACC CAAGCCGTAAC	29 (64)	SOE-PCR (*sec61-S179P*; T535C)
5' SOE SEC61 C1058G (S353C)	CATTAATGTCTTTATGCGA AGCTCTTCTGGAC	32 (61)	SOE-PCR (*sec61-S353C*; C1058G)
3' SOE SEC61 C1058G (S353C)	GTCCAGAAGAGCTTCGCA TAAAGACATTAATG	32 (61)	SOE-PCR (*sec61-S353C*; C1058G)
3' SEC61 3'UTR #1765 *Hin*dIII	aagcttGCGCATTTGCTTAAG CAAGGATACC	25 (58)	SOE-PCR(*sec61* mutants) (#1765=bp downstream of ATG)
3' SEC61 3'UTR #1765 *Xho*I	ctcgagGCGCATTTGCTTAA GCAAGGATACC	25 (58)	Truncated *sec61-302*, *sec61-303*
5' SEC61 CHR #403	GCAAGTAGAAAAACTGAC ACTGGTTCACG	29 (60)	*sec61* integration (primer position: chromosomal part of *SEC61* upstream of integrated *sec61*)
3' pRS306 URA3 #621 (621 bp downstream of URA3 ATG)	GTTGACCCAATGCGTCTC CCTTGTC	25 (61)	*sec61* integration (primer position: URA3 marker)
5' *Sal*I Ydj1	gtcgacATGGTTAAAGAAAC TAAGTTTTACGATATTCTA GG	35 (57)	Control PCR for *sec61* integration (target: Ydj1p)
3' Ydj1 *Xba*I	tctagaTCATTGAGATGCACA TTGAACACCTTC	27 (57)	Control PCR for sec61 integration (target: Ydj1p)
Oligo-d(T) 18 rev	TTTTTTTTTTTTTTTTTT	18 (28)	*HAC1* mRNA splice assay
RT-PCR_ACT1 fwd	ATTCTGAGGTTGCTGCTTT G	20 (50)	Control *HAC1* mRNA splice assay
RT-PCR_ACT1 rev	GTGGTGAACGATAGATGG AC	20 (52)	Control *HAC1* mRNA splice assay
RT-PCR_HAC1 fwd	CTGGCTGACCACGAAGAC GC	20 (58)	*HAC1* mRNA splice assay
RT-PCR_HAC1 rev	TTGTCTTCATGAAGTGATG	20	*HAC1* mRNA splice assay

	A	(46)	
T3	ATTAACCCTCACTAAAGGGA	20 (48)	Sequencing
T7	TAATACGACTCACTATAGGG	20 (48)	Sequencing
SEC61 PBW11 SEQ	AAATAGAGGGAGGGGTGTGG	20 (54)	Sequencing

* Tm = 4 x (G+C) + 2 x (A+T) [°C]

2.1.5 ANTIBODIES

Antibodies used in this study are listed in Table 2.7.

Table 2.7. Primary and secondary antibodies used in this study.

Antibody	Use & Dilution	Source
anti-alpha factor (rabbit)	Western blot: 1:2000 IP: 1:100 (per 1.5 OD_{600})	KB Römisch
anti-BiP (rabbit)	Western Blot: 1: 2000	KB Römisch
anti-CPY (rabbit)	Western Blot: 1: 2000 IP: 1:100 (per 1.5 OD_{600})	KB Römisch
anti-Eug1 (rabbit)	Western Blot: 1: 5000	KB Römisch
anti-FLAG M2 monoclonal (mouse)	Proteasome binding assay: 1:2000	Sigma-Aldrich: cat. # F1804 (affinity purified antibody)
anti-FLAG M2 polyclonal (rabbit)	Proteasome binding assay: 1:2000	Sigma-Aldrich: cat. # F7425 (affinity purified antibody)
Agarose-linked anti-FLAG M2	Proteasome purification: 1: 100 (using yeast cytosol extracted from cells with 10000 OD_{600})	Sigma-Aldrich: cat. # A2220
anti-HA (rabbit)	Western Blot: 1: 5000 IP: 1:250 (per 1.5 OD_{600})	Rockland: cat. # 600-401-384S (Anti-HA epitope tag antibody)
anti-mouse (rabbit)	Western Blot: 1: 1000000	Sigma-Aldrich: cat. # A9044
anti-Pdi1p (rabbit)	Western Blot: 1: 5000	KB Römisch
anti-Sbh1p (rabbit)	Western Blot: 1: 5000	KB Römisch
anti-Sec61p (C-terminal) (rabbit)	Western Blot: 1: 2000	KB Römisch (Affinity purified antibody)
anti-Sec61p (N-terminal) (rabbit)	Western Blot: 1: 2000	KB Römisch (Affinity purified antibody (N-terminal peptide: PFESFLPEVIAPERKC))
anti-rabbit (HRP) (goat)	Western Blot: 1:20000 (X-ray) 1:200000 (Biorad Gel Documentation CCD camera)	Rockland™: cat. # 611-1302

2.1.6 ENZYMES

Enzymes routinely used in this study are listed in Table 2.8.

Table 2.8. Enzymes used in this study and their sources.

Enzyme	Company
Restriction enzymes	
*Eco*RI	New England Biolabs (NEB)
*Hin*dIII	NEB
*Msc*I	NEB
*Xba*I	NEB
*Xho*I	NEB
*Sac*I	NEB
*Sal*I	NEB
*Sfi*I	NEB
Polymerases	
KAPA HiFi™ Hot Start Polymerase	Peqlab
Sp6 RNA polymerase	Promega
T7 RNA polymerase	Promega
Reverse transcriptase	
Maxima® RT	Fermentas
Ligase	
Fast-Link™ DNA Ligation Kit	Biozym (Epicentre®)
Other enzymes	
FastAP™ Thermosensitive Alkaline Phosphatase	Thermo Fisher Scientific Inc.
Lyticase	Römisch Lab

2.1.7 MEDIA AND BUFFERS

S. cerevisiae and *E. coli* media routinely used in the course of this study are listed in Table 2.9 and 2.11 respectively. All other media and all buffers are listed in the respective section of this chapter.

Table 2.9. *S. cerevisiae* media used routinely in this study.

Medium	Composition
YP (Yeast Extract, Peptone)	1 (w/v) % Yeast Extract, 2 (w/v) % Peptone (For solid media: 2 (w/v) % Agar-Agar)
YPD* (Yeast Extract, Peptone, Dextrose)	1 (w/v) % Yeast Extract, 2 (w/v) % Peptone, 2 (w/v) % Glucose (For solid media: 2 (w/v) % Agar-Agar)
Minimal Medium**	0.67 (w/v) % Yeast Nitrogen Base without Amino Acids, 0.13 (w/v) % Synthetic Complete Drop-Out Mixture*** (-Ade, -His, -Leu, -Lys, -Trp, -Ura), 2 (w/v) % Glucose, Amino Acids according auxotrophies (ref. Table 2.10) (For solid media: 2 (w/v) % Agar-Agar)

* Glucose was autoclaved separately at a concentration of 50 % and added to the YP solution prior to use.
** For the preparation of minimal medium, all components were dissolved in MilliQ-water and sterile filtered. For 1 L solid media 800 ml water containing agar-agar were autoclaved while all other components were dissolved in 200 ml MilliQ water and filter-sterilized. The two solutions were mixed prior to pouring the minimal medium plates. The supplements Ade, His, Leu, Lys, Trp and Ura were added according to the strains' auxotrophies as listed in Table 2.10.
*** The composition of the synthetic complete "drop-out" mixture used is listed in Table 2.10.

OD_{600} = 1: 2.7 x 10^7 cells (diploid yeast), 2.8 x 10^8 cells (haploid yeast)

Table 2.10. Composition of Synthetic Complete amino acid drop-out mixture* for *S. cerevisiae.*

Formula	mg/l
Adenine	18
L-Alanine	76
L-Arginine HCl	76
L-Asparagine	76
L-Aspartic acid	76
L-Cysteine	76
L-Glutamine	76
L-Glutamic acid	76
Glycine	76
L-Histidine	76
myo-Inositol	76
L-Isoleucine	76
L-Leucine	380
L-Lysine	76
L-Methionine	76
para-Aminobenzoic acid	8
L-Phenylalanine	76
L-Proline	76
L-Serine	76
L-Threonine	76
L-Tryptophan	76
L-Tyrosine	76
Uracil	76
L-Valine	76

* Drop-out mix without Ade, His, Leu, Lys, Trp, and Ura according to Kaiser *et al.*, 1994. The remaining amino acids were added according to the auxotrophies of the strains used.

Table 2.11. *E. coli* media used routinely in this study.

Medium	Composition
LB (Lysogeny Broth)	0.5 % (w/v) Yeast Extract, 1 % (w/v) Tryptone, 0.05 % (w/v) NaCl, 1.0 mM NaOH (For solid media: 2 % Agar-Agar)
LB-Amp	LB with 100 µg/ml Ampicillin* (For solid media: 2 % Agar-Agar)
LB-Kan	LB with 50 µg/ml Kanamycin*
SOC (Super Optimal broth with Catabolite repression)	2 % (w/v) Tryptone, 0.5 % (w/v) Yeast Extract, 0.05 % (w/v) NaCl

* Antibiotics stock solutions were sterile filtered and added to the media prior to use at the designated concentration.

2.2 METHODS

2.2.1 STERILIZATION

All glassware and media were sterilized by autoclaving at 100 kPa and 120 °C for 20 min if not stated otherwise.

2.2.2 GROWTH OF *S. CEREVISIAE*

S. cerevisiae cells were grown at 30 °C in YPD or in minimal medium with continuous shaking at 225 rpm or on YPD or drop out plates at 30 °C if not stated otherwise (ref. Table 2.9 and 2.10).

2.2.3 GROWTH OF *E. COLI*

E. coli cells were grown at 37 °C, if not stated otherwise, in LB medium with continuous shaking at 225 rpm or on LB medium plates (ref. Table 2.11).

2.2.4 POLYMERASE CHAIN REACTION

During Polymerase Chain Reaction (PCR) specific DNA sequences are selectively amplified. This is achieved using short single-stranded oligonucleotides, which are designed to specifically bind to the template DNA at the 5' and 3' end of the target sequence. During the course of the reaction the template DNA is denatured which enables the oligonucleotides to anneal to the template. This allows for the DNA polymerase to bind and synthesize the complementary DNA strand(s).

PCRs essentially consist of three steps and about 20-35 cycles (mainly depending on the DNA polymerase used and the target sequence; ref. Table 2.13). During the first step, the PCR mix (ref. Table 2.12) containing the template DNA is denatured at a high temperature, resulting in single-stranded DNA. Single-stranded DNA is needed in the second step. Primer annealing (step 2) is performed at a lower, sequence-specific temperature to ensure specific binding of the primer pair to the template DNA. During the elongation step (step 3) DNA polymerase extends the primers and adds nucleotides complementary to the template DNA. The target sequence is exponentially amplified by cycling of the three steps 20-35 times.

During this study the DNA polymerase KAPAHiFi™ Hot Start DNA Polymerase (1 U/µl; Peqlab) was routinely used for PCRs if not stated otherwise. The reaction setup was as described in Table 2.12. Temperature and duration of each step (ref. Table 2.13) were optimized for each reaction/sequence. The peqSTAR 2X Gradient Thermocycler (Peqlab) was used routinely for PCRs. The correct size of each PCR product was verified by agarose gel electrophoresis (ref. 2.2.8).

During this study PCR was performed in order to amplify full-length *sec61* and truncated *sec61* containing the appropriate point mutation(s) (ref. Figure 2.1.3.2). *S. cerevisiae SEC61* (amplified from pBW11, ref. Table 2.5) was used as the template. Gene-specific primers (ref. Table 2.6) for the amplification of the *SEC61* gene and for the introduction of the respective point mutation(s) were designed using the *SEC61* sequence (www. yeastgenome.org). The resulting PCR products were cloned into pRS315 (full-length *sec61*) and pRS306 (truncated *sec61*) to create the respective constructs.

Table 2.12. Standard reaction mixture for PCRs.

PCR Reaction		
Component	**Volume (µl)**	**Final concentration/ Quantity**
5X KAPAHiFi™ Reaction Buffer	10	1X
KAPA dNTP Mix (10 mM each)	1.5	0.3 mM
Forward primer (10 µM)	1.5	0.3 µM
Reverse primer (10 µM)	1.5	0.3 µM
Template DNA	1	10 ng plasmid DNA
KAPAHiFi™ Hot Start DNA Polymerase (1 U/µl)	1	0.02 U/µl
dH_2O	to 50	---

Table 2.13. Standard thermal cycler program for PCRs.

Step	Operation	Temperatur (°C)	Duration
1	Initial template denaturation	95	5 sec
2	Template denaturation	98	20 sec
3	Primer annealing	57*	15 sec
4	Primer extension	72	30 sec/ kb
Steps 2 to 4 were cycled 35 times			
5	Final primer extension	72	5 min
6	Store	4	∞

* Primer annealing for the generation of all *sec61* mutants was performed at 57 °C. For all other PCRs (eg. *HAC1* mRNA splice assay) primer annealing was performed at the Tm given in Table 2.6 or in the respective section of this chapter.

2.2.4.1. SPLICE OVERLAP EXTENSION (SOE) PCR

PCR-driven overlap extension was used for site-directed mutagenesis during this study in order to generate the desired *sec61* mutants. During SOE-PCR overlapping gene fragments are generated that are then used as templates in order to generate the fused (full-length) product. By choosing appropriate internal primers overlapping, complementary 3' ends in the intermediate fragments are created and the desired nucleotide exchange is introduced. The intermediate fragments are then fused together in a final PCR using flanking primers (Ho *et al.*, 1989; Horton *et al.*, 1989; ref. Figure 2.2.4.1.1).

During SOE-PCR segments of the target sequence (*SEC61*) were amplified using template DNA (pBW11) and specific sets of primers (ref. Table 2.6). Mutagenic primers were designed complementary to each other (about 30 bp) containing the desired nucleotide exchange in the centre

of the primer. This results in two fragments that share a complementary sequence of about 30 bp at their 3' end (fragment 1) and 5' end (fragment 2). During a second PCR using the flanking primers, the complementary overlapping sequences hybridize which leads to the extension of the full-length PCR product (ref. Figure 2.2.4.1.1). Flanking primers also contained restriction sites (*Hin*dIII (or *Eco*RI/*Xho*I for *sec61-302* and *sec61-302*; ref. Table 2.6) for cloning into pRS315 (full-length *sec61*) or pRS306 (truncated *sec61*).

The SOE-PCR protocol was essentially as previously described (Heckman and Pease, 2007). The reaction setups were as described in Table 2.14.

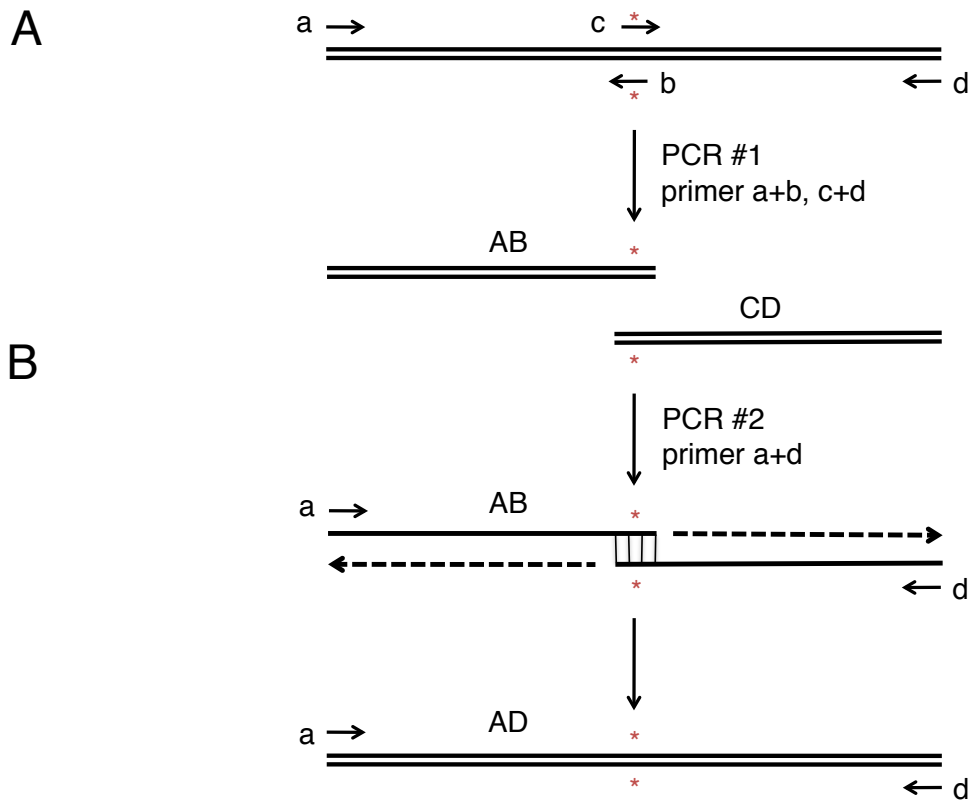

Figure 2.2.4.1.1. SOE-PCR. (A) Site-directed mutagenesis using PCR-driven overlap extension is achieved by using flanking primers (a and d) and mutagenic primers (b and c) to generate the overlapping intermediate PCR products AB (primer a + b) and CD (primer c + d). (B) Fragments AB and CD are then used as templates in the next PCR using the flanking primers a and d. The intermediates hybridize at their overlapping complementary 3' ends and are fused together generating the full-length PCR product AD (adapted from Heckman & Pease, 2007).

Table 2.14. SOE-PCR setups for the generation of *sec61* mutants*.

***SEC61* mutation**	**Fragment No.**	**Primer Pair**	**Template**
sec61-S179P (full-length)	S179P #1	5' *Hin*dIII SEC61 5'UTR #-445 3# SOE SEC61 T535C	pBW11
	S179P #2	5' SOE SEC61 T535C 3' SEC61 3'UTR #1765 *Hin*dIII	
	S179P #3 (S179P #1 + 2 fusion)	5' *Hin*dIII SEC61 5'UTR #-445 3' SEC61 3'UTR #1765 *Hin*dIII	S179P #1 S179P #2
sec61-S353C (full-length)	S353C #1	5' *Hin*dIII SEC61 5'UTR #-445 3' SOE SEC61 C1058G	pBW11
	S353C #2	5' SOE SEC61 C1058G 3' SEC61 3'UTR #1765 *Hin*dIII	
	S353C #3 (S353C #1 + 2 fusion)	5' *Hin*dIII SEC61 5'UTR #-445 3' SEC61 3'UTR #1765 *Hin*dIII	S353C #1 S353C #2
sec61-S179P/S353C (full-length)	S179P/S353C #1	5' *Hin*dII SEC61 5'UTR #-445 3' SOE SEC61 T535C	pBW11
	S179P/S353C #2	5' SOE SEC61 T535C 3' SOE SEC61 C1058G	
	S179P/S353C #3	5' SOE SEC61 C1058G 3' SEC61 3'UTR #1765 *Hin*dIII	
	S179P/S353C #4 (S179P/S353C #1 + 2 fusion)	5' *Hin*dIII SEC61 5'UTR #-445 3' SOE SEC61 C1058G	S179P/S353C #1 S179P/S353C #2
	S179P/S353C #5 (S179P/S353C # 3 + 4 fusion)	5' *Hin*dIII SEC61 5'UTR #-445 3' SEC61 3'UTR #1765 *Hin*dIII	S179P/S353C #3 S179P/S353C #4
truncsec61-S179P (truncated)	truncS179P #1	5' *Hin*dIII SEC61 #57 3' SOE SEC61 T201G	pBW11
	truncS179P #2	5' SOE SEC61 T201G 3' SOE SEC61 T535C	
	truncS179P #3 (S179P #1+ 2 fusion)	5' *Hin*dIII SEC61 #57 3' SOE SEC61 T535C	truncS179P #1 truncS179P #2
	truncS179P #4	5' SOE SEC61 T535C 3' SEC61 3'UTR #1765 *Hin*dIII	pBW11
	truncS179P #5 (S179P/S353C # 3 + 4 fusion)	5' *Hin*dIII SEC61 #57 3' SEC61 3'UTR #1765 *Hin*dIII	truncS179P #3 truncS179P #4
truncsec61-S353C (truncated)	truncS353C #1	5' *Hin*dIII SEC61 #57 3' SOE SEC61 T201G	pBW11
	truncS353C #2	5' SOE SEC61 T201G 3' SOE SEC61 C1058G	
	truncS353C #3 (S353C #1 + 2 fusion)	5' *Hin*dIII SEC61 #57 3' SOE SEC61 C1058G	truncS353C #1 truncS353C #2
	truncS353C #4	5' SOE SEC61 C1058G 3' SEC61 3'UTR #1765 *Hin*dIII	pBW11
	truncS353C #5 (truncS353C #3 + 4 fusion)	5' *Hin*dIII SEC61 #57 3' SEC61 3'UTR #1765 *Hin*dIII	truncS353C #3 truncS353C #4
truncsec61-S179P/S353C (truncated)	truncS179P/S353C #1	5' *Hin*dIII SEC61 #57 3' SOE SEC61 T201G	pBW11
	truncS179P/S353C #2	5' SOE SEC61 T201G 3' SOE SEC61 T535C	
	truncS179P/S353C #3 (truncS179P/S353C #1 + 2 fusion)	5' *Hin*dIII SEC61 #57 3' SOE SEC61 T535C	truncS179P/S353C #1 truncS179P/S353C #2
	truncS179P/S353C #4	5' SOE SEC61 T535C 3' SOE SEC61 C1058G	pBW11
	truncS179P/S353C #5	5' SOE SEC61 C1058G	

	truncS179P/S353C #5	3' SEC61 3'UTR #1765 *Hin*dIII	
	truncS179P/S353C #6 (truncS179P/S353C # 4 + 5 fusion)	5' SOE SEC61 T535C 3' SEC61 3'UTR #1765 *Hin*dIII	truncS179P/S353C #4 truncS179P/S353C #5
	truncS179P/S353C #7 (truncS179P/S353C #3 + 6 fusion)	5' *Hin*dIII SEC61 #57 3' SEC61 3'UTR #1765 *Hin*dIII	truncS179P/S353C #3 truncS179P/S353C #6
truncsec61-302 (truncated)	trunc302 #1	5' *Eco*RI SEC61 #57 3' SOE SEC61 T201G	Plasmid #14 (C. Ng)
	trunc302 #2	5' SOE SEC61 T201G 3' SEC61 3'UTR #1765 *Xho*I	
	trunc302 #3 (trunc302 # 1 + 2 fusion)	5' *Eco*RI SEC61 #57 3' SEC61 3'UTR #1765 *Xho*I	trunc302 #1 trunc302 #2
truncsec61-303 (truncated)	trunc303 #1	5'*Eco*RI SEC61 #57 3' SOE SEC61 T201G	Plasmid #18 (C. Ng)
	trunc303 #2	5' SOE SEC61 T201G 3' SEC61 3'UTR #1765 *Xho*I	
	trunc303 #3 (trunc303 #1 + 2 fusion)	5' *Eco*RI SEC61 #57 3' SEC61 3'UTR #1765 *Xho*I	trunc303 #1 trunc303 #2

* Table 2.14 describes the PCR setup, i.e. combination of templates and primers for the generation of each individual *sec61* mutant.

2.2.5 LARGE SCALE EXTRACTION OF PLASMID DNA

Large-scale extraction of plasmid DNA from *E. coli* was prepared using the GenElute™ HP Plasmid Maxiprep Kit (Sigma-Aldrich). In brief, a single colony was picked from an LB-Amp (or LB-Kan) plate and used to inoculate 150 ml of LB medium (1.0 % (w/v) Tryptone, 0.5 % (w/v) Yeast Extract, 0.05 % (w/v) NaCl, 1.0 mM NaOH) containing either 100 µg/ml Amp or 50 µg/ml Kan (depending on the plasmid's selection marker). The culture was incubated overnight at 37 °C with rapid shaking. The next day, bacteria were harvested by centrifugation (rotor: SLA-3000; Sorvall Evolution® RC centrifuge) at 5400 rpm, RT for 10 min. Plasmid DNA was then extracted using the GenElute™ HP Plasmid Maxiprep Kit according to the supplied protocol as follows. The cell pellet was resuspended in 12 ml of Resuspension/RNase A Solution. For cell lysis 12 ml of Lysis Solution were added to the cells. The mixture was inverted 6 to 8 times. Lysis was for 3 - 5 min at RT. Next, 12 ml of chilled Neutralization Solution were added. The mixture was inverted 4 to 6 times in order to neutralize the lysed cells. Then, 9 ml of Binding Solution were added to the lysate. After careful inversion (1 to 2 times), the lysate was immediately transferred to the barrel of a filter syringe and incubated for 5 min. Columns were equilibrated by adding 12 ml of Column preparation solution to a GenElute™ HP Maxiprep Binding column. The column was centrifuged at 3000 rpm, RT for 2 min (rotor: #11140 (swing-out); SIGMA 4K15 Refrigerated Centrifuge). The eluate was discarded and the cleared lysate was loaded onto the equilibrated column and centrifuged again at 3000 rpm, RT for 2 min. The process was repeated until all of the lysate had been passed through the column. The plasmid DNA bound to the ion exchange resin on the column. In order to remove impurities, the column was

washed with 12 ml of Wash 1 Solution (centrifugation at 3000 rpm, RT for 2 min) followed by a wash with 12 ml of Wash 2 Solution (centrifugation at 3000 rpm, RT for 5 min). The Binding column was transferred to a clean collection tube. Plasmid DNA was eluted by adding 3 ml of Elution Solution to the column, which was centrifuged at 3000 rpm, RT for 5 min. The eluate was transferred to a SS34 polycarbonate tube. Plasmid DNA was precipitated with 0.1 volumes of 3.0 M sodium acetate pH 5.2 and 0.7 volumes of isopropanol and pelleted by centrifugation at 16.000 rpm, 4 °C for 30 min (rotor: SS34; Sorvall Evolution® RC). The plasmid DNA was washed with 70 % (v/v) ethanol (EtOH), recentrifuged as before and air-dried. The plasmid DNA was resuspended in a suitable volume of Milli-Q water. Plasmid DNA was stored at – 20 °C.

2.2.6 SMALL SCALE EXTRACTION OF PLASMID DNA: ALKALINE LYSIS MINIPREPS

The Alkaline Lysis methods by Birnboim and Doly (1979) was employed for the extraction of small amounts of plasmid DNA. In brief, 3 ml of sterile LB medium containing 100 µg/ml Amp or 50 µg/ml Kan were inoculated with one single bacterial colony and shaken overnight at 37 °C. 1.5 ml of the cell culture were transferred to a clean microcentrifuge tube and centrifuged at 13400 rpm, RT for 1 min in a bench top centrifuge (MiniSpin®, Eppendorf) to pellet the cells. The pellet was resuspended in 100 µl of E1 Solution (50 mM Glucose, 25 mM Tris-HCl pH 8.0, 1 mM EDTA pH 8.0) containing 1 µg/ml RNase A (Fermentas) and incubated at RT for 5 min. Cells were then lysed by adding 200 µl of E2 Solution (0.2 M NaOH, 1 % (w/v) SDS). The mixture was inverted and placed on ice for 5 min. Next, 150 µl of E3 Solution (3 M Potassium Acetate pH 4.8) were added. The lysate was mixed by inversion placed back on ice for 5 min, followed by centrifugation at 13400 rpm, RT for 5 min to pellet the cell debris and chromosomal DNA. The supernatant was transferred to a clean microcentrifuge tube and mixed with 800 µl of absolute ethanol. After mixing and incubation at RT for 2 min, the sample was centrifuged at 13400 rpm for 3 min to pellet the plasmid DNA. To remove the salts in the sample, the pellet was washed with 1 ml of 70 % (v/v) ethanol. The ethanol was then discarded and the pellet air-dried. The DNA pellet was resuspended in 20 µl of either sterile TE (10 mM Tris-HCl pH 8.0, 1 mM EDTA pH 8.0) or MilliQ-water. Plasmid DNA was stored at – 20 °C.

2.2.7 ETHANOL PRECIPITATION

DNA precipitation was conducted by adding 1/10 volume of 3 M sodium acetate (pH 5.2) and 2.5 volumes of absolute ethanol to the DNA solution. To precipitate small nucleic acids, the mixture was incubated at – 20 °C for a minimum of 30 min. The pellet was then washed with 1 ml of 70 % (v/v) ethanol and air-dried. The DNA was dissolved in a suitable volume of TE (10 mM Tris-HCl pH 8.0, 1 mM EDTA pH 8.0) or sterile dH_2O and stored at – 20 °C.

2.2.8 AGAROSE GEL ELECTROPHORESIS

Agarose gel electrophoresis was performed to separate, identify and purify DNA fragments. In general, DNA samples were mixed with DNA Loading Dye (6X: 50 % (w/v) Sucrose, 0.15 % (w/v) Bromophenol Blue, 0.02 M EDTA) amd loaded onto a 1 % Agarose Gel (1 % (w/v) Agarose, 2 % (v/v) 50X TAE, 90 % (v/v) dH_2O) containing 0.5 μg ml^{-1} Ethidium Bromide (EtBr)). The gel was placed in a Peqlab gel tank containing 1X TAE buffer (**T**ris **A**cetate **E**DTA; 50X: pH 8.4: 20 M Tris-HCl, 10 M Acetic Acid, 0.05 M EDTA). Electrophoresis was then carried out at 100 - 120 V for ~1-2 hr. GeneRuler™ 1 kb DNA ladder (Fermentas) was used as the size standard (0.5 μg loaded). The gel was placed over a transilluminator for visualization of the DNA, which was photographed using the Molecular Imager ChemiDoc™ XRS (Bio-Rad) or the E-Box VX2 Gel Documentation System (Peqlab).

2.2.9 RECOVERY OF DNA FRAGMENTS

In order to recover DNA from agarose gels, the GenElute™ Gel Extraction Kit (Sigma-Aldrich) was used. The appropriate DNA band was excised from the agarose gel using a sterile scalpel, and then transferred into a 1.5 ml microcentrifuge tube. The gel slice was resuspended in 3 gel volumes of Gel Solubilization Solution. The mixture was incubated at 60 °C until the gel was dissolved followed by the addition of 1 gel volume of 100 % isopropanol. The gel solution was loaded onto an equilibrated binding column and spun for 1 min at full speed in a benchtop centrifuge (MiniSpin®, Eppendorf). The flow-through liquid was discarded each time. Next, 700 μl of Wash Solution were added to the binding column and the column centrifuged for 1 min at RT, full speed. Once all of the gel solution had been passed through the binding column, the column was centrifuged as before in order to remove residual Wash Solution. The DNA was eluted by addition of 50 μl Elution Solution to the membrane of the binding column and incubated for 1 min at RT followed by centrifugation for 1 min at full speed. DNA was stored at – 20 °C until needed.

2.2.10 RESTRICTION DIGESTION OF PCR PRODUCTS AND PLASMID DNA

All endonuclease restriction digestions were carried out in a 50 μl reaction mixture containing the appropriate buffer, as recommended by the supplier (NEB, if not stated otherwise), and 10 units of enzyme per μg of DNA. Reaction mixtures were incubated for 1-2 hr at 37 °C (*Sfi*I: 50 °C) and afterwards heat-inactivated as recommended. Plasmid DNA was then analyzed by gel electrophoresis (ref. 2.2.8).

In the case of two enzymes being used, the buffer in which both enzymes exhibit the highest efficiency was used at the appropriate concentration. The standard reaction mixture is outlined in

Table 2.15. For digestions of larger amounts of DNA, the amounts of enzymes and buffer were increased and the amount of water adjusted accordingly.

Table 2.15. Standard reaction mixture for the restriction digestion of DNA.

Component	DNA	Buffer*	Restriction Enzyme	100 X BSA**	dH_2O
Volume (μl)	x ($1\ \mu$g)	5	1 (10 U)	0.5	to 50

* The buffers were those recommended by the suppliers.
** BSA was added depending on the enzyme.

2.2.11 DEPHOSPHORYLATION OF VECTOR DNA

FastAP™ Thermosensitive Alkaline Phosphatase (Thermo Fisher Scientific) was used to hydrolyze 5' phosphate group prior to each ligation in order to avoid re-ligation of the digested vector. The reaction mix (ref. Table 2.16) consisted of 1 unit of FastAP™ Thermosensitive Alkaline Phosphatase, 1/10 volume of 10X FastAP™ buffer and 1 μg of vector DNA. The sample was incubated at 37 °C for 10 min and heat-inactivated at 65 °C for 15 min.

Table 2.16. Reaction mixture for the dephosphorylation of digested vector DNA.

Component	Digested DNA	10X Buffer	FastAP	dH_2O
Volume (μl)	x ($1\ \mu$g)	2	1	to 20

2.2.12 LIGATION OF VECTOR DNA AND INSERT DNA

In general, following digestion of vector and insert DNA with the appropriate enzyme(s) to create matching sticky ends, the ligation was carried out for 10 min at 22 °C in a thermal cycler using the Fast-Link™ DNA Ligation Kit (Biozym). The reaction mixture contained 10X ligation buffer, 2 units of Fast-Link™ DNA ligase (2 U/μl) and a 3:1 ratio of insert to vector. The reaction was heat-inactivated by incubation at 70 °C for 15 min. Ligations were prepared according to the reaction mixture presented in Table 2.17. Generally, 5 μl of the ligation were used to transform *E. coli* cells.

Table 2.17. Standard reaction mixture for the ligation of vector and insert DNA.

Component	10X Ligation buffer	10 mM ATP	Vector DNA	Insert DNA	H_2O	Fast-Link™ Ligase
Volume (μl)	1.5	1.5	x (50 ng)	y (3:1*)	to 14	1

* Molecular ratio insert : vector

2.2.13 MICRODIALYSIS

Microdialysis was carried out after ligation and prior to electroporation to lower salt concentrations in the sample and thus to increase the efficiency of electroporation and to prevent later shorting of the Bio-Rad MicroPulser™ electroporator. Therefore, the ligation products were placed onto a Millipore filter paper (0.25 μm) floating on sterile MilliQ-water in a Petri dish for 1 hr.

2.2.14 TRANSFORMATION OF *E. COLI* CELLS WITH PLASMID DNA

2.2.14.1 PREPARATION OF ELECTROCOMPETENT CELLS

Preparation of electrocompetent cells was performed according to a procedure described by Dower *et al.* (1988). All steps in this protocol were performed at 4 °C or on ice. 1 L of LB was inoculated with 10 ml of an overnight culture (1/100 dilution) of Top10 or DH5α cells. The cells were grown with vigorous shaking at 37 °C until an OD_{600} of 0.5 - 0.6 was reached. The culture was harvested by centrifugation at 5200 rpm for 10 min (rotor: SLA3000, Sorvall Evolution® RC Centrifuge). The supernatant was discarded and the cells were washed with 1 L and 0.5 L of cold sterile MilliQ H_2O respectively and centrifuged as before. The pellets were resuspended in 20 ml of cold 10 % (v/v) glycerol and centrifuged at 3500 rpm for 10 min. Finally, the cells were resuspended in 3 ml of 10 % (v/v) glycerol and 100 μl aliquots of the electrocompetent cells were transferred to sterile microcentrifuge tubes and stored at – 80 °C.

2.2.14.2 TRANSFORMATION OF ELECTROCOMPETENT CELLS

For electroporation, 100 μl aliquots of electrocompetent cells were thawed on ice and the appropriate DNA was added. The cells and DNA were then transferred to a pre-chilled electroporation cuvette (Peqlab #71-2020). The cuvette with a 0.2 cm gap was placed into the cuvette chamber and pulsed using a Bio-Rad MicroPulser™ electroporator at 200 Ω, 2.5 V, 25 μFD. The sample was immediately resuspended in 1 ml ice-cold SOC medium (0.5 % (w/v) Yeast Extract, 2 % (w/v) Tryptone, 10 mM NaCl, 2.5 mM KCl, 10 mM $MgCl_2$, 10 mM $MgSO_4$*$7H_2O$, 20 mM Glucose), transferred to a 1.5 ml microcentrifuge tube and incubated at 37 °C for 1 hr with vigorous shaking to allow cells to recover. Serial dilutions (neat - 10^{-3}) were prepared from the cell suspension and 100 μl plated on LB Agar plates containing the appropriate antibiotic. The plates were incubated at 37 °C overnight. The next day, single colonies were selected for screening. All clones that were found to be real transformants were named, purified and stored at - 80 °C in 50 % (v/v) glycerol.

2.2.14.3 TRANSFORMATION OF CHEMICALLY COMPETENT CELLS

The NEB 5-alpha (high efficiency) chemically competent *E. coli* cells (cat. # C2987, NEB) were used for transformations with the appropriate constructs when transformations using electrocompetent cells was unsuccessful.

Transformation was performed according to the supplier's instructions. In brief, NEB 5-alpha cells were carefully thawed on ice and 50 µl of competent cells were used per transformation. Next, about 5 µl (~ 50 ng DNA) of plasmid DNA was added to the cells and the microcentrifuge tube was gently flicked 5 times to mix DNA and cells. The mixture was incubated on ice for 30 minutes followed by a heat shock at 42 °C for 30 seconds. The mixture was then placed back on ice and incubated for another 5 minutes. For cell recovery the sample was incubated in 950 µl of RT SOC medium at 37 °C and 250 rpm for 1 hr. Following the incubation several serial dilutions (neat - 10^{-3}) were prepared and 100 µl of each dilution plated onto LB agar plates containing the appropriate antibiotic. The plates were incubated at 37 °C overnight. The next day, single colonies were selected for screening. All clones that were found to be real transformants were named, purified and stored at – 80 °C in 50 % (v/v) glycerol.

2.2.15 DNA SEQUENCING

In order to analyze DNA sequences all plasmids were sequenced. Miniprep DNA samples of all transformants of interest were sent for sequencing. Sequencing (single read sequencing) was performed by GATC Biotech AG (Konstanz) according to the sequencing method by Sanger *et al.* (1977). For sequencing of the various *sec61* sequences the primer T3, T7 and SEC61 PBW11 SEQ (ref. Table 2.6) were routinely used if not stated otherwise. The results were analyzed with the Vector NTI® (Invitrogen) software.

2.2.16 PREPARATION OF LYTICASE

Preparation lyticase was accordimg to a protocol from R. Schekman's laboratory. In brief, from a 200 ml overnight culture of the strain RSB805 10 L (8 x 1.25 L) LB-Amp medium were inoculated with 15 ml of the culture. Cells were grown at 37 °C, 200 rpm to an OD_{600} of 0.5. The cultures were then induced with IPTG which was added to a concentration of 0.5 mM each. Inducation was usually for 5 hr at 37 °C, 200 rpm. Cells were harvested for 10 min, 4 °C, 4200 rpm (rotor: SLA3000, Sorvall Evolution® RC Centrifuge). Pellets were resuspended with ∑ 400 ml 25 mM Tris pH 7.4 and pooled. The resulting pellet was centrifuged for 5 min, 4 °C at 8000 rpm. The supernatant was discarded and the pellet resuspended with ~ 200 ml 25 mM Tris pH 7.4/2 mM EDTA. An equal volume of 25 mM Tris pH 7.4/ 40 % sucrose was slowly added to the suspension which was stirred very slowly for 20

min at RT on a magnetic stirrer (RH basic 2 IKAMAG®, IKA®). The suspension was then centrifuged as before and the supernatant discarded carefully (in the cold room) as the resulting pellet was very soft. The pellet was resuspended with 150 ml of ice-cold 0.5 mM $MgSO_4$, slowly stirred in the cold room for 20 min and centrifuged as before. The supernatant containing the lyticase was aliquoted in 15 ml falcon tubes, snap-frozen in liquid nitrogen and stored at – 80 °C. Lyticase activity was determined using the yeast strain RSY255 (or RSY607) (ref. Table 2.18). RSY255 (~ 50 ml) was grown in YPD to an OD_{600} of 2, harvested for 5 min at 4200 rpm (rotor: SS34, Sorvall Evolution® RC Centrifuge), RT and resuspended with 50 mM Tris-HCL pH 7.4/ 10 mM DTT to an OD_{600} of ~ 2 ($OD_{600\ START}$). Aliquots (1 ml) of the yeast culture (duplicates or triplicates) were incubated with various concentrations of lyticase (0.2, 1.0, 2.0, 5.0, 10 µl). Samples were incubated at 30 °C for 30 min and the OD_{600} was immediately measured. The lyticase activity was determined as follows.

Table 2.18. Calculation of lyticase activity (example: $OD_{600\ START}$ = 1.85).

Volume Lyticase (µl/ml)	**0.2**	**0.5**	**1.0**	**2.0**	**5.0**	**10.0**
Lyticase preparation Sample 1	0.75	0.36	0.17	0.04	0.01	0.05
Lyticase preparation Sample 2	0.75	0.36	0.14	0.08	0	0.02
% $OD_{600\ START}$	40.5	19.5	8.4	3.2	-	-
Δ %	**59.5**	80.5	91.6	96.8	-	-
10 % of Δ %	**5.95**					
(10 % of Δ %)/$V_{Lyticase}$	**5.95/0.2 µl**					
Units/ml	**29750 U/ml**					

2.2.17 TRANSFORMATION OF *S. CEREVISIAE*

Transformation of *S. cerevisiae* using the Lithium Acetate method (LiAc/SS-DNA/PEG) procedure was as described by Gietz *et al.* (1995) and Gietz & Woods (2002). Briefly, a 50 ml culture of *S. cerevisiae* was grown overnight at 30 °C with vigorous shaking. The cells were harvested at 5000 rpm for 5 min at RT (rotor: #12169, Sigma 4K15 Refrigerated Centrifuge) and washed in 25 ml of sterile dH_2O. The pellet was resuspended in 1 ml of 100 mM LiAc and centrifuged for 30 sec at 8000 rpm (Microcentrifuge 5415R, Eppendorf), RT. The pellet was then resuspended in 100 mM LiAc to a final volume of 500 µl. Aliquots of 50 µl were used for the transformation. The 50 µl were centrifuged for 30 sec at full speed, RT. For the transformation the ingredients were added in the following order: 240 µl 50 (w/v) % PEG (MW 3350), 36 µl 1 M LiAc, 50 µl of carrier DNA (DNA from salmon testes, 2 mg/ml (Sigma), boiled for 5 min prior to use), 50 µl plasmid DNA* (~ 1 µg). The mixture was vortexed for 1 min (full speed). The transformation was incubated for 30 min at 30 °C

followed by 20 min at 42 °C (water bath). The samples were centrifuged for 1 min at 8000 rpm. The transformation mix was discarded and the cell pellet was taken up in 200 µl TE (10 mM Tris-HCl pH 8.0, 1 mM EDTA pH 8.0). Cells were plated onto the appropriate minimal medium plates and incubated at 30 °C for 2-4 days. The LiAc method was applied to transform the *S. cerevisiae* strains RSY255 (pRS306-*truncsec61* constructs) and JDY638 (pRS315-*sec61* constructs) with the appropriate plasmid DNA (ref. Table 2.5) to create the desired *sec61* strains. Moreover, it was used to transform *sec61* strains etc. with the appropriate CEN plasmids for various assays.

* The transformation with yeast integrative plasmids required the linearization of the respective plasmid DNA prior to transformation (ref. 2.2.18). This allows for directed integration of the respective sequence into the yeast genome.

2.2.18 VERIFICATION OF *S. CEREVISIAE* TRANSFORMANTS

For transformations into RSY255 plasmid DNA was linearized prior to transformation to allow for integration of the respective sequence into the yeast genome. Digestion with *Sfi*I (NEB) was as described in Table 2.15. The reaction mix was incubated at 50 °C for 1 hr and then immediately used for transformation.

Verification of the various *sec61* strains was as follows. Positive transformants in the RSY255 background were picked and plated onto minimal medium plates lacking URA (growth) or LEU (no growth) using appropriate strains as positive and negative controls. True positive transformants were further analyzed. First, genomic DNA was isolated (ref. 2.2.22) which was used in a PCR (ref. 2.2.4) with the primers 5' *Hin*dIII SEC61 5'UTR #-445 and 3' pRS306 URA3 #621 to verify proper integration of the desired *sec61* sequence from the respective pRS306-*truncsec61** construct into the yeast genome.

Transformants (pCEN-*LEU2-sec61**) in the JDY638 (pGAL-*SEC61* promotor) background were verified by plating onto minimal medium w/o LEU (2 % (w/v) Galactose/ 0.2 % (w/v) Raffinose) after the transformation. Plates were incubated at 30 °C for 2-4 days. Transformants that came up were plated onto both YPD and 5-FOA plates (0.002 % (w/v) Uracil, supplements according to auxotrophies (lacking Uracil)*, 0.67 % (w/v) YNB w/o Amino Acids, 2 % (w/v) Glucose, 2 % (w/v) Agar, 0.1 % (w/v) 5-Fluoroorotic acid (Fermentas)). Real positive transformants were able to grow on both plates.

* According to Table 2.10.

2.2.19 *S. CEREVISIAE* GROWTH ON PLATES (DROP TEST)

Drop tests were performed as follows. For overnight cultures 5 ml YPD were inoculated with a single colony of the respective yeast strain and incubated at 30 °C and 220 rpm. The next day the cells were counted in a hemocytometer (Neubauer improved) and the cell number per ml was determined. For each strain serial dilutions in sterile dH_2O were prepared and 5 µl of each dilution were dropped onto YPD or minimal medium (concentrations on plate: 10^5 – 10^0). The plates were incubated at various temperatures (usually: 20, 25, 30 and 37 °C) for 3 days.

2.2.20 *S. CEREVISIAE* TRANSLOCATION ASSAY

The translocation assay was performed in order to verify whether any of the newly generated JDY638 (pGAL-*SEC61*) derivatives with pCEN-*LEU2-sec61** (sec61*: *sec61-S179P, sec61-S353C, sec61-S179P/S353C*) were defective in either co- or posttranslational import compared to *sec61-302*, *sec61-303* and *SEC61*. Each yeast strain was therefore transformed with the reporter plasmids pDN106 (pRS313-*CPY-URA3*; posttranslational import), or pJN203 (pRS313-*PHO8-URA3*; cotranslational import), or the empty vector pRS313 (control) (Sikorski & Hieter, 1989; Ng *et al.*, 1996; 2007). Cells were plated onto HIS-LEU d/o plates and incubated for 2 - 4 days at 30 °C. Overnight cultures of positive transformants were prepared and incubated overnight at 30 °C and 225 rpm. Serial dilutions of each strain were prepared and dropped onto minimal medium w/o HIS/LEU/URA (monitors translocation defect for *URA3* reporter) and w/o HIS/LEU d/o (monitors Sec61p function, i.e. maintenance of *SEC61*-containing plasmid) plates (10^{5}-10^{1}). Plates were incubated at 30 °C for 3 days.

2.2.21 ISOLATION OF *S. CEREVISIAE* RNA

The preparation of yeast RNA was according to Current Protocols in Molecular Biology (ref. chapter 13.12.1: Preparation of yeast RNA by Extraction with Hot Acidic Phenol). In brief, 10 ml of a yeast culture were grown to an OD_{600} of 1 at 30 °C, 220 rpm. Cells were harvested for 5 min at 4 °C, 7000 rpm (rotor: #11140; Sigma 4K15 Refrigerated Centrifuge). The supernatant was discarded and the pellet was resuspended in 1 ml of ice-cold RNase-free dH_2O (DEPC-treated) and transferred to clean RNase-free microcentrifuge tube. The cells were centrifuged at full speed, 4 °C for 10 sec (Microcentrifuge 5415R, Eppendorf). The supernatant was discarded and the pellet resuspended with 400 µl TES Solution (10 mM Tris-HCl pH 7.7, 10 mM EDTA, 0.5 % (w/v) SDS). Next, 400 µl of Acid Phenol (Roti®-Aqua-Phenol, C. Roth) were added and the sample vortexed for 10 sec and incubated at 65 °C for 1 hour with occasional vortexing. After the incubation step, the sample was placed on ice for 5 min, followed by a centrifugation at full speed, 4 °C for 5 min (Microcentrifuge

5415R, Eppendorf). The aqueous (top) phase was transferred to a clean microcentrifuge tube. 400 µl Roti®-Aqua-Phenol were added and the sample was vortexed for 20 sec, incubated on ice for 5 min and centrifuged as before. The resulting aqueous phase was transferred to a clean microcentrifuge tube and mixed with 400 µl chloroform, vortexed for 20 sec and centrifuged as before. The aqueous phase was transferred to a clean microcentrifuge tube and 40 µl of 3 M NaAc (pH 5.3) and 1 ml of ice-cold 100 % ethanol were added. The sample was vortexed and centrifuged as before. The resulting pellet was washed with 1.5 ml 70 % (v/v) ethanol, centrifuged as before and resuspended in 50 µl RNase-free dH_2O (DEPC-treated). The concentration was determined by measuring the OD_{260} of a 1:200 dilution in dH_2O. RNA was stored at – 20 °C.

2.2.22 ISOLATION OF *S. CEREVISIAE* CHROMOSOMAL DNA

Yeast chromosomal DNA was prepared according to Hoffman & Winston (1987). In brief, 10 ml of a yeast overnight culture (in YPD or the appropriate drop-out medium) were harvested at 3000 rpm, RT for 5 min (rotor: #11140, SIGMA 4K15 Refrigerated Centrifuge). The pellet was resuspended in 0.5 ml of cold dH_2O. The cells were transferred to a 1.5 ml microcentrifuge tube and centrifuged for 5 sec at full speed, RT (MiniSpin® Centrifuge, Eppendorf). The supernatant was discarded and the pellet resuspended in 200 µl Breaking Buffer (2 % (v/v) Triton X-100, 1 % (w/v) SDS, 100 mM NaCl, 100 mM Tris-HCl pH 8.0, 1 mM EDTA pH 8.0). Next, 1 volume (~ 0.3 g) of acid-washed glass beads and 200 µl of PCI (Phenol/Chloroform/Isoamyl Alcohol, 25:24:1) were added. The sample was vortexed for 3 min at full speed. Next, 200 µl of TE Buffer (10 mM Tris-HCl pH 8.0, 1 mM EDTA pH 8.0) were added. The sample was vortexed briefly and centrifuged at full speed for 5 min. The resulting aqueous phase was transferred to a clean microcentrifuge tube and 1 ml 100 % EtOH was added. The sample was mixed by inversion and centrifuged for 3 min at full speed. The pellet was resuspended in 400 µl TE Buffer. 15 µl of DNase-free RNase (10 mg/ml, Fermentas) were added and the mixture incubated for 10 min at 37 °C. After the incubation, 10 µl 4 M Ammonium Acetate and 1 ml 100 % EtOH were added, the sample was mixed by inversion and centrifuged at full speed for 3 min. The supernatant was discarded, the pellet dried at RT and resuspended in 100 µl TE buffer. Yeast DNA concentration was determined by measuring the OD_{260} of a 1:200 dilution of the sample in dH_2O.

2.2.23 PREPARATION OF CELL EXTRACTS

For the preparation of yeast cell extracts fresh overnight cultures were used to inoculate 25 ml YPD. Cells were grown to an OD_{600} of 2 at 30 °C, 220 rpm. Next, cells were harvested at 8000 rpm for 1 min (MiniSpin® Centrifuge, Eppendorf) and the supernatant was discarded. The pellet was

resuspended in 120 ml 1X SDS-PAGE Sample Buffer (62.5 mM Tris-HCl pH 6.8, 2 % (w/v) SDS, 5 % (v/v) β-Mercaptoethanol, 0.001 % (w/v) Bromophenol Blue, 10 % (v/v) Glycerol). About 100 µl of glass beads (acid washed glass beads 400 – 600 µm, Sigma) were added and the cells disrupted in the cold room using a bead beater (Mini-Beadbeater-24; Bio Spec Products Inc.). Disruption was conducted 3 times for 1 min (with 1 min incubation on ice between each cycle). The samples were heated for 10 min at 65 °C and centrifuged at 12000 rpm for 1 min. The supernatant was transferred to a clean microcentrifuge tube, mixed and aliquoted into 20 µl, snap frozen in liquid nitrogen and stored at – 20 °C. Samples were analyzed by Western Blot Analysis (ref. 2.2.24).

2.2.24 PROTEIN GEL ELECTROPHORESIS AND WESTERN BLOT ANALYSIS

2.2.24.1 PROTEIN GEL ELECTROPHORESIS

Protein gel electrophoresis (SDS-PAGE) was routinely conducted using NuPAGE® Novex® Pre-Cast Bis-Tris gels (generally 4-12 % gels, 1.5 mm, 10 wells) and the XCell SureLock™ Mini-Cell (both Invitrogen) if not stated otherwise.

Prior to loading an appropriate volume of the protein sample onto the gel, samples were prepared by adding the appropriate volume of 4X SDS-PAGE Sample Buffer (4X: 240 mM Tris-HCl pH 6.8, 8 % (w/v) SDS, 20 % (v/v) β-Mercaptoethanol, 0.004 % (w/v) Bromophenol Blue, 40 % (v/v) Glycerol) and heating samples at 95 °C (60 °C for membrane proteins) for 5 min in a block heater (Thermomixer® comfort (Eppendorf) or block heater SBH200D/3, Stuart®). The samples were run in 1X NuPAGE® MOPS SDS Running Buffer (Invitrogen) at 150-180 V, RT using a Bio-Rad PowerPac™ HC power supply, until the blue dye ran off the bottom of the gel. The PageRuler™ Prestained Protein Ladder or the PageRuler™ Plus Prestained Protein (both Fermentas) were used as the size standard according to the supplier's instructions. The gel was then either stained with Coomassie and dried (ref. 2.2.24.2) or subjected to Western Blot analysis (ref. 2.2.24.3).

2.2.24.2 COOMASSIE STAINING AND DRYING OF PROTEIN GELS

In order to stain proteins for detection on protein gels the EZBlue™ Gel Staining Reagent (Sigma-Aldrich) was used. This reagent is a ready-to-use Coomassie® Brilliant Blue G-250 based stain. Gels were stained according to the supplier's instructions. In brief, after electrophoresis the gel was rinsed 3 times for 5 min with dH_2O. Next, the gel was fixed* for 15 min using Fixing Solution (50 % (v/v) Methanol, 10 % (v/v) Acetic Acid). Following the fixing step, the gel was washed for 15 min with excess dH_2O. The EZBlue™ Gel Staining Reagent (20-40 ml) was added to the gel, which was incubated for 1 hr at RT. The gel was then washed with dH_2O until the background became clear.

The dH_2O was changed frequently to enhance the contrast between the protein bands and the background.
Optional, the protein gel was dried in a gel dryer (Model 583, Bio-Rad) at 80 °C for 1 hr if desired.

* For native gels run in Tris-Glycine Buffer a fixing was not required.

2.2.24.3 WESTERN BLOT ANALYSIS

Western Blotting was employed to identify the desired proteins using appropriate antibodies. Protein transfer and immunoblotting were as follows: Proteins were transferred from the protein gel (ref. 2.2.24.1) onto nitrocellulose (NC) membranes (0.45 μm pore size, Bio-Rad). The blot was assembled using the NC as well as 3 MM Chromatography Paper (Whatman®) and sponges soaked in Transfer Buffer (25 mM Tris, 200 mM Glycine, 20 % (v/v) Methanol, 0.2 % (w/v) SDS). The protein transfer was conducted in Transfer Buffer for 2 hr at 100 V in the cold room using a Trans-Blot® Electrophoretic Transfer Cell (with plate electrodes and super cooling coil, Bio-Rad).
Following the transfer, the membrane was blocked in Blotto (50 mM Tris-HCl pH 7.4, 150 mM NaCl, 2 % (w/v) Milk Powder, 0.1 % (v/v) Tween-20, 5 mM Sodium Azide) for 1 hr shaking at RT. The membrane was then incubated with the primary antibody (diluted in Blotto, ref. Table 2.7) overnight in the cold room shaking. The next day, the membrane was washed twice for 10 min in Blotto followed by 2 washes for 10 min in 1X TBS-T (50 mM Tris-HCl pH 7.4, 150 mM NaCl, 0.1 % (v/v) Tween-20, 5 mM Sodium Azide). Next, the membrane was incubated with the secondary antibody (ref. Table 2.7, generally anti-rabbit 1:200000 in TBS-T for detection with the ChemiDoc™ XRS System) shaking for 1 hr at RT. The membrane was washed 4 times for 10 min with TBS-T.
The blot was prepared for detection using the SuperSignal™ West Dura Extended Duration Chemiluminescent Substrate (Pierce) according to the supplier's instructions. Signals were detected using the Molecular Imager ChemiDoc™ XRS System (Bio-Rad; CCD camera detection) and evaluated/ quantified with the ImageLab™ software (Bio-Rad).

2.2.25 PREPARATION OF ROUGH MICROSOMAL MEMBRANES

The isolation of rough microsomal membranes *from S. cerevisiae* was performed according to Lyman & Shekman (1995) and Pilon *et al.* (1997). Briefly, 2.5-10 L of a yeast culture were grown overnight in YPD at 30 °C and 200 rpm to an OD600 of ~ 2. The cells were harvested at 5000 rpm and RT for 3 min (rotor: SLA3000; Sorvall Evolution® RC centrifuge), the pellet was resuspended in 100 mM Tris-HCl pH 9.4/10 mM DTT to 100 OD_{600}/ml and then incubated for 10 min at RT in order to weaken the cell walls. Cells were pelleted for 5 min at 5000 rpm, RT and then resuspended in Lyticase Buffer (50 mM Tris-HCl pH 7.5, 0.75 X YP, 700 mM Sorbitol, 0.5 % Glucose, 10 mM DTT)

to 100 OD_{600}/ml. Lyticase was added to a final concentration of 40 U per OD_{600} of cells. Incubation was for 20 min at 30 °C, 80 rpm (Multitron Standard Incubation Shaker, Infors HT (Infors AG)). Following the incubation, the cells were chilled on ice for 2 min and then pelleted for 5 min at 5000 rpm, 4 °C. The supernatant was carefully discarded and the pellet washed with 2X JR Buffer (40 mM Hepes-KOH pH 7.4, 400 mM Sorbitol, 100 mM KOAc, 4 mM EDTA) to 250 OD_{600}/ml and centrifuged at 10.000 rpm and 4 °C for 10 min (rotor: SS34, Sorvall Evolution® RC centrifuge). The resulting pellet was resuspended in 2X JR buffer to 500 OD_{600}/ml and frozen at – 80 °C for at least 1 hr.

The spheroplasts were thawed in an ice-cold water bath and mixed with an equal volume of cold MilliQ water. PMSF and DTT were added to a final concentration of 1 mM and the spheroplasts were disrupted with ten strokes of a motor-driven Potter Elvehjem homogenizer (EUROSTAR power basic, IKA®) in the cold room. The lysate was centrifuged for 5 min at 3000 rpm, 4 °C (rotor: SS34; Sorvall Evolution® RC Centrifuge) and the supernatant transferred to a clean polycarbonate SS34 tube and centrifuged at 17500 rpm, 4°C for 15 min to pellet the membranes. The sample was placed on ice and the pellet was resuspended in a minimum volume (~ 0.5 ml) of B88 (20 mM Hepes-KOH pH 6.8; 250 mM Sorbitol; 150 mM KOAc, 5 mM $Mg(OAc)_2$) and gently homogenized on ice using a small teflon pestle and carefully resuspended using a 1000 µl Gilson® pipette. The sample was loaded onto a 1.2 M/1.5 M Sucrose Gradient (20 mM Hepes-KOH pH 7.5, 50 mM KOAc, 2 mM EDTA, 1 mM DTT, 1.2 M or 1.5 M Sucrose) and centrifuged at 44000 rpm, 4 °C for 1 hr (rotor: SW 60 Ti; Optima™ L-90 K Ultracentrifuge). For the sucrose gradient, 1.5 ml of each sucrose solution (1^{st}: 1.5 M, 2^{nd}: 1.2 M) was layered into an SW60Ti tube (Beckman Coulter #344062). ER-derived microsomes were collected at the interphase of the 1.2 M/1.5 M sucrose gradient and washed with 25 ml of cold B88. The sample was centrifuged at 17500 rpm, 4 °C for 15 min (rotor: SS34; Sorvall Evolution® RC Centrifuge). The microsome pellet was carefully resuspended in the appropriate volume of B88. Membrane concentration was measured at OD_{280} in 2 % (w/v) SDS at a 1:100 dilution. The concentration was adjusted to an OD_{280} of ~ 30 with B88 and the samples aliquoted (50 µl), snap-frozen in liquid nitrogen and stored at – 80 °C.

2.2.26 PREPARATION OF RIBOSOME- AND PROTEASOME-STRIPPED MEMBRANES

The preparation of ribosome- and proteasome-stripped membranes (PK-RMs) from RMs by treatment with puromycin and potassium acetate was modified from Neuhof *et al.* (1998). The reaction was set up on ice. In brief, about 3 ml of rough microsomal membranes (~ 5500 eq*) were mixed with an equal volume of 2X Buffer A (3 mM DTT, 100 mM Hepes-KOH pH 7.6, 300 mM KOAc, 10 mM $Mg(OAc)_2$, 2X Protease Inhibitors, 500 mM Sucrose) as well as 12 µl of 100 mM GTP, 3.3 mg of Puromycin and 6 µl of (40 U/µl) RNasin respectively. The sample was homogenized by five strokes with a motor-driven Potter-Elvehjem homogenizer (EUROSTAR power basic, IKA®) and incubated on ice for 1 hour. Next, 1/1000 volume (6 µl) of 100 mM GTP was added, the sample

homogenized as before and incubated at 37 °C for 30 min. Following the incubation, 1/10 volume of 8 M KOAc and 1/100 volume of 1 M $Mg(OAc)_2$ were added and the sample carefully resuspended. The sample was carefully laid on top of a 950 µl Sucrose Cushion (50 mM Hepes-KOH pH 7.6, 1.6 M Sucrose, 500 mM KOAc, 10 mM $Mg(OAc)_2$) in a TLA100.3 thick wall polycarbonate tube (Beckman Coulter #349622) and centrifuged at 100000 rpm, 18 °C for 1 hour, followed by 1 hour at 100000 rpm, 4 °C (rotor: TLA 100.3, Optima™ MAX-XP Benchtop Ultracentrifuge). The supernatant was carefully removed and the PK-RMs were collected at the interphase. In order to isolate the ribosomes at the bottom of the tube, the cushion layer was carefully removed and the ribosomal pellet resuspended in 600 µl of Buffer A (1.5 mM DTT, 50 mM Hepes-KOH pH 7.6, 150 mM KOAc, 5 mM $Mg(OAc)_2$, 1X Protease Inhibitors, 250 mM Sucrose), snap-frozen in liquid nitrogen and stored at – 80 °C. In order to remove the sucrose and puromycin, the PK-RMs were resuspended in 7.5 ml of 50 mM Hepes-KOH pH 7.2, homogenized and centrifuged for 30 min at 100000 rpm, 4 °C. The resulting pellet was resuspended in 6 ml 50 mM Hepes-KOH pH 7.2, homogenized and centrifuged as before. The pellet was resuspended with 3 ml PK-RM Membrane Buffer (50 mM Hepes-KOH pH 7.2, 250 mM Sucrose, 50 mM KOAc, 2 mM $Mg(OAc)_2$), 1 mM β-Mercaptoethanol), homogenized and centrifuged as before. Finally, the pellet was resupended in 0.3 volumes of Membrane Buffer (to a final concentration of ~ 2 eq/µl), aliquoted (25 µl), snap-frozen in liquid nitrogen and stored at – 80 °C. The concentration of PK-RMs was determined by Western Blotting using anti-Sec61p antibody (ref. 2.2.24.1, 2.2.24.3 and Table 2.7). RMs were used as the standard (standards: 0.25 eq, 0.5 eq, 0.75 eq, 1.0 eq, 1.5 eq of RMs).

* 1 eq of microsomes = 50 A_{280} units/µl (Walter & Blobel, 1981).

2.2.27 PREPARATION OF RECONSTITUTED PROTEOLIPOSOMES

Reconstituted proteoliposomes were prepared according to Görlich & Rapoport (1993), Kalies *et al.* (1994) and Jungnickel & Rapoport (1995). Generally, a 200 µl reaction was set up. In brief, 200 eq of PK-RMs (concentration: ~ 2 eq/µl) were solubilized in 66 µl of 3X Solubilizing Buffer (150 mM Hepes-KOH pH 7.6, 1200 mM KOAc, 30 mM $Mg(OAc)_2$, 48 % (v/v) Glycerol, 6 mM DTT, 1X Protease Inhibitors) and Deoxy-BigCHAP (Sigma-Aldrich) was added to a final concentration of 3 % (v/v). Samples were incubated on ice for 30 min and then centrifuged at 14000 rpm, 4 °C for 5 min (Microcentrifuge 5415R, Eppendorf) in order to remove undissolved membranes. The supernatant was transferred to a clean 2 ml microcentrifuge tube containing 200 µl washed SM-2 Bio-Beads (Biorad) and 5 µl of Phosphatidylcholine/Phosphatidyl-ethanolamin (PC/PE = 4:1 → c = 20 µg/µl; ref. 2.2.28). SM2 BioBeads were prepared by washing 200 µl of the beads (stored in ethanol) three times with 200 µl of cold dH_2O, followed by three washes with 200 µl of Wash Buffer (50 mM Hepes-KOH pH 7.6, 400 mM KOAc, 16 % (v/v) Glycerol, 1 mM DTT). The beads were vortexed for 3 sec

and centrifuged for 1 min at full speed, 4 °C (Microcentrifuge 5415R) each time. The reaction mix was vortexed for 1 min and placed in a thermomixer (Thermomixer® comfort, Eppendorf) in the cold room overnight and mixed at 1100 rpm, 8-12 °C. The next day, the sample was centrifuged at full speed, 4 °C for 5 min (Microcentrifuge 5415R), the supernatant transferred to a clean microcentrifuge tube and the beads were washed three times with cold dH_2O. The supernatant and the washes were pooled and transferred to an ultracentrifuge TLA100.3 1.5 ml tube (Beckman Coulter #357448; used with adapters Beckman Coulter #355919) and proteoliposomes pelleted at 77000 rpm, 4 °C for 30 min (rotor: TLA100.3, Optima™ MAX-XP Benchtop Ultracentrifuge). The resulting pellet was resuspended in 100 µl of Binding Buffer (20 mM Hepes-KOH pH 7.2, 120 mM KOAc, 5 mM $Mg(OAc)_2$, 1 mM DTT, 5 mM ATP, 250 mM Sucrose), aliquoted (10 µl), snap-frozen in liquid nitrogen and stored at –80 °C. Reconstituted membranes were quantified by Western Blot analysis using anti-Sec61p antibody (ref. 2.2.24.1, 2.2.24.3 and Table 2.7) and using RMs as the standard (standards: 0.25 eq, 0.5 eq, 0.75 eq, 1.0 eq, 1.5 eq of RMs).

2.2.28 PREPARATION OF PHOSPHATIDYLCHOLINE/PHOSPHATIDYLETHANOLAMINE

The Phosphatidylcholine/Phosphatidylethanolamine (PC/PE) mix was prepared as follows: 320 µl of PC (10 mg/ml; Avanti-polar® Polar Lipids Inc. #840055C) were mixed with 80 µl of PE (10 mg/ml; Avanti-polar® Polar Lipids Inc # 840026C), 60 µl 10 % (v/v) Deoxy-BigCHAP (Sigma) and 2 µl 1 M DTT. The reaction mix was dried in a vacuum concentrator (Concentrator Plus; Eppendorf) at RT for a few hours and the resulting pellet dissolved in 250 µl of 96 % (v/v) ethanol. The reaction mix was dried as before overnight. The pellet was dissolved in 200 µl Ro-Buffer (16 % (v/v) Glycerol, 50 mM Hepes-KOH pH 7.6) (final concentration: 20 µg/µl (PC/PE = 4:1)). The sample was aliquoted (10 µl), snap-frozen in liquid nitrogen and stored at - 80 °C.

2.2.29 PREPARATION OF *S. CEREVISIAE* CYTOSOL FOR PROTEASOME PURIFICATION

The preparation of yeast cytosol was conducted according to Current Methods in Molecular Biology (ref. Chapter 13.13.5-9). In brief, 10 L of KRY333 were grown in YPD at 200 rpm, 30 °C overnight to an OD_{600} of 2. The cells were harvested by centrifugation at 5000 rpm, RT for 5 min (rotor: SLA3000; Sorvall Evolution® RC Centrifuge). The cell pellets were resuspended in 400 ml of cold dH_2O, pooled and centrifuged as before. After resuspension of the pellet with 3-5 ml of B88 (20 mM Hepes-KOH, pH 6.8; 250 mM Sorbitol; 150 mM KOAc, 5 mM $Mg(OAc)_2$), cells were frozen in liquid nitrogen. First, about 500 ml of liquid nitrogen were poured into a Tri-Pour® plastic beaker (VWR®), which was placed on a magnetic stirrer. The liquid nitrogen was stirred at moderate speed using a large magnetic stir bar. The cells were poured slowly into the liquid nitrogen. Once the cells were frozen,

the liquid nitrogen was decanted. The resulting frozen material was transferred to 50 ml falcon tubes and stored at – 80 °C. Next, about 500 ml of liquid nitrogen were added to a stainless-steel blender (Rio™ Commercial Bar Blender, Hamilton Beach®) running at the lowest setting (in the cold room). Once the cells had been added the blender was run at the highest setting. Lysis was performed for 10 min with addition of liquid nitrogen every minute to maintain the volume of the liquid nitrogen. After 10 min the blender was turned off, the liquid nitrogen evaporated, and the powder transferred to 50-ml falcon tubes. The powder was stored at – 80 °C until needed.

2.2.30 PURIFICATION OF *S. CEREVISIAE* PROTEASOME 26S HOLOENZYME AND 19S RP SUBCOMPLEX

The purification of *S. cerevisiae* 26 S proteasome and 19S RP (Regulatory Particle) was according to Verma *et al*. (2000), Leggett *et al*. (2002) and Lee *et al*. (2004a) using the yeast strain KRY333 which expresses a FLAG®-tagged version of the *rpt1* 19S RP subunit. Briefly, cytosol was prepared as described in 2.2.29. The frozen cytosol was thawed in a cold water bath, mixed with an equal volume of Buffer A (50 mM Tris-HCL pH 7.5, 150 mM NaCl, 10 % (v/v) Glycerol, 5 mM $MgCl_2$) and then centrifuged at 17500 rpm, 4 °C for 45 min (rotor: SS34, Sorvall Evolution® RC Centrifuge). For purification of 26S proteasomes, ATP (pH 7.0) was added to a final concentration of 5 mM to all solutions. Following the centrifugation, the supernatant was carefully taken off and mixed with Buffer A-equilibrated anti-FLAG® M2 agarose beads (Sigma-Aldrich #A2220) in a 50 ml falcon tube. The sample was incubated for 4 hr (up to overnight) at 4 °C with gentle agitation. Equilibration of the FLAG® M2 agarose beads was as follows: In brief, the appropriate amount of beads was transferred to a disposable PD-10 column (Amersham Biosciences, GE Healthcare) using a blue pipette tip, which had been cut off. The column had been rinsed once with Buffer A. The beads were then equilibrated by adding 3 column volumes of 0.1 M Glycine-HCl (pH 3.5) followed by 5 column volumes of Buffer A. The bead bed was never allowed to run dry. About 500 µl of beads were used per 50 ml of supernatant prepared from a yeast culture of 10000 OD_{600}. Following the incubation, the whole sample was passed through a PD-10 column and the beads were washed twice with Buffer 88 (20 mM Hepes-KOH pH 6.8, 250 mM Sorbitol, 150 mM KOAc, 5 mM $Mg(OAc)_2$) followed by two washes with Buffer 88/0.2 % Triton X-100 (B88, 0.2 % (v/v) Triton X-100). Again, the gel bead was not allowed to run dry. The beads were carefully resuspended in B88 (final volume: 2 ml), transferred to a clean 2 ml microcentrifuge tube and eluted with 150 µg/ml FLAG® peptide at 4 °C for 4 hr (or overnight) on a rotating wheel. Following the elution the sample was purified by passing it through a PD-10 column and the eluate was concentrated at 3000 rpm, 4 °C (SIGMA 4K15 Refrigerated Centrifuge) using a Centricon® YM-100 centrifugal filter (Merck Millipore) until a final concentration of 1-2 µg/µl was reached.

The resulting 19S RP or 26S proteasomes were aliquoted (10 µl), snap-frozen in liquid nitrogen and stored at – 80 °C. Protein concentration was determined using the Pierce™ 660nm Protein Assay Reagent (Pierce, Thermo Fisher Scientific) according to the supplier's instructions and a microplate reader (Bio-Rad, measuring at 655 nm).
Samples taken throughout the purification (i.e. cytosol, flow through, washes ans purified sample) were analyzed by SDS-PAGE (ref. 2.2.24.1).

2.2.30.1 PEPTIDASE ACTIVITY ASSAY

Proteasome activity was monitored using the fluorogenic peptide substrate N-Succinyl-Leu-Leu-Val-Tyr-7-Amido-4-Methylcoumarin (Suc-LLVY-AMC, Sigma #S6510). The assay was performed as described by Leggett *et al.* (2002). The substrate is cleaved in the presence of active proteasome (i.e. by the chymotryptic-like peptidase activity of the proteasome). The resulting free AMC fluoresces and can be monitored on a UV transilluminator. The activity assay was perfomed as an in-gel activity assay. In brief, native gel electrophoresis was performed using a 4 % nondenaturing polyacrylamide gel (40 % (v/v) Acrylamide (37.5:1), 1X Native Gel Buffer, 1 mM ATP, 1 mM DTT, 1 % (v/v) 10 % (w/v) APS, 0.1 % (v/v) TEMED). 5X Native Gel Loading Buffer (250 mM Tris-HCl pH 7.4, 50 % (v/v) Glycerol, 0.007 % (w/v) Xylene Cyanol) was added to each sample (usually 1-5 µg of proteasome were loaded) and the gel was run in 1X Native Gel Buffer (5X: 450 mM Tris-borate pH 8.35, 25 mM $MgCl_2$, 2.5 mM EDTA) containing 1 mM ATP and 1 mM DTT at 100 V, 4 °C until the tracking dye ran off the bottom of the gel (~ 2 hr). The gel was then incubated in Buffer A (10 % (v/v) Glycerol, 25 mM Tris-HCl pH 7.4, 10 mM $MgCl_2$, 1 mM ATP, 1 mM DTT) containing 100 µM Suc-LLVY-AMC and 0.02 % (w/v) SDS* for 15 min at 30 °C and visualized on a UV transilluminator at 365 nm.

* Optional: SDS was added to capture 20S CP activity.

2.2.31 PROTEASOME BINDING ASSAY

The proteasome binding assay was performed as described by Kalies *et al.* (2005). In brief, 20 eq of reconstituted proteoliposomes (ref. 2.2.27) were mixed with 2 pmole of 19S RP proteasomal subunit or the 26S holoenzyme (ref. 2.2.30) in 30 µl Binding Buffer (20 mM Hepes-KOH pH 7.2, 250 mM sucrose, 120 mM KOAc, 5 mM $Mg(OAc)_2$, 5 mM ATP, 1 mM DTT). The reaction mix was first incubated on ice for 20 min followed by 10 min at RT. Next, 270 µl of Sucrose Cushion (20 mM Hepes-KOH pH 7.2, 2.5 M Sucrose, 120 mM NH_4OAc, 5 mM $Mg(OAc)_2$, 5 mM ATP, 1 mM DTT) were added and the sample was vortexed for 10 sec. 800 µl of Separating Cushion (20 mM Hepes-KOH pH 7.2, 1.8 M Sucrose, 120 mM NH_4OAc, 5 mM $Mg(OAC)_2$, 5 mM ATP, 1 mM DTT) were

added to a polycarbonate thickwall tube (rotor: TLS-55, Beckman Coulter #343778). The Separating Cushion was carefully underlaid with the sample (300 µl). The sample was topped off with 200 µl of binding buffer and centrifuged at 55000 rpm, 4 °C for 1 hr (rotor: TLS55, Optima™ MAX-XP Benchtop Ultracentrifuge). After ultracentrifugation, the sample was divided into nine fractions (from top to bottom) using a 200 µl pipette tip which had been cut off. For TCA precipitation, an equal volume of ice-cold TCA was added to each fraction. The samples were vortexed briefly and incubated on ice for 30 min, followed by centrifugation at full speed, 4 °C for 10 min (Microcentrifuge 5415R, Eppendorf). The supernatants were taken off with a gel-loading tip and 500 µl of ice-cold Acetone added to the pellets. The samples were vortexed and centrifuged as before. The supernatants were taken off and the pellet dried at RT. About 20 µl of 2X SDS-PAGE Sample Buffer (125 mM Tris-HCl pH 6.8, 4 % (w/v) SDS, 10 % (v/v) β-Mercaptoethanol, 0.002 % (w/v) Bromophenol Blue, 20 % (v/v) Glycerol) were added to each pellet and the proteins resolved by SDS-PAGE (ref. 2.2.24.1). Western Blotting was performed as described in 2.2.24.3 using anti-FLAG® M2 antibody (1:2000, Sigma #F7425) as the primary antibody and anti-rabbit HRP (1:200000, Rockland™ #611-1302) as the secondary antibody (ref. Table 2.7).

2.2.32 UNFOLDED PROTEIN RESPONSE ASSAYS

2.2.32.1 QUANTITATIVE LIQUID ß-GALACTOSIDASE ASSAY

The quantitative liquid ß-galactosidase assay was essentially as described by Miller (1972), Guarente (1983) and Staglar *et al.* (1998). All yeast strains of interest were transformed with the plasmids (ref. Table 2.5) pJC30 (*UPRE-LacZ* reporter construct) and pJC31 (control for pJC30) as described in 2.2.17.

20 ml cultures* were grown in minimal medium (LEU-TRP d/o medium for pRS315-*sec61***) at 30 °C, 220 rpm to an OD_{600} of about 0.5. Aliquots of 1 ml were centrifuged at 8000 rpm (MiniSpin® centrifuge, Eppendorf), 4 °C for 5 min. The pellets were resuspended in 1 ml Z Buffer (pH 7; 60 mM Na_2HPO_4, 40 mM NAH_2PO_4, 10 mM KCl, 1 mM $MgSO_4$) containing 0.27 (v/v) % β-mercaptoethanol. Next, 100 µl chloroform and 50 µl 0.1 (w/v) % SDS were added to the samples, which were agitated on a vortex mixer (Vortex-Genie 2®, Scientific Ind.™) for 10 sec. The samples were then pre-incubated for 5 minutes at 28 °C (water bath). The reaction was induced with the addition of 200 µl 4 mg/ml 2-nitrophenyl-β-D-galactopyranoside (ONPG) in Z Buffer. The samples were incubated at 28 °C (water bath) until a pale yellow colour was visible (for strains transformed with pJC30). ONPG is converted to a yellow product by β-galactosidase, which absorbs light at a wavelength of 420 nm. The reaction was stopped by adding 500 µl of 1 M Na_2CO_3, the samples were centrifuged at full speed (MiniSpin® Centrifuge), RT for 10 minutes and the OD_{420} of the supernatant was measured in

a quartz cuvette (Hellma® Analytics). Generally, for each strain samples were prepared in triplicates. The activity is expressed as β-galactosidase units as follows:

β-Gal units = 1000 x [OD_{420}/(OD_{600} x v x t)]

OD_{420}: optical density of the product (o-nitrophenol)
OD_{600}: optical density of the culture
v: volume of culture used in the assay (ml)
t: time elapsed during the assay (after ONPG addition)

* All cultures were prepared in duplicates or triplicates. One culture was used as a positive control. In brief, when an OD_{600} of about 0.4 was reached tunicamycin (Tm) was added to a final concentration of 1 µg/ml. The cultures were then incubated for another hour at 30 °C, 220 rpm and the assay conducted as described above.

**: pRS315-*sec61-S179P*, pRS315-*sec61-S353C*, pRS315-*sec61-S179P/S353C*, pRS315-*sec61-302*, pRS315-*sec61-303*

2.2.32.2 GROWTH DEFECTS ON TUNICAMYCIN PLATES (DROP TEST)

In order to monitor growth defects of the appropriate strains on plates containing tunicamycin drop tests were performed as in 2.2.19. Briefly, 5 ml cultures of the respective strains were prepared and the cells counted using a hemocytometer (Neubauer improved). Serial dilutions were prepared and 5 µl of each dilution were dropped onto YPD (+/- 0.25 µg/ml Tm, 0.5 µg/ml Tm) plates or minimal medium plates (+/- 0.25 µg/ml Tm, 0.5 µg/ml Tm). Plates were incubated at various temperatures (routinely: 20, 25, 30 and 37 °C) for 3 days.

2.2.32.3 *HAC1* MRNA SPLICE ASSAY

Upon induction of the UPR the *HAC1* mRNA is spliced. Thus, the comparison of the two species, $HAC1^u$ and $HAC1^i$ (u = uninduced; i = induced), allows for the evaluation of the UPR status of various yeast strains.

Cultures of the appropriate strains were prepared in minimal medium and grown at 30 °C, 220 rpm to an OD_{600} of 1. For positive controls each strain was grown in the presence of tunicamycin. In this case, when an OD_{600} of 1 was reached, 2 µg/ml Tm were added to the cultures. The cultures were then incubated for another 3 hr at 30 °C, 220 rpm. 10 ml of each culture were used to isolate yeast RNA according to 2.2.21.

The RNAs were used in reverse transcription reactions to generate cDNA. As the reverse transcriptase the Maxima® Reverse Transcriptase (Fermentas) was used. RNAs were diluted to a final concentration of 0.1 µg/µl. The reaction setup was as shown in Table 2.19. The samples were incubated for 30 minutes at 50 °C, followed by an inactivation at 85 °C for 5 minutes.

Table 2.19. Reverse transcription reaction mixture.

Component	Volume (µl)	Final concentration
RNA	1	0.1 µg
Oligo(dT_{18})-primer (100 mM)	1	100 pmol
dNTP mix (10 mM)	1	0.5 mM
RNase-free dH_2O	to 14.5	to 14.5 µl
5X RT buffer	4	1X
RNasin (40 U/µl)	0.5	20 U
Maxima® RT	1	200 U

1 µl of each cDNA was used in a PCR using the *HAC1*- as well as the *ACT1*-specific primers (ref. Table 2.6). The PCR setup was as described in Table 2.12. The thermal cycler program was as described in Table 2.13 with the following exceptions: primer annealing (step 3) was at 50 °C, primer extension (step 4) was for 45 sec, final primer extension was for 3 min and steps 2 to 4 were cycled 24 times.

10 µl of the PCR product were run on a 1 % Agarose Gel in 1X TAE Buffer (50X TAE pH 8.4: 20 M Tris-HCl, 10 M Acetic Acid, 0.05 M EDTA) at 100 V and RT for 1 hr (ref. 2.2.8). Bands were visualized and photographed using the E-BOX VX2 gel documentation system (PEQLAB).

2.2.33 PULSE-CHASE EXPERIMENTS

2.2.33.1 PULSE LABELING

Pulse chase experiments were performed as described by Gillece *et al.*, (1999) and Verma *et al.* (2000). In brief, cells were grown overnight at 30 °C, 220 rpm in Growth Medium (0.67 % (w/v) Yeast Nitrogen Base (YNB) w/o Amino Acids (AA), 0.13 % (w/v) SC drop-out mix*, 0.2 % (w/v) Casamino Acids (CAA), 5 % (w/v) Glucose, Supplements as required by the strain's auxotrophies**) to an OD_{600} of 0.5–1. Cells were harvested at 3000 rpm, RT for 5 min (rotor: SS34, Sorvall Evolution® RC Centrifuge). The cells were washed twice with Labeling Medium (0.67 % (w/v) YNB w/o AA and Ammonium Sulfate, 5 % (w/v) Glucose, Supplements as required by the strain's auxotrophies**) and resuspended in Labeling Medium to an OD_{600} of 6 (pulse chase experiments) or 4 (pulse experiments). Aliquots of 1.5 OD_{600} (pulse chase experiments) or 2 OD_{600} (pulse experiments) were transferred to clean 1.5 ml microcentrifuge tubes. The samples were pre-incubated at 30 °C, 600 rpm for 30 min (Thermomixer® comfort, Eppendorf). Cells were then pulsed with 0.35 mCi/ml EXPRESS^{35}S^{35}S Protein Labeling Mix (Perkin Elmer) and incubated for 2, 5 or 10 min (depending on

the substrate) at 600 rpm, 30 °C. Following the pulse, cells were immediately transferred to ice and labeling was terminated by adding 750 µl of cold Tris-Azide Buffer (20 mM Tris-HCl pH 7.5, 20 mM Sodium Azide). The cells were then centrifuged for 1 min at full speed, RT (Microcentrifuge 5415R, Eppendorf), the pellets resuspended in 1 ml of Resuspension Buffer (100 mM Tris-HCl pH 9.4, 10 mM DTT, 20 mM Ammonium Sulfate) and incubated for 10 min at RT. The samples were centrifuged as before and resuspended in 150 µl of Lysis Buffer (20 mM Tris-HCl pH 7.5, 2 % (w/v) SDS, 1 mM PMSF, 1 mM DTT). Acid washed glass beads (~ 150 µl; 450-600 µm, Sigma) were added and the cells disrupted in a Mini-Beadbeater-24 (Bio Spec Products Inc.) for 2 x 1 min with an incubation of 1 min on ice in between bursts. Next, the samples were heated at 90 °C for 5 min (membrane proteins: 5 min at 60 °C) in a block heater (SBH200D/3, Stuart®). 3 x 250 µl of IP Buffer w/o SDS (150 mM NaCl, 1 % (v/v) Triton X-100, 15 mM Tris-HCl pH 7.5, 2 mM Sodium Azide) were added and the samples vortexed (Vortex-Genie® 2, Scientific Ind.™), centrifuged as before each time and the supernatants pooled in a clean 2 ml microcentrifuge tube. Immunoprecipitation using the appropriate antibody/antiserum and preparation for gel electrophoresis were as described in 2.2.33.3.
For pulse-chase experiments, the chase was initiated as described in 2.2.33.2.

* According to Kaiser *et al.*, 1994 (Formedium™; ref. Table 2.10).
** Table 2.10

2.2.33.2 CHASE

For pulse-chase experiments, the chase was initiated by adding 250 µl of 2X Chase Mix (0.6 mg/ml Cysteine, 0.8 mg/ml Methionine, 2.6 mg/ml Ammonium Sulfate and 200 mg/ml Casamino Acids (CAA)) to the cells. For time-course experiments, multiple aliquots per strain were prepared. The samples were incubated at 600 rpm, 30 °C (Thermomixer® comfort, Eppendorf) over the desired period of time. Samples were taken at appropriate time points (e.g. t = 0, 5, 10, 15, 20, 30, 60 min), i.e. the chase was immediately terminated after each time point by the addition of cold Tris-Azide Buffer (20 mM Tris-HCl pH 7.5, 20 mM Sodium Azide). The samples were centrifuged at full speed, RT for 1 min (Microcentrifuge 5415R, Eppendorf) and resupended in 1 ml of fresh Tris-Azide Buffer and placed on ice until all samples were taken. The cells were then centrifuged for 1 min at full speed, RT, the pellets resuspended in 1 ml of Resuspension Buffer (100 mM Tris-HCl, pH 9.4, 10 mM DTT, 20 mM Ammonium Sulfate) and incubated for 10 min at RT. The samples were centrifuged as before and resuspended in 150 µl of Lysis Buffer (20 mM Tris-HCl pH 7.5, 2 % (w/v) SDS, 1 mM PMSF, 1 mM DTT). Acid washed glass beads (~ 150 µl; 450-600 µm, Sigma) were added and the cells disrupted in a Mini-Beadbeater-24 (Bio Spec Products Inc.) for 2 x 1 min with an incubation of 1 min on ice between bursts. Next, the samples were heated at 90 °C for 5 min (membrane proteins:

5 min at 60 °C) in a block heater (SBH200D/3, Stuart®) and 3 x 250 µl of IP Buffer w/o SDS (150 mM NaCl, 1 % (v/v) Triton X-100, 15 mM Tris-HCl pH 7.5, 2 mM NaN_3) were added. The samples were briefly vortexed (Vortex-Genie® 2, Scientific Ind.™) and centrifuged as before each time and the supernatants pooled in a clean 2 ml microcentrifuge tube. Immunoprecipitation using the appropriate antibody/antiserum and preparation for gel electrophoresis were as described in 2.2.33.3.

2.2.33.3 IMMUNOPRECIPITATION

The samples were prepared for the preclear by adding 60 µl of 20 % (w/v) Protein A Sepharose™ CL-4B (GE Healthcare) in IP Buffer with SDS (150 mM NaCl, 1 % (v/v) Triton X-100, 15 mM Tris-HCl pH 7.5, 2 mM Sodium Azide, 0.1 % (w/v) SDS). Preclear of the samples was on a rotating wheel for 30 min, at RT. Following the incubation the samples were centrifuged for 2 min at full speed, RT (Microcentrifuge 5415R, Eppendorf) and each supernatant was transferred to a clean microcentrifuge tube containing 60 µl of 20 % (w/v) Protein A Sepharose™ CL-4B as well as the appropriate antibody/antiserum (ref. Table 2.7). The samples were incubated either overnight at 4 °C (cold room) or at RT for 2 hours on a rotating wheel. Next, the samples were centrifuged for 2 min at full speed, RT (Microcentrifuge 5415R, Eppendorf), followed by two washes each with 1 ml of IP Buffer with SDS and 1 ml of Urea Wash (2 M Urea, 200 mM NaCl, 1 % (v/v) Triton X-100, 100 mM Tris-HCl pH 7.5, 2 mM Sodium Azide) and one wash each with 1 ml of ConA Wash (500 mM NaCl, 1 % (v/v) Triton X-100, 20 mM Tris-HCl pH 7.5, 2 mM NaN_3) and 1 ml of Tris-NaCl Wash (50 mM, 10 mM Tris-HCl pH 7.5, 2 mM NaN_3). The samples were vortexed (Vortex-Genie® 2, Scientific Ind.™) briefly, centrifuged for 1 min at full speed, RT, and the supernatants discarded each time. After the washes, 20 µl of 2X SDS-PAGE Protein Sample Buffer (125 mM Tris-HCl pH 6.8, 4 % (w/v) SDS, 10 % (v/v) β-Mercaptoethanol, 0.002 % (w/v) Bromophenol Blue, 20 % (v/v) Glycerol) were added and the samples incubated at 95 °C for 5 min (membrane proteins: 60 °C) in a block heater (SBH200D/3, Stuart®). Samples were centrifuged for 10 sec at full speed, RT and the supernatant carefully loaded onto a protein gel using a gel-loading tip to avoid transfer of sepharose. Generally, proteins were resolved using a 4-12 % Bis-Tris gel (NuPAGE® Novex® Pre-Cast gels) as described in 2.2.24.1. Following the electrophoresis protein gels were incubated in Fixative 1 (10 % (v/v) Acetic Acid, 40 % (v/v) Methanol, 2 % (v/v) Glycerol) for 15 min and in Fixative 2 (50 % (v/v) Methanol, 1 % (v/v) Glycerol) for 30 min, shaking. Gels were then dried at 80 °C for 1 hour in a gel dryer (Model 583, Bio-Rad) and exposed to Storage Phosphor Screens (GE Healthcare). Usually an exposure of 1 - 3 days was sufficient. Radioactivity was visualized using a phosphorimager (Typhoon Trio™ Variable Mode Imager, GE Healthcare). Signal were analyzed and quantified using the ImageQuant™ TL software (GE Healthcare).

2.2.34 *IN VITRO* TRANSCRIPTION, TRANSLATION, TRANSLOCATION AND RETROTRANSLOCATION

2.2.34.1 PREPARATION OF *S. CEREVISIAE* CYTOSOL FOR *IN VITRO* ASSAYS

Concentrated yeast cytosol was prepared using the yeast strain KRY275 according to Sorger & Pelham (1987) and McCracken & Brodsky (1996). 10 L yeast cells were grown in YPD to an OD_{600} of ~ 2 at 30 °C with vigorous shaking. The cells were harvested at 5000 rpm, RT for 3 min (rotor: SLA3000, Sorvall Evolution® RC Centrifuge). The pellets were resuspended in 400 ml dH_2O, the pellets pooled and recentrifuged as before. The resulting pellet was resuspended in a minimal amount of B88 (< 3-5 ml) (20 mM Hepes-KOH pH 6.8, 250 mM Sorbitol, 150 mM KOAc, 5 mM $Mg(OAc)_2$). For freezing the cells, about 500 ml of liquid nitrogen were added to a Tri-Pour® plastic beaker (VWR®), which was placed on a magnetic stirrer. The liquid nitrogen was stirred at moderate speed using a large magnetic stir bar. The cells were poured slowly into the liquid nitrogen. Once the cells were frozen, the liquid nitrogen was decanted. The resulting frozen material was transferred to 50 ml falcon tubes and stored at – 80 °C. Next, about 500 ml of liquid nitrogen were added to a stainless-steel blender (Rio™ Commercial Bar Blender, Hamilton Beach®) running at the lowest setting (in the cold room). Once the cells had been added the blender was run at the highest setting. The yeast was lysed for 10 min with addition of liquid nitrogen every minute to maintain the volume of the liquid nitrogen. After 10 min the blender was turned off, the liquid nitrogen evaporated, and the powder transferred to 50-ml falcon tubes. The powder was stored at – 80 °C until needed. The powder was then thawed in a cold water bath. As the material started to melt, about 0.5 ml B88 per 40 ml of broken yeast was added to the powder. DTT was added to a final concentration of 1 mM. The lysate was centrifuged at 9200 rpm for 10 min at 4 °C (rotor: SS34, Sorvall Evolution® RC Centrifuge). The supernatant was collected and centrifuged as before. The resulting supernatant was transferred to polycarbonate tubes (Beckman Coulter #349622) and centrifuged at 74600 rpm, 4 °C for 1 hour (rotor: TLA100.3, Optima™ MAX-XP Benchtop Ultracentrifuge). The resulting cytosol was aliquoted (100 µl), snap-frozen in liquid nitrogen and stored at – 80 °C. Protein concentration was determined using the Pierce™ 660nm Protein Assay Reagent (Pierce, Thermo Fisher Scientific) according to the supplier's instructions. Cytosol with a concentration > 20 mg/ml was best for ER-associated degradation (ERAD) assays.

2.2.34.2 PREPARATION OF *S. CEREVISIAE* TRANSLATION EXTRACT

Yeast translation extract was prepared as modified from Schekman *et al.* (1994) and Baker *et al.* (1988). The preparation was performed under RNase-free conditions. In brief, 10 L of the protease-deficient yeast strain GPY60 (Table 2.4) were grown in YPD to an OD_{600} = 2 - 4. The cells were

harvested by centrifugation (5000 rpm, RT, 3 min, rotor: SLA3000, Sorvall Evolution® RC Centrifuge) and washed with RNase-free water. The yeast pellets were pooled and resuspended in a small volume of cold RNAs-free Buffer A (100 mM KOAc, 2 mM MgOAc, 20 mM Hepes-KOH pH 7.4, 1 mM PMSF, 2 mM DTT) to yield a "thick paste". The material was poured in a thin stream into a plastic beaker containing 500 µl liquid nitrogen and a large magnetic stir bar in order to freeze the cells. The material was stirred slowly until all cells were frozen. The frozen cells could be stored at – 80 °C for up to a year at this point. Next, for liquid nitrogen lysis, the frozen cells were added to a stainless steel blender (Rio™ Commercial Bar Blender, Hamilton Beach®) containing liquid nitrogen*. The cells were continuously blended under liquid nitrogen for 10 min at high speed (with ~ 100 ml of liquid nitrogen added every minute). The resulting yeast cell powder was transferred into 50 ml falcon tubes and stored at – 80 °C until needed.

The cell powder was thawed in a water bath at RT. As soon as it started to melt, 40 ml** Buffer A (100 mM KOAc, 2 mM MgOAc, 20 mM Hepes-KOH pH 7.4, 1 mM PMSF, 2 mM DTT) were added and the powder was continued to thaw until all ice particles had melted. The cell lysate was transferred to 50 ml polycarbonate tubes (SS34) and centrifuged at 9000 rpm, 4 °C for 10 min (rotor: SS34). The supernatant was carefully transferred to a 45Ti tube (RNase-free) and centrifuged at 36000 rpm, 4 °C for 30 min (rotor: 45 Ti; Optima™ L-90 K Ultracentrifuge). The resulting clear yellowish supernatant was collected, avoiding the lipid layer on top and the white material above the pellet and along the sides of the tube. In order to determine the concentration of ribosomal RNA in the extract at this point of the preparation the OD_{260} of a 1:200 dilution in dH_2O was measured.

The supernatant was then loaded onto a Sephadex® G-25 (GE Healthcare) Econo-Column (393 ml; of the BioLogic LP System, Bio-Rad) column ("S100"). The S100 column was equilibrated with 2 column volumes of Buffer A + 14 % (v/v) glycerol and run with a flow rate of 1 ml/min. Fractions of 3 ml were collected (Model 2110 Fraction Collector, Bio-Rad) as soon as a yellowish band was visible in the lower part of the column. This band contains the fractions that show the highest activity. The OD_{260} of each fraction was measured as before. Fractions with an $OD_{260} > 30$ were pooled (excluding borderline fractions) and the OD_{260} of the pool measured. Translation extracts worked most efficiently when the OD_{260} of the pool was in the range of 60 – 100. The extract was snap-frozen in liquid nitrogen in 1 ml aliquots and stored at – 80 °C.

* The blender was run at low speed and the liquid nitrogen immediately added. Once the cells were added the blender was run at the highest setting.

** 10 ml Buffer A per 10 g of frozen cells

2.2.34.3 LINEARIZATION AND RE-ISOLATION OF PLASMID DNA

For *in vitro* translation the appropriate mRNA was prepared using linearized plasmid DNA containing the desired gene (pDJ100: pαF3Q; ref. Table 2.5 and Table 2.15). Linearisation of plasmid DNA and the transcription reaction was performed under RNAse-free conditions. Generally, a 400 µl digest was set up containing 150 U restriction enzyme (NEB; ref. Table 2.15), 40 µg plasmid DNA and 1X restriction buffer. Plasmid DNA was digested at 37 °C for 2 hr. After the incubation the DNA was re-isolated as follows. 400 µl of P/C/I/H/I (50 % (v/v) Phenol, 48 % (v/v) Chloroform, 2 % (v/v) Isoamyl Alcohol, 0.1 % (w/v) 8-Hydroxy-quinoline) were added to each microcentrifuge tube, which was vortexed (Vortex-Genie® 2, Scientific Ind.™) for 3 sec and centrifuged for 1 min at full speed (Microcentrifuge 5415R, Eppendorf). The upper phase was collected and transferred to a clean RNAse-free microcentrifuge tube. The lower phase was extracted with 100 µl dH_2O (i.e. vortexed and centrifuged as before). The upper phase was collected and combined with the previous upper phase. To the upper phases 500 µl C/I (96 % (v/v) Chloroform/ 4 % (v/v) Isoamyl Alcohol) were added, the sample vortexed and centrifuged as before. The upper phase was transferred to a clean RNase-free microcentrifuge tube and 50 µl 3 M NaAc and 1 ml 95 % (v/v) ethanol were added. Incubation was for 30 min at – 70 °C. The sample was then centrifuged at full speed, 4 °C for 10 min in a pre-cooled desktop centrifuge (Microcentrifuge 5415R, Eppendorf) and the supernatant discarded. The pellet was resuspended in 1.5 ml 70 % (v/v) ethanol, centrifuged as before and the supernatant discarded. The pellet was dried for 5 min at RT in the fume hood and resuspended in a final volume of 188 µl DEPC-H_2O. The DNA concentration was determined by measuring the OD_{260} of a 1:100 dilution of the sample in dH_2O.
The DNA concentration was calculated as follows:

OD_{260} = 1 equals 50 µg/ml for double-stranded DNA

2.2.34.4 *IN VITRO* TRANSCRIPTION REACTION

The *in vitro* transcription of linearized plasmid DNA was according to Rothblatt & Meyer (1986). The transcription reaction was prepared at RT as shown in Table 2.20. Transcription reactions were performed under RNase-free conditions.

Table 2.20. *In vitro* transcription reaction setup.

Component	Volume (µl)	Final Concentration
5X Transcription Buffer	80	1X
0.5 M DTT	8	10 mM
10 mM GTP	4	0.1 mM
GpppG (Cap)	20	0.25 mM
10 mM CTP	20	0.5 mM
10 mM UTP	20	0.5 mM
10 mM ATP	20	0.5 mM
- Vortex -		
RNasin (2500 U/ml)	20	1.2 U/µl
- Vortex -		
linearized plasmid DNA	40 (40 µg)	0.1 µg/µl
SP6 RNA polymerase	20	1 U/µl
DEPC-H_2O	to 400	---
- Vortex -		

Incubation was for 1 hour at 40 °C in a Thermomixer® comfort (Eppendorf). Following the incubation, the sample was EtOH-precipitated by 40 µl 3 M NaAc and 1 ml 100 % (v/v) ethanol. The sample was mixed, incubated at – 70 °C for 30 min and then centrifuged at full speed and 4 °C for 10 min (Microcentrifuge 5415R, Eppendorf). The supernatant was discarded and 1.5 ml 70 % (v/v) ethanol added to the pellet. The sample was centrifuged as before, the supernatant discarded and the pellet air-dried at RT for 5 min. The pellet was resuspended in a final volume of 188 µl DEPC-dH_2O. The RNA concentration and purity of the sample was determined by measuring the optical density at 260 and 280 nm (OD_{260} and $OD_{280;}$ 1 OD_{260} = 40 µg/ml RNA) of a 1: 200 dilution of the sample in dH_2O. For optimal purity, the OD_{260}/OD_{280} should be > 2 (otherwise the sample contains significant protein impurities).

2.2.34.5 *IN VITRO* TRANSLATION REACTION

Prior to the translation of the appropriate substrate (*in vitro* transcribed α-factor precursor (ppαf) or mutant α-factor precursor (pΔgpαf); ref. 2.2.34.4) the S-100 translation extract (ref. 2.2.34.2) was nuclease-treated. Generally, 1.8 ml of the S-100 yeast translation extract was thawed at RT and combined with 50 µl micrococcal nuclease (20 kU/ml; NEB) and 25 µl 40 mM $CaCl_2$ (Sigma-Aldrich). The sample was incubated at 20 °C (water bath) for 20 min. Following the incubation 25 µl 100 mM EGTA (Sigma-Aldrich) were added and the sample incubated at 20 °C for another 5 min.

A translation reaction was generally set up as described in Table 2.21. The reaction mixture was carefully resuspended and incubated at 20 °C (water bath) for 50 min. After the incubation the sample was snap-frozen in liquid nitrogen in 50 µl aliquots and stored at – 80 °C until needed.

Table 2.21. Standard *in vitro* translation reaction setup.

Component	Volume
Nuclease-treated Translation Extract	450 µl
3X Translation Buffer*	450 µl
RNasin (25000U/ml)	15 µl
Creatine Phosphokinase (10 mg/ml)	27 µl
DEPC-H_2O	to 1.35 ml
mRNA	125 µg
L-[^{35}S]-Methionine	0.5 mCi

* 3X Translation buffer (75 mM Creatine Phosphate, 2.25 mM ATP, 300 µM GTP, 120 µm Amino Acids, 360mM KOAc, 6 mM $Mg(OAc)_2$, 66 mM Hepes-KOH pH 7.4, 5.1 mM DTT)

2.2.34.6 *IN VITRO* TRANSLOCATION ASSAY

In vitro assays were performed as described by Lyman and Shekman (1995) and McCracken & Brodsky (1996) and Pilon *et al.*, (1997). For *in vitro* translocation reactions ^{35}S-methionine-labeled ppαf and pΔgpαf were transcribed and translated as above (ref. 2.2.34.4 and 2.2.34.5). For a 60 µl translocation reaction the set-up was as described in Table 2.22. For negative controls either microsomes or ^{35}S-Met-labeled pΔgpαf were omitted from the reaction. The reactions were set up on ice, mixed very gently and incubated at 20 °C for 50 minutes. Following the incubation, an equal volume of ice cold 20 % (w/v) TCA was added to the sample. The sample was agitated on a vortex mixer (Vortex-Genie® 2, Scientific Ind.™) for 10 seconds, chilled on ice for 15 min and centrifuged for 5 min at 4 °C, full speed (Microcentrifuge 5415R, Eppendorf). The supernatant was removed using a gel-loading tip and the pellet washed in sufficient ice-cold acetone to cover the pellet. The sample was centrifuged as before and dried at RT for 10 min. The pellet was then taken up in 25 µl 2X SDS-PAGE Sample Buffer (125 mM Tris-HCl pH 6.8, 4 % (w/v) SDS, 10 % (v/v) β-Mercaptoethanol, 0.002 % (w/v) Bromophenol Blue, 20 % (v/v) Glycerol) and the sample incubated for 15 min at 70 °C (Thermomixer® Comfort, Eppendorf). Radiolabeled proteins were resolved using an 18 % denaturing SDS-polyacrylamide gel containing 4 M urea (ref. Table 2.23). The gel was run overnight at 90 V, RT until the dye front was near the bottom of the gel. The next day, the gel was incubated (shaking) 4 x 10 min in Fixative 1 (10 % (v/v) Acetic Acid, 40 % (v/v) Methanol, 2 % (v/v) Glycerol), followed 30 minutes in Fixative 2 (50 % (v/v) Methanol, 1 % (v/v) Glycerol). The gel was then dried in a gel dryer (Model 583, Bio-Rad) for 1 hour at 80 °C and the gel exposed to a storage phosphor screen (GE Healthcare). Generally, a 1- to 3-day exposure to a storage phosphor screen was sufficient to monitor the desired signal. Radioactivity was visualized using a phosphorimager (Typhoon™ Trio variable mode imager, GE Healthcare). Translocation efficiencies were quantified using the ImageQuant™ TL (GE Healthcare) software.

For time-course experiments, multiple reactions were set up as follows: 470 µl B88, 60 µl 10X ARS, 20 µl microsomes and 50 µl *in vitro* translated ^{35}S-Met-labeled ppαf or pΔgpαf. The reaction was set up on ice, gently resuspended and aliquoted into 60 µl aliquots. The samples were incubated at 20 °C over a time course of 60 min (samples were taken at time points t = 0, 5, 10, 15, 20, 30, 60 min).

Samples were immediately placed on ice and the reactions stopped with the addition of an equal volume of ice-cold 20 % (w/v) TCA. The samples were prepared for SDS-PAGE as described above.

* 10X ARS was aliquoted (100 µl, single-use tubes), snap-frozen in liquid nitrogen and stored at – 80 °C.

Table 2.22. Standard translocation reaction setup.

Component	Volume
B88*	47 µl
Microsomes (OD_{280} = 30)	2 µl
10X ATP**	6 µl
^{35}S-Met-labeled pΔgpαf***	5 µl

* B88: 20 mM Hepes-KOH pH 6.8; 250 mM Sorbitol, 150 mM KOAc, 5 mM $Mg(OAc)_2$
** 10 X ARS: 10 mM ATP, 500 mM Creatine Phosphate, 2 mg/ml Creatine Phosphokinase, B88 to volume
*** ~ 200000 cpm per reaction of *in vitro* translated ^{35}S-Met-labeled ppαf or pΔgpαf

Table 2.23. Composition of 18 % denaturing polyacrylamide 4 M urea gels.

Component	Separating gel (40 ml)	Stacking gel (25 ml)
Acrylamide*	24 ml	4.15 ml
1.5 M Tris-HCl pH 8.8	10 ml	---
0.5 M Tris-HCl pH 6.8	---	6.25 ml
20 % (w/v) SDS	200 µl	125 µl
Urea	9.6 g	6 g
dH_2O	---	10 ml
TEMED**	16.7 µl	15 µl
10 % APS**	200 µl	200 µl

* Rotiphorese® Gel 30 (Carl Roth®)
** TEMED and APS were added after the urea was dissolved completely.

2.2.34.7 *IN VITRO* RETROTRANSLOCATION ASSAY

The *in vitro* retrotranslocation assay was performed in order to examine the retrotranslocation and degradation efficiencies of Δgpαf in *sec61* mutant microsomes. Prior to the actual retrotranslocation reaction the retrotranslocation substrate pΔgpαf had to be translocated into ER-derived microsomes. This was accomplished by an *in vitro* translocation assay as described in 2.2.32.6 using *in vitro* transcribed and translated pΔgpαf (ref. 2.2.34.4 and 2.2.34.5). For retrotranslocation assays time-course experiments were conducted. Therefore, multiple translocation reactions were set up as a single "master" translocation reaction (∑600 µl: 10 x 60 µl) as described in 2.2.32.6 (ref. Table 2.22). The translocation reaction was incubated for 50 min at 20 °C in a water bath. Next, the membranes were pelleted at full speed and 4 °C for 5 min (Microcentrifuge 5415R, Eppendorf) and gently washed with 600 µl cold B88 (20 mM Hepes-KOH, pH 6.8, 250 mM Sorbitol, 150 mM KOAc, 5 mM $Mg(OAc)_2$). To the microcentrifuge tube containing the membranes the appropriate amount of cold B88 was added to a final volume of 600 µl. Further, 60 µl of 10X ARS (400 mM Creatine Phosphate,

2 mg/ml Creatine Phosphokinase, 10 mM ATP; prepared in B88) were added. Initiation of retrotranslocation and degradation was started by the addition of cytosol to 1-3 mg/ml in the final volume of 600 µl. The reaction mix was then divided into 60 µl aliquots which were incubated at 30 °C over a time course of 60 min (samples were taken at t = 0, 5, 10, 15, 20, 30, 60 min). Samples were immediately placed on ice and the reactions stopped with the addition of 60 µl 20 % (w/v) TCA. The samples were agitated on a Vortex mixer for 10 seconds and incubated on ice for 15 min. The samples were then centrifuged at full speed for 15 min, at 4 °C and the supernatant removed with a gel-loading tip. Next, sufficient ice-cold acetone was added to cover each pellet. Samples were agitated on a Vortex mixer for 10 seconds and centrifuged as before. The supernatant was removed with a gel-loading tip and the pellets air-dried and resuspended in 25 µl 2X SDS-PAGE Sample Buffer (125 mM Tris-HCl pH 6.8, 4 % (w/v) SDS, 10 % (v/v) β-Mercaptoethanol, 0.002 % (w/v) Bromophenol Blue, 20 % (v/v) Glycerol). The samples were heated at 70 °C for 15 min (Thermomixer® Comfort, Eppendorf). Proteins were resolved using an 18 % denaturing polyacrylamide gel containing 4 M urea (ref. Table 2.23) and 1X Running Buffer (5X: 0.5 % (w/v) SDS, 1.5 % (w/v) Tris Base, 7.2 % (w/v) Glycine). Gels were run overnight at RT and 90 V. The next day, when the dye front was near the bottom of the gel, the plates were disassembled and the gels fixed and dried as in 2.2.34.6. Exposure of the gels to storage phosphor screens was 2-3 days. Radioactivity was visualized using a phosphorimager (Typhoon™ Trio variable mode imager, GE Healthcare). The amount of degradation was quantified using the ImageQuant™ TL software (GE Healthcare).

2.2.35 PEGYLATION ASSAY

For the anaylsis of conformational changes in mutant Sec61p compared to wild-type Sec61p the PEGylation reagent Methyl-PEG_8-N-hydroxysuccinimide ester ($MS(PEG)_8$, Thermo Fisher Scientific) was used to modifiy accessible primary amines (in lysine residues and the N-terminus) in the protein.

In brief, generally in a final volume of 20 µl 2 µl (OD_{280} = 30) PKRMs (ref. 2.2.26) of the respective *sec61* mutants or the wild-type (*SEC61*) were carefully resuspended with the appropriate volume of Buffer 88 (20 mM Hepes-KOH pH 6.8, 250 mM Sorbitol, 150 mM KOAc, 5 mM $Mg(OAc)_2$), followed by the addition of 20 mM of $MS(PEG)_8$*. Samples were incubated for 30 min at 24 °C in a Thermomixer® comfort (Eppendorf) and reactions were stopped by addition of 1 µl 8 M ammonium acetate solution and incubated on ice for 15 min. Samples were analyzed by SDS-PAGE and Western Blot analysis (ref. 2.2.24) using the anti-Sec61p (N-terminal) and anti-Sbh1p (control) antibody (Römisch lab, ref. Table 2.7). Detection of signals and determination of relative mobility of PEGylated proteins was using the ChemiDoc™ XRS system and the Image Lab™ software (both Bio-Rad). The PageRuler™ (Fermentas, Thermo Fisher Scientific) was used as the molecular weight

standard.

* The MS(PEG)$_8$ stock solution was prepared in water-free DMSO (Thermo Fisher Scientific) and the amount of DMSO in each sample was kept under 10 % (v/v).

3 RESULTS

3.1 OVERVIEW

Sec61p, the pore-forming component of the translocon in *S. cerevisiae*, is an ER membrane protein consisting of ten TMDs (TMD 1-10; ref. Figure 3.1.1). The N- and C-termini of the protein as well as L 2, 4, 6 and 8 are located in the cytosol while L1, 3, 5 and 7 are located in the ER lumen (ref. Figure 3.1.1; Mothes *et al.*, 1994; Wilkinson *et al.*, 1996; Raden *et al.*, 2000; van den Berg *et al.*, 2004). During cotranslational and posttranslational protein import into the ER, Sec61p associates with other proteins to form the Sec61 complex or the SEC complex respectively (Johnson & van Waes, 1999; Park & Rapoport, 2012).

Besides its role during protein import, Sec61p has been suggested to be involved in protein dislocation during ERAD (Hilt & Wolf, 1996; McCracken & Brodsky, 1996; Wiertz *et al.*, 1996a; Johnson & Haigh, 2000; Römisch, 2005). It is still controversial, however, whether Sec61p directly forms the retrotranslocation channel or whether it is one of its components (Pilon *et al.,* 1997, Plemper *et al.*, 1997; Gillece *et al.*, 1999; Schäfer & Wolf, 2009).

One of the crucial steps during ERAD is the degradation of misfolded proteins by the 26S proteasome in the cytosol. It has been demonstrated that during ERAD the proteasome binds to the ER via Sec61p (Lee *et al.*, 2004b; Kalies *et al.,* 2005; Römisch, 2005; Ng *et al.*, 2007).

In a previous study, *sec61* mutants, *sec61-302* (D168G, S179P, F263L, S353C) and *sec61-303* (D168G, F263L), were isolated which showed defects in protein import into the ER for a cotranslational import substrate (ref. Figure 3.1.1). Only *sec61-302*, however, additionally displayed reduced proteasome binding (Ng *et al.*, 2007). As *sec61-302* and *sec61-303* share two point mutations it has been suggested that one or both of the two remaining amino acid substitutions, S179P and/or S353C, are responsible for the observed reduction in proteasome affinity (Ng *et al.*, 2007). As the amino acid substitution S179P is located at the cytoplasmic end of TMD 5, while the S353C mutation is located in L7, S179P seems to be the more promising candidate for further studies (Ng *et al.*, 2007).

In order to elucidate which domain in Sec61p mediates binding to the 26S proteasome during ERAD, I asked which of the two amino acid substitutions, S179P or S353C, is responsible for the reduced proteasome affinity. The *sec61* mutants generated in this study (ref. 3.2.1. and 3.2.2.) were further characterized using various genetic and biochemical methods.

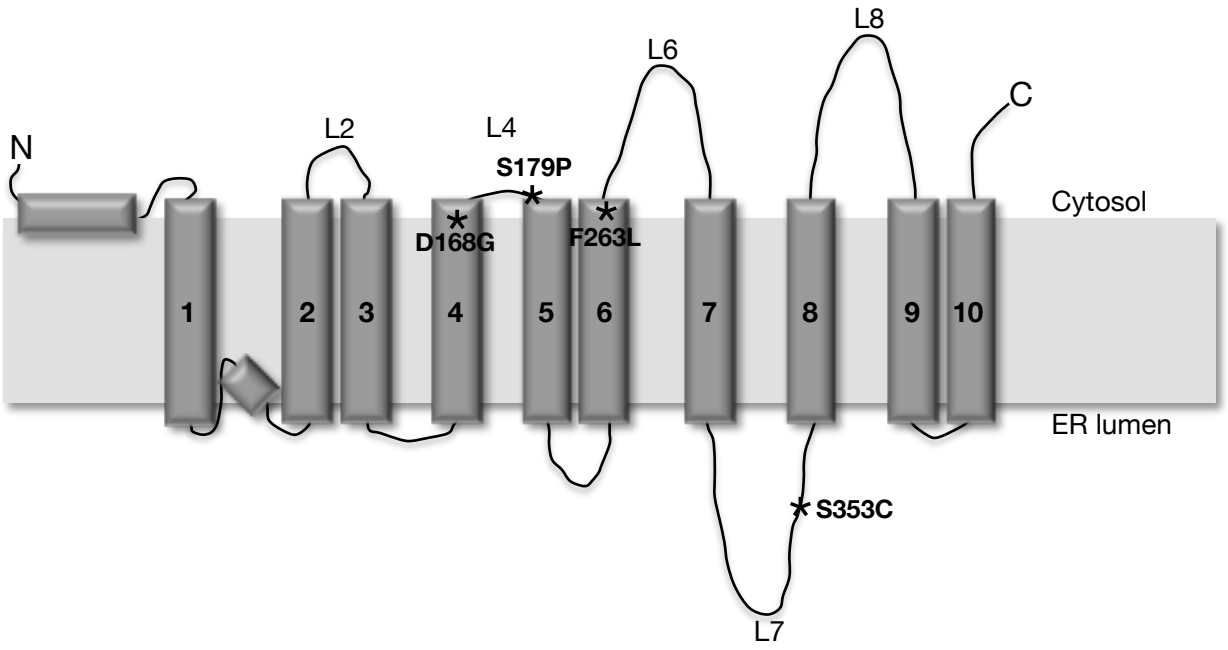

Figure 3.1.1. Topology model of Sec61p. Shown is a simplified topology model of the ER membrane protein Sec61p. The protein consists of ten TMDs (TMD 1 - 10) and four cytosolic loops (L 2, 4, 6 and 8) as well as four ER-lumenal loops (L1, 3, 5 and 7, not indicated). Both termini are located in the cytosol. Positions of point mutations (i.e. the resulting amino acid substitutions) in the *sec61* mutants *sec61-302* (amino acid substitutions: D168G, S179P, F263L, S353C) and *sec61-303* (D168G, F263L) are indicated (★). Both mutants share two of the same point mutations (D168G, F263L) and are defective in cotranslational protein import into the ER. Since only *sec61-302* shows reduced proteasome binding, S179P and/or S353C have been suggested to mediate the observed binding defect (Ng *et al.*, 2007; adapted from Wilkinson *et al.*, 1997; Raden *et al.*, 2000; van den Berg *et al.*, 2004)

3.2 GENERATION OF *S. CEREVISIAE SEC61* MUTANTS

3.2.1 GENERATION AND VERIFICATION OF THE *SEC61* MUTANTS *SEC61-S179P*, *SEC61-S353C* AND *SEC61-S179P/S353C*

As this study was based on previous work on *sec61* mutants, including *sec61-302* (D168G, S179P, F263L, S353C) and *sec61-303* (D168G, F263L), the same genetic background (JDY638 (pGAL-*SEC61*), ref. Table 2.4) was used to create the desired *sec61* mutants (Ng *et al.*, 2007). This was done to be able to use *sec61-302* and *sec61-303* as controls and thus compare results from previous studies (i.e. the reporter plasmid translocation assays and proteasome binding experiments) with those obtained from this study.

The desired *sec61* mutants, designated *sec61-S179P*, *sec61-S353C* and *sec61-S179P/S353C*, were generated by SOE-PCR (ref. 2.2.4.1) followed by the transformation (ref. 2.2.17) of the *S. cerecisiae* strain JDY638 with the respective construct (ref. 2.1.3; Ho *et al.*, 1989; Horton *et al.*, 1989; Gietz *et al.*, 1995).

During SOE-PCR plasmid pBW11 (ref. Table 2.5) consisting of the full-length wild-type *SEC61* gene cloned into the centromeric vector pRS315 was used as the template along with the appropriate oligonucleotides (ref. Table 2.6; Ho *et al.*, 1989; Horton *et al.*, 1989; Sikorski & Hieter, 1989; Stirling *et al.*, 1992; Wilkinson *et al.*, 1996). The desired point mutations T535C (*sec61-S179P*) and/or C1058G (*sec61-S353C*) were introduced into *SEC61* using specific mutagenic primers (ref. Table 2.6 and Table 2.14). The resulting mutant full-length *sec61* sequences, containing *Hin*dIII restriction sites at the 5' and the 3' ends, were cloned into the *Hin*dIII restriction site of the centromeric vector pRS315 (*CEN*, *ARS*, *LEU2*; Sikorski & Hieter, 1989). Next, the resulting plasmids (pRS315-*sec61-S179P*, pRS315-*sec61-S353C*, pRS315-*sec61-S179P/S353C*; ref. Table 2.5) were transformed into chemically competent *E. coli* cells (ref. 2.2.14.3) and plasmid DNA preparations (ref. 2.2.6) from resulting single colonies (clones) were verified by sequencing (ref. 2.2.15) (Sanger *et al.*, 1977; Birnboim & Doly, 1979). The DNA of positive clones was then used to transform the *S. cerevisiae* strain JDY638 using the lithium acetate method (Gietz *et al.* 1995; Ng *et al.*, 2007). The procedure is outlined in Figure 3.2.1.1.A. In *S. cerevisiae* strain JDY638 the expression of *SEC61* is under the control of the *GAL1* promoter, which was achieved using a cassette amplified with the kanamycin resistence gene and the *GAL1* promoter (*kanr-pGAL-SEC61*) (Ng *et al.*, 2007; J. Brown, personal communication). Selection of positive transformants was initially on Synthetic Complete (SC) plates without leucine (SC -LEU), containing 2 % (w/v) galactose and 0.2 % (w/v) raffinose, at 30 °C for three days. Cells expressing mutant *sec61* only were grown on rich medium (YPD) and SC -LEU plates both containing 2 % (w/v) glucose. This allows for the selection of those transformants, which are viable expressing mutant *sec61* (*pCEN-LEU2-sec61*). At the same time the expression of wild-

type *SEC61*, which is under the control of the *GAL1* promoter, is repressed. Thus, successful transformations led to growth of selected transformants on YPD and SC –LEU plates.

Results are shown in Figure 3.2.1.1.B. Following the selection of positive transformants on SC -LEU (2 % (w/v) galactose/ 0.2 % (w/v) raffinose) plates (not shown), two single colonies per transformation were plated onto SC -LEU plates (Figure 3.2.1.1.B Top) and YPD (Figure 3.2.1.1.B Bottom), both containing 2 % (w/v) glucose. The cells were grown at 30 °C for three days. The two wild-type strains JDY638 and RSY255 (*SEC61*) were used as controls. While the former does not grow on medium containing glucose (i.e. no growth on SC -LEU and YPD), the latter does, but needs leucine for growth (i.e. growth on YPD only). Thus, both control strains behaved as expected. As seen in Figure 3.2.1.1.B, all of the *sec61* mutants (*sec61-S179P*, *sec61-S353C*, *sec61-S179P/S353C*) selected were viable as they grew on YPD (Bottom) as well as on SC -LEU medium (Top). Thus, the *sec61* mutants could be used during further for analyses.

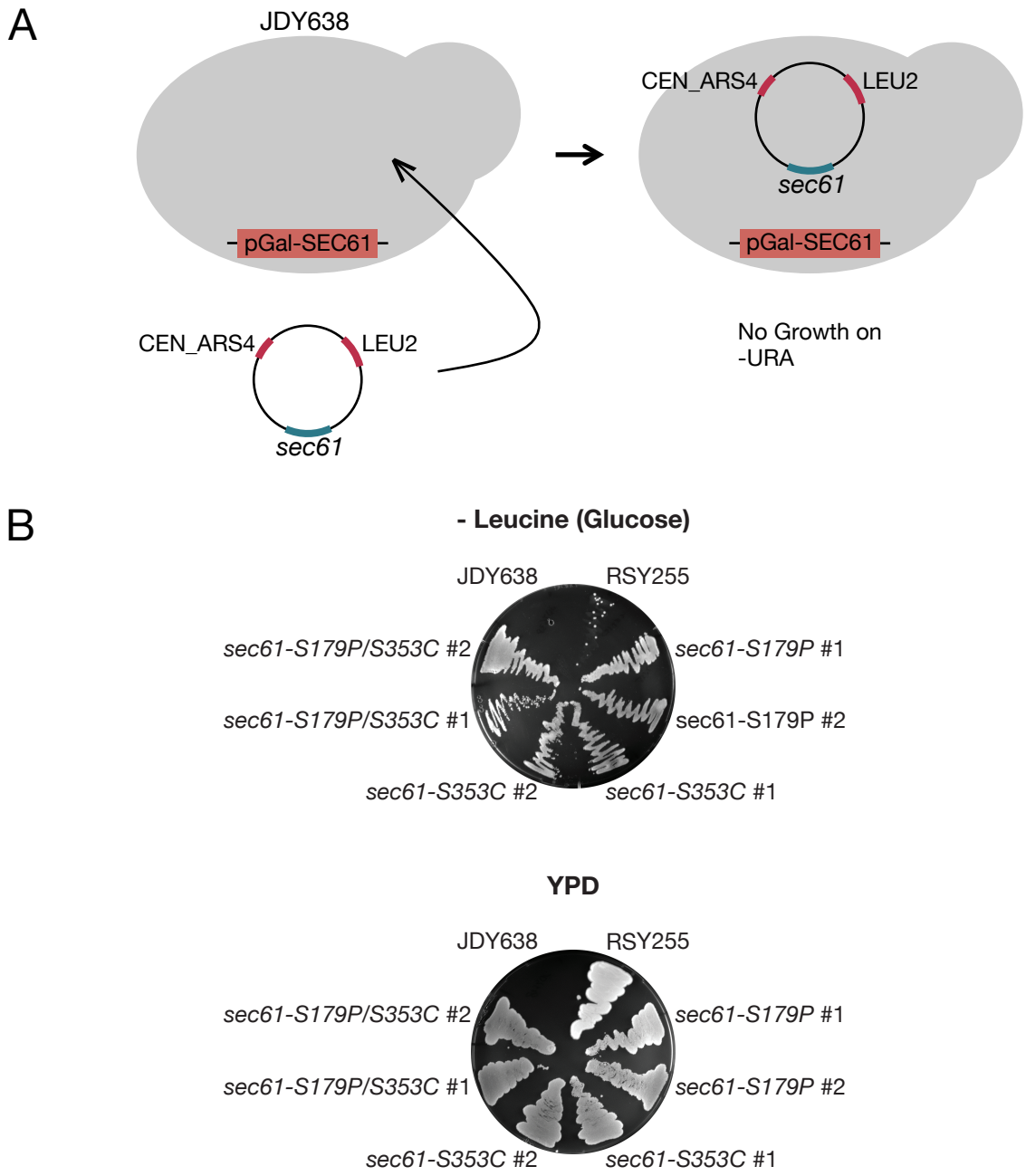

Figure 3.2.1.1 Generation and verification of *sec61* mutants in the JDY638 background. (A) Schematic representation of JDY638 (*kanr-pGAL-SEC61*) transformation with constructs expressing mutant *sec61* (pRS315-*sec61-S179P*, pRS315-*sec61-S353C,* pRS315-*sec61-S179P/S353C*). Initial selection was on SC plates without leucine (2 % (w/v) galactose/ 0.2 % (w/v) raffinose) (not shown) to select for the plasmid only. Viability of cells expressing mutant *sec61* only was monitored on YPD and SC -LEU plates (2 % (w/v) glucose) to test for function of mutant Sec61p. (B) JDY638 derivatives (*pCEN-LEU2-sec61*) were grown on SC plates without leucine d/o (Top) and YPD (Bottom) plates for 3 days at 30 °C in order to select for transformants containing the *sec61* expression plasmid. JDY638 and RSY255 were used as controls.

3.2.2 GENERATION AND VERIFICATION OF THE *SEC61* INTEGRATION MUTANTS *SEC61-S179P*, *SEC61-S353C*, *SEC61-S179P/S353C*, *SEC61-302* AND *SEC61-303*

The *sec61* integration mutants, designated *sec61-S179P*, *sec61-S353C*, *sec61-S179P/ S353C, sec61-302* and *sec61-303*, were created to be used in the *in vitro* retrotranslocation assay using pαf, a soluble ERAD substrate, and the *in vitro* translocation assay using wild-type ppαf, the precursor of 3gpαf (Caplan *et al.*, 1991; McCracken & Brodsky, 1996; Brodsky, 2010).

The respective integration constructs consisted of the appropriate truncated *sec61* sequences cloned into the yeast integrative vector pRS306 (*URA3*; Sikorski & Hieter, 1989). Truncated versions of the mutated *sec61* sequences *sec61-S179P*, *sec61-S353C*, *sec61-S179P/S353C* (ref. 3.2.1), *sec61-302* and *sec61-303* were created using SOE-PCR (ref. 2.2.4.1 and Table 2.14) (*sec61-302* and *sec61-303*: ref. Ng *et al.*, 2007). This was achieved by using the appropriate centromeric plasmids (pRS315-*sec61*-S179, pRS315-*sec61*-S353C and pRS315-*sec61*-S179P/S353C, ref. Table 2.5) containing the respective full-length *sec61* sequences, described in 3.2.1, as templates for the amplification of each truncated *sec61* sequence. Further, the *sec61* integration mutants *sec61-302* and *sec61-303* were created using plasmids from a previous study, containing the respective mutant full-length *sec61* sequences cloned into pRS315, as templates (*sec61-302*: plasmid #14; *sec61-303*: plasmid #18; Ng *et al.*, 2007). The truncation of each *sec61* sequence at the 5' end was achieved by using a specific primer (5' *Hin*dIII SEC61 #57; ref. Table 2.6), which truncated the *sec61* sequences + 57 base pairs (bp) relative to the start codon (ATG) of the gene.

In order to be able to integrate the respective *sec61* sequences into the yeast strain RSY255 (ref. Table 2.4) linearization of the respective integrative plasmid in the region of the truncated *sec61* sequence was necessary prior to transformation. As there was no unique restriction site available in the desired region of the *sec61* sequence that could be used for linearization, a silent mutation was introduced at nucleotide position 201 (+ 201 bp relative to the ATG; nucleotide exchange: T201G → amino acid substitution: R67R) of *SEC61* which created an *Sfi*I restriction site (ref. Table 2.6 and Table 2.14). The introduction of a restriction site at this position created a sufficient recombinogenic stretch between the restriction site and the first point mutation in *sec61-302* and *sec61-303*, A503G (amino acid substitution: D168G). This allows for efficient integration of the respective *sec61* sequences into the yeast genome, as the recombinogenic ends of the linearized integrative constructs direct the *sec61* sequences to the appropriate homologous site in the yeast genome.

Following SOE-PCR, the resulting truncated *sec61* sequences were cloned (ref. 2.2.12) into the yeast integrative vector pRS306 (Sikorski & Hieter, 1989). Chemically competent DH5α *E. coli* cells were transformed (ref. 2.2.14.3) and plasmid DNA (ref. 2.2.5) of resulting single colonies was prepared and sent for sequencing (ref. 2.2.15). Once, the appropriate *sec61* mutants were obtained, the yeast strain RSY255, which is routinely used for *in vitro* assay, was transformed with the

respective linearized plasmid (ref. 2.2.17 and Table 2.5; Ho *et al.*, 1989; Horton *et al.*, 1989; Gietz *et al.*, 1995).

The linearized integration constructs enter the chromosome by homologous recombination as shown in Figure 3.2.2.1.A. The recombinogenic ends of the linearized constructs direct the plasmid to integrate at the wild-type *SEC61* locus homologous to the ends of the linearized sequence. Upon successful integration, the chromosome contains one complete copy of the mutant *sec61* gene followed by the pRS306 backbone, including the *URA3* marker, and a truncated version of *SEC61* (*#sec61*).

Following the transformation, positive tansformants were selected on SC -URA plates (- Uracil) at 30 °C for three days. Growth of transformants (two per transformation) that came up on SC -URA plates were restreaked onto the same plates to verify their ability to grow on SC -URA medium.

Integration of the respective *sec61* sequences into the genome of RSY255 at the correct chromosomal locus was verified by PCR. Following the selection of real transformants (ref. Figure 3.2.2.1.B), chromosomal DNA (ref. 2.2.22) of several positive transformants was prepared. The isolated chromosomal DNAs were used as templates for the PCR (ref. 2.2.18) along with a set of specific primers (Forward primer: 5' *Hin*dIII SEC61 5' UTR #-445; Reverse primer: 3' pRS306 URA3 #621; ref. Table 2.6). The primers were chosen to bind in the chromosomal part of *SEC61* (- 445 bp relative to the ATG) upstream of the integrated *sec61* sequence as well as in the backbone of the pRS306-based plasmid (i.e. the *URA3* marker; + 621 bp relative to the ATG of *URA3*). This allows for verification of properly integrated *sec61* sequences. Only upon integration at the *SEC61* locus, a PCR product of 5556 bp could be amplified. The control primers (5' *Sal*I YDJ1 and 3' YDJ1 *Xba*I; ref. Table 2.6) targeted *YDJ1* (Ydj1p). The amplified product using these primers was 1230 bp in size. *YDJ1* codes for Ydj1p, a cytoplasmic type I Hsp40 co-chaperones belonging to the Hsp40/DnaJ family. Ydj1p is involved in the regulation of Hsp70s and Hsp90s and also protein translocation across membranes, protein folding and ubiquitin-dependent degradation (Caplan & Douglas, 1991; Caplan *et al.*, 1992; Kimura *et al.*, 1995; Lee *et al.*, 1996).

Thus, positive transformants were expected to display two bands, one at 1230 bp (*YDJ1*) and one band at 5556 bp (*sec61* int. (integrated)). Chromosomal DNA of RSY255 (*SEC61*) was used as a control. Here, only a band at 1230 bp was expected. Of the positive transformants shown in Figure 3.2.2.1.B, chromosomal DNA was prepared and tested. The results are shown in Figure 3.2.2.1.C. For each transformant tested, the integration into the genome of RSY255 at the *SEC61* locus was successful (*sec61* int.: lanes 2-6 and 9-11) as the desired band of 5556 bp was successfully amplified. The control PCRs were also positive (*YDJ1*: lanes 2-6 and 9-11), as for all transformants the 1230 bp band could be amplified. As a further control, PCRs using chromosomal DNA of untransformed RSY255 (*YDJ1*. lanes 1 and 8) were performed. While for PCRs performed with DNA of the *sec61* integration strains bands were detected for *YDJ1* as well as for *sec61* (*sec61* int.), for the PCR using RSY255 chromosomal DNA, only a band at 1230 bp should be detectable using both

primer sets (*sec61* int./YDJ1: lanes 1 and 8). This was as expected. Thus, the generation of the *sec61* integration strains *sec61-S179P*, *sec61-S353C*, *sec61-S179P/S353C*, *sec61-302* and *sec61-303* was successful and the transformants could be used for *in vitro* studies.

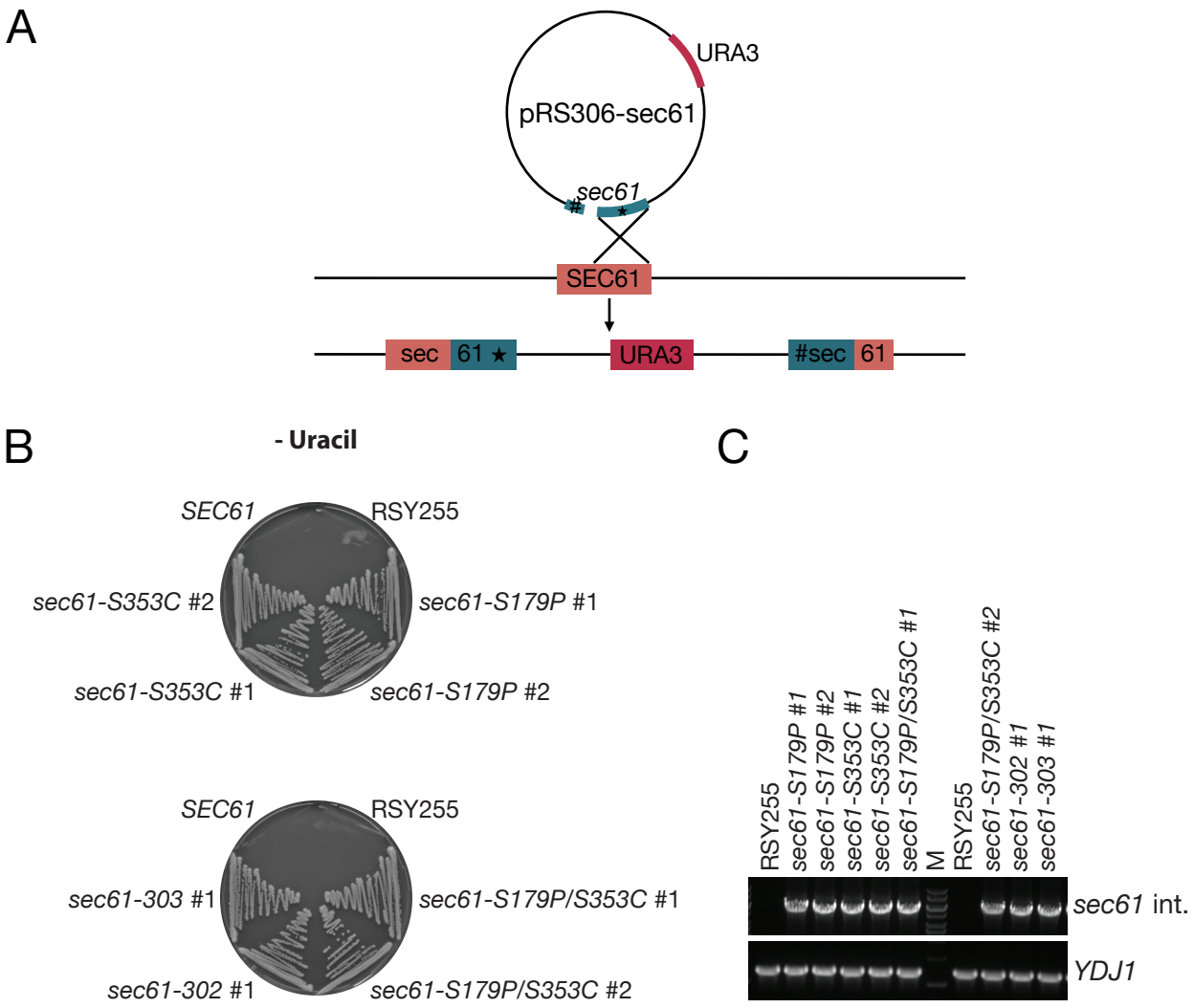

Figure 3.2.2.1 Generation and verification of *sec61* integration mutants. (A) Schematic representation of sequence integration into the yeast genome by homologous recombination. Yeast transformation with the linearized integration plasmid pRS306-*sec61*, containing the appropriate truncated *sec61* gene, leads to the integration of the sequence at the *SEC61* locus homologous to the digested sequence, resulting in one complete copy of *sec61* containing the appropriate point mutation(s) (sec61★) followed by the pRS306 backbone sequence including *URA3* and a truncated version of *SEC61* (#sec61). (B) RSY255 was transformed with the linearized (*Sfi*I) plasmids pRS306-*truncsec61** (*: S179P; S353C; S17PP/S353C; 302; 303). Selection of positive transformants was on SC -URA plates at 30 °C for 3 days. Controls: JDY638 (*SEC61*) and RSY255 (both: no growth on - Uracil). (C) Verification of integration of the appropriate *sec61* sequence at the *SEC61* locus was by PCR using chromosomal DNA of positive transformants and specific primers (*sec61* int. (5556 bp): lanes 2-6 and 9-11). Control primers targeted *YDJ1* (*YDJ1* (1230 bp): lanes 1-6 and 8-11). Chromosomal DNA of untransformed RSY255 (*YDJ1* and *sec61* int.: lanes 1 and 8) was used as another control. (int. = integrated).

3.3 GROWTH ANALYSIS OF THE *SEC61* MUTANTS

The JDY638 derivatives *sec61-S179P*, *sec61-S353C* and *sec61-S179P/S353C* that are described in 3.2.1, were initially tested for growth (i.e. viability) at various temperatures.

Serial dilutions (10^5 – 10^0 cells) of each strain were plated onto rich medium (YPD), minimal medium (SC) and on the same media containing the ER stress inducer tunicamycin (Tm). The plates were all incubated at the designated temperaures (37 °C, 30 °C, 25 °C and 20 °C) for three days (ref. Figure 3.3.1). The two *sec61* mutants isolated in a previous study, *sec61-302* and *sec61-303,* were included in the analysis. Both strains were in the same genetic background (JDY638) as the newly generated mutants (Ng *et al.*, 2007). Further, *sec61-3* (G341E; maps to the ER-lumenal loop 7) and *sec61-32* (C150Y; maps to the ER-lumenal end of TMD 4) were used as controls. The mutant *sec61-32* has been shown to be cold-sensitive (Cs) for growth and protein translocation into intact cells (Pilon *et al.*, 1997, Pilon *et al.*, 1998). The mutant *sec61-3* has been described to be cold- (Cs) and temperature-sensitive (Ts) (Sommer & Jentsch, 1993; Stirling *et al.*, 1992; Pilon *et al.*, 1997; Wilkinson *et al.*, 1997). Further, membranes isolated from both strains have been shown to be deficient in translocation into the ER as well as in ER degradation, as shown in an *in vitro* retrotranslocation assay reproducing the export of an ERAD substrate from the ER for degradation in the cytosol (Pilon *et al.*, 1998).

Results are shown in Figure 3.3.1. As seen in Figure 3.3.1 (YPD, - Tm), none of the *sec61* mutants *sec61-S179P*, *sec61-S353C*, *sec61-S179P/S353C*, *sec61-302* and *sec61-303* exhibited growth defects on rich medium compared to wild-type cells at the temperatures tested. While at 30 °C and 25 °C (10^5-10^1 cells) growth was optimal, it was reduced at 20 °C (10^5-10^2 cells) and 37 °C (10^5-10^3 cells) for all strains. The control strains, *sec61-3* (Cs, Ts) and *sec61-32* (Cs), displayed impaired growth at 20 °C (restrictive temperature: 18 °C). At this temperature the effect for *sec61-32* (reduced growth at 10^5 cells) was more pronounced as for *sec61-3* (10^5-10^4 cells). Moreover, *sec61-3* (reduced growth even at 10^5 cells) displayed reduced growth at 37 °C (restrictive temperature) as described previously (Stirling *et al.*, 1992; Sommer & Jentsch, 1993; Pilon *et al.*, 1998). Growth at 25 °C and 30 °C of both strains was comparable to the wild-type (*SEC61*). It has, however, to be noted that *SEC61* is not the isogenic wild-type for *sec61-3* and *sec61-32*. Since the two mutants grew as described previously at the restrictive and permissive temperatures, growth rates of the two control strains were compared to this wild-type (Sommer & Jentsch, 1993; Pilon *et al.*, 1997, 1998).

As none of the *sec61* mutants, except *sec61-3* and *sec61-32*, displayed growth defects on rich medium at any of the temperatures tested, growth was also tested on minimal medium (SD), i.e. under more restrictive nutritional conditions (Figure 3.3.1, SD, - Tm). As for growth experiments on YPD, growth of the *sec61* mutants (JDY638 derivatives) on SD medium was comparable to the wild-type (*SEC61*) at all temperatures tested. For all strains tested, however, single colonies were smaller when grown on SD medium. While growth of the JDY638 derivatives at 30 °C and 25 °C (both 10^5-10^2 cells) was comparable to growth on YPD, it was reduced at 37 °C (10^5-10^4 cells) and 20 °C (10^5-

10^3 cells). Further, on SD medium, the *sec61* mutants *sec61-3* and *sec61-32* showed the same growth defects at 20 °C (*sec61-3*: 10^5-10^4 cells; *sec61-32*: reduced growth at 10^5-10^4 cells) and 37 °C (*sec61-3*: strongly reduced growth at 10^5 cells), which were a little more pronounced than those observed for growth on YPD, while growth at 25 °C (10^5-10^2 cells) and 30 °C (10^5-10^2 cells) was comparable to the wild-type (*SEC61*).

Further growth analyses were performed in the presence of the UPR inducer tunicamycin (Tm). The antibiotic tunicamycin interferes with N-linked glycosylation in the ER, leading to increased ER stress and eventually to the induction of the UPR (Kuo & Lampen, 1974; Duksin & Mahoney, 1982; Langan & Slater, 1991; Torrez-Quiroz *et al.*, 2010).

First, strains were grown on YPD plates containing 0.25 µg/ml Tm for three days at the respective temperatures (ref. Figure 3.3.1, YPD, + Tm). Growth on medium containing Tm was monitored in order to analyze whether any of the mutations in *SEC61* lead to a reduced capacity of the respective strain to recover from an increase in ER stress compared to any of the other strains. I reasoned that if either of the mutations in *SEC61* affected protein translocation across the ER membrane, and especially dislocation, this would affect the cells' ability to recover from the accumulation of unglycosylated proteins in the ER. This would result in growth defects on medium containing (Tm). As shown in Figure 3.3.1 (YPD, + Tm), the *sec61* mutants, *sec61-S179P*, *sec61-S353C, sec61-S179P/S353C, sec61-302* and *sec61-303* showed growth rates comparable to the corresponding wild-type (*SEC61*) when Tm was added at a concentration of 0.25 µg/ml, i.e. no severe growth defect was visible. Upon addition of Tm to the medium, however, the growth of these strains was altogether reduced compared to growth on rich medium alone, indicating that under the conditions tested none of the *sec61* mutants was more severely affected than the wild-type (*SEC61*) at neither temperature. At 25 °C, 30 °C and 37 °C growth was reduced by one dilution step compared to growth of these strains on YPD only. At 20 °C a reduction in growth of two dilution steps was detected (ref. Figure 3.3.1, YPD, +/- Tm). It has been shown previously that the mutation in *sec61-3* (isolation via an UPR screen) leads to an activation of the UPR in this strain (Sommer & Jentsch, 1993). Thus, I expected *sec61-3* to be sensitive to Tm. For *sec61-32*, I reasoned that this strain, as it is Cs and defective in protein import and export, would also be sensitive to the antibiotic (Pilon *et al.*, 1007; Pilon *et al.*, 1998). The control strains *sec61-3* and *sec61-32* showed a reduction in growth at all temperatures compared to the remaining strains. As expected, this effect was more pronounced at 20 °C (almost two dilution steps) and 37 °C (growth even more compromised at 10^5 cells) for *sec61-3* and at 20 °C (unable to form single colonies at 10^5 cells) for *sec61-32*. Thus, growth defects at the restrictive temperatures are more severe under the influence of the ER stress inducer.

Additionally, growth was tested on minimal medium containing two concentrations of Tm (0.25 µg/ml and 0.5 µg/ml). The higher concentration was chosen, as on YPD in the presence of 0.25 mg/ml Tm, the effects were only subtle. As seen in Figure 3.3.1 (SD, + Tm), growth of the JDY638 derivatives at 30 °C in the presence of 0.25 µg/ml Tm was only slightly reduced compared to growth on SD alone.

This effect was slightly more pronounced when 0.5 µg/ml Tm were added to the medium. Here, a reduction in growth of almost one dilution step compared to growth on SD (- Tm) was observed. The same was found for mutants *sec61-3* and *sec61-32* at this temperature. When grown at 25 °C in the presence of 0.25 µg/ml Tm, growth of the JDY638 derivatives was comparable growth on SD (- Tm). When 0.5 µg/ml Tm was added to the medium, a reduction in growth of one dilution step was observed. However, as for growth at 30 °C, growth rates of all *sec61* mutants were comparable to the wild-type (*SEC61*). At a Tm concentration of 0.25 µg/ml, *sec61-3* grew on SD as without the addition of Tm. For this strain growth was reduced by almost two dilution steps at a Tm concentration of 0.5 µg/ml. The effect was more severe for *sec61-32*. While growth at 0.25 µg/ml Tm was comparable to growth on SD without Tm, at a concentration of 0.5 µg/ml hardly any growth was detected. At 20 °C a reduction in growth rate by about two dilution steps was observed for the JDY638 derivatives in the presence of 0.25 µg/ml Tm. At the higher Tm concentration hardly any growth was detected at this temperature. The mutant *sec61-3* displayed growth comparable to growth on SD alone at the lower Tm concentration, while at the higher concentration there was hardly any growth. As for *sec61-32* growth was already compromised on SD without the addition of Tm, there was no growth at both Tm concentrations. Finally, at 37 °C there was a slight reduction in growth for the JDY638 derivatives at the lower Tm concentration, which was slightly more pronounced at 0.5 µg/ml Tm. Since for the mutant *sec61-3* there was hardly any growth on SD alone, growth was still compromised when Tm was added. The mutant *sec61-32*, although at this temperature overall growth was stronger than for the JDY638 derivatives, growth was reduced by almost to dilution steps when 0.2 µg/ml Tm were added. This effect was more pronounced when 0.5 µg/ml Tm was added.

Under the conditions tested, the newly generated *sec61* mutants as well as *sec61-302* and *sec61-303* are viable and are not cold-sensitive or temperature-sensitive as e.g. *sec61-3* or *sec61-32* (Stirling *et al.*, 1992; Sommer & Jentsch, 1993; Pilon *et al.*, 1997; Pilon *et al.*, 1998; Ng *et al.*, 2007). Comparing their abilities to grow on rich medium or minimal medium to the corresponding wild-type (*SEC61*), they do not show any growth defects on either medium and drop out medium (ref. Figure 3.3.1, YPD, SD). Even when Tm (i.e. upon ER stress induction) was added the *sec61* mutants grow comparable to the wild-type (*SEC61*). The results therefore imply that the mutations in *SEC61* in the respective *sec61* mutants (*sec61-S179P*, *sec61-S353C*, *sec61-S179P/S353C*, *sec61-302* and *sec61-303*) do not affect the function of Sec61p as severely as e.g. those found in *sec61-3* and *sec61-32*. Even the *sec61* mutants *sec61-302* and *sec61-303*, which are defective in cotranslational protein import into the ER, displayed no growth defects, suggesting that the import defect is not severe enough to disturb cell viability under the conditions tested.

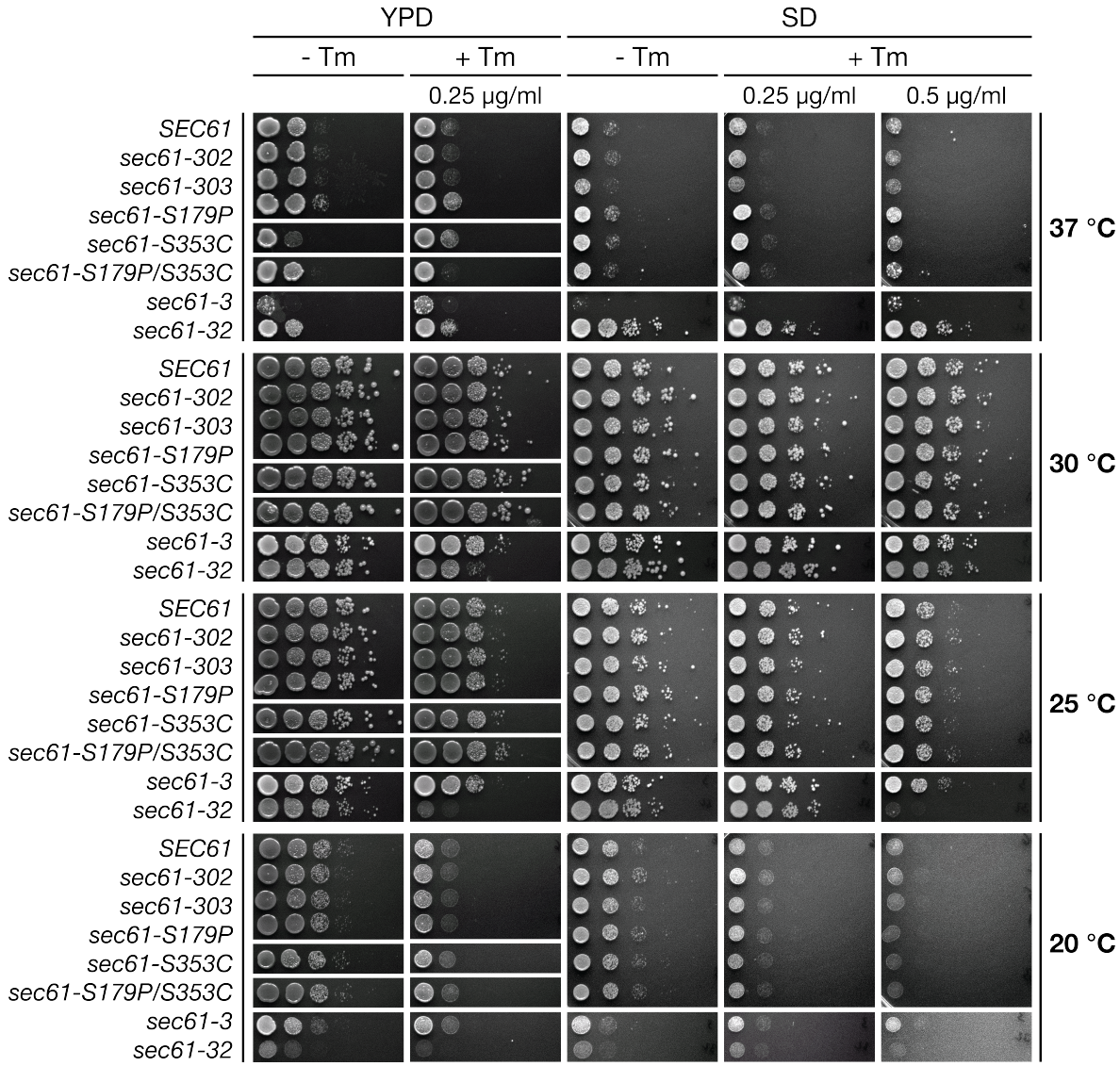

Figure 3.3.1. Growth analyses of the *sec61* mutants. Growth analyses were performed using the *sec61* mutants *sec61-S179P*, *sec61-S353C* and *sec61-S179P/S353C*, generated in this study, as well as *sec61-302* and *sec61-303* (all in the JDY638 background; Ng *et al.*, 2007). Serial dilutions (10^5-10^0 cells) of each yeast strain were dropped onto the respective plates and incubated at 20, 25, 30 and 37 °C for 3 days. Initially growth was monitored on rich medium in the absence (YPD, -Tm) or presence (YPD, +Tm) of tunicamycin. In order to analyze whether any of the strains showed growth defects under more restrictive nutritional conditions the growth analyses were repeated using minimal medium (SD, - Tm). Again, in order to evaluate the impact of induced ER stress on the growth of the different *sec61* mutants (i.e. on their capacity to cope with the accumulation of misfolded proteins in the ER), growth was additionally monitored in the presence of tunicamycin (SD, +Tm). Growth rates were compared to the corresponding *SEC61* wild-type strain. The mutants *sec61-3* and *sec61-32* were used as controls. Plates were photographed using the E-Box VX2 Gel Documentation System (Peqlab).

3.4 TESTING FOR TRANSLOCATION DEFECTS USING *URA3*-REPORTER FUSION PROTEINS

The *sec61* mutants *sec61-302* and *sec61-303* isolated in a previous study are defective in cotranslational protein import into the ER (Ng *et al.*, 2007). In the study mentioned, protein import capacities of the *sec61* mutants *sec61-301* (R67C), *sec61-302* (D168G, S179P, F263L, S353C) and *sec61-303* (D168G, F263L) were monitored using a *URA3*-reporter plasmid translocation assay and results compared to the corresponding wild-type (*SEC61*) (all in the JDY638 background; Ng *et al.,* 1996; Ng *et al.*, 2007). The assay was performed using reporter constructs for co- and posttranslational translocation (Ng *et al.*, 1996, 2007). As all of the above *sec61* mutants showed defects in cotranslational import, but only membranes of the mutant *sec61-302* displayed reduced proteasome binding, it was reasoned that the two amino acid substitutions D168G and F263L, which *sec61-302* and *sec61-303* share, mediate the cotranslational import defect observed in these mutants. Therefore, it has been concluded that the two remaining amino acid substitutions in *sec61-302*, F179P and/or S353C, are responsible for the reduction in proteasome affinity (Ng *et al.*, 2007).

In order to analyze whether the amino acid substitutions S179P and/or S353C cause a cotranslational import defect on their own, I repeated the reporter translocation assay using the mutants *sec61-S179P*, *sec61-S353C* and *sec61-S179P/S353C* described in 3.2.1 (ref. 2.2.20). The mutant *sec61-302* was used as a control as well as the corresponding wild-type (*SEC61*) strain. All strains were in the JDY638 background in order to compare the data with previous results (Ng *et al.*, 2007).

For the reporter translocation assay the JDY638 derivatives *SEC61*, *sec61-302*, *sec61-S179P*, *sec61-S353C* and *sec61-S179P/S353C* (Ng *et al.*, 2007; this study), which are uracil auxotrophic strains, were transformed with a plasmid containing a reporter construct for either cotranslational import, pJEY203 (Ng *et al.*, 2007) or posttranslational import, pDN106 (Ng *et al.*, 1996), or the empty pRS313 vector (Sikorski & Hieter, 1989). The reporter plasmid pNY203 (pRS313-*PHO8-URA3*) expresses a fusion protein of the first 70 amino acids of *PHO8* and the whole open reading frame (ORF) of *URA3*. The fusion sequence is under the control of the PHO5 promoter (Ng *et al.*, 2007). *PHO8* encodes alkaline phosphatase, which is involved in the dephosphorylation of phosphotyrosyl peptides in *S. cerevisiae* and is cotranslationally imported into the ER (Donella-Deana *et al.*, 1993). *URA3* encodes the Orotidine-5'-phosphate (OMP) decarboxylase which is involved in the *ne novo* biosynthesis of pyrimidines in the cytosol (Lacroute, 1968). The fusion protein is cotranslationally imported into the ER. The second reporter plasmid used in this experiments was pDN106 (pRS313-*CPY-URA3*), which has been created by fusing the promoter sequence of *PRC1* (CPY) and its amino-terminal 110 amino acids in frame with *URA3*. The initiator methionine of Ura3p was replaced by glycine as a linker. As for pJEY203, the resulting recombinant gene was cloned into the yeast centromeric vector pRS313 (Sikorski & Hieter, 1989; Ng *et al.*, 1996).

The *PRC1* (CPY) portion of the fusion gene encodes the yeast vacuolar carboxy peptidase Y, which is involved in protein degradation in the vacuole (van den Hazel *et al.*, 1996). The fusion protein is posttranslationally imported into the ER.

Following the transformation of the *sec61* mutants and the wild-type (*SEC61*) with the reporter constructs or the empty vector, transformants were selected on minimal medium containing glucose but lacking histidine and leucine (-HIS/LEU) at 30 °C for three days. For the assay, serial dilutions (10^4-10^1 cells) of an overnight culture of each strain were plated onto minimal medium plates lacking HIS/LEU (+ Uracil) and onto the same plates also lacking uracil (-HIS/LEU/URA; - Uracil), respectively. Growth on minimal medium -HIS/LEU plates selects for the reporter plasmid and the plasmid encoding the *sec61* mutants whereas growth on minimal medium -HIS/LEU/URA plates monitors translocation defects. In *sec61* mutants with disturbed protein translocation the Ura3p fusion protein remains in the cytosol and thus allows growth on plates lacking uracil (ref. Figure 3.4.1.A).

The results are shown in Figure 3.4.1.B. On minimal medium -HIS/LEU (+ Uracil) plates all of the *sec61* mutants transformed with the reporter plasmids and the control grew comparable to wild-type (*SEC61*) cells (Figure 3.4.1.B, + Uracil, PHO8, CPY, pRS313). This is in concordance with data from growth experiments that have shown that the *sec61* mutants analyzed are all viable, i.e. Sec61p function is not disturbed to the extent that cell viability is compromised (ref. 3.3).

As shown in Figure 3.4.1.B, growth on minimal medium -HIS/LEU/URA (- Uracil) plates, which monitors translocation defects, was only detectable for *sec61-302* transformed with the reporter plasmid for cotranslational import (pRS313-*PHO8-URA3*). This supports data from a previous study, which has shown that the mutant *sec61-302* is defective in protein import of the cotranslational import substrate Pho8p (Ng *et al.*, 2007). For the remaining *sec61* mutants tested as well as for the wild-type (*SEC61*) no growth on minimal medium -HIS/LEU/URA (- Uracil) plates was detectable when transformed with either pRS313-*PHO8-URA3* or pRS313-*CPY-URA3*. The vector pRS313 was used as a negative control (Figure 3.4.1.B, none, pRS313). The fact that the cells failed to grow indicates that the reporter fusion protein was translocated into the ER, i.e. none of these strains is defective in co- or posttranslational protein import.

Since none of the *sec61* mutants created in this study (ref. 3.2.1) display defects in co- or posttranslational protein import during the reporter plasmid translocation assay, I reasoned that these mutants would be great tools for elucidating which domain(s) of Sec61p are involved protein dislocation (ERAD), i.e. proteasome binding during retrotranslocation. Hence, defects that might be detectable here could then be solely attributed to the effect of the amino acid exchange S179P and/or S353C on Sec61p's function during these processes and would thus not be a result of disturbed protein import.

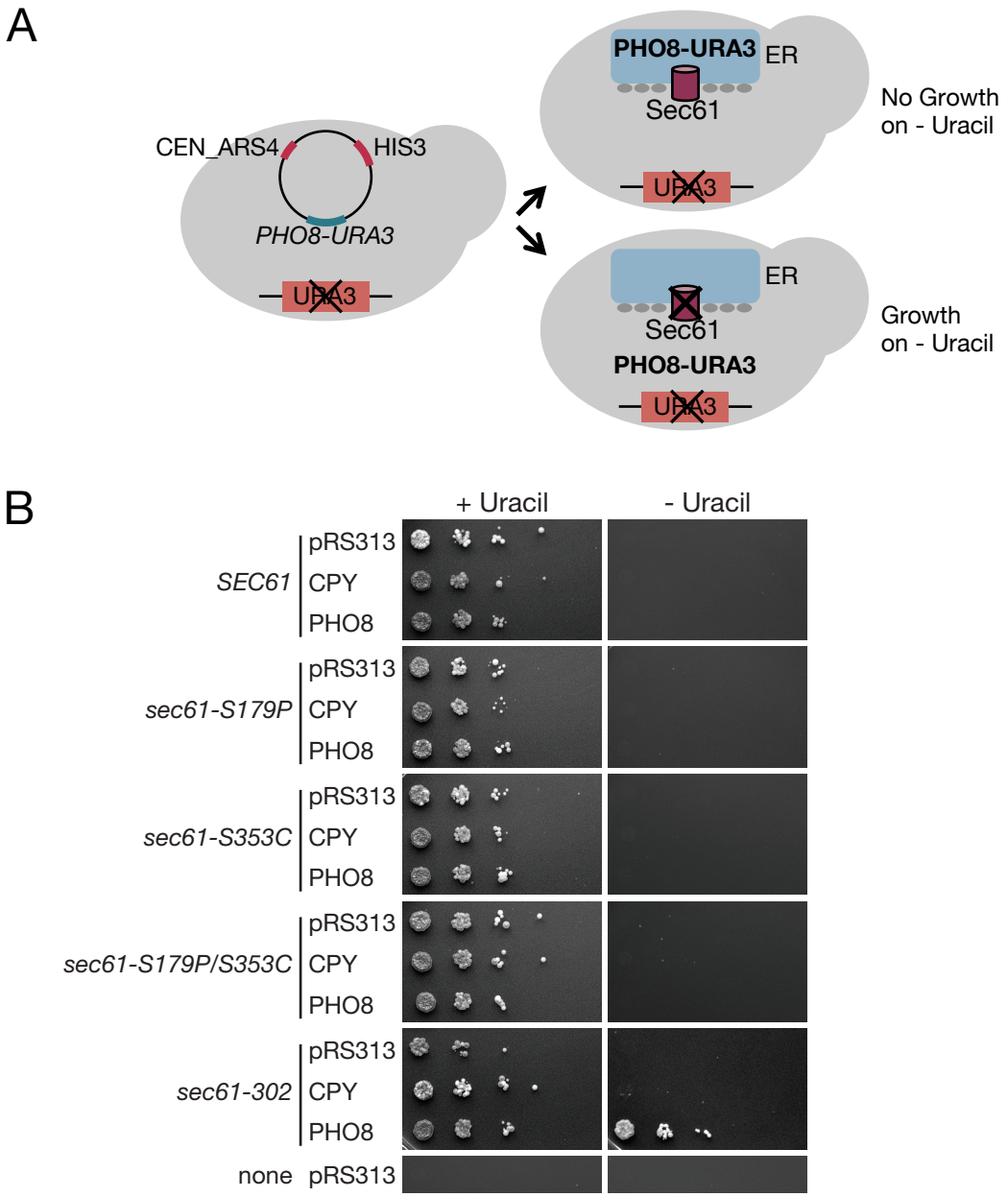

Figure 3.4.1. **Detection of translocation defects using a reporter translocation assay.** (A) Schematic representation of the reporter translocation assay. Yeast strains transformed with the reporter plasmid for cotranslational (pRS313-*PHO8-URA3* (shown), or posttranslational import (pRS313-*CPY-URA3*), or the empty vector pRS313 (control) were grown on minimal medium plates lacking leucine and histidine (not shown). Translocation defects of the respective reporter fusion protein results in growth on minimal medium lacking histidine, leucine and uracil (- Uracil). (B) Serial dilutions (10^4-10^0 cells) of the indicated JDY638 derivatives, transformed with either of the reporter plasmids or pRS313, were grown at 30 °C for 3 days on minimal medium lacking histidine and leucine (+ Uracil; controls for Sec61p function) and on the same plates lacking uracil (- Uracil; controls for translocation defects) (N = 3; Sikorski & Hieter, 1989; Ng *et al.*, 1996; Ng *et al.*, 2007).

3.5 PROTEASOME BINDING ASSAY

In a previous study the *sec61* mutant *sec61-302* (D168G, S179P, F263L, S353C) was shown to display reduced proteoliposome binding to purified 19S RP (Ng *et al.*, 2007). From the binding experiments and additional data it has been suggested that the amino acid substitutions S179P and/or S353C are responsible for the reduction in proteasome affinity (Ng *et al.*, 2007). S179P being the only residue accessible from the cytosol has been speculated to be the more likely candidate (Ng *et al.*, 2007). Therefore, in order to elucidate which of the two point mutations cause the reduction in proteasome affinity, I performed binding experiments using the mutants *sec61-S179P*, *sec61-S353C* and *sec61-S179P/S353C*.

3.5.1 PURIFICATION OF 19S REGULATORY PARTICE

For proteasome binding assays the 19S proteasome subcomplex was isolated by affinity purification (ref. 2.2.30). In this study the *S. cerevisiae* strain KRY333 was routinely used to purifiy 19S RP (ref. Table 2.4). The strain expresses a version of the 26S proteasome that is FLAG®-tagged on Rpt1p of the 19S RP base subunit (ref. Figure 3.5.1.1.A; Verma *et al.*, 2000). The presence of the Flag®-tag does not disturb proteasome function, such as assembly and activity (Verma *et al.*, 2004; Sone *et al.*, 2004). FLAG®-tagged 19S RPs were used routinely for proteasome binding assays as it has been shown that binding of the 26S proteasome to ER membranes is mediated by the base subunit of the 19S RP (Ng *et al.*, 2007).

Cytosol of *S. cerevisiae* strain KRY333 was prepared and 19S RP immunoprecipitated overnight using anti-FLAG® M2 agarose beads. Immunoprecipitated 19S RP was eluted using FLAG® peptide and concentrated to 1 -2 *µ*g/*µ*l. In order to monitor the sufficiency and success of the purification, samples were taken during the purification. This was also done to ensure purity of the 19S RP preparation as a contamination with 26S proteasomes was not desired. Samples of the cytosol and washes following the immunoprecipitaion, as well as of the purified 19S RPs were analyzed by SDS-PAGE (ref. 2.2.24.1) and stained with Coomassie (ref. 2.2.24.2).

As shown in Figure 3.5.1.1.B the purification of FLAG®-tagged 19S RP was successful (lane 6: 19S RP). The distinct protein pattern that the 19S RP display when resolved by SDS-PAGE was as shown previously (Verma *et al.*, 2000; Leggett, Glickman and Finley, 2005; Ng *et al.*, 2007). Lane 2 (Cytosol) shows the protein content of the samples before the incubation of the yeast lysate with anti-FLAG resin. Lane 5 shows the sample enriched in 19S RP in the course of the purification. Also, the loss of 19S RP during washes following the incubation with the anti-FLAG resin was minimal (lane 3: Wash 1 and lane 4: Wash 2). Hence, the purification was successful and the 19S RP proteasomes could be used for proteasome binding assays (ref. 3.5.2).

As results from the binding experiments were compared to those from a previous study, contaminations with 26S proteasomes had to be avoided. In addition to the Coomassie stain, a proteasomal activity assay was performed in order to assess the puritiy of the preparation. As a control purified 26S from the same yeasts strain were used.

The peptidase activity of proteasomal preparations was monitored using an in gel activity assay (ref. 2.2.30.1). Native gel electrophoresis of purified proteasomal preparations (about 5 μg of 26S, 20S C and 19S RP) was performed using 4 % nondenaturing polyacrylamide gels. Gels were immediately incubated with the fluorogenic peptide substrate N-succinyl-Leu-Leu-Val-Tyr-7-amido-4-methylcourmarin (Suc-LLVY-AMC) for 10 min at 30 °C (Glickman *et al.*, 1998b; Verma *et al.*, 2000). Suc-LLVY-AMC is a fluorogenic chymotrypsin substrate for the 20S proteasome. The 20S proteasome consisting of four heptameric rings, two outer α-rings and two inner β-rings, harbours chymotrypsin-like activity (Hiller *et al.*, 1996; Verma *et al.*, 2000). The protease-active sites (β 1, 2 and 5) which perform the proteolysis reactions during protein degradation are located in the 20S CP lumen (Finley, 2009). Suc-LLVY-AMC is cleaved due to the chymotrypsin-like enzyme activity of active proteasomes, resulting in the free fluorophore 7-amido-4-methylcoumarin (AMC), which can then be monitored under UV light (360 nm). Thus, samples containing active 20S CP are fluorescent under UV light (Hiller *et al.*, 1996).

Results are shown in Figure 3.5.1.1.C. Shown are the results from the peptidase activity assay (RIGHT) as well as the coomassie stain (LEFT) of the same gel. The Coomassie stain revealed all three samples used in the peptidase activity assay (26S: lane1; 20S CP: lane2; 19S RP: lane 3). Further, the 19S RPs (lane 3) do not run as a distinct band, which has been shown before (Verma *et al.*, 2000). As expected, a fluorescent signal was detectable for the control samples containing 26S (lane 1) and 20S CP (lane 2), respectively (ref. Figure 3.5.1.1.C, RIGHT). The double band in lane 1 can be attributed to the existence of singly (R_1P) and doubly (R_2P) capped proteasomes in the 26S preparation. For the sample containing 19S RP (lane 3) no fluorescent band was detectable. This, too, was as expected, as this sample does not contain 20S CP. Thus, there was no contamination of the 19S RP preparation detectable.

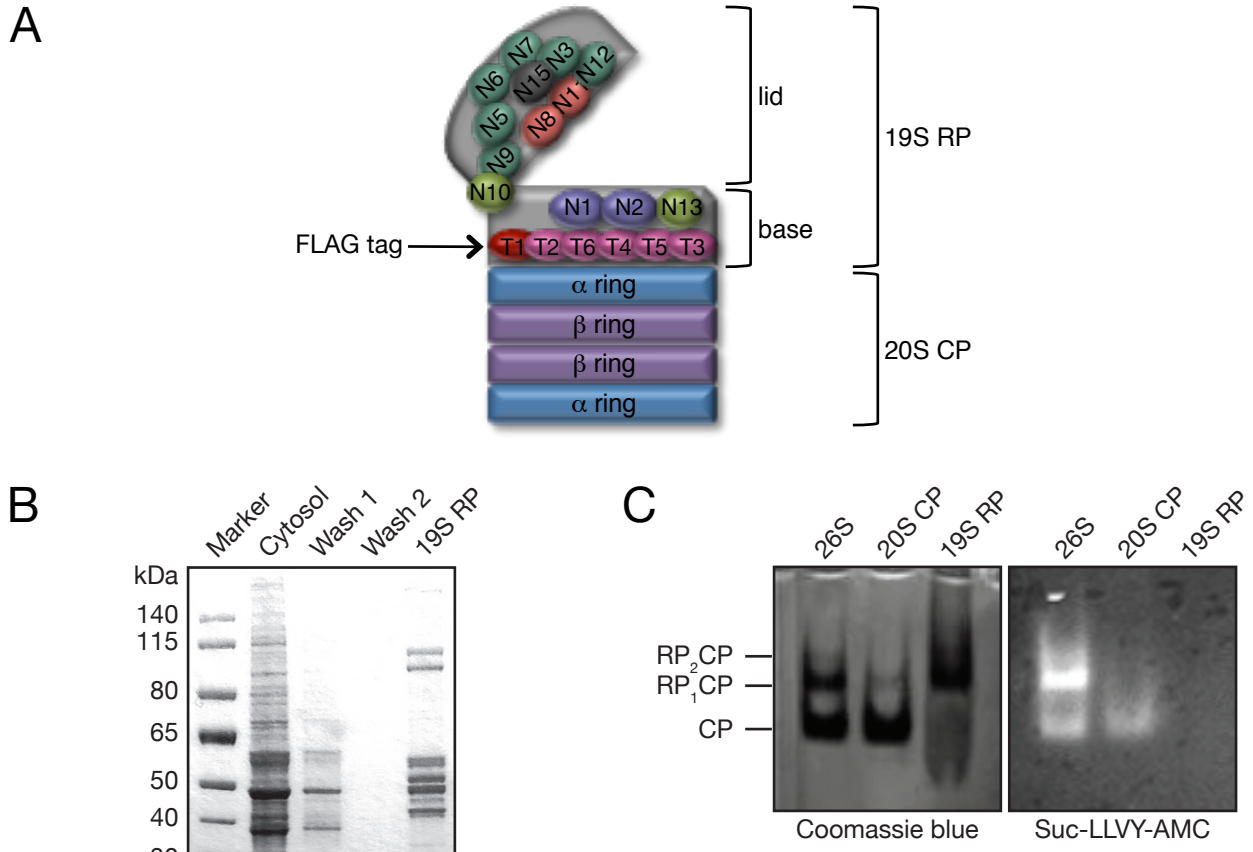

Figure 3.5.1.1 Affinity purification of the 19S RP. (A) Schematic representation of the 26S proteasome and its subunits 19S RP and 20S CP. The position of the FLAG®-tag for purification is indicated. The Rpt1-FLAG® strain KRY333 was routinely used for the purification of 19S RPs and 26S proteasomes (control). Isolation of 26S proteasomes was in the presence of ATP (adapted from Hanna & Finley, 2007). (B) Affinity purification of FLAG®-tagged 19S RP was from cleared yeast lysate using anti-FLAG® M2 agarose (Sigma). Bound proteins were eluted with 100 µg/ml FLAG® peptide (Sigma), concentrated using a Centricon® YM-100 centrifugal filter and quantified using the Pierce™ 660nm Protein Assay Reagent (Thermo Scientific). Sample of the cytosol and after various washes during the purification and 5 µg of 19S proteasome were resolved on a NuPAGE® Novex® 4-12 % Pre-Cast gel at 150 V using 1X MOPS Running Buffer (Invitrogen). The gel was then stained using the EZBlue™ gel staining reagent (Sigma) and dried in a gel dryer (Model 583, BioRad). (C) Peptidase activity of proteasomal preparations (i.e. purified FLAG®-tagged 19S RP and 26S from the same strain as control; 20S CP purified from KRY332) was evaluated using an in-gel activity assay (RIGHT). The fluorogenic chymotrypsin substrate Suc-LLVY-AMC was used as the substrate. Proteasome samples were resolved on a 4 % nondenaturing polyacrylamide gel containing DTT, ATP and glycerol. The gel was incubated for 10 min at 30 °C in the presence of 100 µM substrate and 1 mM ATP. Visualization of fluorescent bands was upon exposure to UV light (360 nm). The same gel was stained with Coomassie blue as a control (LEFT).

3.5.2 PROTEASOME BINDING ASSAYS

As mentioned earlier, the mutant *sec61-302*, apart from being defective in cotranslational import, also displays a reduction in proteasome affinity (Ng *et al.*, 2007). The point mutations S179P (cytoplasmic end of TMD 5 of Sec61p) and/or S353C (loop 7 of Sec61p) which *sec61-302* shares with the remaining three *sec61* mutants *sec61-S179P*, *sec61-S353C* and *sec61-S179P/S353* did not cause defects in co- or posttranslational import into the ER (ref. 3.2.1 and 3.4). In order to analyze which of these point mutations is responsible for the reduction in proteasome binding observed in *sec61-302*, I performd proteasome binding assays (ref. 2.2.31).

For proteasome binding assays, I isolated rough microsomes (RMs) from the *sec61* mutants *sec61-302* (D168G, S179P, F263L, S353C), *sec61-S179P*, *sec61-S353C* and *sec61-S179P/S353C* and the corresponding wild-type strain (*SEC61*) (ref. 2.2.25). Prior to the actual binding assay I treated RMs with puromycin and high salt (potassium acetate) (ref. 2.2.26). The aminonucleoside antibiotic puromycin (from *Streptomyces alboniger*) is an analogue of the 3' end of a tyrosyl-tRNA, which causes premature chain termination during translation (Darken, 1964; Pesta, 1971). Treatment with puromycin and high concentrations potassium acetate causes release of nascent chains from ribosomes and the dissociation of the ribosomes from the membranes (Görlich *et al.*, 1992). The purpose of this step is to free up the maximal number of proteasome binding sites (i.e. Sec61 channel) in the microsomes prior to the binding experiment. I then solubilized the stripped *S. cerevisiae* microsomal membranes (PK-RMs) and reconstituted total protein into proteoliposomes (RECs) (ref. 2.2.27; Kalies *et al.*, 2005). The reconstitution step is required when using *S. cerevisiae* membranes during proteasome binding assays, as the use of intact yeast PK-RMs produces data that are not interpretable and the use of proteoliposomes also increases overall binding of proteasomes to the membranes (Kalies *et al.*, 2005; Ng *et al.*, 2007).

It has been speculated that the binding of 19S RP to the membranes is not efficient enough when using yeast PK-RMs and hence, no differences between wild-type and mutant membranes are detectable when using PKRMs instead of reconstituted proteoliposomes during binding experiments and the use of proteoliposomes also increases overall binding to the membranes (Kalies *et al.*, 2005; Ng *et al.*, 2007). Reconstituted proteoliposomes were produced by treating PK-RMs with Deoxy-BigCHAP, a detergent dissolving the membranes, followed by the reconstitution of total protein using phosphatidylcholine (PC) and phosphatidylethanolamine (PE) membranes (ref. 2.2.27 and 2.2.28). During the reconstitution of total protein into proteoliposomes 50 % of all ER membrane proteins are expected to be in the inside-out orientation. Therefore, the amount of yeast proteoliposomes had to be adjusted accordingly. Reconstituted proteoliposomes were quantified (i.e. determination of Sec61p contents) was by immunoblotting with anti-Sec61p antibody using different concentrations of RMs of the appropriate strain as the standard (not shown).

For the proteasome binding assays, reconstituted proteoliposomes prepared from PK-RMs of the wild-type (*SEC61*) and the *sec61* strains were incubated with purified 19S RP (ref. 3.5.1 and 2.2.31).

In brief, reconstituted proteoliposomes (20 eq*) from the appropriate *S. cerevisiae* strain were incubated with of purified *S. cerevisiae* 19S RP (2 pmol). After binding was complete, membranes were floatated in 1.8 M sucrose, resulting in a distribution of unbound 19S RP at the bottom and membranes with bound 19S RP at the top of the sucrose gradient (ref. Figure 3.5.2.1.A). Following the ultracentrifugation step, the gradients were fractionated from the top (9 fractions). Proteins in each fraction were then resolved by SDS-PAGE (ref. 2.2.24) and proteasome binding was detected by immunoblotting for the FLAG®-tagged Rpt1 subunit (ref. 2.2.24.3). Reconstituted proteoliposomes were quantified prior to the assays, and proteasome binding efficiencies (i.e. bound fractions (1 - 3) vs unbound fractions (7 - 9)) evaluated using the ChemiDoc™ XRS system and the Image Lab™ software (both Bio-Rad).

The results are shown in Figure 3.5.2.1.B and 3.5.2.1.C. Proteasome binding to reconstituted proteoliposomes results in a signal in the top fractions, indicating an interaction between Sec61p in the ER membrane and the proteasomal 19S RP (Figure 3.5.2.1.B *SEC61*, lanes 2-4). Mock binding assays containing 19S RP alone were used as a control (ref. Figure 3.5.2.1.B no membranes). For proteasome binding assays using only 19S RP, there should only be a signal detectable in the bottom fractions of the gradient (unbound) as there are no membranes for the proteasomal subunits to bind to in the sample. The results of the control experiment was as expected (ref. Figure 3.5.2.1.B no membranes, lanes 7-9). For *sec61-302* membranes (19 % bound), which were used as another control, a reduction in 19S RP binding compared to wild-type membranes (39 % bound) could be detected (ref. Fig. 3.5.2.1.B and 3.5.2.1.C *SEC61* and *sec61-302*). Membranes of the mutant *sec61-S179P* did not show a defect or reduction 19S RP binding (38 % bound). In the mutants *sec61-S353C* (17 % bound) and *sec61-S179P/S353C* (30 % bound), however, a reduction in membrane-19S RP interaction could be detected (ref. Fig. 3.5.2.1.B and 3.5.2.1.C *sec61-S353C and sec61-S179P/S353C*). For the latter, the proteasome binding defect was less pronounced compared to *sec61-S353C* and *sec61-302*.

As shown in Figure 3.5.2.1.B I was able to reproduce results from proteasome binding assays with *sec61-302* showing that ER membranes from this strain have reduced affinity for 19S RP (Ng *et al.*, 2007). Surprisingly, the mutation in *sec61-S179P* did not affect 19S RP binding compared to wild-type membranes (Figure 3.5.2.1.B and 3.5.2.1.C *sec61-S179P*). In *sec61-S353C* and *sec61-S179P/S353C* I saw a reduction in the interaction between membranes and 19S RP, leading to the conclusion that the point mutation S353C, and not S179P as initially anticipated, is responsible for the reduced interaction of 19S RP with mutant Sec61p in *sec61-302*, *sec61-S353C* and *sec61-S179P/S353C* (ref. Figure 3.5.2.1.B and 3.5.2.1.C). The results presented here, together with those from the reporter plasmid translocation assay (ref. 3.4), strongly suggest that among the mutations in *sec61-302*, D168G and/or F263L are responsible for the cotranslational import defect, whereas S353C probably causes the observed reduction in binding of 19S RP to membranes derived from *sec61-302*, *sec61-S353C* and *sec61-S179P/S353C* (Ng *et al.*, 2007; this study). This finding is

striking, as S353C is located in the ER-lumenal loop 7, a region of Sec61p inaccessible from the cytoplasmic side of the membrane. One possible explanation for the observed effect could be that the amino acid substitution S353C has a certain impact on the conformation of Sec61p, leading to a conformational change (distortion) of the protein, which in turn could mask the proteasomal binding site on the cytosolic face of the protein. I therefore attempted tot rule out this possibility during the course of this study (also ref. 2.9).

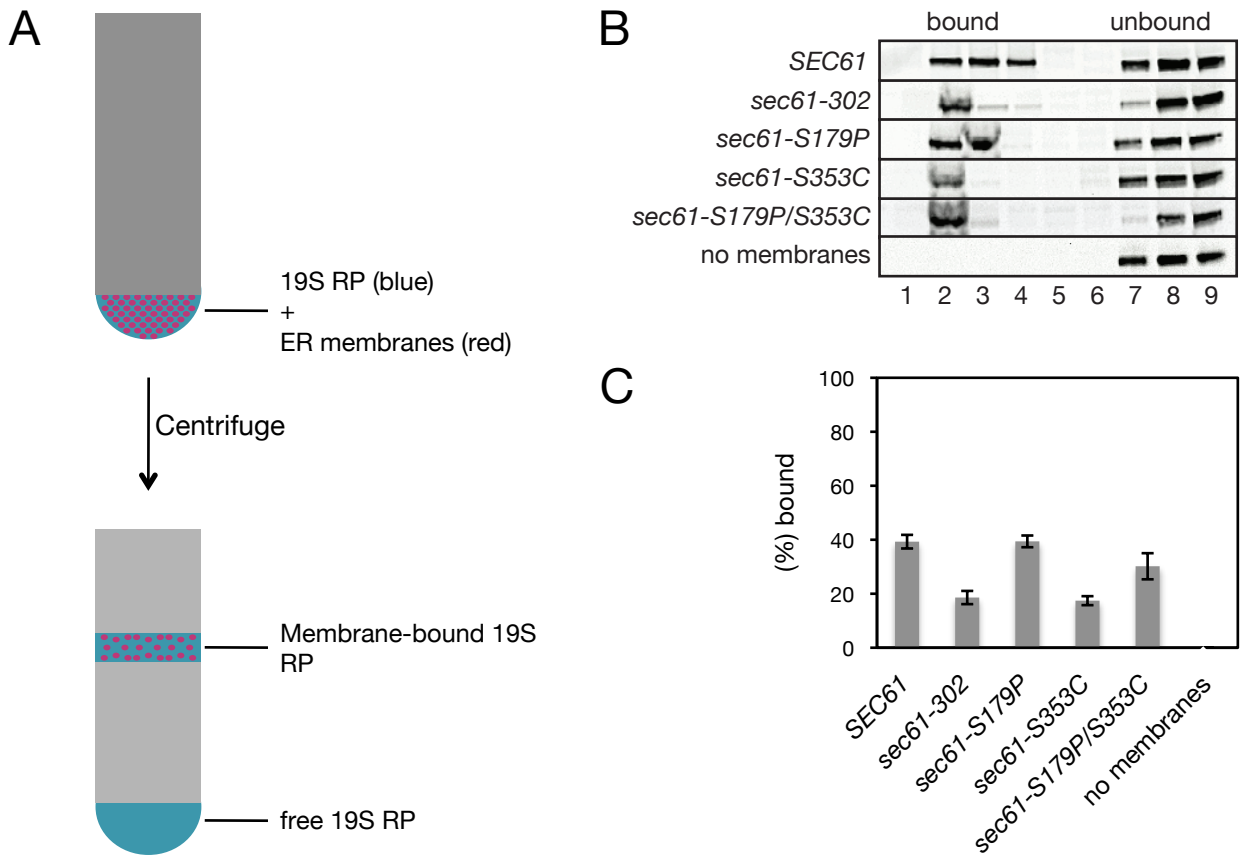

Figure 3.5.2.1 Proteasome binding assay. (A) Schematic representation of the proteasome binding assay. ER-derived membranes (BLUE), i.e. reconstituted proteoliposomes from yeast RMs, of the wild-type (*SEC61*) and the mutant *sec61* strains were incubated with purified 19S RP (RED) in the presence of ATP. Sample were loaded under a sucrose gradient and subjected to ultracentrifugation. The distribution of the proteasomes and ER membranes before and after flotation through a 1.8 M sucrose cushion is shown. Free proteasomes stay in the fraction at the bottom of the gradient while proteasomes bound to membranes float with the membranes to the top. After ultracentrifugation the gradient was fractionated from the top. Proteasomes in each fraction were detected by SDS-PAGE and immunoblotting. (B) 20 eq* of reconstituted proteoliposomes were incubated with 2 pmol 19S RP proteasomal subcomplex FLAG®-tagged on Rpt1p and analyzed by flotation through a 1.8 M sucrose gradient. Gradients were fractionated from top to bottom and subjected to SDS-PAGE and immunoblotting with anti-FLAG® antibody. Detection of signals was using chemiluminescence and a CCD camera system (ChemiDoc™ XRS, Bio-Rad). The positions of 19S RP bound to yeast membranes and of unbound proteasomal subunits are indicated. (N = 3) (C) Binding efficiencies were quantified using the Image Lab™ software (Bio-Rad). Results of three experiments (N = 3) were averaged and the amount (%) of 19S RP bound to membranes for each strain are shown. Error bars indicate the standard error. * 1 eq of microsomes = 50 A_{280} units/µl (Walter & Blobel, 1981).

3.6 ANALYSES OF UPR INDUCTION IN THE *SEC61* MUTANTS

The UPR is induced as a response to ER stress, such as the accumulation of misfolded proteins in the ER, which, if not cleared from the ER, are toxic to the cell (Menzel *et al.*, 1997; Ng *et al.*, 2000; Ron & Walter, 2007). In *S. cerevisiae* the induction of the UPR involves the activation of the Ire1p-mediated signal transduction pathway, resulting in the upregulation of the expression of genes involved in ERAD, such as ER chaperones (Cox *et al.*, 1993; Mori *et al.*, 1993). This pathway ensures cell homeostasis as it enables the cell to cope with the high load of those species and mediate their degradation (Lee, 1987; Kozutsumi *et al.*, 1988; Travers *et al.*, 2000). As the UPR pathway is tightly linked to ERAD, a UPR induction would be expected when Sec61p function is disturbed (Pilon *et al.*, 1997; Casagrande *et al.*, 2000; Friedlander *et al.*, 2000; Travers *et al.*, 2000; Tsai *et al.*, 2002; Kostova & Wolf, 2003).

3.6.1 DETECTION OF UPR INDUCTION IN THE *SEC61* MUTANTS USING THE QUANTITATIVE LIQUID β-GALACTOSIDASE ASSAY

Initially, the quantitative liquid β-galactosidase assay was employed to monitor the constitutive UPR activation in the newly generated *sec61* mutants (JDY638 background; ref. 3.2.1) (ref. 2.2.32.1; Miller, 1972; Guarente, 1982; Stagljar *et al.*, 1998).

The induction of the UPR was measured by using the plasmid pJC30 (*TRP1*, *CEN/ARS*), containing the 22 bp Unfolded Protein Response Element (UPRE) of *KAR2* (BiP) upstream of the *LacZ* gene under the control of the disabled *CYC1* promoter (Guarente & Mason, 1983; Sorger & Pelham, 1987; Sikorski & Hieter, 1989; Mori *et al.*, 1992, Cox *et al.*, 1993; Cox & Walter, 1996). The UPRE, a sequence found in the promoter region of UPR-activated genes, induces *Lacz* gene expression as a response to UPR activation (Miller, 1972; Guarente, 1982). As a control the same plasmid, pJC31, lacking the *UPRE* was used (Cox *et al.*, 1993; Kawahara *et al.*, 1997; Cox & Walter, 1996; Menzel *et al.*, 1997).

Upon UPR induction, cells containing the reporter plasmid pJC30 express β-galactosidase. The enzyme activity in turn is measured by the conversion of ortho-nitrophenyl-β-D-galactopyranoside (ONPG), a β-galactoside. ONPG is a chromogenic substrate, resulting in ortho-nitrophenol when hydrolyzed by the enzyme (Miller *et al.*, 1972). The product has a yellow colour and absorbs light at a wavelength of 420 nm (Miller *et al.*, 1972). The amount of o-nitrophenol formed can be measured by determining the absorbance at 420 nm. Thus, this simple quantitative colorimetric measure allows for an indirect determination of enzyme activity by measuring the formation of yellow colour.

The strains *sec61-S179P*, *sec61-S353C*, *sec61-S179P/S353C*, *sec61-302*, *sec61-303* and the corresponding wild-type (*SEC61*) as well as the strains *sec61-3*, *DER1* and *Δder1* were transformed with the reporter plasmids and transformants selected on the respective minimal medium. The

mutant *sec61-3* as well as *DER1* and *Δder1* were used as controls. The *sec61-3* mutant, which was isolated via a UPR screen, is defective in ERAD and therefore is expected to display an increased UPR even when the UPR is not induced using tunicamycin (Tm) (Sommer & Jentsch, 1993; Pilon *et al.*, 1997; Zhou & Shekman, 1999). Der1p has been shown to be part of the ERAD machinery (Knop *et al.*, 1996). In the absence of Der1p ER stress is increased, which in turn activates the UPR (Knop *et al.*, 1996; Taxis *et al.*, 2003). Therefore, in the *Δder1* strain, a strong UPR inducation is expected .

For the actual assay, cells were grown in minimal medium to an OD_{600} of 0.5 at 30 °C. For the assay 1 OD_{600} per sample was harvested. As a control each strain was grown in the presence of 1 *µ*g/ml tunicamycin (Tm). The antibiotic interferes with the glycosylation in the ER, thereby inducing the UPR due to increased ER stress (Kuo & Lampen, 1974; Duksin & Mahoney, 1982; Langan & Slater, 1991; Torrez-Quiroz *et al.*, 2010). The antibiotic was added at an OD_{600} of 0.4 (this was usually sufficient) and cells grown for another hour. Triplets of each strain were prepared. The cells were permeabilized and resulting lysates pre-incubated in a 28°C water bath. Lysates were then incubated with ONPG until the samples turned yellow (i.e. strains transformed with pJC30). Reactions were stopped and supernatants were measured in spectrophotometer at 420 nm.

Averaged results of four independent experiments are shown in Figure 3.6.1.1. The *sec61* mutants *sec61-S179P* (~ 3.1 β-gal units), *sec61-S353C* (~ 3.7 β-gal units), *sec61-S179P/S353C* (~ 3.7 β-gal units), *sec61-302* (~ 2.3 β-gal units) and *sec61-303* (~ 2.7 β-gal units) did not show an elevated UPR in the absence of tunicamycin (- Tm) compared to the corresponding wild-type (*SEC61*: ~ 3.5 β-gal units). When tunicamycin was added (+ Tm) an onset of the UPR was detected in all strains. The *sec61* mutants generated in this and another study, i.e. *sec61* mutants *sec61-S179P* (~ 8.3 β-gal units), *sec61-S353C* (~ 7.9 β-gal units), *sec61-S179P/S353C* (~ 8.6 β-gal units), *sec61-302* (~ 9.9 β-gal units) and *sec61-303* (~ 8.1 β-gal units), showed an activation of the UPR when tunicamycin was added that was still comparable to the wild-type (*SEC61*: ~ 9.6 β-gal units) (Ng et al., 2007). This effect, however, was less pronounced compared to the control strains.

The controls *sec61-3* (~ 11.4 β-gal units) and *Δder1* (~ 12.8 β-gal units), displayed an elevated β-galactosidase activity compared to the wild-type (*SEC61*: ~ 3.5 β-gal units; *DER1*: (~ 2.2 β-gal units) or the remaining *sec61* mutants without the addition of tunicamycin (- Tm), suggesting a constitutively elevated UPR under the experimental conditions tested. This was as expected. The effect was even more pronounced when the cells were treated with tunicamycin (+ Tm): *sec61-3* (~ 17.4 β-gal units), *Δder1* (~ 20.5 β-gal units) and *DER1* (~ 7.9 β-gal units). Moreover, in the deletion mutant *Δder1* the β-galactosidase levels were higher compared to *sec61-3*. The fact that for all strains the β-galactosidase units are comparable when tunicamycin was added suggests that the concentration used results in a maximum induction of the UPR. As seen in Figure 3.6.1.1, values gained from strains transformed with pJC31 (control) are shown in the same column of respective strain transformed with pJC30. They represent the background of the individual samples and

therefore display low β-galactosidase units.

The fact that under the conditions tested, the *sec61* mutants only displayed an increase in β-galactosidase activities in the presence of tunicamycin suggests that the point mutations in *SEC61* in these mutants do not have a severe enough impact on Sec61p function to cause ER stress and thus an induction of the UPR.

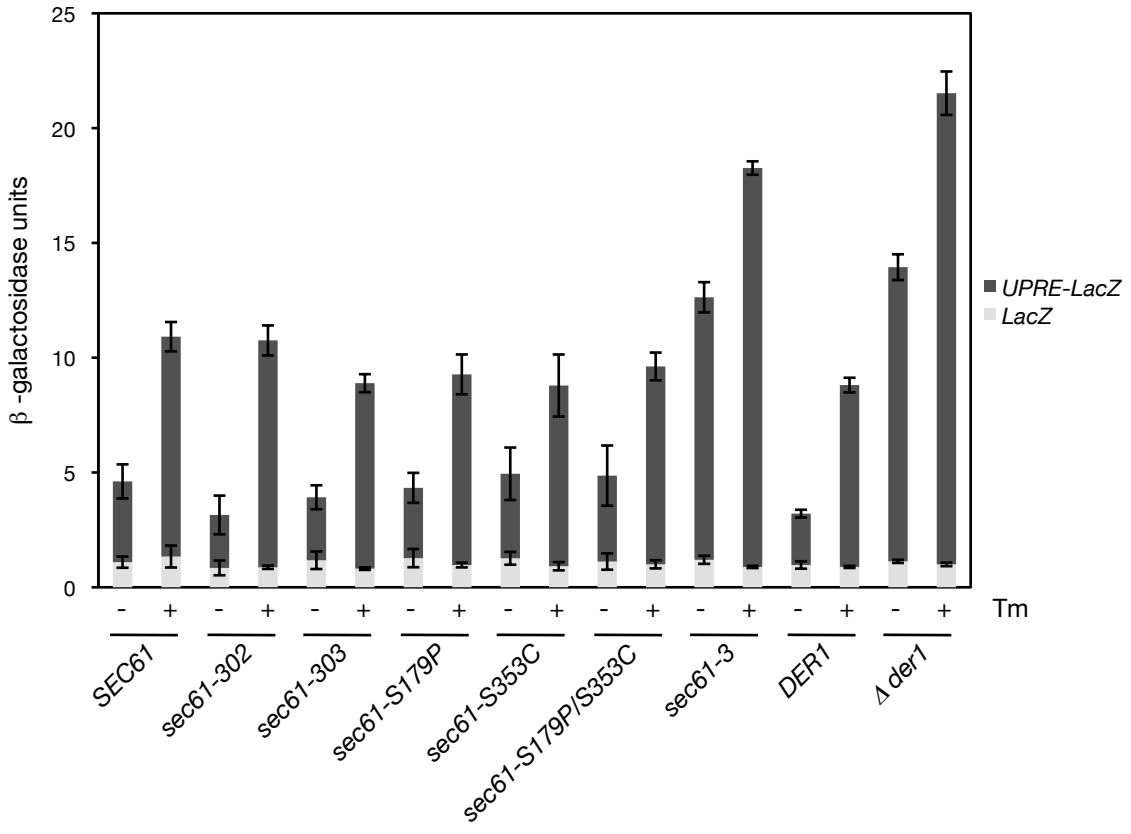

Figure 3.6.1.1. Analysis of UPR induction in the *sec61* mutants using the liquid quantitative β-galactosidase assay. The indicated *sec61* mutants, the corresponding wild-type (*SEC61*) as well as the control strains *DER1*, *Δder1*, *sec61-3* co-expressing a reporter plasmid containing *UPRE-CYC1-LacZ* (pJC30) or the same plasmid lacking *UPRE* (pJC31: control) were grown in the respective minimal medium at 30 °C to an OD_{600} of 0.5. The UPR was induced using 1 µg/ml Tm. Tm was added at an OD_{600} of 0.4 and incubation was continued for 1 hour. Lysates of 1 OD_{600} were prepared using chloroform and 0.1 % (w/v) SDS. Samples were pre-incubated for 5 min in a 28 °C water-bath, followed by the addition of 200 µl ONPG (4 mg/ml). Samples were incubated at 28 °C until the substrate turned yellow. The reactions were stopped using 0.5 ml 1 M Na_2CO_3 and supernatants measured at a wavelength of 420 nm. β-galactosidase units were normalized to the OD_{600} of cells used for the assay. For each experiment, triplets of each strain (+/- Tm) were analyzed. Results from four (N = 4) independent experiments were averaged and graphed. Error bars indicate the standard error.

3.6.2 DETECTION OF THE UPR INDUCTION IN THE *SEC61* MUTANTS ON THE RNA LEVEL

In order to further assess UPR induction in the *sec61* mutants I employed an assay monitoring *HAC1* mRNA splicing (ref. 2.2.32.3).

In *S. cerevisiae*, upon induction of the UPR the *HAC1* pre-mRNA (HAC^u mRNA) is spliced releasing an intron (ref. 1.4). The resulting exons are ligated by a tRNase (Cox & Walter, 1996; Shamu and Walter, 1996; Kawahara *et al.*, 1997; Bertolotti *et al.*, 2000; Papa *et al.*, 2003; Credle *et al.*, 2005; Zhou *et al.*, 2006; Oikawa *et al.*, 2007; Lee *et al.*, 2008). The resulting species, HAC^i mRNA, encodes the transcription factor Hac1p, which is transported to the nucleus where it induces the expression of UPR target genes (Cox & Walter, 1996; Mori *et al.*, 1996; Travers *et al.*, 2000; Kimata *et al.*, 2006). The two *HAC1* species, HAC^u and HAC^i, differ in size. While the unspliced form, HAC^u (*u* = uninduced), displays a size of 720 bp, the spliced form, HAC^i (*i* = induced), is 470 bp in size. Thus, the formation of the spliced *HAC1* mRNA species ($HAC1^i$) is a direct measure for the induction of the UPR in the cells.

The strains *sec61-S179P*, *sec61-S353C*, *sec61-S179P/S353C*, *sec61-302*, *sec61-303* and the corresponding wild-type (*SEC61*), as well as *sec61-3*, *Δder1* and *DER1* were grown in minimal medium at 30 °C to an OD_{600} of 1. As a control the UPR was induced in all strains by treatment with 2 µg/ml tunicamycin (Tm) for another 3 hours when an OD_{600} of 1 was reached. Additionally, *sec61-3* was grown at 17 °C in the presence and absence of tunicamycin (+/- Tm) for another 3 hours when an OD_{600} of 1 was reached. The RNA of each strain was isolated and the cDNA prepared which was used as the template during PCR. Specific primers targeting *HAC1* or *ACT1* (control) were used during the PCRs. Amplification of *ACT1*, encoding actin, was used as a loading control.

Results are shown in Figure 3.6.2.1. Induction of the UPR using tunicamycin (+ TM) was successful in all strains, indicating that induced UPR is detectable. The magnitude of $HAC1^i$ formation in the *sec61* mutants *sec61-S179P*, *sec61-S353C*, *sec61-S179P/S353C*, *sec61-302* and *sec61-303* was comparable to the wild-type (*SEC61*) when the UPR inducer was added (ref. Figure 3.6.2.1 TOP: + Tm). In the absence of tunicamycin (- Tm) there was no HAC^i species detectable in these strains (TOP: - TM).

In the control strain *sec61-3* an induction of the UPR was detecable even in the absence of tunicamycin (- Tm) at both temperatures tested (ref. Figure 3.6.2.1 BOTTOM: - TM, 17 °C and 30 °C) (Sommer & Jentsch, 1993). At 17 °C a slightly stronger UPR induction was detected (ref. Figure 3.6.2.1 BOTTOM: - Tm, 17 °C). When tunicamycin was added this effect was even more pronounced (ref. Figure 3.6.2.1 BOTTOM: + Tm, 17 °C and 30 °C). The same was true for *Δder1* (Knop *et al.*, 1996). This strain showed an induction of the UPR in the absence (- Tm) and presence (+ Tm) of tunicamycin, which too was in concordance with results from the liquid quantitative β-galactosidase assay (ref. Figure 3.6.1.1). The corresponding wild-type (*DER1*) behaved as expected, i.e. no HAC^i species was detectable under normal growth conditions (- Tm), but could be detected when tunicamycin was added (ref. Figure 3.6.2.1 BOTTOM: + Tm).

Thus, the results further indicate that in the *sec61* mutants analyzed, except *sec61-3*, the UPR is not induced under normal growth conditions supporting data from the liquid quantitative β-galactosidase assay (ref. 3.6.1).

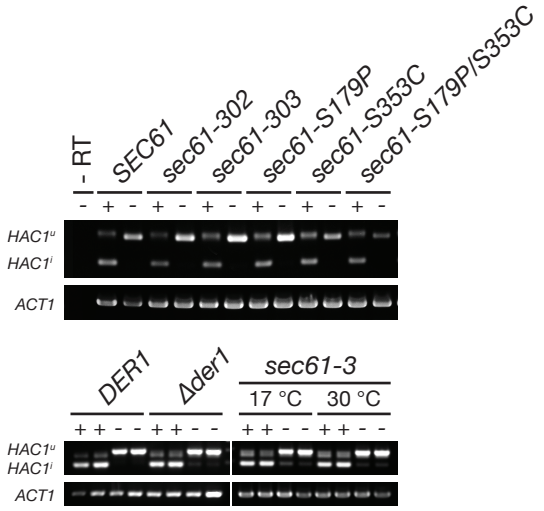

Figure 3.6.2.1. Analysis of UPR induction in the *sec61* mutants using the *HAC1* pre-mRNA splicing assay. Total RNA of each strain was prepared from cultures grown in minimal medium at 30 °C to an OD_{600} of 1. For positive controls, cultures were grown in the presence of 2 μg/ml TM for another 3 hours when an OD_{600} of 1 was reached. For *sec61-3* RNA was additionally prepared from cultures grown at 17 °C (+/- Tm). Here, cells were grown to an OD_{600} of 1 at 30 °C and then shifted to 17 °C for another 3 hours. Total RNA (0.1 μg) was subjected to RT-PCR using an Oligo(dT_{18})-dT primer to produce cDNA. The resulting cDNA (1 μg) was subjected to PCR of *HAC1* with a set of primers targeting *HAC1* to monitor the UPR. PCR fragments derived from $HAC1^u$ mRNA ($HAC1^u$ = uninduced; ~ 720 bp) and $HAC1^i$ mRNA (i = induced; ~ 470 bp) are indicated. *ACT1* RT-PCR was conducted as a loading control. Samples were resolved on a 1 % agarose gel. As a control PCR was conducted without RT-PCR product (- RT) (here: RT = Reverse Transcription).

3.6.3 GROWTH ANALYSES OF THE *SEC61* MUTANTS IN THE *ΔIRE* BACKGROUND

Additionally, I conducted growth analyses of the *sec61* mutants in the sensitized genetic background of *Δire1*.

IRE1, encoding Ire1p, is required for the UPR (Cox *et al.*, 1993). It has been shown that under normal growth conditions *IRE1* is not needed (Nikawa & Yamashita, 1992; Cox e*t al.*, 1993). Upon accumulation of misfolded proteins in the ER, however, it is vital as a central component of the UPR (Cox *et al.*, 1993). Therefore, this assay is a sensitive method for detecting even slight defects in retrotranslocation of misfolded proteins due to mutations in *SEC61*.

The strains *IRE1* (wild-type) and *Δire1* were transformed (ref. 2.2.17) with linearized integration plasmids (pRS306-*truncsec61**) containing the truncated versions of the mutant *sec61* sequences to create the respective integration mutants (ref. 3.2.2; Ho *et al.*, 1989; Horton *et al.*, 1989; Gietz *et al.*, 1995). Transformants were selected on the appropriate minimal medium and integration of the individual sequences at the correct locus was verified using chromosomal DNA and specific primers (Forward primer: 5' *Hin*dIII SEC61 5' UTR #-445; Reverse primer: 3' pRS306 URA3 #621; ref. Table 2.6) (ref. 2.2.18; data not shown).

Results are shown in Figure 3.6.3.1. Serial dilutions (10^5-10^0 cells) of each strain grown at 30 °C were plated onto rich medium (YPD) lacking (- TM) or containing (+ Tm) the UPR inducer tunicamycin (Kuo & Lampen, 1974; Duksin & Mahoney, 1982; Langan & Slater, 1991; Torrez-Quiroz *et al.*, 2010). Plates were grown at various temperatures (20 °C, 25 °C, 30 °C and 37 °C) for 3 days. As seen in Figure 3.6.3.1, none of the mutants *IRE1 sec61-S179P*, *IRE1 sec61-S353C*, *IRE1 sec61-S179P/S353C*, *IRE1 sec1-302* and *IRE1 sec61-303* exhibited growth defects on rich medium (YPD) at the temperatures tested when compared to the wild-type (*IRE1 SEC61*) (YPD, - Tm). While growth at 37 °C (10^5-10^1 cells), 30 °C (10^5-10^1 cells) and 25 °C (10^5-10^1 cells) was optimal for these strains, a reduction in growth was detectable at 20 °C (10^5-10^4 cells). In the presence of tunicamycin (+ Tm) growth of these strains was still comparable to the wild-type (*IRE1 SEC61*) at all temperatures. At 37°C (10^5-10^1 cells), 30 °C (10^5-10^1 cells) and 25 °C (10^5-10^1 cells) growth in the presence of 0.25 µg/ml tunicamycin (YPD, + Tm, 0.25 µg/ml) was least affected when compared to growth in the absence on tunicamycin (YPD, -Tm). At 20 °C (10^5 cells) a strong reduction in growth was detected in the presence of the lower tunicamycin concentration (YPD, +Tm, 0.25 µg/ml). This effect was even more pronounced (i.e. hardly any growth) when cells were grown in the presence of the higher tunicamycin concentration (YPD, + Tm, 0.5 µg/ml). At 37 °C (10^5-10^1 cells) and 30 °C (10^5-10^1 cells) growth at the higher tunicamycin concentration was comparable to growth on rich medium only (YPD, - Tm) and on medium containing 0.25 µg/ml tunicamycin. At 25 °C (10^5-10^4 cells) the addition of 0.5 µg/ml tunicamycin (YPD, + Tm, 0.25 µg/ml) led to further reduction in growth compared to growth on rich medium alone (YPD, - Tm) or in the presence of 0.25 µg/ml tunicamycin (YPD, + Tm, 0.25 µg/ml).

The mutants *Δire1 sec61-S179P*, *Δire1 sec61-S353C*, *Δire1 sec61-S179P/S353C*, *Δire1 sec61-302 and Δire1 sec61-303* displayed growth comparable to the *Δire1 SEC61* strain on rich medium alone (YPD, - Tm) at all temperatures tested (37 °C: 10^5-10^1 cells; 30 °C: 10^5-10^1 cells; 25 °C: 10^5-10^1 cells; 20 °C: 10^5-10^4 cells). Moreover, growth of these strains was comparable to the respective *sec61* mutants in the *IRE1* background at 25 °C, 30 °C and 37 °C. At 20 °C (10^5-10^4/10^3 cells) growth of *Δire1 sec61-S179P*, *Δire1 sec61-S353C*, *Δire1 sec61-S179P/S353C*, *Δire1 sec61-302 and Δire1 sec61-303* was a little more efficient compared to the same *sec61* mutants in the *IRE1* background at the same temperature (YPD, 20 °C).

All *sec61* mutants in the *Δire1* background displayed an extreme sensitivity towards tunicamycin. This was as described before, as ER stress is lethal to cells in the absence of the protective UPR (Cox *et al.*, 1993). For these mutants no growth was detected at the various temperatures tested when grown in the presence of the lower as well as the higher tunicamycin concentration (+ Tm: 0.25 µg/ml, 0.5 µg/ml).

Results from this and the remaining assays monitoring the UPR (ref. 3.6.1 and 3.6.2) in the *sec61* mutants indicate that the UPR is not induction these mutants under normal growth conditions.

*: -S179P, -S353C, -S179P/S353C, -302, -303

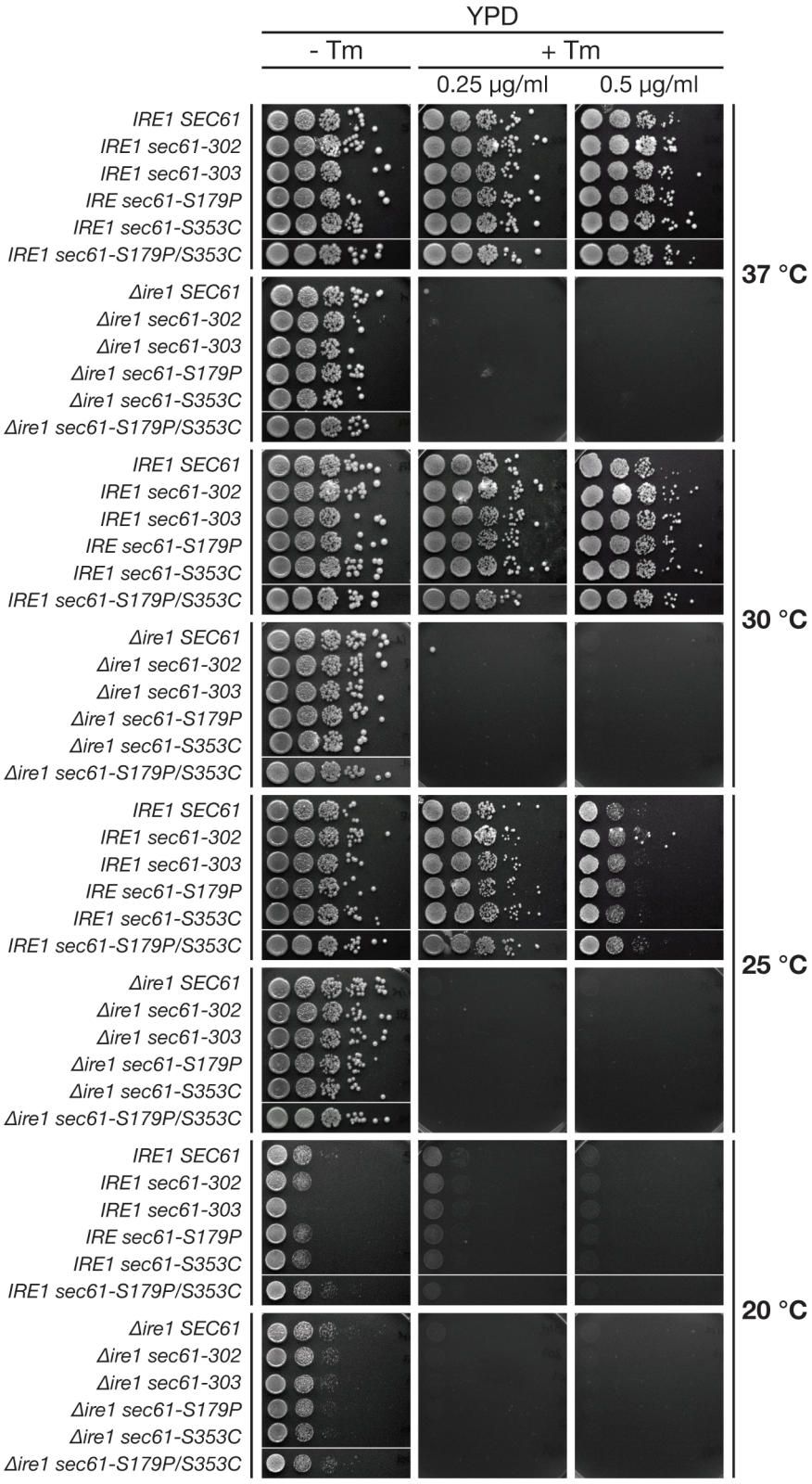

Figure 3.6.3.1. Growth analyses of the *sec61* mutants in the *IRE1* and *Δire1* bakground. Serial dilutions (10^5-10^0 cells) of the indicated strains, grown overnight at 30 °C, were grown on rich medium (YPD) in the presence (+ Tm) or absence (- Tm) of tunicamycin (0.25 µg/ml or 0.5 µg/ml). Plates were incubated for 3 days at the indicated temperatures and photographed using the E-Box VX2 Gel Documentation System (Peqlab).

3.7 ERAD IN THE *SEC61* MUTANTS

The *sec61-S353C* mutant created in this study is a candidate for analyzing the domains of Sec61p that are directly involved in proteasomal degradation during ERAD, as it has no defects in growth or protein translocation into the ER (ref. 3.3 and 3.4). Thus, any defects in protein degradation (ERAD) cannot be an indirect result of impaired protein import.

Pulse-chase experiments using the *sec61* mutants *sec61-S179P*, *sec61-S353C* and *sec61-S179/S353C*, together with *sec61-302*, *sec61-303* and the corresponding wild-type (*SEC61*) were performed in order to investigate whether any of the mutants, especially *sec61-S353C, sec61-S179P/S353C* and *sec61-302*, are defective in the degradation of substrates of various ERAD pathways (CPY*, Δgpαf, KWW and Ste6-166p) (Ng *et al.*, 1996; Vashist *et al.*, 2001; Vashist & Ng, 2004; Ng *et al.*, 2007).

3.7.1 CPY*$_{HA}$ ERAD IN THE *SEC61* MUTANTS

The first ERAD substrate studied was the mutant *S. cerevisiae* vacuolar protease carboxypeptidase Y (CPY), CPY*, a soluble, glycosylated secretory protein that is translocated posttranslationally into the ER (Knop *et al.*, 1996b; Ng *et al.*, 1996). CPY* is a model ERAD (ERAD-L) substrate which has been extensively studied. This mutated form of CPY is the result of a point mutation in the gene *PRC1*, leading to the amino acid substitution of glycine to arginine at position 255 (G255R; allele: *prc1-1*). Due to this point mutation, the protein misfolds irreversibly and consequently cannot move further along the secretory pathway and reach its correct native conformation (Finger *et al.*, 1993). CPY* is rather recognized by the ERQC machinery, retrotranslocated into the cytosol and degraded by the 26S proteasome (Hiller *et al.*, 1996; Kostova & Wolf, 2003). Import into the ER, however, is not disturbed and CPY* can also be fully glycosylated (Finger *et al.*, 1993).

Wild-type CPY, encoded by *PRC1*, is a vacuolar C-terminal exopeptidase, belonging to a family of highly conserved serine carboxypeptidases. CPY is, among other vacuolar proteinases, vital for the proteolytic capacity of the vacuole (Chiang & Schekman, 1991; Stennicke *et al.*, 1996; van den Hazel *et al.*, 1996). It contains four glycosylation sites (positions: Asn13, Asn87, Asnl68, Asn368) and further contains disulfide bonds (Knop *et al.*, 1996; Kostova & Wolf, 2003). It is synthesized as a precursor (ppCPY; cytosolic form), which is imported into the ER, where the signal sequence is cleaved off (pCPY) and CPY becomes promptly N-glycosylated (inactive p1 or ER form). CPY is then further modified in the Golgi apparatus leading to the p2 or Golgi form. Once it reaches its final destination, the vacuole, CPY is activated by proteolytic cleavage resulting in the mature or vacuolar form (mCPY) (Steven *et al.*, 1982). Thus, for CPY there are several species and molecular weights possible during its maturation: ppCPY (prepro CPY, ~ 59 kDa), pCPY (pro CPY, ~ 57 kDa), p1 CPY (ER form, 67 kDa), p2 CPY (Golgi form, 69 kDa), mCPY (mature form, 61 kDA).

The degradation of CPY* in the *sec61* mutants (JDY638 background, ref. 3.2.1) *sec61-S179P*, *sec61-S353C*, *sec61-S179P/S353C*, *sec61-302*, *sec61-303* and the corresponding wild-type (*SEC61*) was analyzed by pulse-chase experiments (Ng *et al.*, 2000; Ng *et al.*, 2007). Pulse-chase experiments were performed as described in 2.2.33. In brief, initially all of the above strains were transformed with the plasmid pDN431 (*CEN, URA3*), carrying the gene encoding an epitope-tagged version of CPY*, CPY*$_{HA}$ (Sikorski & Hieter, 1989; Ng *et al.*, 1996; Ng *et al.*, 2000). This recombinant version of CPY* was created by site-directed mutagenesis and was finally cloned into the vector pDN201 (Sikorski & Hieter, 1989; Ng *et al.*, 1996; Ng *et al.*, 2000). It has been shown to behave as a proper ERAD substrate in pulse-chase experiments, where it is degraded in the same manner and with similar degradation kinetics as CPY* (Finger *et al.*, 1993; Biederer *et al.*, 1997; Ng *et al.*, 2000; Taxis *et al.*, 2002). The degradation of CPY*$_{HA}$ in wild-type cells has been shown to be with a half-life ($t_{1/2}$) of around 30 min, compared to untagged CPY* ($t_{1/2}$ ~ 20 min) (Finger *et al.*, 1993; Ng *et al.*, 2000; Vashist *et al.*, 2004). Transformants were selected on minimal medium lacking leucine and uracil.

For pulse-chase experiments the cells were grown in growth medium containing the appropriate supplements to an OD_{600} of about 1, and aliquots of 1.5 OD_{600} were preincubated for 30 minutes in labeling medium (i.e. growth medium lacking ammonium sulfate, methionine and cysteine). Preincubation was performed to use up the remaining methionine and cysteine in the samples. Cells were pulse-labeled by adding 0.35 mCi/ml of L-[^{35}S]-methionine/cysteine (EXPRE^{35}S^{35}S [^{35}S]-Protein Labeling Mix, Perkin Elmer) for 10 min at 30 °C, followed by a chase to monitor degradation kinetics of the ERAD model substrate (ref. Vashist *et al.*, 2001). Initiation of the chase was by the addition of chase mix containing unlabeled cysteine and methionine. The chase was up to 90 min as indicated (ref. Figure 3.7.1.1.A). After various time points, the chase was terminated by adding ice-cold Tris-azide buffer. Cells were lysed by agitation in a Mini-Beadbeater-24 (BioSpec Products Inc.) and CPY*$_{HA}$ immunoprecipitated from lysate with 10 µl polyclonal anti-CPY serum (rabbit; Römisch lab) overnight at 4 °C. For the CPY*$_{HA}$ pulse-chase experiments the CPY antibody, instead of the anti-HA antibody (Rockland™), was used for economic reasons. The amount of antibody used was sufficient to be saturating for the immunorecipitation of protein from 1.5 OD_{600} cells (data not shown). Following the immunoprecipitation, the samples were analyzed by SDS-PAGE (ref. 2.2.24.1), using 4–12 % Bis-Tris gels (NuPAGE® Novex® Pre-Cast gels, Invitrogen). Dried gels were then exposed to storage phosphor screens (GE Healthcare). Usually an exposure of 2-3 days was most sufficient. Proteins were visualized using a phosphorimager system (Typhoon Trio™ Variable Mode Imager, GE Healthcare). Signals were analyzed and quantified using the ImageQuant™ TL software (GE Healthcare.

Results of a representative pulse-chase experiment are shown in Figure 3.7.1.1.A. Using the CPY antibody, a faster migrating band around 60 kDa (*), in addition to the band corresponding to CPY*$_{HA}$ (~ 67 kDa), could be detected. The upper band represents CPY*$_{HA}$. The additional band represents

mature chromosomal CPY (mCPY) (ref. Figure 3.7.1.1.A, *). In order to confirm this, pulse-chase experiments with the wild-type (*SEC61*) and *sec61-302* (cotranslational import defect) strain were performed, using the anti-HA antibody (Rockland™) for immunoprecipitations (data not shown). Using the anti-HA antibody, the band at ~ 60 kDa was not detected throughout the course of the experiment, indicating that it corresponds to chromosomal CPY. Degradation kinetics for the two strains using the anti-HA antibody were comparable to those when the CPY antibody was used (data not shown). This experiment also indicates that under the experimental conditions tested, there was no accumulation of pre-pro-CPY*$_{HA}$ in the cells, which is in concordance with data showing that the *sec61* mutants analyzed are not defective in posttranslational import (ref. 3.4).

As shown in Figure 3.7.1.1, CPY*$_{HA}$ was degraded rapidly in the wild-type strain (*SEC61*) with a $t_{1/2}$ of ~ 20 min (ref. Figure 3.7.1.1.B, *SEC61*). The results show that there was no delay in CPY*$_{HA}$ turnover in the *sec61* mutants analyzed. The *sec61* mutant defective in protein translocation into the ER (ref. 3.4) but not in proteasome binding (ref. 3.5.2), *sec61-303* ($t_{1/2}$ ~ 21 min), showed no stabilization of the substrate. In *sec61-S179P* ($t_{1/2}$ ~ 21 min) CPY*$_{HA}$ had degradation kinetics similar to the wild-type. None of the *sec61* mutants displaying a reduction in proteasome binding, *sec61-S353C* ($t_{1/2}$ ~ 19 min), *sec61-S179P/S353C* ($t_{1/2}$ ~ 21 min) and *sec61-302* ($t_{1/2}$ ~ 24 min), showed a significant delay in CPY*$_{HA}$ turnover. At the end of the 90 min chase 93 – 97 % of the substrate had been degraded in all strains.

The fact that none of the *sec61* mutants, especially those with reduced proteasome binding, were defective in the degradation of CPY*$_{HA}$, could be attributed to several things. The reduction in proteasome binding observed in *sec61-S353C*, *sec61-S179P/S353C* and *sec61-302* might not be severe enough to also affect ERAD. It is also possible that the *sec61* mutants tested are merely not disturbed in the degradation of CPY*$_{HA}$. Thus, as no defect in ERAD of the soluble, glycosylated, posttranslationally imported ERAD-L substrate CPY*$_{HA}$ was detected, further ERAD substrates were analyzed, in order to assess substrate stability in each strain (ref. 3.7.2 – 3.7.5; Swanson *et al.*, 2001; Vashist *et al.*, 2001).

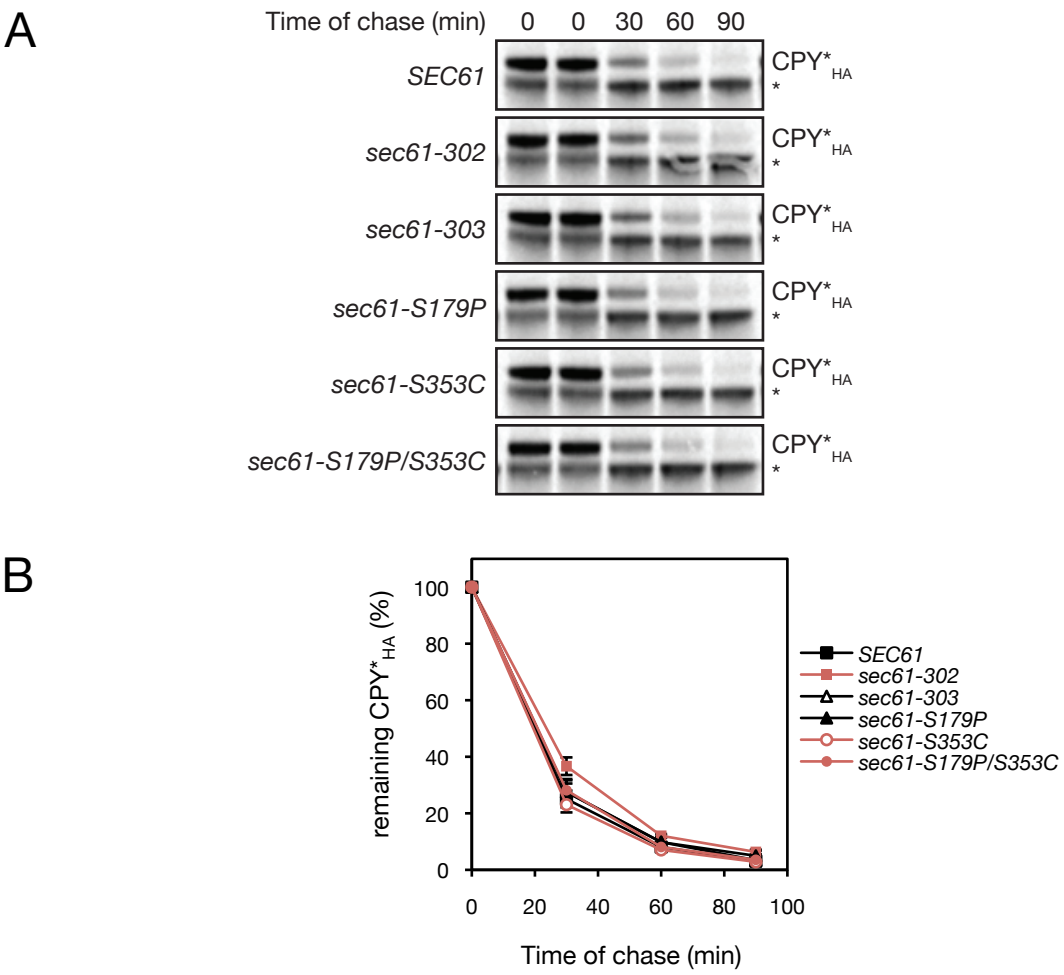

Figure 3.7.1.1 Degradation of mutant Carboxypeptidase Y (CPY*) in the *sec61* mutants. (A) For pulse-chase experiments, *sec61* and wild-type (*SEC61*) cells expressing CPY^*_{HA} from the plasmid pDN431 (*CEN*, *URA3*), were grown to an OD_{600} ~ 1 in growth medium containing the appropriate supplements. Aliquots of 1.5 OD_{600} were preincubated in labeling medium, lacking methionine and cysteine, at 30 °C for 30 min, followed by pulse-labeling with 0.35 mCi/ml ^{35}S-methionine/cysteine (EXPRE^{35}S^{35}S [^{35}S]-Protein Labeling Mix, Perkin Elmer) at 30 °C for 10 min. Cells were chased for the indicated periods of time, lysed by bead beating and CPY^*_{HA} was immunoprecipitated from lysates using 10 µl of CPY antibody (Römisch lab) and analyzed by SDS-PAGE on 4-12 % Bis-Tris gels (NuPAGE® Novex® Pre-Cast gels, Invitrogen). Dried gels were exposed to storage phosphor screens for 2 days and signals detected using a phosphorimager. Shown is a representative result of three independent experiments (N = 3). (B) CPY^*_{HA} degradation efficiencies of the various strains were determined by analyzing and quantifying the band intensities (A) using the ImageQuant™ TL software (GE Healthcare). Data of three independent experiments were averaged and graphed accordingly. Error bars indicate the standard error.

3.7.2 MUTANT ALPHA FACTOR PRECURSOR ERAD IN THE *SEC61* MUTANTS

ERAD of mutant *S. cerevisiae* alpha factor (α-factor) precursor, Δgpαf, in the *sec61* mutants and the corresponding wild-type strain (*SEC61*) was monitored using pulse-chase experiments (ref. 2.2.33). The Δgpαf is a soluble, unglycosylated ERAD substrate, which is degraded via the ERAD-L pathway (Hansen *et al.*, 1986; Rothblatt and Meyer, 1986; Waters and Blobel, 1986).

In *S. cerevisiae*, mating involves the secretion and response to peptide pheromones such as the alpha factor (Sprague *et al.*, 1983). The α-factor, a peptide of 13 amino acids, encoded by the genes *MFα1* (mainly) and *MFα2*, is secreted by alpha cells during the mating process (Stötzler *et al.*, 1976; Kurjan & Hershowitz, 1982; Singh *et al.*, 1983; Caplan *et al.*, 1991). Wild-type ppαf (~ 18 kDa) consists of an N-terminal signal peptide (19 amino acids) followed by a proregion (64 amino acids), containing three glycosylation sites (**Asn**-X-Thr; positions: 23, 57, 67). The proregion is followed by 4 tandem repeats of mature alpha factor sequence, which are each preceeded by a spacer peptide (Brake *et al.*, 1983; Waters *et al.*, 1988; Caplan *et al.*, 1991). The ppαf is imported posttranslationally into the ER where the signal sequence is cleaved off by signal peptidase (Waters *et al.*, 1988). The resulting pro-α-factor (pαf; ~ 16 kDa) is promptly glycosylated upon entry into the ER. Glycosylated alpha factor precursor, designated 3gpαf (~ 28 kDa), is transported from the ER to the Golgi where it is proteolytically processed and eventually secreted (Emter *et al.*, 1983; Julius *et al.*, 1983, 1984a, 1984b; Dmochowska *et al.*, 1987; Fuller *et al.*, 1988).

As the wild-type pre-pro-α-factor, the mutant α-factor precursor, pΔgpαf (~ 18 kDa), is efficiently imported into the ER. Upon entry into the ER, the signal sequence is cleaved off (McCracken & Brodsky, 1996). The resulting Δgpαf (~ 16 kDa) is an ERAD substrate, as deletion of all three glycosylation sites in the proregion by site-directed mutagenesis (N23Q, N57Q, N67Q) probably results in misfolding (Caplan *et al.*, 1991; Mayinger & Meyer, 1993; McCracken & Brodsky, 1996; Werner *et al.*, 1996). Retrotransloction of Δgpαf to the cytosol has been shown to be via the Sec61p channel (Pilon *et al.*, 1997). Moreover, the degradation of Δgpαf has been shown to be independent of polyubiquitination and dependent on ATP and the proteasome 19S RP (McCracken & Brodsky, 1996; Werner *et al.*, 1996; Lee *et al.*, 2004a).

For pulse-chase experiments (ref. 2.2.33), the *sec61* mutants (JDY638 background, ref. 3.2.1), *sec61-S179P*, *sec61-S353C*, *sec61-S179P/S353C*, *sec61-302*, *sec61-303* and the corresponding wild-type (*SEC61*) were transformed with the expression plasmid p416pΔgpαf (*CEN*, *URA3*, ref. Table 2.5) carrying a gene encoding the unglycosylated pre-pro-alpha-factor derivative pΔgpαf (McCracken & Brodsky, 1996; Ng *et al.*, 2007). From this plasmid the mutant pre-pro-α-factor is conditionally expressed under the control of the MET25 promoter, i.e. the gene is transcribed in the absence of methionine and expression is repressed in the presence of methionine in the medium (Mumberg *et al.*, 1994).

Expression of mutant α-factor precursor in each cell clone can be very variable, making the evaluation of results difficult (Römisch, personal communication). Therefore, clones with similar expression levels were selected to perform pulse-chase experiments (data not shown).

For pulse chase experiments, cells were grown overnight in growth medium, containing all required supplements, to an OD_{600} of about 1. Aliquots of 1.5 OD_{600} were preincubated in labeling medium, lacking methionine and cysteine, for 30 minutes, followed by pulse-labeling with 0.35 mCi/ml of L-[^{35}S]-Methionine/Cysteine (EXPRE^{35}S^{35}S [^{35}S]-Protein Labeling Mix, Perkin Elmer) for 5 min at 30 °C. Following the labeling, a chase was initiated by adding chase mix, containing unlabeled methionine and cysteine. The chase was over a period of 30 minutes with samples taken at the indicated intervalls (t = 0, 5, 15, 30 min) (ref. Figure 3.7.2.1.A). Termination of the chase was by adding ice-cold Tris-azide buffer. The cells were then lysed using a Mini-Beadbeater-24 (BioSpec Products Inc.) and the Δgpαf precipitated from lysates with 10 µl of polyclonal anti-α-factor serum (Römisch lab) overnight at 4 °C. The amount of antiserum used was sufficient to be saturating for the immunoprecipitation of protein from 1.5 OD_{600} cells (data not shown). The samples were then analyzed by SDS-PAGE, using 4 -12 % Bis-Tris gels (NuPAGE® Novex® Pre-Cast gels, Invitrogen). The gels were dried, exposed to storage phosphor screen (GE Healthcare) generally for 2-3 days and signals detected using a phosphorimager (Typhoon Trio™ Variable Mode Imager, GE Healthcare). Signals were analyzed and quantified using the ImageQuant™ TL software (GE Healthcare).

The results of a representative pulse-chase experiment are shown in Figure 3.7.2.1.A and B. In the pulse-chase experiments, the half-life ($t_{1/2}$) of intracellular Δgpαf in *SEC61* wild-type cells was ~ 13 min. This was in good agreement with previous data (Caplan *et al.*, 1991). The *sec61* mutant *sec61-303* ($t_{1/2}$ ~ 14 min) did not affect the half-life of Δgpαf. The *sec61* mutants displaying reduced proteasome binding (ref. 3.5.2), *sec61-302* ($t_{1/2}$ ~ 18 min), *sec61-S353C* ($t_{1/2}$ ~ 20 min) and *sec61-S179P/S353C* ($t_{1/2}$ ~ 16 min), did not show significant stabilization of Δgpαf (Ng *et al.*, 2007). For these strains $t_{1/2}$ was increased compared to the wild-type (*SEC61*). Not only were the half-lives of Δgpαf similar, but also the amounts of substrate degraded at the end of the chase, were comparable in all strains (93 – 98 %; ref. Figure 3.7.2.1.B). For the *sec61-S179P* mutant ($t_{1/2}$ ~ 19 min) an increased $t_{1/2}$ was detected as well. As seen in Figure 3.7.2.1.B a faint band (*) above the band displaying the degradation kinetics of Δgpαf (~ 16 kDa) was detected in all samples with a decrease in intensity of the band over the course of the pulse-chase experiment. Although the band displays the same molecular weight as pΔgpαf (~ 18 kDa) the possibility that it could be attributed to pΔgpαf was excluded. As the translocation in the pulse-chase experiment was very efficient, detection of pΔgpαf would be expected only in the pulse sample (t = 0 min). Thus, the upper band (*) is probably nonspecific.

Taken together, the data from pulse-chase experiments monitoring the degradation kinetics of CPY^*_{HA} (ref. 3.7.1) and Δgpαf suggest that none of the *sec61* mutants, especially those impaired in proteasome binding (*sec61-302*, *sec61-S353C* and *sec61-S179P/S353C*), are deficient in the degradation of these two ERAD-L substrates. I therefore investigated whether the *sec61* mutants had any effects on ERAD of substrates that are not soluble and thus substrates of another ERAD pathway (ERAD-C).

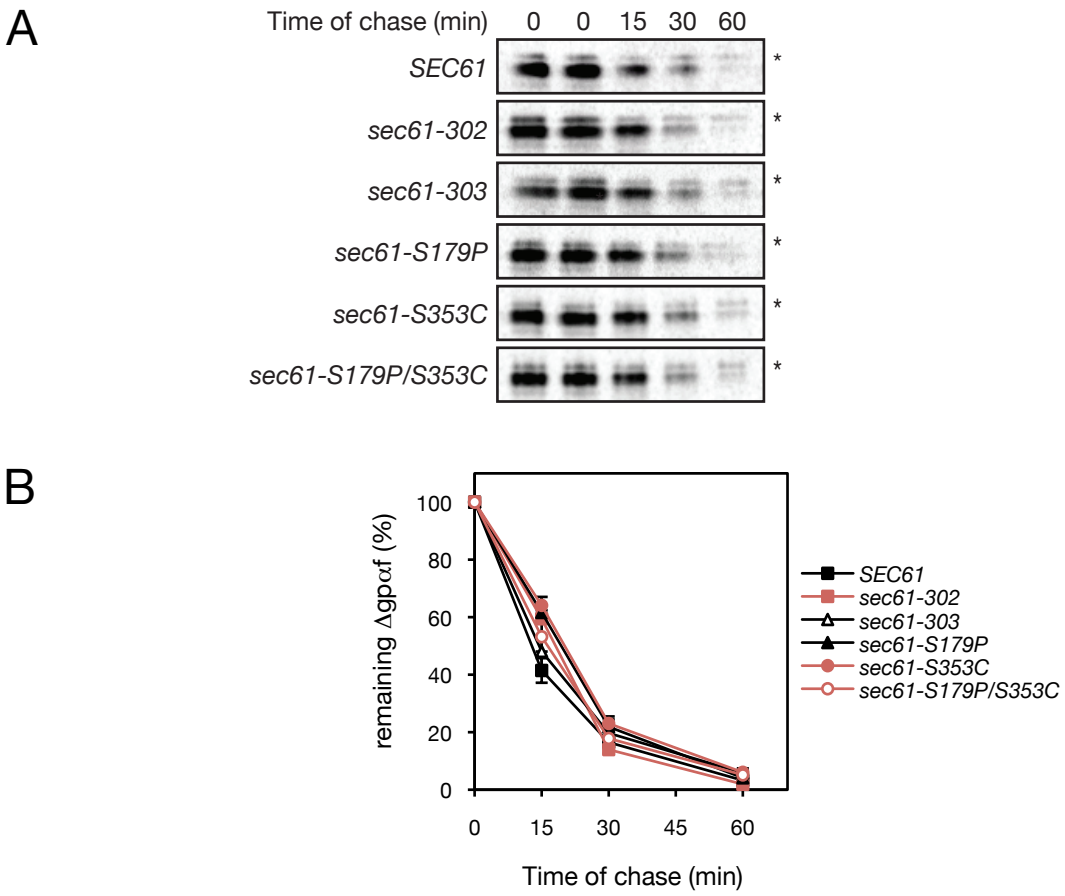

Figure 3.7.2.1 Degradation of mutant alpha factor precursor (Δgpαf) in the *sec61* mutants. (A) For pulse-chase experiments, *sec61* and wild-type (*SEC61*) cells expressing pΔgpαf from the plasmid pDN431 (*CEN*, *URA3*), were grown to an OD_{600} of ~ 1 in growth medium containing the appropriate supplements. Aliquots of 1.5 OD_{600} were preincubated in labeling medium lacking methionine and cysteine at 30 °C for 30 min, followed by pulse-labeling with 0.35 mCi/ml ^{35}S-methionine/cysteine (EXPRE^{35}S^{35}S [^{35}S]-Protein Labeling Mix, Perkin Elmer) at 30 °C for 5 min. Cells were chased for the indicated periods and the chase was terminated by adding ice-cold Tris-azide buffer. Cells were lysed by bead-beating and Δgpαf precipitated from the lysates using 10 µl of anti-α-factor serum (Römisch lab). Samples were analyzed by SDS-PAGE using 4-12 % Bis-Tris gels (NuPAGE® Novex® Pre-Cast gels, Invitrogen) and phosphor-imaging. (B) Δgpαf degradation efficiencies of the various strains were determined by analyzing and quantifying the band intensities (A) using the ImageQuant™ TL software (GE Healthcare). Results of two independent experiments (N = 2) were averaged and graphed. Error bars indicated the standard error.

3.7.3 KWW ERAD IN THE *SEC61* MUTANTS

Since Sec61p has been shown to be involved in ERAD of the soluble ERAD substrate ΔgpαF, I tested the degradation of two soluble ERAD substrates that were unglycosylated (ΔgpαF, ref. 3.7.2) and glycosylated (CPY^*_{HA}, ref. 3.7.1) and degraded via the ERAD-L pathway (McCracken & Brodsky, 1996; Pilon *et al.*, 1997; Ng *et al.*, 2000; Vashist *et al.*, 2001). Next, I investigated ERAD of a transmembrane substrate that was also degraded via ERAD-L, the chimeric protein KWW (Vashist & Ng, 2004).

The ERAD substrate KWW (KHN lumenal domain/Wsc1p transmembrane domain/Wsc1p cytosolic domain) is a chimeric integral membrane protein in which the luminal domain of Wsc1p was replaced with KHN (Vahist *et al.*, 2001; Vashist & Ng, 2004). The protein further displays a type I membrane orientation (Vahist *et al.*, 2001; Vashist & Ng, 2004). The lumenal domain of KWW, KHN, consists of the signal sequence of *S. cerevisiae* Kar2p fused to the Simian Virus 5 HA-Neuraminidase ectodomain. It contains O-linked sugars that are modified upon transport to the Golgi, making it possible to determine the proteins localization. It further contains four N-linked glycosylation sites (Loayza *et al.*, 1998; Vashist *et al.*, 2001; Vashist & Ng, 2004). The integral membrane protein Wsc1p, forming the cytosolic and transmembrane domain of KWW, is a signaling protein (nonessential) with one transmembrane domain. It is located at the plasma membrane (Lodder *et al.*, 1999; Vashist *et al.*, 2001; Vashist & Ng, 2004). KWW is misfolded in the lumenal domain leading to its degradation via the ERAD-L pathway (Vashist & Ng, 2004).

The turnover of KWW in the *sec61* mutants (ref. 3.2.1; *sec61-S179P*, *sec61-S353C*, *sec61-S179P/S353C*, *sec61-302*, *sec61-303*) and the corresponding wild-type strain (*SEC61*) was monitored using pulse-chase experiments (ref. 2.2.33) (Ng *et al.*, 2007). Prior to pulse-chase experiments, the strains were transformed with the expression plasmid pSM101 (*CEN*, *URA*), containing the gene encoding HA epitope-tagged KWW. The KHN portion of KWW was created using the expression plasmid pSM70, containing the fusion gene of the first 45 amino acids of Kar2p (signal sequence and cleavage site) to the C-terminal 528 amino acids of the SV5 HN gene. In pSM70, a triple HA epitope tag was added in frame with the C-terminus of KHN (Vashist *et al.*, 2001). The HA epitope tag was taken from pCS124 (C. Shamu, Harvard University). Insertion of the resulting gene was into pDN251, containing the moderate *PRC1* promoter (Ng *et al.*, 1989; Ng *et al.*, 1996; Vashist *et al.*, 2001). The sequences encoding tagged KHN as well as the transmembrane and the cytosolic domain of *WSC1* were ligated into pSM70, resulting in pSM101 (Vashist & Ng, 2004).

For pulse-chase experiments, cells were grown overnight to an OD_{600} of about 1 in growth medium containing all supplements required. Preincubation of 1.5 OD_{600} aliquots was in labeling medium, lacking methionine and cysteine, for 30 min. The cells were pulse-labeled for 10 min at 30 °C with 0.35 mCi/ml of L-[^{35}S]-Methionine/Cysteine (EXPRE^{35}S^{35}S [^{35}S]-Protein Labeling Mix, Perkin Elmer) as described previously (Vashist & Ng, 2004). The chase, which was initiated by adding chase mix

containing unlabeled methionine and cysteine, was for 90 min with samples taken at the indicated intervals (t = 0, 30, 60 and 90 min; Figure 3.7.3.1.A). The chase was terminated with the addition of ice-cold Tris-azide buffer, followed by the preparation of lysates using a Mini-Beadbeater-24 (BioSpec Products Inc.). KWW was precipitated from the resulting lysates with 4 µl of anti-HA antibody (Rockland™) at 4 °C overnight. Prior to the experiments, the amount of antibody needed to immunoprecipitate all KWW from 1.5 OD_{600} was determined by titration (data not shown). Samples were resolved on 4 -12 % Bis-Tris gels (NuPAGE® Novex® Pre-Cast gels, Invitrogen). The gels were dried, exposed to a storage phosphor screen (GE Healthcare) for 2 days and signals detected using a phosphorimager system (Typhoon Trio™ Variable Mode Imager, GE Healthcare). Signals were analyzed and quantified using the ImageQuant™ TL software (GE Healthcare).

Results are shown in Figure 3.7.3.1.A and B. In *SEC61* wild-type cells, the degradation of KWW was took place a half-life of ~ 33 min, which was a similar to published data ($t_{1/2}$ ~ 35 min; Vashist & Ng, 2004). Moreover, KWW, which is around 87 kDa in size when glycosylated, displays a shift in mobility during the time course of the experiment. This has been shown previously to be due to extended O-mannosylation of the protein, as KWW molecules are transported from the ER to the Golgi from where they are retrieved to the ER for degradation (Harty *et al.*, 2001; Vashist *et al.*, 2001, Arvan *et al.*, 2002; Vashist & Ng, 2004). Neither the mutants with a proteasome binding defect (ref. 3.5.2), *sec61-302* ($t_{1/2}$ ~ 39 min), *sec61-S353C* ($t_{1/2}$ ~ 39 min) and *sec61-S179P/S353C* ($t_{1/2}$ ~ 39 min), nor the remaining mutants *sec61-S179P* ($t_{1/2}$ ~ 39 min) and *sec61-303* ($t_{1/2}$ ~ 38 min) displayed significant stabilization of the substrate during pulse-chase analyses, although the half-lives of KWW in each mutant was slightly increased compared to the wild-type (*SEC61*). Overall, degradation kinetics throughout the course of the pulse-chase experiment were comparable to the wild-type (*SEC61*). At the end of the chase period the amounts of KWW degraded were similar for each strain (88-99 %; Figure 3.7.3.1.B).

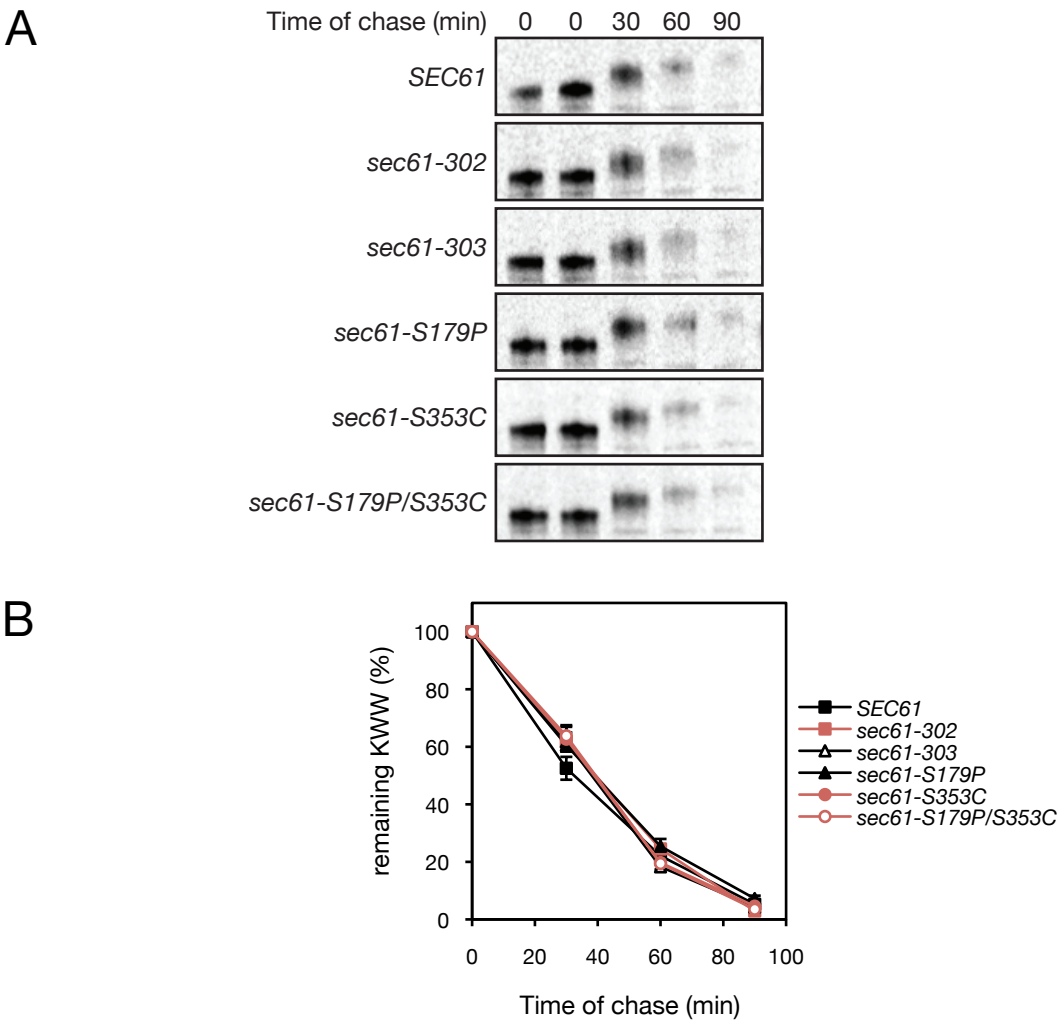

Figure 3.7.3.1 Degradation of KWW in the *sec61* mutants. (A) For pulse-chase experiments, *sec61* and wild-type (*SEC61*) cells expressing KWW from the plasmid pSM101 (*CEN*, *URA3*), were grown to an OD_{600} of ~ 1 in growth medium containing the appropriate supplements. Aliquots of 1.5 OD_{600} were preincubated in labeling medium, lacking methionine and cysteine, at 30 °C for 30 min, followed by pulse-labeling with 0.35 mCi/ml ^{35}S-methionine/cysteine (EXPRE^{35}S^{35}S [^{35}S]-Protein Labeling Mix, Perkin Elmer) at 30 °C for 10 min. Cells were chased for the indicated periods and the chase was terminated by adding ice-cold Tris-azide buffer. Cells were lysed by bead beating and the lysates immunoprecipitated using 4 µl of anti-HA antibody (Rockland™). The lysates were subjected to SDS-PAGE analysis, using 4-12 % Bis-Tris gels (NuPAGE® Novex®, Invitrogen)). Dried gels were exposed to storage phosphor screens (GE Healthcare) for 3 days. Signals were detected using a phosphorimager system. (B) The rate of KWW degradation was determined by analyzing and quantifying the band intensities (A) using the ImageQuant™ TL software (GE Healthcare). Results were graphed accordingly. Averaged results from two independent experiments are shown (N = 2). Error bars indicate the standard error.

3.7.4 STE6-166P ERAD IN THE *SEC61* MUTANTS

Although Sec61p has been shown to be mainly involved in ERAD-L, I also tested whether any of the *sec61* mutants were defective in the degradation of an ERAD-C substrate (Plemper *et al.*, 1997, 1999b; Pilon *et al.*, 1998; Willer *et al.*, 2008; Schäfer & Wolf, 2009).

The ERAD-C pathway not only differs from the ERAD-L (and ERAD-M) pathway regarding the location of the lesion within the aberrant protein, but also in the composition of the underlying complex (Römisch, 2005; Vashist & Ng, 2004; Carvalho *et al.*, 2006; Denic *et al.*, 2006). A role of Sec61p in ERAD-C is still under debate. In a previous study, Sec61p has been implicated to be involved in the degradation of a substrate containing a cytoplasmic degron. ERAD of this substrate has been shown to involve the E3 ligase Doa10p, a central component of the ERAD-C pathway (Scott & Schekman, 2008). These findings, however, have been challenged by another study, which has indicated that the substrate is degraded by yet another ERAD pathway (ERAD-T) involving Hrd1p, questioning a role of Sec61p in ERAD-C (Rubenstein *et al.*, 2012).

As a substrate for the ERAD-C pathway, a mutant form of Ste6p, Ste6-166p, was used. Ste6p, the a-factor transporter in *S. cerevisiae*, is a member of the ATP-binding cassette (ABC) superfamily (Berkower & Michaelis, 1996). As a plasma membrane ABC transporter, Ste6p moves through the secretory pathway to the plasma membrane, where the protein, after pumping a-factor out of the cell, eventually undergoes endocytosis and ubiquitin-dependent degradation in the vacuole (Kuchler *et al.*, 1989; Michaelis, 1993; Kölling & Hollenberg, 1994; Kölling & Losko, 1997). Ste6p consists of 12 transmembrane domains with major extramembrane domains of the protein predicted to be located in the cytosol (Kuchler *et al.*, 1989; Geller *et al.*, 1996).

The nonglycosylated Ste6p mutant Ste6-166p is truncated at the C-terminus, rendering the resulting protein unstable (Loayza *et al.*, 1998). The truncation is due to a mutation (Q1249X) causing premature termination (42 amino acids shorter than Ste6p) (Loayza *et al.*, 1998). Due to the mutation, Ste6-166p is retained in the ER and promptly degraded via the ERAD-C pathway, involving the UPS (Berkower & Michaelis, 1996, Loayza *et al.*, 1998; Vashist & Ng, 2004).

Strains were transformed with the expression plasmid pSM1083, containing the gene encoding HA epitope-tagged Ste6-166p. This plasmid was created by hydroxylamine mutagenesis of the expression plasmid pSM683 (*CEN*, *URA3*, *STE6::HAe*), which contained the HA epitope-tagged *STE6* gene (Berkower *et al.*, 1994; Kaiser *et al.*, 1994; Loayza & Michaelis, 1998; Loayaza *et al.*, 1998).

For pulse-chase experiments positive transformants were grown overnight to an OD_{600} of about 1 in growth medium containing all supplements required. Aliquots of 1.5 OD_{600} were preincubated for 30 minutes in labeling medium, lacking methionine and cysteine and cells were pulse-labeled for 5 min at 30 °C with 0.35 mCi/ml of L-[^{35}S]-methionine/cysteine (EXPRE^{35}S^{35}S [^{35}S]-Protein Labeling Mix, Perkin Elmer) as described previously (Vashist *et al.*, 2001; Vashist & Ng, 2004). Chase initiation was by adding chase mix, containing unlabeled methionine and cysteine. The chase was over a

period of 30 min with samples taken at the indicated intervals (t = 0, 5, 15 and 30 min), followed with the addition of ice-cold Tris-azide buffer to terminate the chase. Cell lysates were prepared using a Mini-Beadbeater-24 (BioSpec Products Inc.) and immunoprecipitated with 4 µl of anti-HA antibody (Rockland™) at 4 °C overnight. Prior to the experiments, the amount of antibody needed to immunoprecipitate all HA-tagged protein from 1.5 OD_{600} was determined by titration using *SEC61* and *sec61-302* strains (data not shown). Samples were resolved on 4 -12 % Bis-Tris gels (NuPAGE® Novex® Pre-Cast gels, Invitrogen). The gels were dried, exposed to storage phosphor screen (GE Healthcare) for 2-3 days and signals detected using a phosphorimager system (Typhoon Trio™ Variable Mode Imager, GE Healthcare). Signals were analyzed and quantified using the ImageQuant™ TL software (GE Healthcare).

The results of a representative pulse-chase experiment are shown in Figure 3.7.4.1.A and B. In the *SEC61* wild-type, Ste6-166p was degraded with a half-life of ~ 9 minutes, which was similar to previously published data (Vashist *et al.*, 2001; Vashist & Ng, 2004). The *sec61* mutants displaying a proteasome binding defect (ref. 3.5.2) *sec61-302* ($t_{1/2}$ ~ 9 min), *sec61-S353C* ($t_{1/2}$ ~ 7 min) *and sec61-S179P/S353C* ($t_{1/2}$ ~ 5 min) also showed degradation efficiencies comparable to or faster than the wild-type (*SEC61*). In *sec61-S179P* and *sec61-303* Ste6-166p was degraded with a half-life of 7 min and 10 min, respectively. It has to be mentioned that for *sec61-S179P/S353C*, and to a much lesser extent *sec61-S353C*, the signal was not as strong as for the other mutants tested, which may have affected results (ref. Figure 3.7.4.1.A). Even when the experiment was repeated the signal intensities remained weaker for these strains. However, signals, which were detectable, were quantified for *sec61-S353C* and *sec61-S179P/S353C*. Due to time constraints the experiment could not be repeated with newly transformed *sec61-S353C* and *sec61-S179P/S353C*. Thus, it could not be ruled out whether the observed weaker signal intensities were due to technical issues or whether they were mutant-specific and indicate that the mutants are defective in the biogenesis of polytopic TM proteins.

As seen in Figure 3.7.4.1.B the amounts of Ste6-166p after the 30-min chase were comparable in wild-type and mutant strains (95-99 %; Figure 3.7.4.1.B).

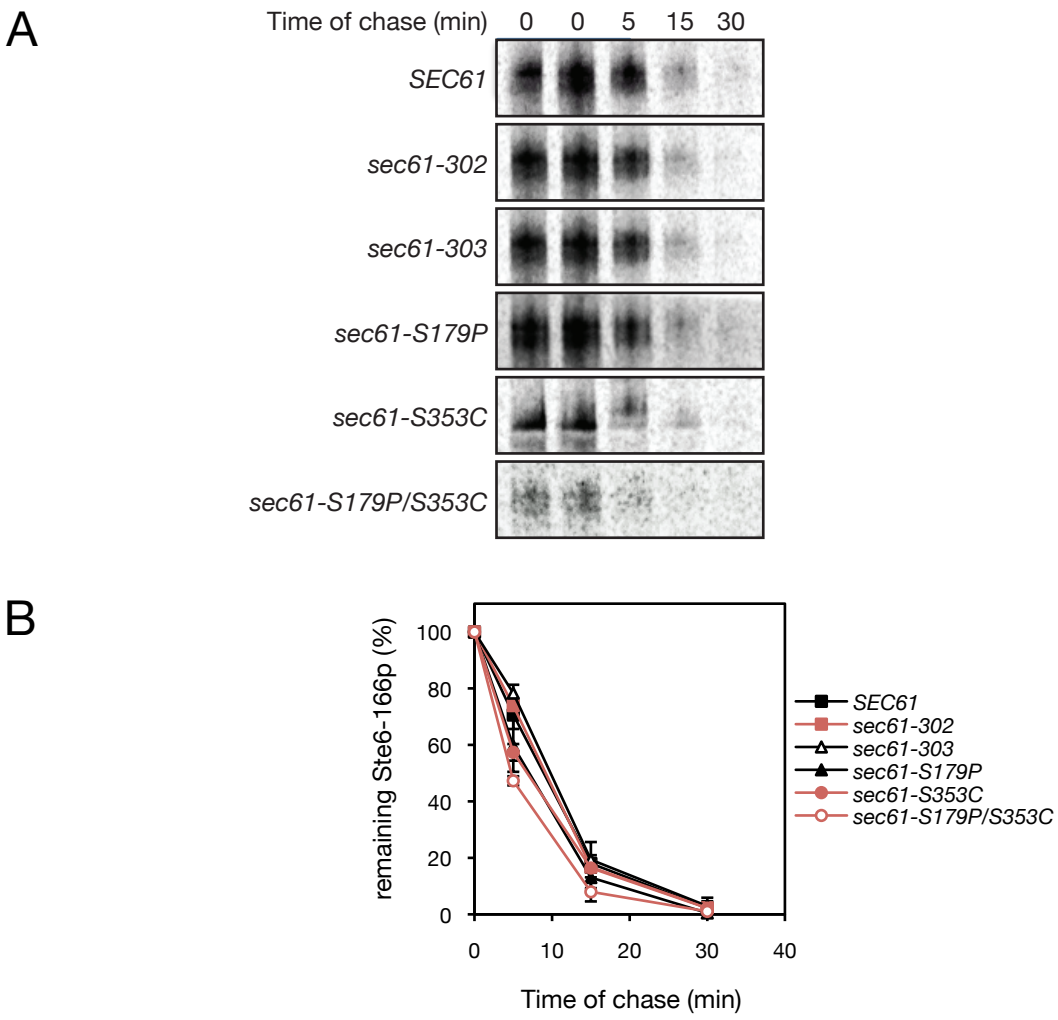

Figure 3.7.3.1 Degradation of Ste6-166p in the *sec61* mutants. (A) For pulse-chase experiments, *sec61* and wild-type (*SEC61*) cells expressing Ste6-166p from the plasmid pSM1083 (*CEN*, *URA3*), were grown to an OD_{600} of ~ 1 in growth medium containing the appropriate supplements. Aliquots of 1.5 OD_{600} were preincubated in labeling medium, lacking methionine and cysteine, at 30 °C for 30 min, followed by pulse-labeling with 0.35 mCi/ml ^{35}S-methionine/cysteine (EXPRE^{35}S^{35}S [^{35}S]-Protein Labeling Mix, Perkin Elmer) at 30 °C for 5 min. The chase was initiated by adding chase mix, containing unlabeled methionine and cysteine, to a final concentration of 2 mM. Cells were chased for the indicated periods and the chase was terminated by adding ice-cold Tris-azide buffer. Cells were lysed by bead beating, Ste6-166p immunoprecipitated from lysates using 4 µl of anti-HA antibody (Rockland™) and analyzed by SDS-PAGE, on 4-12 % Bis-Tris gels (NuPAGE® Novex® Pre-Cast gels, Invitrogen). Gels were dried and exposed to storage phosphor screens (GE Healthcare) for 2-3 days and signals detected using a phosphorimager system. (B) The rate of Ste6-166p degradation was determined by analyzing and quantifying the band intensities (A) using the ImageQuant™ TL software (GE Healthcare). Results of two experiments (N = 2) were averaged and graphed accordingly. Error bars indicate the standard error.

3.8 ANALYSIS OF *IN VITRO* TRANSLOCATION AND ERAD IN THE *SEC61* MUTANTS

3.8.1 *IN VITRO* TRANSLOCATION OF PPαF INTO *SEC61* MICROSOMES

Since under the conditions tested, none of the *sec61* mutants showed striking ERAD defects *in vivo*, I next analyzed the mutants' abilities to degrade the ERAD substrate ΔgpαF *in vitro*.

A cell-free assay system was used to assess the effects of the mutations in *SEC61* on posttranslational translocation (McCracken & Brodsky, 1996). This was done by measuring the translocation rate of the *S. cerevisiae* alpha factor precursor (pre-pro-alpha factor, ppαf) into ER-derived rough microsomes (RM). Wild-type ppαf (~ 18 kDa) is signal-cleaved and promptly gylcosylated upon import into the ER (ref. 3.7.1) resulting in the formation of 3gpαf (fully glycosylated, ~ 28 kDa) (Emter *et al.*, 1983; Julius *et al.*, 1983, 1984a; Fuller *et al.*, 1988; Waters *et al.*, 1988; Brodsky, 2010).

In vitro translocation assays using ppαf (ref. 2.2.34.6) were performed prior to examining degradation efficiencies of ΔgpαF in order to test import capacities of microsomal membranes isolated from the *sec61* mutants and the corresponding wild-type (*SEC61*) (ref. 3.2.2). *In vitro* translocation and retrotranslocation assays rely on the quality of ER-derived microsomes, which has an essential impact on the translocation capacities of the membranes. As sufficient import (~ 50 %) is mandatory for retrotranslocation assays, translocation reactions were established to optimize the amounts of microsomes and ppαf necessary to gain efficient translocation. Since none of the *sec61* mutants analyzed have been shown to be defective in posttranslational import employing a reporter plasmid translocation assay (ref. 3.4), *in vitro* import of wild-type alpha factor precursor was expected to be functional in properly prepared microsomes. Moreover, as mentioned earlier, undisturbed import into the ER would also be beneficial for evaluating *in vitro* retrotranslocation assays, as ERAD defects in *sec61* mutants competent for import could be linked directly to the respective mutation in *SEC61*.

For ER import assays, microsomal membranes of the wild-type (*SEC61*) strain as well as the *sec61* mutants *sec61-302*, *sec61-303*, *sec61-S179P*, *sec61-S353C*, *sec61-S179P/S353C* and *sec61-3*, grown at 30 °C, were prepared (Lyman & Schekman, 1995; Pilon *et al.*, 1997). Wild-type ppαf was transcribed from plasmid pDJ100 (ref. Table 2.5), containing the ppαf gene under the control of the bacteriophage promoter SP6, using SP6 polymerase (ref. 2.2.34.4; Hansen *et al.*, 1986; Rothblatt & Meyer, 1986). In order to obtain radiolabeled ppαf, *in vitro* translation of the transcript was in the presence of ^{35}S-labeled methionine (Perkin Elmer) (ref. 2.2.34.5; McCracken & Brodsky, 1996; Brodsky, 2010).

Radiolabeled ppαf was translocated into wild-type or mutant microsomes (2 µl of OD_{280} = 30) at 24 °C in the presence of ATP, an ATP-regenerating system and *S. cerevisiae* wild-type cytosol (Sorger & Pelham, 1987; Baker *et al.*, 1988; McCracken & Brodsky, 1996). The optimal temperature for the

in vitro assays has been shown to be 24 °C (Pilon *et al.*, 1997). The assays were performed as time course experiments with reactions terminated at various time points (t = 0, 0, 5, 10, 15, 20 and 30 min) by precipitation with ice-cold trichloroacetic acid (to 10 %). As controls, the translocation reactions were prepared lacking either membranes (- RM) or ppaf (- ppaf) and incubated for 30 minuted as above. As a result, only untranslocated ppaf should be detected in the first case, while in the second case, there should be no signal. Samples were resolved on 4 -12 % Bis-Tris gels (NuPAGE® Novex® Pre-Cast gels, Invitrogen). The gels were dried, exposed to storage phosphor screen (GE Healthcare) for 2-3 days and signals detected using a phosphorimager system (Typhoon Trio™ Variable Mode Imager, GE Healthcare). Signals were analyzed and quantified using the ImageQuant™ TL software (GE Healthcare). Translocation efficencies were measured by the formation of triply glycosylated 3gpαf.

As seen in Figure 3.8.1.1.A and B, none of the *sec61* mutants, except *sec61-3*, were severely defective in posttranslational import of ppαf *in vitro*. This confirmed data from reporter plasmid translocation assays in this and a previous study, which have shown that there is no posttranslational import defect detectable in the *sec61* mutants analyzed (ref. 3.4; Ng *et al.*, 2007). Import of ppαf in all *sec61* mutant membranes was only slightly slower compared to import into wild-type membranes. While after 30 min ~ 57 % of ppaf were imported into wild-type membranes, the mutants *sec61-302* (46 %), *sec61-303* (43 %), *sec61-S179P* (48 %), *sec61-S353C* (39 %) and *sec61-S179P/S353C* (47 %) showed only moderately reduced import rates, and the initial kinetics (0 - 10 min) were almost identical to wild-type. The import efficiencies of all *sec61* mutants, except *sec61-3*, was around 39 – 48 % after 30 min and thus sufficient for subsequent ERAD experiments (Figure 3.8.1.1.B). It has to be noted, however, that import kinetics of ppαf in the strains is slower compared to published results ($t_{1/2}$ = 2-5 min at 20 °C), indicating that the

As a control for the translocation assay, membranes isolated from *sec61-3* were used. In this mutant the underlying point mutation (G341E) is located in the same region as S353C. Further, although *sec61-3* has been shown to be defective in posttranslational import, the defect is not as severe as in *sec61-32* (Pilon *et al.*, 1997, 1998). Moreover, microsomal membranes from *sec61-3* have been shown to be defective in degradation of Δgpαf (Pilon *et al.*, 1997, 1998). Under the conditions tested here, import of ppαf into *sec61-3* microsomal membranes was also reduced (29 % translocated after 30 min). The import defect was not as previously described, which is very likely due to the fact that the membranes were isolated and tested at the strain's permisse temperature (Pilon *et al.*, 1998).

As the results in Figure 3.8.1.1.A and B show, the amount of ppαf imported into the microsomes increases steadily during the time course. Therefore, for the retrotranslocation assays the translocation of mutant alpha factor pΔgpαf was incubated for 60 min in order to ensure maximum import (ref. 3.8.2).

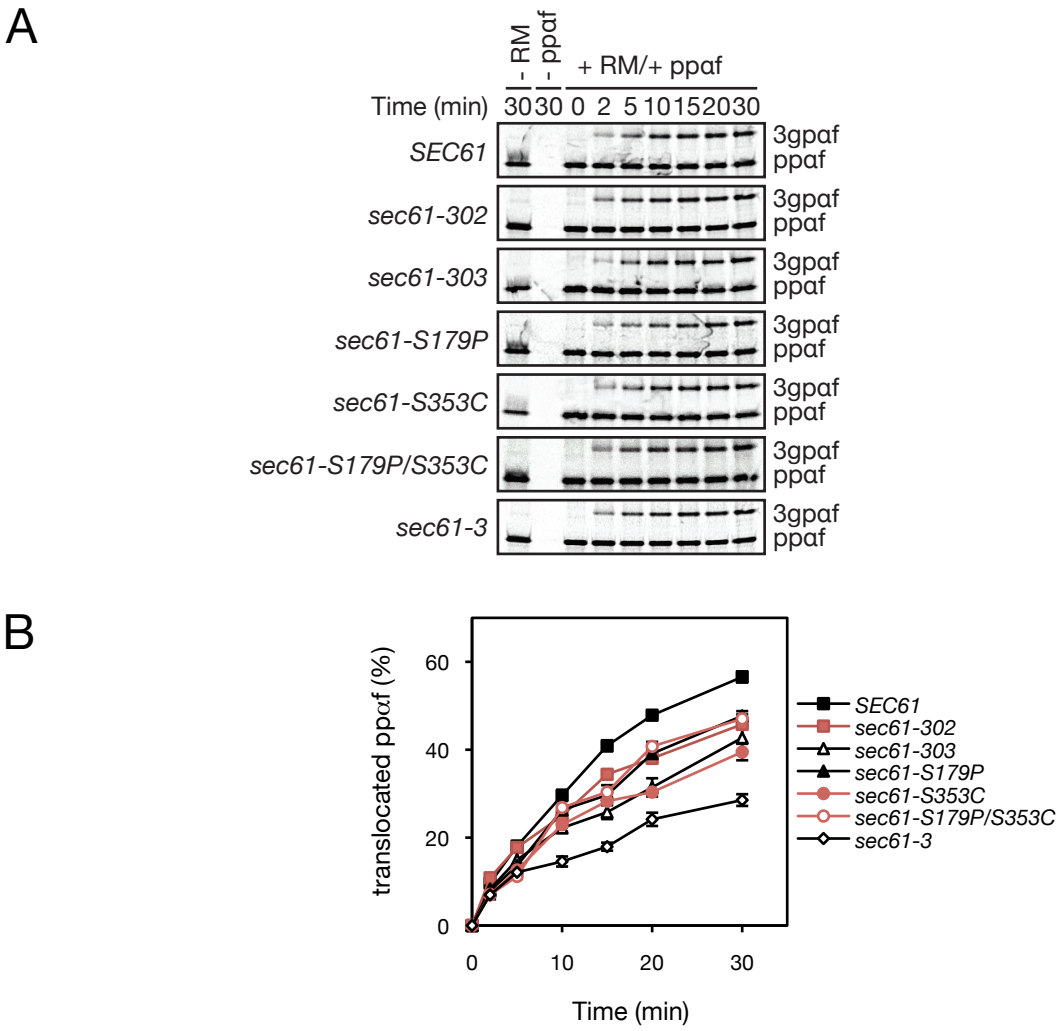

Figure 3.8.1.1. *In vitro* import of ppαf into *sec61* microsomes. (A) ER-derived microsomes (2 µl of OD_{280} = 30) of *sec61* mutants and the corresponding wild-type (*SEC61*) were incubated with ^{35}S-labeled ppαf in the presence of ATP and an ATP-regenerating system at 24 °C for the indicated period of time. Translocation was measured by the formation of fully glycosylated alpha factor (3gpαf, ~ 28 kDa). As controls import reactions were performed lacking either microsomes (- RM) or ppαf (- ppαf). Samples were resolved on 4-12 % Bis-Tris gels (NuPAGE® Novex® Pre-Cast gels, Invitrogen). Gels were dried and exposed to storage phosphor screens (GE Healthcare) for 2-3 days. Signals were detected using a phosphorimager. (B) Import of ppαf was quantified using the ImageQuant™ TL software (GE Healthcare). Results of two independent experiments (N = 2) were averaged and graphed. Error bars indicate the standard error.

3.8.2 *IN VITRO* ERAD OF ΔGPαF IN THE *SEC61* MUTANTS

ERAD involves the retrotranslocation of misfolded secretory and transmembrane proteins from the ER to the cytosol where they are degraded by the 26S proteasome (Hiller *et al.*, 1996; Plemper & Wolf, 1999; Kostova & Wolf, 2003; Meusser *et al.*, 2005; Römisch, 2005; Nakatsukasa & Brodsky, 2008; Schäfer *et al.*, 2008; Vembar & Brodsky, 2008). Sec61p, the pore-forming component of the translocation channel, has been shown to be involved in retrotranslocation and a role as the dislocon has been proposed (Pilon *et al.*, 1997; Plemper *et al.*, 1998; Schäfer & Wolf, 2009).

An *in vitro* retrotranslocation assay was employed to analyze whether membranes derived from the *sec61* mutants (ref. 3.2.2) were defective in the dislocation of mutant pro-alpha factor (Δgpαf), an ERAD substrate whose dislocation into the cytosol is dependent on 19S RP binding to the Sec61 channel (McCracken & Brodsky, 1996). This was done in additon to the pulse-chase analyses (ref. 3.7.2) using the same substrate to see if the slight increase in $t_{1/2}$ in S353C-containing mutants was exacerbated *in vitro*. As described earlier (ref. 3.7.2), mutant pre-pro-alpha factor (pΔgpαf), unable to acquire N-linked oligosaccharides, is efficiently imported into the ER, where the signal sequence is removed (Mayinger & Meyer, 1993). In *S. cerevisiae*, the resulting species, Δgpαf, has been shown to be dislocated from the ER and degraded in the cytosol by the 26S proteasome *in vitro* and *in vivo* (Caplan *et al.*, 1991; Mayinger & Meyer, 1993; McCracken & Brodsky, 1996; Werner *et al.*, 1996; Lee *et al.*, 2004a).

For the cell-free assay, unglycosylated pre-pro-α-factor was transcribed and translated *in vitro* using the plasmid paF3Q (ref. 2.2.34.4 and 2.2.34.5). The gene encoding pΔgpαf, was created by site-directed mutagenesis, resulting in the replacement of all three oligosaccharide-accepting asparagine residues in ppαf with glutamines (N23Q, N57Q, N67Q; Krieg & Melton, 1984; Kunkel *et al.*, 1987; Mayinger & Meyer, 1993). Since pΔgpαf, as well as ppαf, is transported into the ER posttranslationally, radiolabeled substrate could be prepared prior to use (Caplan *et al.*, 1991). Radiolabeled pΔgpαf was translocated posttranslationalley into wild-type (*SEC61*) and mutant ER-derived microsomes at 24 °C for 60 minutes in the presence of ATP (ref. 2.2.34.6 and 3.8.1). For each *S. cerevisiae* strain, equal amounts of membranes (2 µl of OD_{280} = 30) and radiolabeled Δgpαf (5 µl translation) were used. Following import of pΔgpαf into microsomes at 24 °C, the membranes were washed, resulting in signal-cleaved Δgpαf in the lumen of membranes (t = 0). In order to initiate retrotranslocation of Δgpαf, membranes were incubated with 0 mg/ml, 1 mg/ml, 2 mg/ml and 3 mg/ml wild-type (KRY257) cytosol, ATP and an ATP-regenerating system (ARS) at 30 °C for the indicated periods of time (t = 0, 5, 10, 15, 20, 30, 60 min) (ref. 2.2.34.7). Incubations were terminated by precipitation with trichloroacetic acid and samples analyzed on 18 % polyacrylamide/4 M urea gels. The gels were dried, exposed to storage phosphor screen (GE Healthcare) for 2-3 days and signals detected using a phosphorimager (Typhoon Trio™ Variable Mode Imager, GE Healthcare). Signals were analyzed and quantified using the ImageQuant™ TL software (GE Healthcare).

First, the cytosol concentration at which maximal export and degradation kinetics could be detected was assessed using wild-type (*SEC61*) membranes. As seen in Figure 3.8.2.1.A and B, there was no export in the absence of cytosol was (0 mg/ml cytosol). This confirmed that retrotranslocation depends on cytosol containing functional 26S proteasomes, as shown previously (McCracken & Brodsky, 1996; Werner *et al.*, 1996; Pilon *et al.*, 1997). Also visible on the gel was pΔgpαf which was not degraded because it is material aggregated on the cytosolic face of the microsomes and therefore cannot be removed by the membrane washes and cannot translocate (McCracken & Brodsky, 1996; Pilon *et al.*, 1997). Further, maximum Δgpαf degradation efficiency was detectable when 3 mg/ml cytosol ($t_{1/2}$ ~ 18 min) were used and slightly lower efficiencies when 1 mg/ml ($t_{1/2}$ ~ 22 min) and 2 mg/ml ($t_{1/2}$ ~ 20 min) cytosol were used. At 1 mg/ml cytosol, however, there was a lag phase detectable in the first 5 min of the reaction (ref. Figure 3.8.2.1.B). Therefore, retrotranslocation assays were initially performed using 3 mg/ml cytosol.

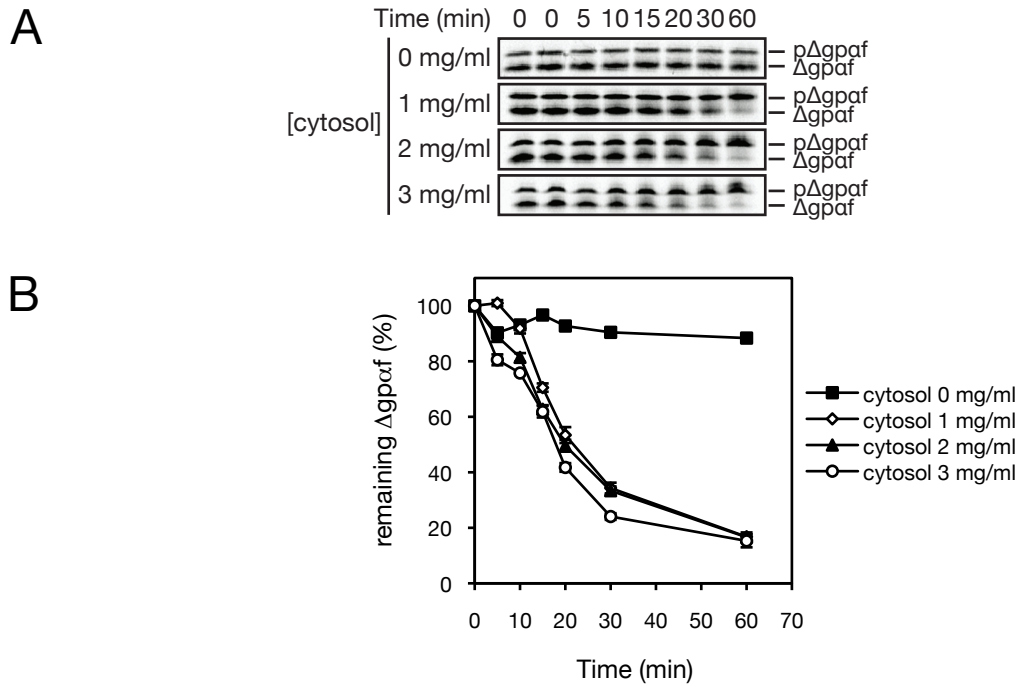

Figure 3.8.2.1. *In vitro* ERAD of Δgpαf in *SEC61*. (A) Wild-type (*SEC61*) microsomes were used initially to determine efficient cytosol concentrations for the assay. ^{35}S-labeled pΔgpαf was introduced into wild-type microsomes (2*µ*l of OD_{280} = 30) at 24 °C. The membranes were washed and incubated at 30 °C in the presence of ATP, an ATP-regenerating system and 0, 1, 2 or 3 mg/ml wild-type cytosol (KRY275) for the indicated periods of time. Incubations were terminated by adding trichloroacetic acid (to 10 %). Samples were analyzed on 18% polyacrylamide/4M urea gels and exposed to storage phosphor screens (GE Healthcare) for 2-3 days. Signals were detected using a phosphorimager system. (B) Degradation of Δgpαf was quantified using the ImageQuant™ TL software (GE Healthcare). Results of two independent experiments (N = 2) were averaged and graphed. Error bars indicate the standard error.

As shown in Figure 3.8.2.2.A and B, when the *in vitro* retrotranslocation assay was performed using 3 mg/ml cytosol, ΔgpαF degradation in wild-type (*SEC61*) microsomes was with a $t_{1/2}$ of ~ 15 min. This was in good agreement with data from a previous study (Pilon *et al.*, 1997). Microsomes from *sec61-3*, used as a control, have been shown to be deficient in export even at the permissive temperature (Pilon *et al.*, 1997). Membranes isolated from *sec61-3* behaved during *in vitro* retrotransocation assays as described previously, i.e. degradation was drastically reduced (Pilon *et al.*, 1997). After a period of 60 minutes ~ 24 % of ΔgpαF had been dislocated from *sec61-3* membranes (ref. Figure 3.8.2.2.A and B).

Membranes of the mutants *sec61-S179P* ($t_{1/2}$ ~ 18) and *sec61-303* ($t_{1/2}$ ~ 24 min) showed only slightly slower kinectics than the wild-type (*SEC61*). Further, after an incubation of 60 minutes the amounts of ΔgpαF retrotranslocated from membranes of *sec61-S179P* (~ 79 %), *sec61-303* (~ 74 %) were also comparable to the wild-type (~ 83 %). Also, in these mutants initiation of retrotransloaction was slightly delayed, but afterwards kinetics were similar as well as maximal export of ΔgpαF. In contrast, export of ΔgpαF from *sec61-302*, *sec61-S353C* and *sec61-S179P/S353C* microsomes had a longer initial lag phase and genuinely slower degradation kintetics, resulting in $t_{1/2}$ of ~ 55 min, 33 min and 49 min, and maximal export after 60 min of only 52 %, 64 % and 55 %, respectively. Strikingly, those were the mutants with reduced affinity of the Sec61 channel for 19S RP (ref. 3.5.2).

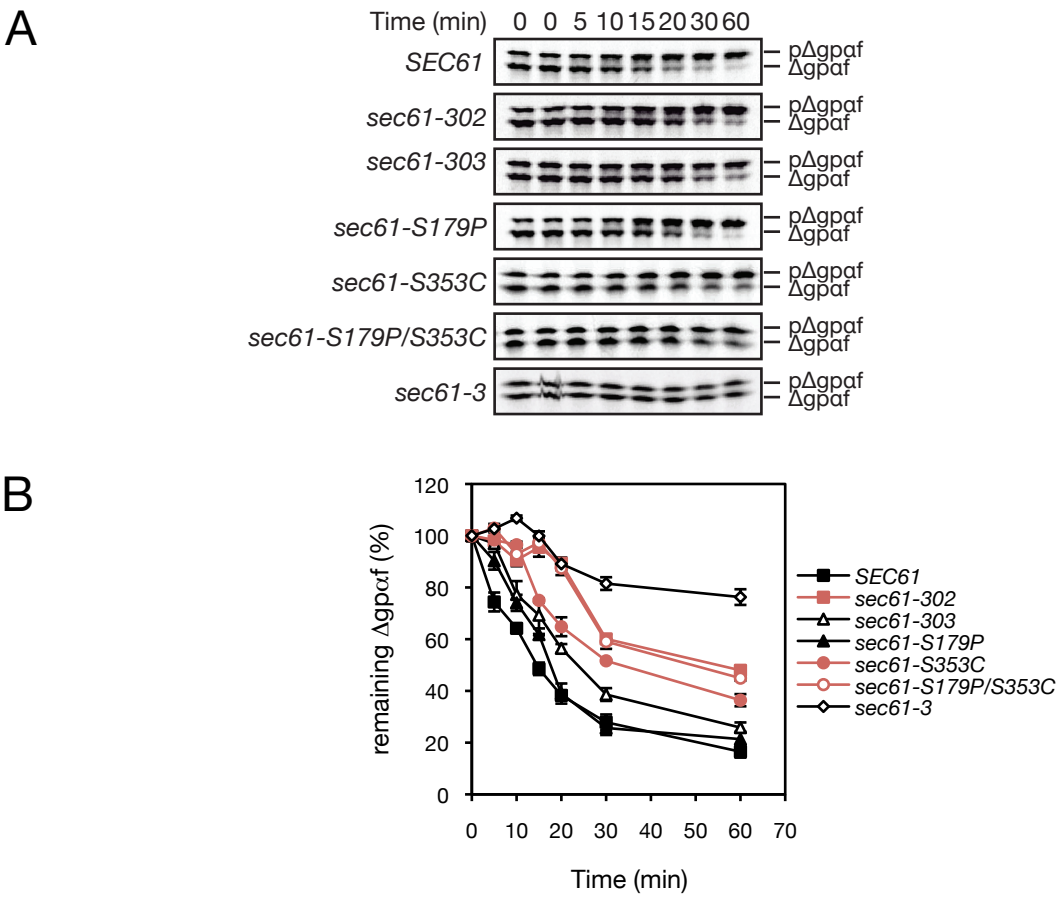

Figure 3.8.2.2. *In vitro* ERAD of Δgpαf in the *sec61* mutants (I). (A) Membranes of the designated *sec61* mutants and the corresponding wild-type (*SEC61*) were loaded with ^{35}S-labeled Δgpαf and incubated at 30 °C in the presence of ATP, an ATP-regenerating system and 3 mg/ml wild-type cytosol (KRY275) for the indicated periods of time. Incubations were terminated by precipitation with trichloroacetic acid (to 10 %). Sample analysis was on 18 % polyacrylamide/4 M urea gels, which were exposed to storage phosphor screens (GE Healthcare) for 2-3 days. Signals were detected using a phosphorimager system. Membranes from *sec61-3* were used as a control. The band showing a lower mobility is pΔgpαf associated with microsomes. (B) Degradation of Δgpαf was quantified using the ImageQuant™ TL software (GE Healthcare). Results of two independent experiments (N = 2) were averaged and graphed. Error bars indicate the standard error.

As 26 S proteasomes are present in excess when using a cytosol concentration of 3 mg/ml, assays were repeated using 1 mg/ml cytosol (ref. Figure 3.8.2.3.A and B). This was done in order to analyze whether a lower proteasome concentration would have a limiting effect on Δgpαf export and degradation in the mutants with a 19S RP binding defect. Membranes derived from the export-deficient strain *sec61-3* displayed a severe reduction in export at 1 mg/ml cytosol compared to wild-type (Pilon *et al.*, 1998). After a period of 60 min ~ 75 % of remaining Δgpαf were detectable, which was comparable to results shown in Figure 3.8.2.2. As expected degradation of Δgpαf in wild-type membranes was slower at 1 mg/ml cytosol ($t_{1/2}$ = 23 min; ref. Figure 3.8.2.1), and indistinguishable

from ERAD in *sec61-303* ($t_{1/2}$ = 22 min) and *sec61-S179P* microsomes ($t_{1/2}$ = 24 min) (ref. Figure 3.8.2.3). At 1 mg/ml, however, in all *sec61* mutants containing the S353C replacement (*sec61-302*: $t_{1/2}$ = 46 min; *sec61-S353C*: $t_{1/2}$ = 45 min; *sec61-S179P/S353C*: $t_{1/2}$ = 42 min) Δgpαf was degraded with a 2-fold increased $t_{1/2}$ compared to wild-type. This suggests that in the presence of limiting amounts of proteasomes the Sec61p-19S RP interaction becomes limiting for export of Δgpαf from the ER to the cytosol.

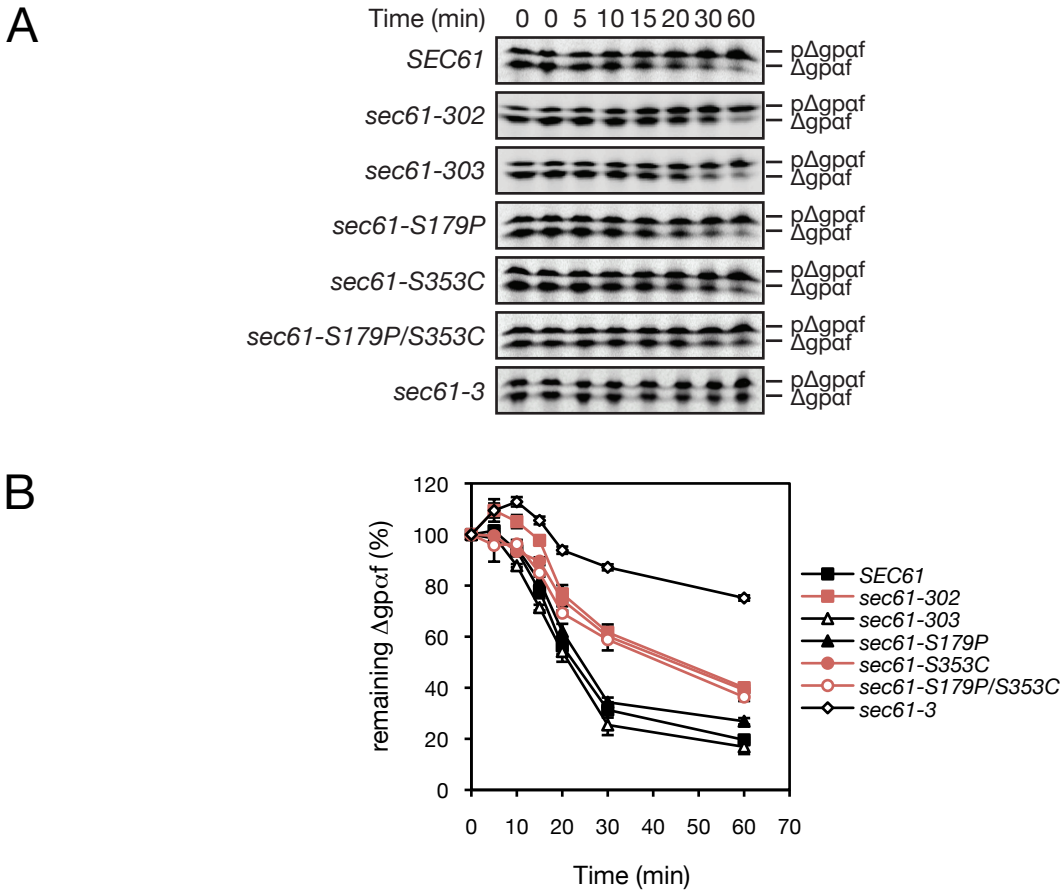

Figure 3.8.2.3. *In vitro* ERAD of Δgpαf in the *sec61* mutants (II). (A) Membranes (2*µ*l of OD_{280} = 30) of the wild-type (*SEC61*) strain and the designated *sec61* mutants were loaded with Δgpαf and incubated at 30 °C in the presence of ATP, an ATP-regenerating system and 3 mg/ml wild-type cytosol (KRY275) for the indicated periods of time. Incubations were terminated by precipitation with trichloroacetic acid (to 10 %). Samples were analyzed on 18% polyacrylamide/4 M urea gels, which were exposed to storage phosphor screens (GE Healthcare) for 2-3 days. Signals were detected using a phosphorimager system. The band showing a lower mobility is pΔgpαf associated with microsomes. (B) Degradation of Δgpαf was quantified using the ImageQuant™ TL software (GE Healthcare). Results of two independent experiments (N = 2) were averaged and graphed. Error bars indicate the standard error.

3.9 DETECTION OF CONFORMATIONAL CHANGES IN MUTANT SEC61P

As proteasome binding assays (ref. 3.5.2) indicated that the amino acid substitution S353C is responsible for the reduction in 19S RP binding to reconstituted proteoliposomes derived from the respective *sec61* mutants, I was interested in identifying whether the observed defect was due to a conformational change in mutant Sec61p (Ng *et al.*, 2007). Such a conformational change might have an impact on the accessibility of the proteasome binding site on the cytoplasmic face of Sec61p, making it less accessible for the proteasome.

In order to understand whether there is a conformational change in Sec61p in those *sec61* mutants causing a defect in proteasome binding, I used the following approach: The PEGylation reagent Methyl-PEG_8-NHS ester* ($MS(PEG)_8$; Pierce®, Thermo Scientific) was used in order to modify all accessible lysine (K) residues (and the N-terminus) of the wild-type or mutant Sec61p (ref. 2.2.35 and Figure 3.9.1).

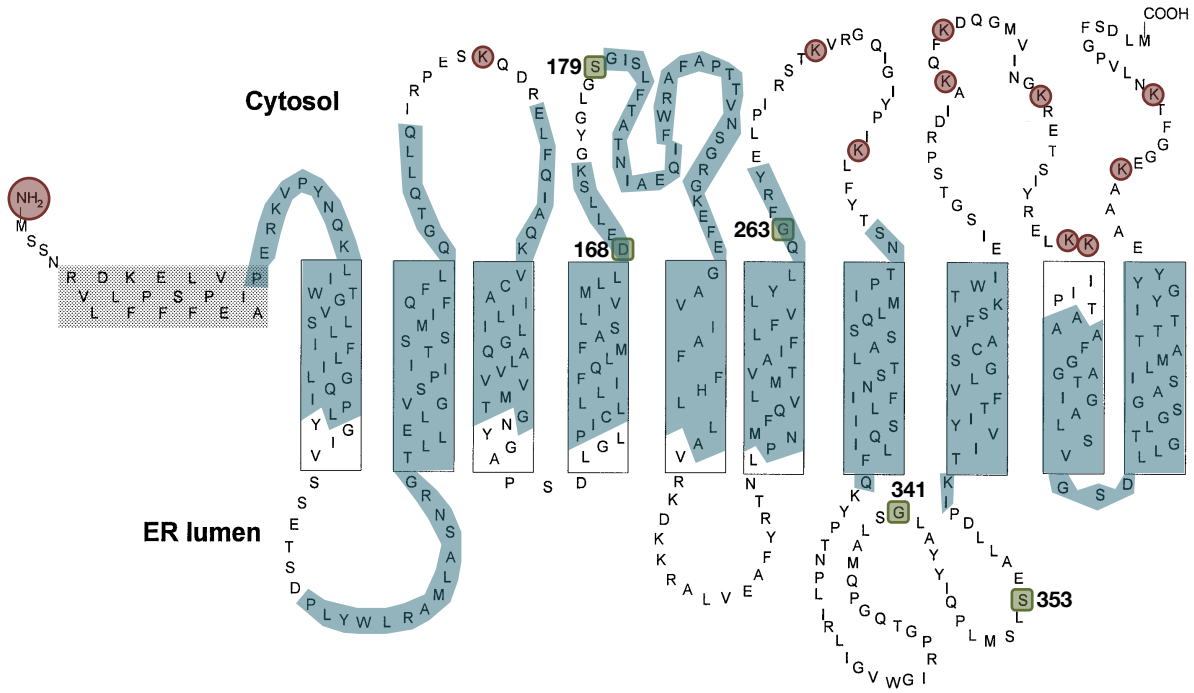

Figure 3.9.1. Topology model of Sec61p (modified). Shown is the topology model of Sec61p including positions of amino acids in the protein. Positions of theoretically accessible primary amines (lysine residues (K); RED) on the cytoplasmic face of Sec61p, the amino terminus (RED) and positions of amino acid substitutions in Sec61p of *sec61-302*, *sec61-S179P*, *sec61-S353C* and *sec61-3* (GREEN) are indicated. Positions of transmembrane domains according to the *M. jannashii* crystal structure are also outlined (BLUE) (taken from Wilkinson *et al.*, 1997; modified according to van den Berg *et al.*, 2004).

$MS(PEG)_8$ belongs to a group of polyethylene glycol (PEG) compounds containing methyl- and amine-reactive N-hydroxysuccinimide (NHS) ester groups at opposite ends of the molecule (Harris & Zalipsky, 1997; Veronese & Harris, 2002). The reagent contains eight PEG units, resulting in a spacer length of 30.8 Å. For each successfully modified lysine (K) residue, the modifier adds 0.51 kDa to the protein (Morar *et al.*, 2006). Protein modifications using $MS(PEG)_8$ occur at the primary amines in lysine (K) residue side chains and the N-terminus of proteins (Morar *et al.*, 2006). During the PEGylation reaction, the NHS-ester reacts efficiently with primary amines, resulting in the formation of amide bonds while releasing the NHS group. During this reaction the PEG chains, containing terminal methyl groups, are covalently attached to the protein (Veronese & Harris, 2002; Morar *et al.*, 2006). $MS(PEG)_8$ is a hydrophilic reagent, a property which is transferred to the modified protein and thus could have an impact on the protein's mobility.

Due to its hydrophobic character, Sec61p (53 kDa) displays an abnormal migration behaviour during SDS-PAGE (Wilkinson *et al.*, 1996; Pilon *et al.*, 1998). Here, Sec61p generally migrates at about 37 kDa (Wilkinson *et al.*, 1996; Pilon *et al.*, 1998). Since the hydrophilic property of $MS(PEG)_8$ is transferred to Sec61p upon successful PEGylation, I anticipated that the migration behaviour of the

protein might change. This would be favourable for the detection of minor changes in the molecular weight of mutant Sec61p. If, however, the hydrophobic character of Sec61p was too dominant, then the detection of subtle differences in the molecular weight (e.g. 1.2 kDa, which would correlate with two $MS(PEG)_8$ modifications) would be difficult.

On the cytosolic face of Sec61p there are theoretically 10 accessable lysine (K) residues (plus 1 N-terminus) according to data from the *M. jannaschii* crystal structure (ref. Figure 3.9.1; van den Berg *et al.*, 2004). Thus, upon successful PEGylaton of all theoretically available lysine (K) residues, an overall increase in molecular weight of 6.6 kDa would be possible using $MS(PEG)_8$.

For the PEGylation assay, PK-RMs (2 µl of OD_{280} = 30 in 20 µl reaction volume) of the *sec61* mutants *sec61-S179P*, *sec61-S353C*, *sec61-S179P/S353C*, *sec61-302* and *sec61-3*, as well as the corresponding wild-type (*SEC61*) strain were prepared. PK-RMs were prepared by treatment with puromycin and potassium acetate (ref. 2.2.26; Neuhof *et al.*, 1998). The treatment causes the release of ribosomes and peripheral proteins from the microsomal membranes, i.e. of proteins that might block access to Sec61p. Using ER-derived PK-RMs, only lysine (K) residues on the cytosolic face of the protein as well as its N-terminus are modified. Thus, if one of the mutations in *SEC61* indeed causes a conformational change in Sec61p, this could be detected as e.g. a reduction in molecular weight of modified mutant Sec61p compared to modified wild-type Sec61p.

Prior to the actual experiment, the ideal experimental conditions were determined. In two independent experiments the concentration of the PEGylation reagent and the incubation time yielding maximal PEGylation efficiency were determined. As $MS(PEG)_8$ is moisture-sensitive, the reagent had to be dissolved in water-free DMSO to avoid hydrolysis of the compound's reactive group. Thus, the reagent was added last to the reaction. Initial PEGylation experiments using $MS(PEG)_8$ were performed in collaboration with Michael Lafontaine.

In order to determine the time of incubation that is needed to achieve maximal PEGylation of Sec61p, PK-RMs (2 µl of OD_{280}) derived from the wild-type (*SEC61*) strain were incubated in amine-free buffer (B88) at RT (24 °C) using 2.5 mM $MS(PEG)_8$ for various periods of time (t = 5, 10, 20, 30 min). Reactions were stopped with ammonium acetate and incubated on ice for 15 min. Following the incubation, samples were analyzed by SDS-PAGE on 4 -12 % Bis-Tris gels (NuPAGE® Novex® Pre-Cast gels, Invitrogen) and immunoblotting using the anti-Sec61p (N-terminal) and anti-Sbh1p (control) antibody (Römisch lab). Detection of signals and determination of relative mobility of PEGylated proteins was using the ChemiDoc™ XRS system and the Image Lab™ software (both Bio-Rad). The PageRuler™ (Fermentas, Thermo Scientific) was used as the molecular weight standard.

Results are shown in Figure 3.9.2.A. Following PEGylation, distinct protein bands could be detected (t = 5 – 30 min). The untreated wild-type PK-RMs, however, displayed a weaker band, which was probably due to antibody distribution on the nitrocellulose membrane. Additionally, upon successful PEGylation of Sec61p an increase in protein size could be detected. This increase reached a maximum after an incubation period of about 20 min. Therefore, in the following experiments an

incubation of 30 min was chosen to alow for maximal PEGylation. Generally, signals of PEGylated proteins were less distinct compared to the untreated control (ref. Figure 3.9.2.A, *SEC61*: 30 min, - $MS(PEG)_8$). This could have been due to PEGylation of Sec61p's N-terminus, which could impede access of the anti-Sec61p (N-terminal) antibody. The use of anti-Sec61p (C-terminal) antibody, however, resulted in too much background and thus was not used for detection (data not shown).

Next, the $MS(PEG)_8$ concentration required for efficient PEGylation of Sec61p was determined. Here, the experiment was conducted as before using various concentrations of the PEGylation reagent ([$MS(PEG)_8$] = 0, 0.5, 1.0, 1.5, 2.0, 2.5, 3.0, 4.0, 5.0, 10, 15, 20 mM) and incubating the samples for 30 min. Results are shown in Figure 3.9.2.B. For all $MS(PEG)_8$ concentrations used there was an increase in protein size detectable, indicating successful PEGylation of wild-type Sec61p. More precisely, compared to the untreated sample (0 mM), between 0.5 and 5 mM reagent used bands showing slower migration of the protein was detected. Using these concentrations, however, PEGylation seemed not as efficient as at concentrations between 10 and 20 mM. Here, a further increase in Sec61p size was detectable. As between 15 and 20 mM $MS(PEG)_8$ no further increase in protein size was detected, we assumed that maximal PEGylation was achieved. Thus, for PEGylation experiments an $MS(PEG)_8$ concentration of 20 mM was used.

The assay using PK-RMs (2 µl of OD_{280}) of the *sec61* mutants *sec61-302*, *sec61-S353C*, *sec61-S179P* and *sec61-3* and the corresponding wild-type (*SEC61*) was performed as described above. Membranes were incubated with 20 mM of $MS(PEG)_8$ at 24 °C for 30 min and samples analyzed as before. In Figure 3.9.2.C, a representative result of the PEGylation experiment is shown. PEGylated wild-type (*SEC61*) PKRMs (ref. Figure 3.9.2.C *SEC61*: + $MS(PEG)_8$) displayed an increase in molecular weight of ~ 2.9 kDa, compared to untreated wild-type PKRMs (*SEC61*: - $MS(PEG)_8$), which would correlate with a successful PEGylation of about 6 lysine (K) residues (or 5 lysine (K) residues and the N-terminus). It has to be noted that not all lysine residues seem to be accessible for PEGylation which might be due to the overall conformation of Sec61p or the size of the modifier. PKRMs of *sec61-S179P* showed an increase in molecular weight of ~ 2.8 kDa which was similar to the wild-type (*SEC61*), suggesting that the amino acid substitution S179P does not cause a conformational change in Sec61p. A slight increase in molecular weight for *sec61-302* (Δ kDa ~ 1.3 kDa) and *sec61-S353C* (Δ kDa ~ 1.2 kDa) was detected compared to the untreated sample (- $MS(PEG)_8$). This suggests that for both mutants fewer lysine (K) residues were accessible (*sec61-302*: ~ 2-3 lysine (K) residues; *sec61-S353C*: ~ 2 lysine (K) residues) for PEGylation than in the wild-type (*SEC61*) Sec61p, indicating that this might indeed be due to a conformational change of Sec61p in these mutants. The ERAD-deficient mutant *sec61-3* (G341E) was used as a control, as in this mutant the underlying amino acid substitution is located in the same region as the substitution S353C of *sec61-S302*, *sec61-S353C* and *sec61-S179P/S353C* (Sommer & Jentsch, 1993; Pilon *et al.*, 1998; Ng *et al.*, 2007). Interestingly, for *sec61-3* (Δ ~ 1.5 kDa) the increase in protein size would correlate with 3 modifications) with $MS(PEG)_8$ and was comparable to *sec61-302* and *sec61-S353C*.

Moreover, signals for PEGylated Sec61-3p were fainter compared to the untreated samples (*sec61-3*: - MS$(PEG)_8$) and the other mutants, indicating that modified Sec61-3p is instable. Thus, the above results could give a first indication that due to the amino acid substitution S353C in *sec61-302* and *sec61-S353C* a conformational change in mutant Sec61p is induced affecting proteasome binding by e.g. masking the proteasome binding site on the cytoplasmic face of Sec61p.

The preliminary data gained from the PEGylation assays were not significant enough to provide strong evidence for a conformational change in Sec61p in the respective mutants. Therefore, I aimed at modifying the assay to be able to get significant results, which would give an insight into the conformation of mutant Sec61p. I therefore used the reagent EZ-Link® Sulfo-NHS-LC-LC-Biotin** (spacer length: 30.5 Å; molecular weight: 0.67 kDa) which also modifies primary amines (Pierce, Thermo Scientific). The biotin (0.244 kDA) moiety binds streptavidin (Sigma) with high affinity (Hofmann *et al.*, 1982; Hermanson, 2008). The homotetramer streptavidin has a molecular weight of about 60 kDa, with each of the subunits being able to bind one biotin molecule (Green, 1975; Weber, 1989). This property of the modifier was employed to detect a conformational change in mutant Sec61p. Binding of streptavidin to the biotin moiety on modified primary amines would thus yield in a substancial increase in molecular weight per successful biotinylation.

Retardation assays using the biotinylation/streptavidin approach, however, could not be established successfully (data not shown). No discrete protein bands could be detected during Western Blot analysis using the reagent, but a smear over the whole lane. Unfortunately, due to time constraints, the assay could not be optimized.

* Succinimidyl-([N-methyl]-ethyleneglycol) ester

** Sulfosuccinimidyl-6-(biotinamido)-6-hexanamido hexanoate

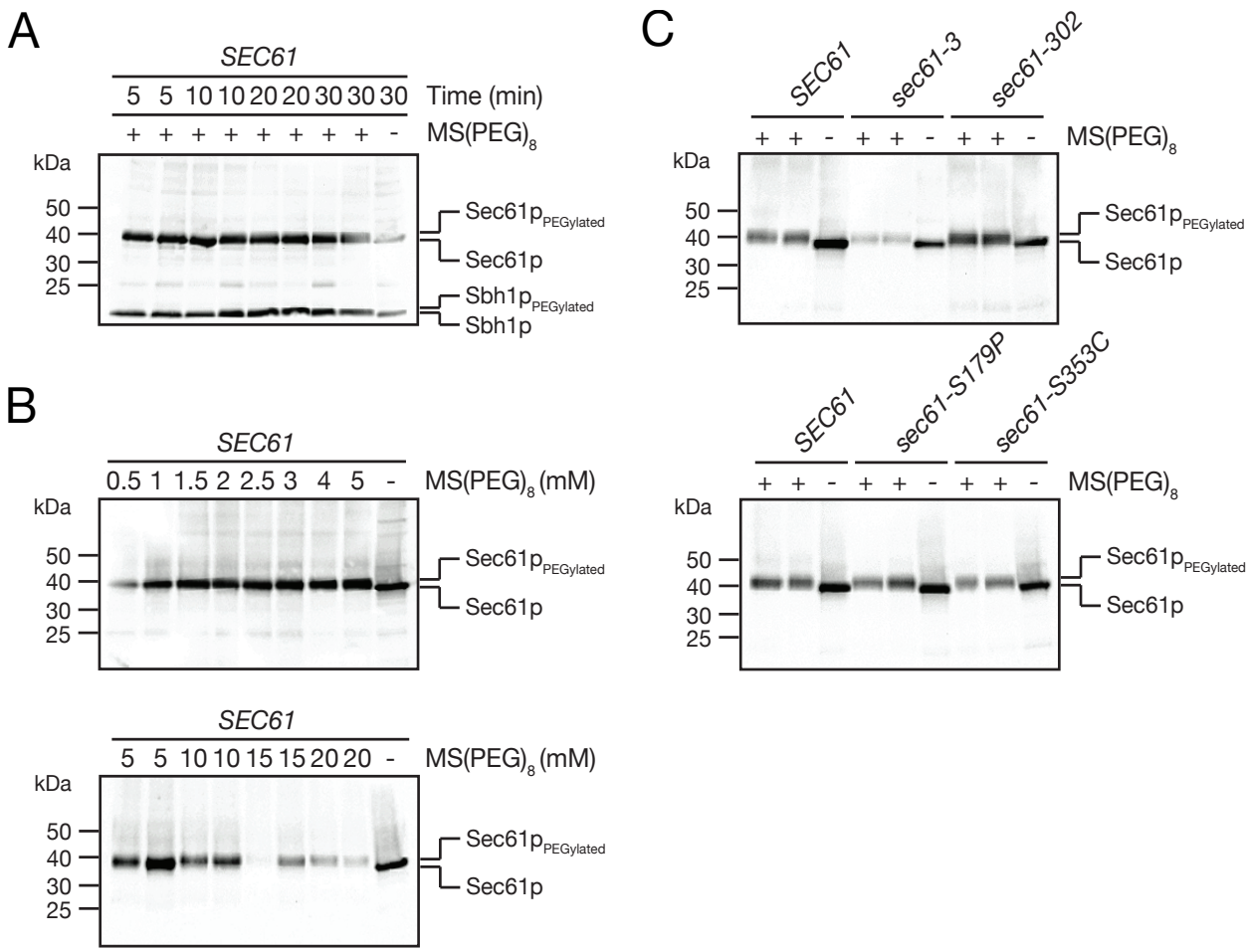

Figure 3.9.2. Analysis of a conformational change in mutant Sec61p. (A) Determination of optimal incubation time for the PEGylation of wild-type Sec61p. Wild-type (*SEC61*) PKRMs (2 µl of OD_{280} = 30) were incubated in B88 in the presence of 2.5 mM $MS(PEG)_8$ at 24 °C over the indicated periods of time. As a control untreated PKRMs (- $MS(PEG)_8$; i.e. water-free DMSO instead of $MS(PEG)_8$) were incubated for 30 min. Reactons were stopped by adding 1 µl 8M ammonium acetate solution followed by an incubation for 15 min on ice. Samples were analyzed by SDS-PAGE on 4-12 % BisTris gels (NuPAGE® Novex® Pre-Cast gels, Invitogen) and immunoblottig with Sec61p antibody (N-terminal) and Sbh1p antibody (both Römisch lab). Detection of bands was using the SuperSignal™ West Dura Extended Duration Chemiluminescent Substrate (Pierce) and the Molecular Imager ChemiDoc™ XRS System (BioRad; CCD camera detection). (B) Determination of optimal $MS(PEG)_8$ concentration for PEGylation of Sec61p. Wild-type (*SEC61*) PKRMs (2 µl of OD_{280} = 30) were incubated at 24 °C in B88 in the presence of the indicated $MS(PEG)_8$ concentrations over 30 min. Detection of signal was as in A (except: no Sbh1p detection). Untreated wild-type PK-RMs were used as a control. (C) PKRMs of the wild-type (SEC61) and the indicated *sec61* mutants were PEGylated using 20 mM $MS(PEG)_8$ for 30 min. Untreated PKRMs were used as controls. Detection of signals was as in A (except: no Sbh1p detection).

4 DISCUSSION

The eukaryotic cell is confronted with a high load of proteins that need to undergo correct folding or assembly in order to function properly (Schubert *et al.*, 2000; Trombetta & Parodi, 2003). Proteins that fail to fold or assemble correctly are toxic to the cell and thus threaten cell homeostasis (Goldberg, 2003; Römisch, 2004). Folding of secretory proteins (and membrane proteins) takes up a central role in overall protein folding, as those proteins make up approximately 30 % of all eukaryotic proteins (Ghaemmaghami *et al.*, 2003). A quality control mechanism (ERQC; ref. 1.3.2) within the first compartment of the secretory pathway, the ER, ensures that only properly folded proteins move further along the secretory pathway to their final destinations, while misfolded proteins are subjected to the ERAD (ref. 1.6). The complexity of protein folding and of processes linked with it such as ERQC, ERAD as well as the UPR (ref. 1.4), is seen in the variety of protein aggregation diseases such as the neurodegenerative disorders Alzheimer's, Parkinson's, Huntington's and Creutzfeld-Jakob (CJD) disease as well as α1-antitrypsin deficiency and cystic fibrosis (Qu *et al.*, 1996; Werner *et al.*, 1996; Imai *et al.*, 2001; Harding & Ron, 2002; Araki *et al.*, 2003; Forman *et al.*, 2003; Gow & Sharma. 2003; Pereira *et al.*, 2004 Lukacs & Verkman, 2012; Mendoza *et al.*, 2012; Rabeh *et al.*, 2012).

The ERAD pathway involves the recognition of damaged or misfolded proteins in the ER, their ubiquitination and subsequent degradation by 26S proteasomes in the cytosol (McCracken & Brodsky, 1996; Römisch, 2005; Mehnert *et al.*, 2010; Smith *et al.*, 2011). Since the components of the UPS (ref. 1.5) act in the cytosol, a prerequisite of protein degradation is the dislocation of misfolded proteins from the ER to the cytosol (Jensen *et al.*, 1995; Ward *et al.*, 1995; Werner *et al.*, 1996; Wiertz *et al.*, 1996b).

While the nature of the dislocation channel is still under debate, various studies suggest Sec61p as a possible candidate for the channel-forming component during protein dislocation of ERAD-L substrates and at least some transmembrane proteins (MHC class I HC, Pdr5*) (ref. 1.6.1; Wiertz *et al.*, 1996b; Pilon *et al.*, 1997, 1998; Plemper *et al.*, 1997; 1998; Gillece *et al.*, 1999; Schmitz *et al.*, 2000; Römisch, 2005; Willer *et al.*, 2008; Schäfer & Wolf, 2009). Not only has Sec61p been shown to associate with some ERAD-L substrates, it also interacts with components of the ERAD-L pathway, such as Hrd1p, as well as with 26S proteasomes (Wiertz *et al.*, 1996b; Plemper *et al.*, 1999a; Ng *et al.*, 2007; Schäfer & Wolf, 2009). Although there are studies that argue against a role of Sec61p during dislocation, in no case the evidence is compelling and the available evidence strongly suggests that Sec61p is at least part of the dislocon (Carvalho *et al.*, 2006, 2010; Denic *et al.*, 2006; Sato *et al.*, 2006; Wahlmann *et al.*, 2007; Garza *et al.*, 2009). Deciphering the ERAD pathway requires an understanding of the contribution of its individual components, such as Sec61p.

In a previous study from our group in collaboration with Jeremy Brown, two *sec61* mutants, *sec61-302* (D168G, S179P, F263L and S353C) and *sec61-303* (D168G and F263L), were isolated

displaying a defect in cotranslational protein import (Ng *et al.*, 2007). Additionally, only *sec61-302* specifically displayed a reduction in proteasome binding (Ng *et al.*, 2007). Considering the dimensions of the α-subunit's TMDs derived from the crystal structure of the *M. jannaschii* SecY complex, the single amino acid substitutions are located in TMD 4 (D168G), in the cytosolic loop (L) 4 close to the cytosolic end of TMD 5 (S179P), in TMD 6 close its cytosolic end (F263L) and in the ER-lumenal L 7 (S353C) of Sec61p (ref. Figure 3.9.1; Wilkinson *et al.*, 1996; van den Berg *et al.*, 2004; Ng *et al.*, 2007).

Since the two amino acid substitutions D168G and F263L, shared by *sec61-302* and *sec61-303*, did not cause a reduction in proteasome binding to membranes isolated from *sec61-303*, it was suggested that one of the remaining amino acid substitutions, S179P or S353C, is responsible for the observed reduction in proteasome binding (Ng *et al.*, 2007). In order to elucidate whether S179P or S353C mediate the observed binding defect, I generated the respective *sec61* mutants by SOE-PCR in the same genetic background as *sec61-302* and *sec61-303* (JDY638), which were also included in my analyses (ref. 3.2; Ng *et al.*, 2007).

4.1 TEMPERATURE- AND STRESS-SENSITIVITY OF THE *SEC61* MUTANTS

I initially analyzed *sec61-S179P*, *sec61-S353C* and *sec61-S179P/S353C* with respect to cell viability on rich and minimal medium at various temperatures in the absence or presence of the glycosylation inhibitor tunicamycin, to evaluate the effects of any of the point mutations in *SEC61* on its functions (ref. 3.3; Kuo & Lampen, 1974; Duksin & Mahoney, 1982). Growth in the presence of tunicamycin leads to misfolded protein accumulation in the ER and thus a sensitivity towards tunicamycin can be associated with defects in ERAD (Travers *et al.*, 2000; Tran *et al.*, 2011). The *sec61* mutants were viable (ref. Figure 3.3.1). I found that none of my new *sec61* mutants displayed severe growth defects at any of the temperatures tested, the only exception being *sec61-S353C* which showed a slight temperature sensitivity at 37 °C (ref. Figure 3.3.1). None of the remaining *sec61* mutants displayed cold- or temperature-sensitivity, suggesting that none of the point mutations in *SEC61* affected protein translocation into the ER at any temperature (ref. Figure 3.3.1). The same was true when cells were grown on minimal medium, i.e. under more restrictive nutritional conditions (ref. Figure 3.3.1). Here, in the absence as well as in the presence of tunicamycin, growth of my mutants was comparable to the corresponding wild-type (*SEC61*) (ref. Figure 3.3.1). For the growth experiments I used two previously isolated *sec61* mutants, *sec61-3* (Cs, Ts) and *sec61-32* (Ts), as controls (Stirling *et al.*, 1992; Sommer & Jentsch, 1993; Pilon *et al.*, 1997, 1998). Both *sec61* mutants displayed the same growth defects in my hands as shown previously (ref. Figure 3.3.1; Pilon *et al.*, 1998). The cold- and temperature-sensitivities of *sec61-3* and *sec61-32* had been suggested to be due to the impact of higher or lower temperature on the mobility or structure of the membrane protein Sec61p (Pilon *et al.*, 1998). The fact that none of the *sec61* mutants display a

striking cold- or temperature-sensitivity indicates that the underlying point mutations in the respective mutants do not affect Sec61p stability and thus function (Pilon *et al.*, 1997).

Alignments of Sec61p amino acid sequences from temperate organisms and extremophiles suggest that amino acid substitutions in the ER-lumenal L 7 of Sec61p have an impact on channel function at extreme temperatures (Römisch *et al.*, 2003). In Antarctic and Arctic fish species amino acid substitutions in L 7 may improve channel function in the cold (Römisch *et al.*, 2003). The effect at 37 °C for *sec61-S353C* could support this idea. At 37 °C a conformational change in Sec61p caused by the S353C substitution might be enhanced resulting in instability of the protein. Instability might lead to reduced viability at this temperature. Temperature-sensitivity of *sec61-S353C* was not exceeded when the mutant was grown in the presence of tunicamycin, which suggests that it was independent of ERAD (ref. Figure 3.3.1). The fact that neither *sec61-302* nor *sec61-S179P/S353C* display temperature-sensitivity could be due to the existence of S179P on the cytosolic face of Sec61p in these mutants. Although only speculative, this amino acid substitution on the opposite side of the Sec61 channel could counteract the effect of S353C on the Sec61p structure leading to the observed temperature sensitivity (ref. 3.3). This compensatory effect of the amino acid substitution S179P in sec61-S179P/S353C may be due to the contribution of proline to the overall protein structure. Proline increases the rigidity of protein structures (Prajapati *et al.*, 2007). At residue 179 in Sec61p, located in the cytoplasmic L 4 close to the cytosolic end of TMD5, it might have a stabilizing effect against the conformational change induced by S353C (Ng *et al.*, 2007).

Stability and expression levels of Sec61p in my *sec61* mutants, although I did not specifically investigate these, did not seem to be affected (data not shown). Comparison of equal amounts of RMs (measured in equals; 1 eq = 50 A_{280} units/μl), derived from *sec61* mutants and the corresponding wild-type (*SEC61*) grown at the permissive temperature, when quantifying PK-RMs and reconstituted proteoliposomes prior to proteasome binding assays, revealed that the amounts of mutant Sec61p as well as signal intensities were comparable to the wild-type (*SEC61*) (data not shown; Walter & Blobel, 1981). This, together with the fact that in my *sec61* mutants cell viability was not affected, further emphasizes that none of the point mutations in the *sec61* mutants derived from *sec61-302* affected Sec61p stability or function during import.

4.2 PROTEIN TRANSLOCATION INTO THE ER IN THE *SEC61* MUTANTS

In yeast, Sec61p is the pore-forming component during co- and posttranslational protein import into the ER (ref. 1.2; Stirling *et al.*, 1992; Panzner *et al.*, 1995, Römisch, 1999). In order to investigate whether the amino acid substitutions S179P and S353C cause the defect in co-translational import into the ER detected in *sec61-302* and *sec61-303*, I employed a reporter translocation assay using plasmids encoding protein substrates for co- (p*PHO8-URA3*) or posttranslational (p*CPY-URA3*) ER import (ref. 3.4; Ng *et al.*, 1996; Ng *et al.*, 2007).

Translocation of the two reporter fusion proteins Pho8p-Ura3p and CPYp-Ura3p into the ER, if disturbed due to Sec61p dysfunction, leads to the accumulation of the respective fusion protein in the cytosol (Ng *et al.*, 2007). This in turn enables the cells (*ura3* auxotrophs) to grow on medium lacking uracil as the Ura3p part of the protein remains in the cytosol (Ng *et al.*, 1996; Ng *et al.*, 2007). The mutants *sec61-302* and *sec61-303* were identified screening specifically for co-translational import defects using these plasmids (Ng *et al.*, 1996; Ng *et al.*, 2007). For *sec61-302*, which was used as a control in the assay, I could reproduce the defect in cotranslational ER import (ref. Figure 3.4.1; Ng *et al.*, 2007). Defects in protein translocation into the ER for my new *sec61* mutants were not apparent when employing the reporter translocation assay (ref. Figure 3.4.1).

Since none of the *sec61-302* derivatives I generated displayed defects in co- or posttranslational protein import into the ER in this assay, the defect in cotranslational translocation found in *sec61-302* and *sec61-303* can be attributed to the amino acid substitutions D168G and/or F263L, which are present in both mutants (Ng *et al.*, 2007). The individual contributions of the amino acid substitutions D168G and F263L to the observed cotranslational import defect in *sec61-302* and *sec61-303*, however, were not investigated. It has been suggested that pore opening could be mediated by shifts in helices lining the Sec61 channel (van den Berg *et al.*, 2004). These shifts might be promoted by a rearrangement of L 4, which is located between TMD 4 and TMD 5 (van den Berg *et al.*, 2004). As the amino acid substitution D168G is located close to L 4 it might affect this rearrangement (van den Berg *et al.*, 2004). Another *sec61* mutant with a point mutation in TMD 4 of Sec61p, *sec61-24* (L162P; Cs), also displays a translocation defect at the permissive temperature (Pilon *et al.*, 1998). For this and other classic *sec61* mutants, adjacent to the N-terminal side of the lateral gate, it has been suggested that the mutants might interfere with the structural transition between the open and closed conformation of the gate (Pilon *et al.*, 1998; Trueman *et al.*, 2011).

The results further indicate that the conformational change in Sec61p induced by the ER-lumenally located amino acid substitution S353C does not affect co- or posttranslational import into the ER (ref. 4.1).

The essential role of Sec61p during protein translocation into the ER generally complicates the analysis of its involvement in ERAD. In many *sec61* mutants defects in misfolded protein degradation coincide with defects in protein import into the ER. Therefore, it has been argued that the ERAD defects observed in these mutants may be caused indirectly by lack of ER import of one or more ERAD factors (Jentsch & Sommer, 1993; Pilon *et al.*, 1997, 1998; Zhou & Schekman, 1999). Only *sec61* mutants defective in export, but with normal ER import capacity, are therefore suitable to demonstrate a direct role of the Sec61 channel in ERAD (Pilon *et al.*, 1997). Thus, the fact that none of the *sec61* mutants that I created in this study (*sec61-S179P*, *sec61-S353C* and *sec61-S179P/S35C*) is defective in protein translocation into the ER, makes them excellent tools for further studies of the role of the Sec61 channel in ERAD. Therefore, these mutants were not only useful for elucidating the domains in Sec61p involved in proteasome binding, but also for directly

demonstrating the importance of this interaction for ERAD, without any interfering impact of disturbed ER import.

4.3 PROTEASOME BINDING IN THE *SEC61* MUTANTS

ERAD (ref. 1.6) eliminates misfolded or unassembled proteins from the ER (Römisch, 2005). The selection of ERAD substrates occurs in the ER by the ERQC (ref. 1.3) (Ellgaard & Helenius, 2003). Proteolysis of these substrates by the cytoplasmic UPS (ref. 1.5) requires their dislocation from the ER to the cytosol (Voges *et al.*, 1999; Goldberg, 2003; Römisch, 2005). The central role of the 26S proteasome, the most downstream component of the UPS, in ERAD has been demonstrated in several studies (ref. 1.5.2): Misfolded secretory and transmembrane proteins accumulate in the cytosol (or even in the ER) upon addition of proteasome inhibitors, and mutations in 20S CP and 19S RP subunits cause ERAD defects (Wiertz *et al.*, 1996b; Huppa & Ploegh, 1997; Mayer *et al.*, 1998; Yang *et al.*, 1998). In some, but not all cases, export and degradation of ERAD substrates is coupled (Hiller *et al.*, 1996; Loayza *et al.*, 1998; Plemper *et al.*, 1998, Kalies *et al.*, 2005; Ng *et al.*, 2007). The extraction mechanism of ERAD substrates from the ER is not fully understood so far. Cdc48p, which binds to the Sec61 channel, is involved in export of many ERAD substrates from the ER (Kalies *et al.*, 2005; Brodsky, 2012). It can also act together with the 19S RP of the 26S proteasome during extraction of proteins from the ER and during degradation of substrates, which are difficult to unfold (Isakov & Stanhill. 2011; Morris *et al.*, 2014). The 19S RP can also promote misfolded protein extraction from the ER on its own in mammalians and yeast (Lee *et al.*, 2004a; Ng *et al.*, 2007; Wahlman *et al.*, 2007). In a cell-free system, proteasomes in the presence of ATP promote export from the ER and degradation of a soluble ERAD substrate (Lee *et al.*, 2004a; Wahlman *et al.*, 2007). For this ERAD substrate export and degradation can be uncoupled, and the 19S RP is the only cytosolic factor required for dislocating the substrate from the ER into the cytosol *in vitro* (Lee *et al.*, 2004a). Binding of the 19S RP to the Sec61 channel has been demonstrated, the exact binding site on the Sec61p cytosolic face, however, has not been elucidated so far (Kalies *et al.*, 2005; Ng *et al.*, 2007). Ribosomes and proteasomes bind competitively to the Sec61 channel but to different sites or domains (Ng *et al.*, 2007). Binding is mediated by the ATP-bound form of the 19S RP base (Ng *et al.*, 2007). The exact proteasomal binding site in the Sec61 channel had not been identified prior to my work (Kalies *et al.*, 2005; Ng *et al.*, 2007).

I performed binding experiments with reconstituted proteoliposomes derived from my *sec61* mutants and purified 19S RPs to elucidate which of the amino acid substitutions, S179P or S353C, is responsible for the defect in proteasome binding in *sec61-302* (ref. 3.5.2; Verma *et al.*, 2000; Kalies *et al.*, 2005; Ng *et al.*, 2007). The mutant *sec61-302* was included as a control (Ng *et al.*, 2007). Using reconstituted proteoliposomes rather than RMs treated with puromycin and high salt (PK-RMs) to remove ribosomes was shown in the past to improve specific binding of proteasomes to

yeast membranes and thus the interpretability of results (Kalies *et al.*, 2005).

19S RP binding to reconstituted membranes isolated from *sec61-S353C*, *sec61-S179P/S353C* and *sec61-302* was reduced, while binding to *sec61-S179P* was comparable to wild-type (*SEC61*) (ref. Figure 3.5.2.1; Ng *et al.*, 2007). Affinity of *sec61-S179P/S353C* for 19S RP, however, was higher than of *sec61-S353C* and *sec61-302* membranes (ref. Figure 3.5.2.1). This might be explained by the stabilizing effect of the proline residue in S179P on the Sec61p structure which might counteract the conformational change in Sec61p caused by S353C (ref. 4.1). This, however, does not explain the reduction in proteasome binding in *sec61-302* (Ng *et al.*, 2007). In this mutant proteasome binding was comparable to *sec61-S353C* (ref. Figure 3.5.2.1). Whether the remaining substitutions D168G and F263L have an additive effect on Sec61p's conformation or stability and thus on proteasome binding was not tested, but on their own they do not affect 19S RP binding (ref. *sec61-303*; Ng *et al.*, 2007). My results indicate that the point mutation in *SEC61* leading to the amino acid substitution S353C in the ER lumen, and not S179P on the cytosolic face of the channel, as suspected originally, is responsible for the reduced proteasome binding observed in *sec61-302* (ref. 3.5.2; Ng *et al.*, 2007).

The observation that the amino acid substitution S353C (corresponding point mutation: C1058G) and not S179P (corresponding point mutation: T535C) leads to a reduction in proteasome binding was surprising, as Sec61p's L 7 is located in the ER lumen and thus cannot directly mediate proteasome binding (Wilkinson *et al.*, 1996; van den Berg *et al.*, 2004). The cold-sensitive mutant *sec61-32* (C150Y), which is the *sec61* mutant displaying the most severe ERAD defect known to date, also displays a reduction in proteasome binding, although binding defects were not as pronounced as in *sec61-302* (Pilon *et al.*, 1997; 1998; Ng *et al.*, 2007). The underlying amino acid substitution in *sec61-32*, C150Y, is located towards the lumenal end of TMD 4 and, just as S353C, cannot directly mediate the effect on binding to the 19S RP (Pilon *et al.*, 1997; Ng *et al.*, 2007). Thus, for this mutation it has also been suggested that the point mutation induces a conformational change, which affects 19S RP binding (Ng *et al.*, 2007).

Initially, I anticipated that S179P is responsible for the observed defect in proteasome binding in *sec61-302*, due to its location in cytosolic L 4 of Sec61p (van den Berg *et al.*, 2004; Ng *et al.*, 2007). Moreover, in a previous study, other mutations in lumenal loops of Sec61p had no effect on proteasome binding (ref. *sec61-301*; Ng *et al.*, 2007). Cytosolic L 4, however, has been proposed to act as a hinge during rearrangement of TMD 4 and TMD 5 during channel opening rather than as the direct proteasome binding site (van den Berg *et al.*, 2004; Ng *et al.*, 2007). Further, it has been suggested that S179P could not constitute the entire proteasome binding site due to its proease-insensitivity (Kalies *et al.*, 2005). Conformational rearrangement of Sec61p as a prerequisite for proteasome binding, as such a conformational change could expose the proteasome binding site, has also been suggested (Kalies *et al.*, 2005; Ng *et al.*, 2007). The N-terminus of Sec61p, conserved between *S. cerevisiae* and mammals, has been suggested as a possible proteasome binding site,

which might become more exposed as a result of a conformational change if there were movement around L4 (van den Berg *et al.*, 2004; Kalies *et al.*, 2005; Ng *et al.*, 2007).

My work together with data from Tretter *et al.* (2013) shows that a conformational change hinging on ER-lumenal L 7 of Sec61p is central for generating the 19S RP binding site in Sec61p. It might be possible that Sec61p's L 7, when triggered accordingly by respective binding partners in the ER, is involved in the mediation of a conformational change in Sec61p which might, in turn, make the proteasome binding site on the cytosolic face of the channel accessible. Considering the fact that binding of ribosomes and proteasomes to Sec61p, although to different sites, is competitive, such a conformational change exposing the proteasome binding site during ERAD, and maybe masking that of the ribosome at the same time, could be advantageous for the cell, as a switch from import to export could be regulated according to the cell's needs (Lee *et al.*, 2004b; Kalies *et al.*, 2005). In order to be able to fully understand the nature of proteasome binding to the retrotranslocation channel structural analysis of Sec61p associated with proteasomes would be useful. Recent advances in high resolution EM should make it possible to generate a Sec61 channel-19S RP structure (ref. Voorhees *et al.*, 2014).

The proposed conformational change in Sec61p induced by S353C might only partially expose or even partially masks the proteasome binding site on the cytoplasmic face of Sec61p, since proteasome binding in *sec61-302*, *sec61-S353C* and *sec61-S179P/S353C* is not completely blocked (ref. 3.5.2; Ng *et al.*, 2007). It is also possible that S353C interferes with ER-lumenal factors, such as chaperones, that might trigger channel opening during ERAD.

A comparison between the wild-type (*SEC61*) and *sec61-S353C* protein sequence indicates that the mutation leading to the S353C substitution causes an extension of L7 and a reduction of the helical propensity N-terminal of the substitution and that in this region a portion of the helix is replaced with an extended strand (data not shown; Jones, 1999; Yachdav *et al.*, 2014). A thus extended L7 would push transmembrane helix 7 towards helix 2 thereby leading to lateral gate stabilization in the closed conformation on the lumenal side. It is conceivable that the extended L7 induces shifts in Sec61p affecting cytosolic ends of TMD 2, TMD 7 and TMD 8, altering the cytosolic face of Sec61p (van den Berg *et al.*, 2004, Park *et al.*, 2014). As a result the channel might appear tightly closed from the cytosol rendering it less appealing for the 26 S proteasome to bind to the channel. This, together with the fact that neither S179P nor S353C cause a defect in co- or posttranslational import into the ER indicates that the conformational change is not severe enough to affect ribosome binding or interaction with the Sec63 complex (ref. 3.4; Kalies *et al.*, 1994; Jonhson & van Waes, 1999). This finding is in concordance with data that have shown that ribosomes and proteasomes bind to different sites on Sec61p (Kalies *et al.*, 2005; Ng *et al.*, 2007). It might, however, be interesting to investigate directly whether S353C has an effect on ribosome interaction with the Sec61 channel.

Proteoliposomes derived from a mutant lacking the entire ER-lumenal L 7 and additional 14 residues of TMD 7, *sec61ΔL7*, displayed a slight increase in proteasome binding compared to the

corresponding wild-type (Tretter *et al.*, 2013). This mutant was not defective for growth at 30 °C or 37 °C, but showed an increase in sensitivity towards tunicamycin at 20 °C (Tretter *et al.*, 2013). Tunicamycin sensitivity was even more pronounced than in the ERAD-deficient mutant *sec61-32* (Pilon *et al.*, 1997, 1998; Tretter *et al.*, 2013). From this study it was concluded that L 7, although important for Sec61p function, is not essential (Tretter *et al.*, 2013). Another *sec61* ER L 7 mutant, *sec61Y345H*, identified in a screen for mice (*sec61-Y344H*) prone to diabetes, causes a delay in misfolded protein export from the ER in intact yeast cells (Wheeler & Gekakis, 2012; Tretter *et al.*, 2013). Binding of 19S RP to this mutant was comparable to the wild-type (Tretter *et al.*, 2013).

In mice bearing the homologous substitution, Y344H (*sec61Y344H*) in Sec61p, the mutation in *SEC61* leads the development of pancreatic β-cells with distended ER cisternae suggesting that cell death of β-cells is elicited by defects in ERAD and via a prolonged induction of the UPR (Lloyd *et al.*, 2010). Studies in mammalian cells revealed that this point mutation leads to calcium leakage from the ER through the Sec61 channel (Schäuble *et al.*, 2012). The leakage could not be turned off by BiP suggesting that the point mutation leads to a partial opening of the channel (Schäuble *et al.*, 2012).

A model of the aforementioned Sec61ΔL7p (Sec61p lacking residues 305-371) suggests that the mutant channel is partially open due to a disturbed interaction between transmembrane helix 2b and 7 of Sec61p (Tretter *et al.*, 2013). More precisely, in this mutant Sec61p the lack of ER lumenal L 7 and the lumenal end of TMD 7, leads to a shift in transmembrane helix 2b towards the cytoplasmic face of the ER membrane which therefore cannot be held in place by TMD 7 (Tretter *et al.*, 2013). In Sec61ΔL7p the most C-terminal residue of the gating motif, N302, which sets the hydrophobicity threshold for signal sequence insertion into the translocation channel, is located at the very C-terminal end of TMD 7 (Trueman *et al.*, 2011; Tretter *et al.*, 2013). Due to the excision in Sec61ΔL7p TMD7 and TMD 8 are only connected by 2 residues, which in turn applies tension onto N302 thereby weakening the hydrogen bonds to its partners in the gating motif resulting in a partial opening of the gate (Tretter *et al.*, 2013). The observed slight increase in proteasome affinity in this mutant might be explained by the partially open Sec61 channel (Tretter *et al.*, 2013).

Preliminary data from PEGylation of the cytosolic domains of Sec61p analyzing possible conformational changes in *sec61* mutants indeed indicated that S353C in *sec61-302* and *sec61-S353C* leads to a conformational change in Sec61p, while Sec61-S179Pp seemed to display a conformation comparable to wild-type Sec61p (ref. 3.9; *sec61-S179P/S353C* was excluded from the experiments). Interestingly, in this assay another mutant with a point mutation in the ER-lumenal L 7, *sec61-3* (G341E), also seemed to adopt a conformation that deviates from wild-type Sec61p (ref. Figure 3.9.2). Due to technical limitations the data from this experiment, however, were not significant enough to be conclusive. During PEGylation assays Sec61-3p seemed to be unstable as the detected signal was significantly weaker compared to the remaining mutant Sec61ps analyzed (ref. 3.9). Sec61p instability in *sec61-3* (G341E) as wells as in *sec61-2* (G213D) was described in

the past (Stirling *et al.*, 1992; Sommer & Jentsch, 1993; Biederer *et al.*, 1996). The observed translocation defects and temperature sensitivities in these mutants are explained by the degradation of the respective mutant Sec61p proteins (Stirling *et al.*, 1992; Sommer & Jentsch, 1993; Biederer *et al.*, 1996).

Although the extracytoplasmic loops of Sec61p are less well conserved than the cytoplasmic loops, the ER-lumenal L 7 of Sec61p contains an array of residues, which are highly conserved among various organisms (*S. cerevisiae*, *S. pompe*, *C. albicans*, *Dictyostelium discoideum*, *C. elegans*, fruit fly, zebrafish, xenopus, mouse, rat, orangutan and human). A comparison of Sec61p protein sequence from *S. cerevisiae* with those of various orthologues shows that especially in the region between residue 340 and residue 353 there is a high density of highly conserved residues (data not shown). The importance of individual highly conserved residues for protein function is seen in mutants such as *sec61-3* (G341E) and the tyrosine in the di-tyrosine motif in *sec61Y345H*, which when mutated have a negative impact on protein function (Stirling *et al.*, 1992; Sommer & Jentsch, 1993; Lloyd *et al.*, 2010; Wheeler & Gekakis, 2012; Tretter *et al.*, 2013). The serine residue at position 353 of Sec61p in *S. cerevisiae* is not as highly conserved. At the corresponding position in Sec61p of organisms such as *C. elegans*, fruit fly, zebrafish, Xenopus, mouse, rat, orangutan and human there is a glycine residue instead (G352). This glycine residue, however, is conserved among the organisms mentioned. But both are small residues and allow a certain flexibility of L 7 in this position, which might be altered in S353C. In addition, the cysteine in the ER lumen might be prone to formation of disufide bonds, which would keep L 7 in position. That mobility around L 7 is crucial for Sec61 channel opening has been shown clearly in a recent structural study from the Rapoport lab (Park *et al.*, 2013).

4.4 CHARACTERIZATION OF UPR-ACTIVATION IN THE *SEC61* MUTANTS

Since ERAD (ref. 1.6) and the UPR (ref. 1.4) are tightly linked pathways, monitoring the UPR can give first hints as to whether ER stress is caused in the respective *sec61* mutants due to dysfunctional Sec61p (Friedlander *et al.*, 2000; Travers *et al.*, 2000).

In none of the *sec61* mutants I investigated, *sec61-S179P*, *sec61-S353C*, *sec61-S179P/S353C*, *sec61-302* and *sec61-303*, the UPR was induced (Figures 3.6.1, 3.6.2 and 3.6.3). This is consistent with the modest effects on ERAD in intact cells (ref. 3.7 and 4.5).

Initially, I monitored UPR induction with a quantitative liquid β-galactosidase assay after transforming the strains with a reporter plasmid containing the *lacZ* gene under the control of a *UPRE* (ref. 3.6.1). Colorimetric measurement of β-galactosidase activity revealed that none of the *sec61* mutants (*sec61-302*, *sec61-303*, *sec61-S179P*, *sec61-S353C* and *sec61-S179P/S353C*) displayed an elevated UPR when compared to the corresponding wild-type (*SEC61*) (ref. Figure 3.6.1.1). There

were also no differences between mutants and wild-type when the UPR inducer tunicamycin was added (ref. Figure 3.6.1.1). The control strains *Δder1* (corresponding wild-type *DER1*) and *sec61-3*, which was isolated via a UPR screen, displayed elevated β-galactosidase activities even in the absence of tunicamycin (ref. Figure 3.6.1.1; Sommer & Jentsch, 1993; Knop *et al.*, 1996; Zhou & Schekman, 1999). When tunicamycin was added to these strains UPR induction was even more pronounced (ref. Figure 3.6.1.1).

I confirmed these results investigating *HAC1* mRNA splicing (ref. 3.6.2; Mori *et al.*, 2010). I could not detect spliced *HAC1* mRNA (*HAC1*^{i}) in any of my *sec61* mutants under normal growth conditions in the absence of tunicamycin (ref. Figure 3.6.2.1). Only in the controls *Δder1* and *sec61-3* spliced *HAC1* mRNA was present in the absence of tunicamycin (ref. Figure 3.6.2.1). The effect was even more pronounced in the presence of tunicamycin (ref. Figure 3.6.2.1). In addition, in *sec61-3* I investigated *HAC1* mRNA at the restrictive temperature (17 °C) and found it to be stronger compared to splicing at 30 °C which, again, was expected (ref. Figure 3.6.2.1; Sommer & Jentsch, 1993). Upon addition of tunicamycin, the UPR was induced resulting in the detection of the spliced *HAC1*^{i} mRNA species in all strains as expected (ref. Figure 3.6.2.1).

Results from investigating synthetic effects of my *sec61* mutants with *Δire1* were in concordance with those from the *HAC1* mRNA splice assay and the β-galactosidase assay (ref. 3.6.3). Since cells lacking *IRE1* are hypersensitive to the accumulation of misfolded proteins in the ER, disturbed protein retrotranslocation due to point mutations in *SEC61* should result in a growth defect (Shamu & Walter, 1996). In the absence of tunicamycin none of the double mutants (*Δire1 sec61-302*, *Δire1 sec61-303*, *Δire1 sec61-S179P*, *Δire1 sec61-S353C* and *Δire1 sec61-S179P/S353C*) displayed growth defects at any of the temperatures tested compared to the wild-type (*SEC61*) (ref. Figure 3.6.3.1). Upon addition of tunicamycin, growth was severely compromised in all strains, i.e. none of the strains were viable (ref. Figure 3.6.3.1). As the tunicamycin concentration used in this experiment very likely was too high to detect growth or even differences in tunicamycin sensitivity in the double mutants the experiment would have to be repeated using lower tunicamycin concentrations.

Data from the UPR assays suggest that, although a reduction in proteasome binding was detected in the S353C-containing mutants, the observed reduction in proteasome binding does not, under the conditions tested, result in significant accumulation of misfolded proteins in the ER (ref. Figure 3.5.2.1, 3.6.1.1, 3.6.2.1 and 3.6.3.1). One explanation for this observation is that the high concentration of proteasomes in the cytosol sufficiently compensates for the proteasome binding defect in intact cells. This was confirmed by my *in vitro* experiments (ref. 4.6).

4.5 ERAD OF SOLUBLE AND TRANSMEMBRANE SUBSTRATES IN THE *SEC61* MUTANTS

I investigated the effect of my new *sec61* mutants on ERAD in intact cells with pulse-chase experiments using the ERAD-L substrates ΔgpαF, CPY* and KWW and the ERAD-C substrate Ste6-166p (ref. 3.7.1, 3.7.2 and 3.7.3; McCracken & Brodsky, 1996; Loayza *et al.*, 1998; Vashist *et al.*, 2001; Vashist & Ng, 2004). I also included *sec61-302* and *sec61-303* in the analyses, as ERAD had not been investigated in theses mutants (Ng *et al.*, 2007). Sec61p has been suggested to be mainly required in ERAD-L, but this may be an effect of the *sec61* mutants selected to test Sec61p-dependence of specific substrates (Pilon *et al.*, 1998; Willer *et al.*, 2008; Schäfer & Wolf, 2009). An involvement of Sec61p in ERAD-C has been suggested, as Sec61p could be isolated with a complex containing Doa10p, but has not been explicitely demonstrated (Stolz *et al.*, 2010). Therefore, I also investigated degradation of the ERAD-C substrate, Ste6-166p (ref. 3.7.4; Vashist & Ng, 2004).

The glycosylated ERAD-L substrates KWW and CPY* employ the same chaperone equipment and other requirements during ERAD, which might explain why degradation of these ERAD-L substrates is not affected in the same way as degradation of ΔgpαF (Vashist & Ng, 2004). In the soluble CPY* a point mutation (G255R) leads to protein misfolding and rapid ERAD (Knop *et al.*, 1996). The chimeric single-spanning transmembrane ERAD substrate KWW, containing a lesion in its ER-lumenal domain, has been shown to be a bonafide ERAD substrate (Vashist & Ng, 2004). Both substrates require the ER-to-Golgi transport for degradation as well as BiP, Cue1p, Hrd1p and Der1p (Vashist *et al.*, 2001; Vashist & Ng, 2004). While for CPY*, which is imported into the ER posttranslationally, the primary driver for export from the ER is Cdc48p, for KWW the main driving force for export from the ER is not known (Vashist *et al.*, 2001; Vashist & Ng, 2004).

Among the ERAD-L substrates tested the unglycosylated ΔgpαF, whose precursor pΔgpαF is translocated into the ER posttranslationally, takes in a distinct role (McCracken & Brodsky, 1996). In this substrate N-glycosylation sites in the proregion were removed which leads to misfolding (McCracken & Brodsky, 1996). The requirements for degradation of ΔgpαF differ from those of CPY* and KWW (Vashist et al., 2001; Vashist & Ng, 2004). Not only is this ERAD-L substrate degraded fastest, it also does not require the ER-to-Golgi transport for degradation, both *in vitro* and *in vivo* (Caplan *et al.*, 1991; McCracken & Brodsky, 1996). ERAD of ΔgpαF, despite the lack of N-linked oligosaccharides, depends on Cne1p, the yeast homologue of mammalian calnexin (McCracken & Brodsky, 1996). In addition to its role as an ER lectin, calnexin displays glycan-independent chaperone functions (Swanton *et al.*, 2003; Fontanini et al., 2004; Helenius & Aebi, 2004). For Cne1p a function similar to the mammalian calnexin has been proposed *in vitro* (Xu *et al.*, 2004). As opposed to most other ERAD substrates investigated so far, degradation of ΔgpαF does not require ubiquitination but export from the ER depends on the 19S RP (McCracken & Brodsky, 1996; Werner *et al.*, 1996; Lee *et al.*, 2004a). Degradation of ΔgpαF also depends on BiP (Vashist *et al.*, 2001;

Vashist & Ng, 2004). Thus, it has been suggested that for ΔgpαF a distinct ER checkpoint might exist (Vashist & Ng, 2004).

The ERAD-C substrate Ste6-166p (Gln1249X leads to truncation of 42 aa), mutant a-factor transporter in yeast, has been suggested to be retained in the ER (Berkower & Michaelis, 1996; Loayza *et al.*, 1998). It is also highly unstable and rapidly degraded (Loayza *et al.*, 1998). Degradation of this ERAD substrate requires the UPS (ref. 1.5) (Loayza *et al.*, 1998; Vashist *et al.*, 2001). It is not clear how or whether Ste6-166p is extracted from the ER membrane for degradation by the proteasome (Loayza *et al.*, 1998). Ste6-166p is degraded independently of Hrd1p, Der1p and BiP, but requires Doa10p for degradation (Loayza *et al.*, 1998; Vashist *et al.*, 2001; Vashist & Ng, 2004). Degradation of mutants Ste6p has been suggested to be independent of Sec61p, although this could also be due to the *sec61* background used in the experiments (Huyer *et al.*, 2004b). In a previous study an alternative pathway for mutant Ste6p degradation was suggested (Huyer *et al.*, 2004a). Ste6-166p was shown to induce the formation of so-called ERACs (ER-associated compartments) from which it was subjected to ERAD without entering the secretory pathway (Huyer *et al.*, 2004a). In a more recent study it was shown that mutant Ste6p is extracted from the ER membrane and that degradation requires polyubiquitination, Cdc48p and ATP (Nakatsukasa *et al.*, 2008).

When I investigated degradation efficiencies of the ERAD-L substrates in the *sec61* mutants, I found that ERAD of Cdc48p-dependent substrate CPY* and the chimeric substrate KWW, was not affected in any of the *sec61* mutants (ref. Figure 3.7.1.1 and 3.7.3.1; Finger *et al.*, 1993; Vashist et al., 2001; Vashist & Ng et al., 2004). ERAD of ΔgpαF on the other hand was moderately affected in the *sec61-302* derivatives (ref. Figure 3.7.2.1).

Degradation of CPY* and KWW was barely affected in the *sec61* mutants (ref. Figure 3.7.1.1 and Figure 3.7.3.1). The half-life of CPY* in the wild-type ($t_{1/2}$ = 21 min) was in agreement with published data (Knop *et al.*, 1996). Degradation efficiencies in the *sec61* mutants were also comparable to the wild-type, except *sec61-302* which displayed slightly slower degradation of the substrate ($t_{1/2}$ ~ 24 min) (ref. 3.7.1; Ng *et al.*, 1996). For KWW, the half-life in the wild-type ($t_{1/2}$ ~ 33 min) was close to the published data ($t_{1/2}$ ~ 35 min) (Vashist & Ng, 2004). The degradation kinetics of all *sec61* mutants was similar ($t_{1/2}$ ~ 38 min) but slightly slower than the wild-type (ref. Figure 3.7.3.1).

The degradation of ΔgpαF was more variable in the *sec61* mutants I investigated (ref. Figure 3.7.2.1). While in *sec61-303* ($t_{1/2}$ ~ 14 min) ERAD degradation of ΔgpαF was not affected, in the *sec61-302* derivatives ($t_{1/2}$ ~ 18 min) degradation of the substrate was slower than in the wild-type ($t_{1/2}$ ~ 13 min) (ref. Figure 3.7.2.1). Especially in *sec61-S353C* turnover of ΔgpαF was affected ($t_{1/2}$ ~ 20 min). I also observed a delay during degradation initiation for ΔgpαF (ref. Figure 3.7.2.1). CPY* and KWW have identical requirements for ERAD, which are distinctive from those for ΔgpαF ERAD. This might explain the difference between these substrates and ΔgpαF with respect to turnover in my *sec61*

mutants (Vashist *et al.*, 2001; Vashist & Ng, 2004).

Degradation of the ERAD-C substrate Ste6-166p was not affected in the *sec61* mutants (ref. Figure 3.7.4.1). For Ste6-166p, however, transformation rates were poor especially for *sec61-S353C* and *sec61-S179P/S353C*. This might explain why the signal for Ste6-166p in *sec61-S353C* and *sec61-S179P/S353C* was weaker compared to the remaining strains, which complicated the interpretation of results (ref. Figure 3.7.4.1). Due to technical difficulties I was not able to repeat the experiment and thus to elucidate whether in the two mutants Ste6-166p signal intensities were weaker due to technical issues or whether the observed effects were mutant-specific defects in the biogenesis of polytopic transmembrane proteins (ref. Figure 3.7.4.1). From the data I did obtain, I concluded that ERAD of this transmembrane ERAD-C substrate was also undisturbed in *sec61S353C* and *sec61-S179P/S353C* mutants (ref. Figure 3.7.4.1).

The results show that degradation of the ERAD-L substrate ΔgpαF, whose export from the ER depends on the 19S RP, is affected the most in *sec61-S353C* (ref. Figure 3.7.3.1). This suggests that the 19S RP-Sec61 channel interaction is important for ERAD. The fact that in *sec61-302* and *sec61-S179P/S353C* degradation of ΔgpαF is less affected supports the idea that, although in these mutants proteasome binding (ref. 3.5.2) is also reduced, the substitution S179P counteracts the effect of S353C on the conformation of Sec61p (ref. 4.4 and Figure 3.5.2.1 and Figure 3.7.3.1).

4.6 ERAD OF ΔGPαF IN A CELL-FREE SYSTEM

The limiting step for export of ΔgpαF from the ER is 19S RP binding to the Sec61 channel (McCracken & Brodsky, 1996; Lee *et al.*, 2004a). In intact cells the effect of ΔgpαF degradation was subtle, as here the high proteasome concentration in the cytosol would compensate for a reduction in 19S RP affinity for mutant Sec61 channel, as in *sec61-S353C* (ref. Figure 3.7.2.1 and 4.5; Kalies *et al.*, 2005; Russell *et al.*, 1999).

ATP and proteasomes are the minimum requirements for *in vitro* ERAD of ΔgpαF (Werner *et al.*, 1996; McCracken & Brodsky, 1996; Verma *et al.*, 2000; Lee *et al.*, 2004b). When I analyzed ATP-dependent ΔgpαF retrotranslocation in a cell-free system using membranes derived from my *sec61* mutants I found a delay in ERAD of ΔgpαF in the *sec61* mutants containing the S353C substitution when proteasomes were limiting (ref. Figure 3.8.2.3; McCracken & Brodsky, 1996). Degradation kinetics of ΔgpαF in the ERAD-deficient *sec61-3* mutant (G341E), which I used as a control, because the underlying point mutation is also located in the ER-lumenal L 7, were in concordance with previous results (Stirling *et al.*, 1992; Sommer & Jentsch, 1993; Pilon *et al.*, 1997, 1998).

Usually, in *in vitro* assays for ER export of ΔgpαF a cytosol concentration of 3 mg/ml is used in which the proteasome concentration is still in the saturating range for the wild-type Sec61 channel (McCracken & Brodsky, 1996; Pilon *et al.*, 1997). The effects using 3 mg/ml cytosol in the *in vitro*

assay were comparable to those in intact cells (ref. Figure 3.7.2.1, Figure 3.8.2.2 and 4.5). In the S353C mutants the reduction in affinity of the Sec61 channel for the 19S RP would be partially compensated by the high proteasome concentration in the cytosol in intact cells and *in vitro* using 3 mg/ml cytosol (McCracken & Brodsky, 1996; Russell *et al.*, 1999; Kalies *et al.*, 2005).

Using a non-saturating concentration of 1 mg/ml cytosol, I observed a delay in ERAD of Δgpαf for the mutants with reduced 19S RP affinity *sec61-302*, *sec61-S353C* and *sec61-S179P/S353C* ($t_{1/2}$ ~ 45 min) compared to the wild-type ($t_{1/2}$ ~ 23 min), which, however, was not as severe as for *sec61-3*, for which export was severely reduced, or *sec61-32* (not tested here) (ref. Figure 3.8.2.3; Stirling *et al.*, 1992; Sommer & Jentsch, 1993; Pilon *et al.*, 1997, 1998). Although export was delayed in my mutants it was not fully compromised. Since *sec61* mutants displaying a reduction in proteasome binding also display a delay in Δgpαf ERAD, my results indicate that Sec61 channel interaction with the 19S RP is important for the dislocation of Δgpαf. The fact that export of Δgpαf from *sec61-S17P/S353C* membranes was affected to the same extent as for *sec61-S353C*, although 19S RP binding was only moderately reduced in this mutant, implies that 19S RP binding to the Sec61 channel, apart from requiring a specific conformation of Sec61p on its cytoplasmic face, also induces a conformational change in the channel necessary for promoting export of misfolded proteins (ref. Figure 3.8.2.3; Vorhees *et al.*, 2014). This would explain that while in the double mutant the amino acid substitution S179P might counteract the destabilizing effect of S353C on Sec61p conformation and thus on proteasome binding, S353C would still inhibit the initial steps for export (ref. 4.4). As the ER-lumenal L 7 might also promote export and act as a binding site of ER-lumenal binding partners required during retrotranslocation, such as ER chaperones, it seems plausible that in *sec61-S179P/S353C* export is still negatively affected while 19S RP binding is only mildly reduced (ref. 3.5.2 and 3.8.2). From my data it is evident that in intact cells the proteasome concentration is sufficient enough to compensate 19S RP binding defects especially in the *sec61-S353C* mutant (ref. 4.3 and 4.5). Therefore, in order to investigate the importance of the 19S RP-Sec61p interaction in ERAD one would have to express *sec61-S353C* with reduced proteasome concentration and test UPR and various ERAD substrates.

Thus, the S353C substitution could not only cause a conformational change in Sec61p that has a negative effect on proteasome binding, it could also impair a conformational change or movement of individual domains in Sec61p which might be necessary for the exposure of the proteasome binding site and for priming of misfolded protein export from the ER.

Another explanation for the observed effects in *sec61-302*, *sec61-S353C* and *sec61-S179P/S353C* might be that a disulfide bond is formed via the cysteine (S353C) with PDI, which is involved in export of Δgpαf, causing the delay in export (Gillece *et al.*, 1999). Although I prefer the first scenario, at this point both scenarios are speculative.

A role of ER-lumenal L 7 during proteasome binding and retrotranslocation would be in addition to its important role during translocon gating as has been demonstrated by Trueman *et al.* (2011). In this

study the effects of *sec61* L7 mutants on Sec61 channel protein function were investigated. The authors found that specific insertion mutations in L 7 caused a delay in channel gating resulting in mostly posttranslational translocation defects (Trueman *et al.*, 2011). Channel gating requires a concerted movement of TMD 7 and TMD 8, a process that is disturbed in the *sec61* L7 insertion mutants (Trueman *et al.*, 2011; Park *et al.*, 2014). The mutations in ER-lumenal L 7 have been proposed to cause breakage of side-chain contacts linking TMD 7 and TMD 8 via the minihelix in L 7, which would lead to an uncoordinated movement of TMD 7 and TMD8 during translocon gating (van den Berg *et al.*, 2004; Trueman *et al.*, 2011). This would result in delayed signal sequence insertion into the signal sequence binding site (Trueman *et al.*, 2011). One of the initial *sec61* L7 mutants in the Trueman study, *sec61* E345-HA, in which the insertion is located eight residues N-terminal of the residue S353, was not defective in import of pCPY into the ER (Trueman *et al.*, 2011). Among the other *sec61* L7 mutants *sec61* I320-HA and *sec61* S340-HA displayed severe defects in CPY translocation (Trueman *et al.*, 2011). This further confirms that specific mutations in ER-lumenal L 7 can result in very different phenotypes.

4.7 CONCLUSION

In this study, by generating *sec61* mutants containing individual point mutations, I was able to identify that the amino acid substitution S353C, located in the ER-lumenal L 7 of Sec61p leads to a reduction in proteasome binding in the mutant *sec61-302* (D168G, S179P, F263L and S353C) (Ng *et al.*, 2007). The respective *sec61* mutants were all viable and showed no defects in growth or co- or posttranslational protein import into the ER, which suggests that import defects in *sec61-302* and *sec61-303* (D168G and F263L), which share two of the same point mutations, can be attributed to the remaining point mutations leading to the amino acid substitutions D168G and F263L (Ng *et al.*, 2007). In the mutants I generated for this study the UPR was not induced, indicating that protein homeostasis was not disturbed due to the amino acid substitutions. At the same time I found that ERAD of the mutant alpha factor precursor, Δgpαf, was disturbed in the *sec61* mutants containing the S353C substitution *in vitro* and *in vivo*. ERAD of other ERAD-L substrates and one ERAD-C substrate was not or barely delayed in the initial phases of degradation.

Although data from this study do not reveal the exact proteasome binding site on the cytoplasmic face of Sec61p, they indicate that the conformation of Sec61p during ERAD determines the efficiency of proteasome binding. My work indicates that the amino acid substitution S353C leads to or prevents a conformational change in Sec61p, hinging on ER-lumenal L 7, which affects the proteasome binding site on the cytoplasmic face of the protein and that the 19S RP/Sec61 channel interaction is important for export of a subset of ERAD substrates. This suggests that a specific conformation of Sec61p is required for efficient interaction with the proteasome as has been speculated previously (Kalies *et al.*, 2005; Ng *et al.*, 2007; Tretter *et al.*, 2013). My results, together

with those from previous work in our group and by others, stress that the large ER-lumenal lL 7 of Sec61p is involved in ERAD (Wheeler & Gekakis, 2012; Tretter *et al.*, 2013). Whether L7 functions as a binding site for chaperone/substrate complexes as a prerequisite for retrotranslocation channel opening or proteasome binding still requires elucidation. Nevertheless, my work identifies a second mutation in Sec61p L 7 which is ERAD-specific, confirming Sec61p's direct role as part of the ERAD machinery.

5 REFERENCES

Abell BM, Pool MR, Schlenker O, Sinning I & High S (2004) Signal recognition particle mediates post-translational targeting in eukaryotes. *EMBO J* **23**:2755-2764.

Abell BM, Rabu C, Leznicki P, Young JC & High S (2007) Post-translational integration of tail-anchored proteins is facilitated by defined molecular chaperones. *J Cell Sci* **120**:1743-1751.

Aebi M, Bernasconi R, Clerc S & Molinari M (2010) N-glycan structures: recognition and processing in the ER. *Trends Biochem. Sci*. **35(2)**:74-82.

Akiyama Y & Ito K (1987) Topology analysis of the SecY protein, an integral membrane protein involved in protein export in *Escherichia coli*. *EMBO J* **6(11)**:3465-3470.

Alder NN, Shen Y, Brodsky JL, Hendershot LM & Johnson AE (2005) The molecular mechanism underlying BiP-mediated gating of the Sec61 translocon of the endoplasmic reticulum. *J Cell Biol* **168**:389-399.

Allan BB, Moyer BD & Balch WE (2000) Rab1 recruitment of p115 into a *cis*-SNARE complex: programming budding COPII vesicles for fusion. *Science* **289**:444-448.

Allen, JF (2003) The function of genomes in bioenergetic organelles. *Philos Trans R Soc Lond B Biol Sci* **358**:19-37.

Amaya Y, Nakano A, Ito K & Mori M (1990) Isolation of a yeast gene, SRH1, that encodes a homologue of the 54K subunit of mammalian signal recognition particle. *J Biochem* **107**:457-463.

Anderson DJ, Walter P & Blobel G (1982) Signal recognition protein is required for integration of actelycholine receptor delta subunit, a transmembrane glycoprotein, into the endoplasmic reticulum membrane. *J Cell Biol* **93**:501-506.

Andrews DW & Johnson AE (1996) The translocon: more than a hole in the ER membrane? *Trends Biochem Sci* **21**:365-369.

Andrews DW, Lauffer L, Walter P &Lingapappa VR (1989) Evidence for a two-step mechanism involved in assembly of functional signal recognition particle receptor. *J Cell Biol* **108**: 797-810.

Aoe T, Lee AJ, van Donselaar E, Peters PJ & Hsu VW (1998) Modulation of intracellular transport by transported proteins: insights from regulation of COPI-mediated transport. *Proc Natl Acad Sci USA* **95**:1624-1629.

Appenzeller-Herzog C & Ellgaard L (2008) The human PDI family: versatility packed into a single fold. *Biochem Biophys Acta* **1783**:535-548.

Appenzeller-Herzog C & Hauri HP (2006) The ER-Golgi intermediate compartment (ERGIC): in search of its identity and function. *J Cell Sci* **119**:2173-2183.

Apweiler R, Hermjakob H & Sharon N (1999) On the frequency of protein glycosylation, as deduced from analysis of the SWISS-PROT database. *Biochim Biophys Acta* **1473**:4-8.

Aragon T, van Anken E, Pincus D, Serafimova IM, Korennykh CA & Walter O (2009) Messenger RNA targeting to endoplasmic reticulum stress signalling sites. *Nature* **457(7230)**:736-740.

Araki E, Oyadomari S & Mori M (2003) Endoplasmic reticulum stress and diabetes mellitus. *Intern Med* 42:7-14.

Arendt CS & Hochstrasser M (1997) Identification of the yeast 20S proteasome catalytic centers and subunit interactions required for active-site formation. *Proc Natl Acad Sci USA* **94**:7156-7161.

Arvan P, Zhao X, Ramos-Castaneda J & Chang A (2002) Secretory pathway quality control operating in Golgi, plasmalemmal, and endosomal systems. *Traffic* **3**:771-780.

Babbitt SE, Kiss A, Deffenbaugh AE, Chang YH, Bailly E, Erdjument-Bromage H, Tempst P, Buranda T, Sklar LA, Baumler J, Gogol E & Skowyra D (2005) ATP hydrolysis-dependent disassembly of the 26S proteasome is part of the catalytic cycle. *Cell* **121**:553-565.

Baboshina OV & Haas AL (1996) Novel multiubiquitin chain linkages catalyzed by the conjugating enzymes E2EPF and RAD6 are recognized by 26S proteasome subunit 5. *J Biol Chem* **271(5)**:2823-2831.

Bacher G, Lütcke H, Jungnickel B, Rapoport TA & Dobberstein B (1996) Regulation by the ribosome of the GTPase of the signal-recognition particle during protein targeting. *Nature* **381**.248-251.

Bacher G, Pool M & Dobberstein B (1999) The Ribosome Regulates the Gtpase of the β-Subunit of the Signal Recognition Particle Receptor. *J Cell Biol* **146(4)**:723-730.

Baker D, Hicke L, Rexach M, Schleyer M & Schekman R (1988) Reconstitution of *SEC* gene product-dependent intercompartmental protein transport. *Cell* **54**:335-344.

Bange G, Wild K & Sinning I (2007) Protein Translocation: Checkpoint Role for SRP GTPase Activation. *Curr Biol* **17(22)**: R980-R982.

Bannykh SI & Balch WE (1997) Membrane dynamics at the endoplasmic reticulum-Golgi interface. *J Cell Biol* **138(1)**:1-4.

Barbin L, Eisele F, Santt O & Wolf DH (2010) The Cdc48-Ufd1-Npl4 complex is central in ubiquitin-proteasome triggered catabolite degradation of fructose-1,6- bisphosphatase. *Biochem Biophys Res Commun* **394**:335-341.

Bard F & Malhotra V (**2006).** The formation of TGN-to-plasma-membrane transport carriers. *Annu Rev Cell Dev Biol* **22**:439-455.

Barlowe C (2000) Traffic COPs of the early secretory pathway. *Traffic* **1**:371-377.

Batey RT, Rambo RP, Lucast L, Rha B & Doudna JA (2000) Crystal structure of the ribonucleoprotein core of the signal recognition particle. *Science* **287**:1232-1238.

Baumeister W, Walz J, Zuhl F & Seemuller E (1998) The proteasome: paradigm of a self-compartmentalizing protease. *Cell* **92**:367-380.

Bayer P, Arndt A, Metzger S, Mahajan R, Melchior F, Jaenicke R & Becker J (1998) Structure determination of the small ubiquitin-related modifier SUMO-1. *J Mol Biol* **280(2)**:275-286.

Bays NW, Gardner RG, Seelig LP, Joazeiro CA & Hampton RY (2001) Hrd1p/Der3p is a membrane-anchored ubiquitin ligase required for ER-associated degradation. *Nat Cell Biol* **3(1)**:24-29.

Becker T, Bhushan S, Jarasch A, Armache JP, Funes S, Jossinet F, Gumbart J, Mielke T, Berninghausen O, Schulten K, Westhof E, Gilmore R, Mandon EC & Beckmann R (2009) Structure of monomeric yeast and mammalian Sec61 complexes interacting with the translating ribosome. *Science* **32:**1369-1373.

Becker B & Melkonian M (1996) The secretory pathway of protists: spatial and functional organization and evolution. *Microbiol Rev* **60(4)**:697-721.

Beckmann R, Bubeck D, Grassucci R, Penczek P, Verschoor A, Blobel G & Frank J (1997) Alignment of conduits for the nascent polypeptide chain in the ribosome-Sec61 complex. *Science* **278**:2123-2126.

Beckmann R, Spahn CA, Eswar N, Hemers J, Penczek PA, Sali A, Frank J & Blobel G (2001) Architecture of the protein-conducting channel associated with the translating 80S ribosome. *Cell* **107(3)**:361-372.

Bedford L, Paine S, Sheppard PW, Mayer RJ & Roelofs J (2010) Assembly, structure and function of the 26S proteasome. *Trends Cell Biol* **20(7)**:391-401.

Beh CT and Rose MD (1995) Two redundant systems maintain levels of resident proteins within the yeast endoplasmic reticulum. *Proc Natl Acad Sci USA* **92(21)**:9820-9823.

Beilharz T, Egan B, Silver PA, Hofmann K & Lithgow T (2003) Bipartite signals mediate subcellular targeting of tail-anchored membrane proteins in *Saccharomyces cerevisiae*. *J Biol Chem* **278**:8219-8223.

Benitez EM, Stolz A & Wolf DH (2011) Yos9, a control protein for misfolded glycosylated and non-glycosylated proteins in ERAD. *FEBS Lett* **585**:3015-3019.

Berkower C, Loayza D & Michaelis S (1994) Metabolic instability and constitutive endocytosis of *STE6*, the a-factor transporter of *Saccharomyces cerevisiae*. *Mol Biol Cell* **5**:1185-1198.

Berkower C & Michaelis S (1996) ATP binding cassette proteins in yeast. In: Membrane Protein Transport, ed. S. Rothman, Greenwich, CT: JAI Press:231-277.

Bernales S, Papa FR & Walter P (2006) Intracellular signaling by the unfolded protein response. *Annu Rev Cell Dev Biol* **22**:487-508.

Bernardi KM, Forster ML, Lencer WI & Tsai B (2008) Derlin-1 facilitates the retro-translocation of cholera toxin. *Mol Biol Cell* **3**:877-884.

Bernstein HD, Poritz MA, Strub K, Hoben PJ, Brenner S & Walter P (1989) Model for signal sequence recognition from amino-acid sequence of 54 kDa subunit of signal recognition particle. *Nature* **340**:482-486.

Bertolotti A, Zhang Y, Hendershot LM, Harding HP & Ron D (2000) Dynamic interaction of BiP and ER stress transducers in the unfolded-protein response. *Nat Cell Biol* **2**:326-332.

Beyer A (1997) Sequence analysis of the AAA protein family. *Protein Sci* **6**:2043-2058.

Bhamidipati A, Denic V, Quan EM & Weissman JS (2005) Exploration of the topological requirements of ERAD identifies Yos9p as a lectin sensor of misfolded glycoproteins in the ER lumen. *Mol Cell* **19**:741-751.

Biederer T, Volkwein C & Sommer T (1996) Degradation of subunits of the Sec61p complex, an

integral component of the ER membrane, by the ubiquitin-proteasome pathway. *EMBO J* **15**:2069-2076.

Biederer T, Volkwein C & Sommer T (1997) Role of Cue1p in ubiquitination and degradation at the ER surface*. Science* **278**:1806-1809.

Bird P, Gething M-J & Sambrook J (1987) Translocation in yeast and mammalian cells: not all signal sequences are functionally equivalent. *J Cell Biol* **105(6)**:2905-2914.

Birnboim HC, Doly J (1979) A rapid alkaline extraction procedure for screening recombinant plasmid DNA. *Nucleic Acids Res* **7**:1513-1523.

Blobel G (1980) Intracellular protein topogenesis. *Proc Natl Acad Sci USA* **77 (3)**:1496-1500.

Blobel G & Dobberstein B (1975a) Transfer of proteins across membranes: I. Presence of proteolytically processed and unprocessed nascent immunoglobulin light chains on membrane-bound ribosomes of murine myeloma, *J Cell Biol*. **67**:835-851.

Blobel G & Dobberstein B (1975b) Transfer of proteins across membranes: II. Reconstitution of functional rough microsomes from heterologous components, *J Cell Biol* **67**:852-862.

Blobel G & Sabatini DD (1971) Ribosome-membrane interaction in eukaryotic cells. *Biomembranes* **2**:193-195.

Böhni PC, Deshaies RJ & Schekman R (1988) *SEC11* is required for signal peptide processing and yeast cell growth. *J Cell Biol* **106**:1035-1042.

Bohn S, Beck F, Sakata E, Walzthoeni T, Beck M, Aebersold R, Förster F, Baumeister W & Nickell W (2010) Structure of the 26S proteasome from *Schizosaccharomyces pombe* at subnanometer resolution. *Proc Natl Acad Sci USA* **107**:20992-20997.

Bonifacino JS & Klausner RD (1994) Degradation of proteins retained in the endoplasmic reticulum. *In*: *Cellular Proteolytic Systems* (Ciechanover A & Schwartz AL eds) *Wiley-Liss Inc.,* New York:137-160.

Bordallo J, Plemper RK, Finger A & Wolf DH (1998) Der3p/Hrd1p is required for endoplasmic reticulum-associated degradation of misfolded lumenal and integral membrane proteins. *Mol Biol Cell* **9(1)**:209-222.

Borgese N, Brambillasca S, Soffientini P, Yabal M & Makarow M (2003a) Biogenesis of tail-anchored proteins. *Biochem Soc Trans* **31**:1238-1242.

Borgese N, Colombo S & Pedrazzini E (2003) The tale of tail-anchored proteins. *J Cell Biol* **161**:1013–1019.

Braakman I & Bulleid NJ (2011) Protein folding and modification in the mammalian endoplasmic reticulum. *Annu Rev Biochem* **80**:71-99.

Braakman I, Helenius J & Helenius A (1992) Manipulating disulfide bond formation and protein folding in the endoplasmic reticulum. *EMBO J* **11 (5)**:1717-1722.

Bradford MM (1976) A rapid and sensitive method for the quantitation of microgram quantities of protein utilizing the principle of protein-dye binding. *Anal Biochem* **72**:248-254.

Brake AJ, Julius DJ & Thorner J (1983) A functional prepro-alpha-factor gene in *Saccharomyces*

yeasts can contain three, four, or five repeats of the mature pheromone sequence. *Mol Cell Biol* **3**:1440-1450.

Brambillasca S, Yabal M, Makarow M & Borgese N (2006) Unassisted translocation of large polypeptide domains across phospholipid bilayers. *J Cell Biol* **175**:767-777.

Brambillasca S, Yabal M, Soffientini P, Stefanovic S, Makarow M, Hegde RS & Borgese N (2005) Transmembrane topogenesis of a tail-anchored protein is modulated by membrane lipid composition. *EMBO J* **24**:2533-2542.

Braun BC, Glickman M, Kraft R, Dahlmann B, Kloetzel PM, Finley D & Schmidt M (1999) The base of the proteasome regulatory particle exhibits chaperone-like activity. *Nat Cell Biol* **1**:221-226.

Braun S, Matuschewski K, Rape M, Thoms S, Jentsch S (2002) Role of the ubiquitin-selective $CDC48^{UFD1/NPL4}$ chaperone (segregase) in ERAD of OLE1 and other substrates. *EMBO J* **21**:615-621.

Braun RJ & Zischka H (2008) Mechanisms of Cdc48/VCP-mediated cell death: from yeast apoptosis to human disease. *Biochim Biophys Acta* **1783**:1418-1435.

Breitfeld PP, Casanova JE, Simister NE, Ross SA, McKinnon WC, Mostov KE (1989) Sorting signals. *Curr Opin Cell Biol* **1(4)**:617-623.

Breyton C, Haase W, Rapoport TA, Kuhlbrandt W & Collinson I (2002) Three-dimensional structure of the bacterial protein-translocation complex SecYEG. *Nature* **418**:662-665.

Briggs, LC, Baldwin GS, Miyata N, Kondo H, Zhang X & Freemont PS (2008) Analysis of nucleotide binding to P97 reveals the properties of a tandem AAA hexameric ATPase. *J Biol Chem* **283**:13745-13752

Brodsky JL (2010) The use of *in vitro* assays to measure endoplasmic reticulum-associated degradation. *Methods in Enzymology* **470**:661-679.

Brodsky JL (2012) Cleaning up: ER-associated degradation to the rescue. *Cell* **151**:1163-1167.

Brodsky JL, Goeckeler J & Schekman R (1995) Sec63p and BiP are required for both co- and post-translational protein translocation into yeast microsomes. *Proc Natl Acad Sci USA* **92**:9643-9646.

Brodsky JL & McCracken AA (1999) ER protein quality control and proteasome-mediated protein degradation. *Semin Cell Dev Biol* **10**:507-513.

Brodsky JL & Schekman R (1993) A Sec63p-BiP complex from yeast is required for protein translocation in a reconstituted proteoliposome. *J Cell Biol* **123**:1355-1363.

Brodsky JL, Werner ED, Dubas ME, JGoeckeler JL, Kruse KB & McCracken AA (1999) The requirement for molecular chaperones during endoplasmic reticulum-associated protein degradation demonstrates that protein export and import are mechanistically distinct. *J Biol Chem* **274**:3453-3460.

Brown JD, Hann BC, Medzihradszky KF, Niwa M, Burlingame AL & Walter P (1994) Subunits of the *Saccharomyces cerevisiae* signal recognition particle required for its functional expression. *EMBO J* **13**:4390-4400.

Buchberger A (2010) Control of ubiquitin conjugation by cdc48 and its cofactors. *Subcell Biochem* **54**:17-30.

Buck TM, Wright CM & Brodsky JL (2007) The activities and function of molecular chaperones in the endoplasmic reticulum. *Semin Cell Dev Biol* **18**:751-761.

Bukau B & Horwich AL (1998) The Hsp70 and Hsp60 chaperone machines. *Cell* **92**:351-366.

Bukau B, Weissman J & Horwich A (2006) Molecular chaperones and protein quality control. *Cell* **125(3)**:443-451.

Burroughs AM, Balaji S, Iyer LM & Aravind L (2007) Small but versatile: the extraordinary functional and structural diversity of the β-grasp fold. *Biol Direct* **2**:18.

Buschhorn BA, Kostova Z, Medicherla B & Wolf DH (2004) A genome-wide screen identifies Yos9p as essential for ER-associated degradation of glycoproteins. *FEBS Lett* **577**:422-426.

Cannon KS, Or E, Clemons Jr WM, Shibata Y, Rapoport TA (2005) Disulfide bridge formation between SecY and a translocating polypeptide localizes the translocation pore to the center of SecY. *J Cell Biol* **169**:219-225.

Cao TB & Saier MH Jr (2003) The general protein secretory pathway: phylogenetic analyses leading to evolutionary conclusions. *Biochim Biophys Acta* **1609(1)**:115-125.

Caplan AJ, Cyr DM & Douglas MG (1992) YDJ1p facilitates polypeptide translocation across different intracellular membranes by a conserved mechanism. *Cell* **71(7)**:1143-1155.

Caplan AJ & Douglas MG (1991) Characterization of *YDJ1*: a yeast homologue of the bacterial dnaJ protein. *J Cell Biol* **114 (4)**:609-621.

Caplan S, Green R, Rocco J & Kurjan J (1991) Glycosylation and structure of the yeast MF alpha 1 alpha-factor precursor is important for efficient transport through the secretory pathway. *J Bacteriol* **173 (2)**:627-635.

Caramelo, JJ, Castro, OA, Alonso LG, De Prat-Gay G & Parodi AJ (2003) UDP Glc:glycoprotein glucosyltransferase recognizes structured and solvent accessible hydrophobic patches in molten globule-like folding intermediates. *Proc. Natl Acad. Sci. USA* **100**:86-91.

Caramelo JJ, Castro OA, de Prat-Gay G & Parodi AJ (2004) The endoplasmic reticulum glucosyltransferase recognizes nearly native glycoprotein folding intermediates. *J Biol Chem* **279**:46280-46285.

Caramelo JJ & Parodi AJ (2007) How sugars convey information on protein conformation in the endoplasmic reticulum. *Semin Cell Dev Biol* **18**:732-742.

Carrie C, Giraud E & Whelan J (2009) Protein transport in organelles: dual targeting of proteins to mitochondria and chloroplasts. *FEBS J* **276**:1187-1195.

Carvalho P, Goder V & Rapoport TA (2006) Distinct ubiquitin-ligase complexes define convergent pathways for the degradation of ER proteins. *Cell* **126**:361-373.

Carvalho P, Stanley AM & Rapoport TA (2010) Retrotranslocation of a misfolded luminal ER protein by the ubiquitin-ligase Hrd1p. *Cell* **143**:579-591.

Casagrande R, Stern P, Diehn M, Shamu C, Osario M, Zúñiga M, Brown PO & Ploegh H (2000)

Degradation of proteins from the ER of *S. cerevisiae* requires an intact unfolded protein response pathway. *Mol Cell* **5**:729-735.

Chandu D & Nandi D (2002) From proteins to peptides to amino acids: comparative genomics of enzymes involved in down-stream events during cytosolic protein degradation. *Appl.Genom. Proteom* **4**:235-252.

Chandu D & Nandi D (2004) Comparative genomics and functional roles of the ATP-dependent proteases Lon and Clp during cytosolic protein degradation. *Res Microbiol* **155**:710-719.

Chapman RE & Walter P (1997) Translational attenuation mediated by an mRNA intron. *Curr Biol* **7**:850-859.

Chau V, Tobias JW, Bachmair A, Marriott D, Ecker DJ, Gonda DK & Varshavsky A (1989) A multiubiquitin chain is confined to specific lysine in a targeted short-lived protein. *Science* **243**:1576-1583.

Chavan MM, Yan A & Lennarz WJ (2005) Subunits of the translocon interact with components of the oligosaccharyl transferase complex. *J Biol Chem* **280(24)**:22917-22924.

Chawla A, Chakrabarti S, Ghosh G & Niwa M (2011) Attenuation of yeast UPR is essential for survival and is mediated by IRE1 kinase. *J Cell Biol* **193(1)**:41-50.

Chen P & Hochstrasser M (1996) Autocatalytic subunit processing couples active site formation in the 20S proteasome to completion of assembly. *Cell* **86**:961-972.

Chen X, van Valkenburgh C, Liang H, Fang H, Green N (2001) Signal peptidase and oligosaccharyltransferase interact in a sequential and dependent manner within the endoplasmic reticulum. *J Biol Chem* **276**: 2411-2416.

Chen Y, Zhang Y, Yin Y, Gao G, Li S, Li S, Jiang Y, Gu X & Luo J (2005) SPD—a Web-based secreted protein database. *Nucleic Acids Res* **33**:D169-173.

Cheng Z, Jiang Y, Mandon EC & Gilmore R (2005) Identification of cytoplasmic residues of Sec61p involved in ribosome binding and cotranslational translocation. *J Cell Biol* **168**:67-77.

Chiang HL & Schekman R (1991) Regulated import and degradation of a cytosolic protein in the yeast vacuole. *Nature* **350**:313-318.

Chirico WJ, Waters MG & Blobel G (1988) 70 K heat shock related proteins stimulate protein translocation into microsomes. *Nature* **332** :805-810.

Chou KC & Elrod DW (1999) Protein subcelluar location predicition. *Protein Eng* **12**:107-118.

Ciechanover A (1998) The ubiquitin-proteasome pathway: on protein death and cell life. *EMBO J* **17(24)**:7151-7160.

Ciechanover A & Brundin P (2003) The ubiquitin proteasome system in neurodegenerative diseases: sometimes the chicken, sometimes the egg. *Neuron* **40(2)**:427-446.

Ciechanover A, Heller H, Elias S, Haas AL & Hershko A (1980) ATP-dependent conjugation of reticulocyte proteins with the polypeptide required for protein degradation. *Proc Natl Acad Sci USA* **77(3)**:1365-1368.

Ciechanover A, Hod Y & Hershko A (1978) A heat-stable polypeptide component of an ATP-dependent proteolytic system from reticulocytes. *Biochem Biophys Res Commun* **81**:1100-1105.

Ciechanover A & Iwai K (2004) The ubiquitin system: from basic mechanisms to the patient bed. *IUBMB Life* **56(4)**:193-201.

Clerc S, Hirsch C, Oggler DM, Deprez P, Jakob C, Sommer T & Aebi M (2009) Htm1 protein generates the N-glycan signal for glycoprotein degradation in the endoplasmic reticulum. *J Cell Biol* **184(1)**:159-172.

Connolly T & Gilmore R (1986) Formation of a functional ribosome-membrane junction during translocation requires the participation of a GTP-binding protein. *J Cell Biol* **103(6)**:2253-2261.

Corsi AK & Schekman R (1996) Mechanism of polypeptide translocation into the endoplasmic reticulum. *J Biol Chem* **271**:30299-30302.

Corsi AK & Schekman R (1997) The lumenal domain of Sec63p stimulates the ATPase activity of BiP and mediates BiP recruitment to the translocon in Saccharomyces cerevisiae. *J Cell Biol* **137(7)**:1483-1493.

Cosson P & Letourneur F (1994) Coatamer interaction with di-lysine endoplasmic reticulum retention motif. *Science* **263**:1629-1631.

Cosson P & Letourneur F (1997) Coatamer (COPI)-coated vesicles: role in intracellular transport and protein sirting. *Curr Opin Cell Biol* **9**:484-487.

Cox JS, Shamu C & Walter P (1993) Transcriptional induction of genes encoding endoplasmic reticulum resident proteins requires a transmembrane protein kinase. *Cell* **73**:1197-1206.

Cox JS & Walter P (1996) A novel mechanism for regulating activity of a transcription factor that controls the unfolded protein response. *Cell* **87**:391-404.

Credle JJ, Finer-Moore JS, Papa FR, Stroud RM & Walter P (2005) On the mechanism of sensing unfolded protein in the endoplasmic reticulum. *Proc Natl Acad Sci USA* **102**:18773-18784.

Crowley KS, Liao S, Worrell VE, Reinhart GD & Johnson AE (1994) Secretory proteins move through the endoplasmic reticulum membrane via an aqueous, gated pore. *Cell* **78**:461-471.

Dahlmann B, Kopp F, Kristensen P & Hendil KB (1999) Identical subunit topographies of human and yeast 20S proteasomes. *Arch Biochem Biophys* **363(2)**:296-300.

Dai RM & Li CC (2001) Valosin-containing protein is a multi-ubiquitin chain-targeting factor required in ubiquitin-proteasome degradation. *Nat Cell Biol* **3**:740-744.

Dalbey RE & von Heijne G (1992) Sinal peptidase in prokaryotes and eukaryotes: a new protease family. *Trends Biochem Sci* **17**:474-478.

Darken MA (1964) Puromycin inhibition of protein synthesis. *Pharmacol Rev* **16**:223-243.

Davies, JM, Brunger AT & Weis WI (2008) Improved structures of full-length p97, an AAA ATPase: implications for mechanisms of nucleotide-dependent conformational change. *Structure* **16**:715-726.

Dawson S, Higashitsuji H, Wilkinson J, Fujita J & Mayer R (2006) Gankyrin: a new oncoprotein

and regulator of pRb and p53. *Trends Cell Biol* **16**:229-233.

Deak PM and Wolf DH (2001) Membrane topology and function of Der3/Hrd1p as a ubiquitin-protein ligase (E3) involved in endoplasmic reticulum degradation. *J Biol Chem* **276(14)**:10663-10669.

Deichsel A, Mouysset J & Hoppe T (2009) The ubiquitin-selective chaperone CDC-48/p97, a new player in DNA replication. *Cell Cycle* **8**:185-190.

Denic V, Quan EM & Weissman JS (2006) A luminal surveillance complex that selects misfolded glycoproteins for ER-associated degradation. *Cell* **126**:349-359.

Deshaies RJ & Joazeiro CA (2009) RING domain E3 ubiquitin ligases. *Annu Rev Biochem* **78**:399-434.

Deshaies RJ, Koch BD, Werner-Washburne M, Craig EA & Schekman R (1988) A subfamily of stress proteins facilitates translocation of secretory and mitochondrial precursor polypeptides. *Nature* **332**:800-805.

Deshaies RJ, Sanders SL, Feldheim DA & Schekman R (1991) Assembly of yeast Sec proteins involved in translocation into the endoplasmic reticulum into a membrane-bound multisubunit complex. *Nature* **349**:806-808.

Deshaies RJ & Schekman R (1987) A yeast mutant defective at an early stage in import of secretory protein precursors into the endoplasmic reticulum. *J Cell Biol* **105(2)**:633-645.

Deshaies RJ & Schekman R (1989) *SEC62* encodes a putative membrane protein required for protein translocation into the yeast endoplasmic reticulum. *J Cell Biol* **109**:2653-2664.

Deshaies RJ & Schekman R (1990) Structural and functional dissection of Sec62p, a membrane-bound component of the yeast endoplasmic reticulum protein import machinery. *Mol Cell Biol* **10(11)**:6024-6035.

Deveraux Q, Ustrell V, Pickart C & Rechsteiner M (1994) A 26S protease subunit that binds ubiquitin conjugates. *J Biol Chem* **269**:7059-7061.

Deville K, Gold VA, Robson A, Whitehouse S, Sessions RB, Baldwin SA, Radford SE & Collinson I (2011) The oligomeric state and arrangement of the active bacterial translocon. *J Biol Chem* **286**:4659-4669.

de Virgilio M, Weninger H & Ivessa NE (1998) Ubiquitination is required for the retro-translocation of a short-lived luminal endoplasmic reticulum glycoprotein to the cytosol for degradation by the proteasome. *J Biol Chem* **273**:9734-9743.

Dill KA (1985) Theory for the folding and stability of globular proteins. *Biochemistry* **24(6)**:1501-1509.

Dill KA, Ozkan SB, Shell MS & Weikl TR (2008) The protein folding problem. *Annu Rev Biophys* **37**:289-316.

Djuranovic S, Hartmann MD, Habeck M, Ursinus A, Zwickl P, Martin J, Lupas AN, Zeth K (2009) Structure and Activity of the N-Terminal Substrate Recognition Domains in Proteasomal ATPases. *Mol Cell* **34**:580-590.

Dmochowska A, Dignard D, Hennig D, Thomas DY & Bussey H (1987) Yeast *KEXI* gene encodes a putative protease with a carboxypeptidase B-like function involved in killer toxin and α-

factor precursor processing. *Cell* **50**:573-584.

Do H, Falcone D, Lin J, Andrews DW & Johnson AE (1996) The cotranslational integration of membrane proteins into the phospholipid bilayer is a multistep process. *Cell* **85**:369-378.

Dobberstein B, Blobel G & Chua NH (1977) *In vitro* synthesis and processing of a putative precursor for the small subunit of ribulose-1,5-bisphosphate carboxylase of *Chlamydomonas reinhardtii*. *Proc Natl Acad Sci USA* **74**:1082-1085.

Dobson CM (2004) Principles of protein folding, misfolding and aggregation. *Semin Cell Dev Biol* **15**:3-16.

Donella-Deana A, Ostojić S, Pinna LA, Barbarić S (1993) Specific dephosphorylation of phosphopeptides by the yeast alkaline phosphatase encoded by *PHO8* gene. *Biochim Biophys Acta* **1177(2)**:221-228.

Dorner AJ, Wasley LC & Kaufman RJ (1992) Overexpression of *GRP78* mitigates stress induction of glucose regulated proteins and blocks secretion of selective proteins in Chinese hamster ovary cells. *EMBO J* **11**:1563-1571.

Dower WJ, Miller JF & Ragsdale CW (1989) High efficiency transformation of *E. coli* by high voltage electroporation. *Nucleic Acids Research* **16(13)**:6127-6145.

Dubiel W & Gordon C (1999) Ubiquitin pathway: another link in the polyubiquitin chain? *Curr Biol* **9**:R554-557.

Duden R (2003) ER-to-Golgi transport: COPI and COPII function. *Mol Membr Biol* **20(3)**:197-207.

Duksin D & Mahoney WC (1982) Relationship of the structure and biological activity of the natural homologues of tunicamycin. *J Biol Chem* **257(6)**:3105-3109.

Duman JG & Forte JG (2003) What is the role of snare proteins in membrane fusion? *Am J Physiol Cell Physiol* **285**:C237-C249.

Duong F (2003) Binding, activation and dissociation of the dimeric SecA ATPase at the dimeric SecYEG translocase. *EMBO J* **22**:4375-4384.

du Plessis DJ, Berrelkamp G, Nouwen N & Driessen A (2009) The lateral gate of SecYEG Opens during protein translocation. *J Biol Chem* **284**:15805–15814.

Effantin G, Rosenzweig R, Glickman MH & Steven AC (2009) Electron microscopic evidence in support of alpha-solenoid models of proteasomal subunits Rpn1 and Rpn2. *J Mol Biol* **386**:1204-1211.

Eisele F, Schafer A & Wolf DH (2010) Ubiquitylation in the ERAD pathway. *Subcell Biochem* **54**:136-148.

Eletr ZM, Huang DT, Duda DM, Schulman BA & Kuhlman B (2005) E2 conjugating enzymes must disengage from their E1 enzymes before E3-dependent ubiquitin and ubiquitin-like transfer. *Nat Struct Mol Biol* **12**:933-934.

Ellgaard L & Helenius A (2003) Quality control in the endoplasmic reticulum. *Nature Rev Mol Cell Biol* **4(3)**:181-191.

Ellgaard L, Molinari M & Helenius A (1999) Setting the Standards: Quality Control in the Secretory Pathway. *Science* **286(5446)**:1882-1888.

Elsasser S & Finley D (2005) Delivery of ubiquitinated substrates to protein-unfolding machines. *Nat Cell Biol* **7(8)**:742-749.

Elsasser S, Gali RR, Schwickart M, Larsen CN, Leggett DS, Müller B, Feng MT, Tübing F, Dittmar GA & Finley D (2002) Proteasome subunit Rpn1 binds ubiquitin-like protein domains. *Nat Cell Biol* **4**:725–730.

Emr S, Glick BS, Linstedt AD, Lippincott-Schwartz J, Luini A, Malhotra V, Marsh BJ, Nakano A, Pfeffer SR, Rabouille C, Rothman JE, Warren G & Wieland FT (2009) Journeys through the Golgi — Taking stock in a new era. *J Cell Biol* **187(4)**:449-453.

Emter O, Mechler B, Achstetter T, Muller H & Wolf DH (1983) Yeast pheromone α-factor is synthesized as a high molecular weight precursor. *Biochem Biophys Res Commun* **116**:822-829.

Enekel C, Lehmann A & Kloetzel PM (1998) Subcellular distribution of proteasomes implicates a major location of protein degradation in the nuclear envelope-ER network in yeast. *EMBO J* **17(21)**:6144-6154.

Esnault Y, Blondel MO, Deshaies RJ, Schekman R & Képès F (1993) The yeast *SSS1* gene is essential for secretory protein translocation and encodes a conserved protein of the endoplasmic reticulum. *EMBO J* **12(11)**:4083-4093.

Esnault Y, Feldheim D, Blondel MO, Schekman R & Képès F (1994) *SSS1* encodes a stabilizing component of the Sec61 subcomplex of the yeast protein translocation apparatus. *J Biol Chem* **269(44)**:27478-27485.

Fagioli C & Sitia R (2001) Glycoprotein quality control in the endoplasmic reticulum. Mannose trimming by endoplasmic reticulum mannosidase I times the proteasomal degradation of unassembled immunoglobulin subunits. *J Biol Chem* **276**:12885-12892.

Fang H & Green N (1994) Nonlethal sec71-1 and sec72-1 mutations eliminate proteins associated with the Sec63p-BiP complex from *S. cerevisiae*. *Mol Biol Cell* **5(9)**:933-942.

Farquhar MG & Hauri HP (1997) Protein sorting and vesicular traffic. In: Berger, EG & Roth (Eds.) The Golgi apparatus. Birkhäuser Verlag, Basel, Switzerland, pp 63-129.

Farquhar MG & Palade GE (1998) The Golgi apparatus: 100 years of progress and controversy. *Trends in Cell Biology* **8**:2-10.

Fasshauer D., Otto H., Eliason W. K., Jahn R., Brunger A. T (1997) Structural changes are associated with soluble N-ethylmaleimide-sensitive fusion protein attachment protein receptor complex formation. *J Biol Chem* **272**:28036-28041.

Fasshauer D, Sutton RB, Brunger AT & Jahn R (1998) Conserved structural features of the synaptic fusion complex: SNARE proteins reclassified as Q- and R-SNAREs. *Proc Natl Acad Sci USA* **95**:15781-15786.

Feldheim D, Rothblatt J & Schekman R (1992) Topology and functional domains of Sec63p, an endoplasmic reticulum membrane protein required for secretory protein translocation. *Mol Cell Biol* **12(7)**:3288-3296.

Feldheim D & Schekman R (1994) Sec72p contributes to the selective recognition of signal peptides by the secretory polypeptide translocation complex. *J Cell Biol* **126(4)**:935-43

Feldheim S, Yoshimura K, Admon A & Schekman R (1993) Structural and functional characterization of Sec66p, a new subunit of the polypeptide translocation apparatus in the yeast endoplasmic reticulum. *Mol Biol Cell* **4(9)**:931-939.

Felici F, Cesareni G & Hughes JMX (1989) The most abundant small cytoplasmic RNA of *Saccharomyces cerevisiae* has an important function required for normal cell growth. *Mol Cell Biol* **9:**3260-3268.

Feng D, Zhao X, Soromani C, Toikkanen J, Romisch K, Vembar SS, Brodsky JL, Keränen S & Jäntti J (2007) The transmembrane domain is sufficient for Sbh1p function, its association with the Sec61 complex, and interaction with Rtn1p. *J Biol Chem* **282(42)**:30618-30628.

Fernández FS, Trombetta SE, Hellman U & Parodi AJ (1994) Purification to homogeneity of UDP-glucose:glycoprotein glucosyltransferasefrom *Schizosaccharomyces pombe* and apparent absence of the enzyme from *Saccharomyces cerevisiae*. *J Biol Chem* **269**:30701-30706.

Ferrell K, Wilkinson CR, Dubiel W, Gordon C (2000) Regulatory subunit interactions of the 26S proteasome, a complex problem. *Trends Biochem Sci* **25**:83-88.

Fewell SW, Day BW & Brodsky JL (2001) Identification of an inhibitor of hsc70-mediated protein translocation and ATP hydrolysis. *J Biol Chem* **276(2)**:910-914.

Finger A, Knop M & Wolf DH (1993) Analysis of two mutated vacuolar proteins reveals a degradation pathway in the endoplasmic reticulum or a related compartment of yeast. *Eur J Biochem* **218**:565-574.

Finke K, Plath K, Panzner S, Prehn S, Rapoport TA, Hartmann E & Sommer T (1996) A second trimeric complex containing homologs of the Sec61p complex functions in protein transport across the ER membrane of *Saccharomyces cerevisiae*. *EMBO J* **15**:1482-1494.

Finley D (2002) Ubiquitin chained and crosslinked. *Nat Cell Biol* **4(5)**:E121-E123.

Finley D (2009) Recognition and Processing of Ubiquitin-Protein Conjugates by the Proteasome. *Annu Rev Biochem* **78**:477-513.

Finley D, Tanaka K, Mann C, Feldmann H, Hochstrasser M, Vierstra R, Johnston S, Hampton R, Haber J, McCusker J, Silver P, Frontali L, Thorsness P, Varshavsky A, Byers B, Madura K, Reed SI, Wolf D, Jentsch S, Sommer T, Baumeister W, Goldberg A, Fried V, Rubin DM, Glickman MH, Toh-e A (1998) Unified nomenclature for subunits of the *Saccharomyces cerevisiae* proteasome regulatory particle. *Trend Biol Sci* **23(7)**:244-245.

Fisher EA & Ginsberg HN (2002) Complexity in the secretory pathway: the assembly and secretion of apolipoprotein B-containing lipoproteins. *J Biol Chem* **277**:17377-17380.

Flaherty KM, DeLuca-Flaherty C & McKay DB (1990) Three-dimensional structure of the ATPase fragment of a 70K heat-shock cognate protein. *Nature* **346**:623-628.

Förster F, Lasker K, Beck F, Nickell S, Sali A & Baumeister W (2009) An atomic model AAA-ATPase/20S core particle sub-complex of the 26S proteasome. *Biochem Biophys Res Commun* **388(2)**:228-233.

Förster F, Lasker K, Nickell S, Sali A & Baumeister W (2010) Towards an integrated structural model of the 26S proteasome*. Mol Cell Proteomics* **9**:1666-1677.

Fons RD, Bogert BA & Hegde RS (2003) The translocon-associated protein complex facilitates the initiation of substrate translocation across the ER membrane. *J Cell Biol* **129(160)**:529-539.

Forman MS, Lee VM-Y & Trojanowski JG (2003) 'Unfolding' pathways in neurodegenerative disease. *Trends Neurosci* **26**:407-410.

Frank J (2006) Three-Dimensional Electron Microscopy of Macromolecular Assemblies. *Oxford University Press*, New York.

Freedman RB, Hirst TR & Tuite MF (1994) Protein disulphide isomerase: building bridges in protein folding. *Trends Biochem Sci* **19**:331-336.

Freemont PS, Hanson IM & Trowsdale J (1991) A novel cysteine-rich sequence motif. *Cell* **64**:483-484.

Friedlander R, Jarosch E, Urban J, Volkwein C & Sommer T (2000) A regulatory link between ER-associated protein degradation and the unfolded-protein response. *Nat Cell Biol* **2**:379-384.

Frohlich KU, Fries HW, Rüdiger M, Erdmann R, Botstein D & Mecke D (1991) Yeast cell cycle protein CDC48p shows full-length homology to the mammalian protein VCP and is a member of a protein family involved in secretion, peroxisome formation, and gene expression. *J Cell Biol* **114**:443-453.

Fujimuro M, Tanaka K, Yokosawa H & Toh-e A (1998) Son1p is a component of the 26S proteasome of the yeast *Saccharomyces cerevisiae*. *FEBS Lett* **423(2)**:149-154.

Fukunaga K, Kudo T, Toh-e A, Tanaka K, Saeki Y (2010) Dissection of the assembly pathway of the proteasome lid in *Saccharomyces cerevisiae*. *Biochem Biophys Res Comm* **396**:1048-1053.

Fulga TA, Sinning I, Dobberstein B & Pool MR (2001) SRβ coordinates signal sequence release from SRP with ribosome binding to the translocon. *EMBO J* **20**:2338-2347.

Fuller RS, Sterne RE & Thorner J (1988) Enzymes required for yeast prohormone processing. *Annu Rev Physiol* **50**:345-362.

Funakoshi M, Sasaki T, Nishimoto T & Kobayashi H (2002) Budding yeast Dsk2p is polyubiquitin-binding protein that can interact with theproteasome. *Proc Natl Acad Sci USA* **99**:745-750.

Gabel CA & Bergmann JE (1985) Processing of the asparagine-linked oligosaccharides of secreted and intracellular forms of the vesicular stomatitis virus G protein: *in vivo* evidence of Golgi apparatus compartmentalization. *J Cell Biol* **101**:460-469.

Gardner RG, Swarbrick GM, Bays NW, Cronin SR, Wilhovsky S, Seelig L, Kim C & Hampton RY (2000) Endoplasmic reticulum degradation requires lumen to cytosol signaling: transmembrane control of Hrd1p by Hrd3p. *J Cell Biol* **151**:69-82.

Gardner MB & Walter P (2011) Unfolded proteins are Ire1-activating ligands that directly induce the unfolded protein response. *Science* **333(6051)**:1891-1894.

Garza RM, Tran PN & Hampton RY (2009) Geranylgeranyl Pyrophosphate Is a Potent Regulator of HRD-dependent 3-Hydroxy-3-methylglutaryl-CoA Reductase Degradation in Yeast. *J Biol Chem* **284(51)**:35368-35380.

Gauss R, Jarosch E, Sommer T & Hirsch C (2006) A complex of Yos9p and the HRD ligase integrates endoplasmic reticulum quality control into the degradation machinery. *Nat Cell Biol* **8**:849-854.

Gauss R, Kanehara K, Carvalho P, Ng DT & Aebi M (2011) A complex of Pdi1p and the mannosidase Htm1p initiates clearance of unfolded glycoproteins from the endoplasmic reticulum. *Mol Cell* **42(6)**:782-793.

Gaynor EC, Graham TR & Emr SD (1994) COPI in ER/Golgi and intra-Golgi transport: do yeast COPI mutants point the way? *Biochim Biophys Acta* **1404**:33-51.

Geller D, Taglicht D, Edgar R, Tam A, Pines O, Michaelis S & Bibi E (1996) Comparative topology studies in *Saccharomyces cerevisiae* and in *Escherichia coli* of the N-terminal half of the yeast ABC protein, Ste6. *J Biol Chem* **271**:13746-13753.

Gething MJ (1999) Role and regulation of the ER chaperone BiP. *Semin Cell Dev Biol* **10**:465-472.

Ghaemmaghami S, Huh WK, Bower K, Howson RW, Belle A, Dephoure N, O'Shea EK & Weissman JS (2003) Global analysis of protein expression in yeast. *Nature* **425**:737-741.

Gierasch L (1989) Signal sequences. *Biochemistry* **28**:923-930.

Gietz RD, Schiestl RH, Willems AR & Woods RA (1995) Studies on the transformation of intact yeast cells by the LiAc/SS-DNA/PEG procedure. *Yeast* **11(4)**:355-360.

Gietz RD & Woods RA (2002) Transformation of yeast by the Lithium acetate/single strand carrier DNA/PEG method. *Methods in Enzymology* **350**:87-96.

Gilbert HF (1997) Protein disulfide isomerase and assisted protein folding. *J Biol Chem* **272**:29399-29402.

Gillece P, Luz JM, Lennarz WJ, de la Cruz FJ & Römisch K (1999) Export of a cysteine-free misfolded secretory protein from the endoplasmic reticulum for degradation requires interaction with protein disulfide isomerase. *J Cell Biol* **147 (7)**:1443-1456.

Gillece P, Pilon M & Romisch K (2000) The protein translocation channel mediates glycopeptide export across the endoplasmic reticulum membrane. *Proc Natl Acad Sci USA* **97**:4609-4614.

Gilmore R, Blobel G & Walter P (1982a) Protein translocation across the endoplasmic reticulum. I. Detection in the microsomal membrane of a receptor for the signal recognition particle. *J Cell Biol* **95(2)**:463-469

Gilmore R, Walter P & Blobel G (1982b) Protein translocation across the endoplasmic reticulum. II. Isolation and characterization of the signal recognition particle receptor. *J Cell Biol* **95(2)**:470-477.

Glick BS (1995) Can hsp70 proteins act as force generating motors ? *Cell* **80**:11-14.

Glick BS (2000) Organization of the Golgi apparatus. *Curr Opin Cell Biol* **12**:450-456.

Glick BS & Malhotra V (1998) The curious status of the Golgi apparatus. *Cell* **95(7)**:883-889.

Glickman MH & Ciechanover A (2002) The ubiquitin-proteasome proteolytic pathway: Destruction for the sake of construction. *Physiol Rev* **82**:373-428.

Glickman MH, Rubin DM, Fried VA & Finley D (1998a) The regulatory particle of the *Saccharomyces cerevisiae* proteasome. *Mol Cell Biol* **18**:3149-3162

Glickman MH, Rubin DM, Fu H, Larsen CN, Coux O, Wefes I, Pfeifer G, Cjeka Z, Viestra R Baumeinster W, Fried V & Finley D (1998b) A subcomplex of the proteasome regulatory particle required for ubiquitin-conjugate degradation and related to the COP9-signalosome and eIF3. *Cell* **94(5)**:615-623.

Glickman MH, Rubin DM, Fu H, Larsen CN, Coux O, Wefes I, Pfeifer G, Cjeka Z, Vierstra R, Baumeister W, Fried V & Finley D (1999) Functional analysis of the proteasome regulatory particle. *Mol Biol Rep* **26(1-2)**:21-28.

Glynn SE, Martin A, Nager AR, Baker TA, Sauer RT (2009) Structures of asymmetric ClpX hexamers reveal nucleotide-dependent motions in a AAA+ protein-unfolding machine. *Cell* **139**:744-756.

Görlich D, Prehn S, Hartmann E, Kalies KU & Rapoport TA (1992) A mammalian homolog of Sec61p and SecYp is associated with ribosomes and nascent polypeptides during translocation. *Cell* **71**:489-503.

Görlich D & Rapoport TA (1993) Protein translocation into proteoliposomes reconstituted from purified components of the endoplasmic reticulum membrane. *Cell* **75**:615-630.

Goldberg AL (2003) Protein degradation and protection against misfolded or damaged proteins. *Nature* **426**:744-756.

Gomez TA, Kolawa N, Gee M, Sweredoski MJ & Deshaies RJ (2011) Identification of a functional docking site in the Rpn1 LRR domain for the UBA-UBL domain protein Ddi1. *BMC Biol* **9**:33.

Gow A & Sharma R (2003) The unfolded protein response in protein aggregating diseases. *Neuromolecular Med* **4**:73-94.

Grant BD & Sato M (2006) Intracelular Trafficking. *WormBook*, ed. The *C. elegans* Research Community, WormBook

Green NM (1975) Avidin. *Adv Protein Chem* **29**:85-133.

Groll M, Bajorek M, Kohler A, Moroder L, Rubin DM, Huber R, Glickman MH, Finley D (2000) A gated channel into the proteasome core particle. *Nat Struct Biol* **7**:1062-1067.

Groll M, Bochtler M, Brandstetter H, Clausen T & Huber R (2005) Molecular machines for protein degradation. *ChemBioChem* **6**:222-256.

Groll M, Ditzel L, Löwe J, Stock D, Bochtler M, Bartunik HD & Huber R (1997) Structure of 20S proteasome from yeast at 2.4 Å resolution. *Nature* **386**:463-471.

Guarente, L (1983) Yeast promoters and *lacZ* fusions designed to study expression of cloned genes in yeast. *Methods Enzymol* **101**:181-191.

Guarente L & Mason T (1983) Heme regulates transcription of the *CYC1* gene of *S. cerevisiae* via an upstream activation site. *Cell* **32**:1279-1286.

Gundelfinger ED, Krause E, Melli M & Dobberstein B (1983) The organization of the 7SL RNA in the signal recognition particle. *Nucleic Acids Res* **11:**7363-7374.

Haas AL & Rose IA (1982) The mechanism of ubiquitin activating enzyme. A kinetic and equilibrium analysis. *J Biol Chem* **257**:10329-10337.

Haas IG & Wabl M (1983) Immunoglobulin heavy chain binding protein. *Nature* **306**:387-389.

Hainzl T, Huang S & Sauer-Eriksson AE (2002) Structure of the SRP19 RNA complex and implications for signal recognition particle assembly. *Nature* **417:**767-771.

Halic M, Gartmann M, Schlenker O, Mielke T, Pool MR, Sinning I & Beckmann R (2006) Signal recognition particle receptor exposes the ribosomal translocon binding site. *Science* **312(5774)**:745-747.

Haltiwanger RS & Lowe JB (2004) Role of glycosylation in development. *Annu Rev Biochem* **73**:491-537.

Hamman BD, Chen JC, Johnson EE & Johnson AE (1997) The aqueous pore through the translocon has a diameter of 40-60 Å during cotranslational protein translocation at the ER membrane. *Cell* **89**:535-544.

Hamman BD, Hendershot LM & Johnson AE (1998) BiP maintains the permeability barrier of the ER membrane by sealing the lumenal end of the translocon pore before and early in translocation. *Cell* **92**:747-758.

Hammond C, Braakman I & Helenius A (1994) Role of N-linked oligosaccharide recognition, glucose trimming, and calnexin in glycoprotein folding and quality control, *Proc Natl Acad Sci USA* **91(3)**:913-917.

Hammond AT & Glick BS (2000) Dynamics of transitional endoplasmic reticulum sites in vertebrate cells. *Mol Biol Cell* **11**:3013-30.

Hammond C & Helenius A (1995) Quality control in the secretory pathway. *Curr Opin Cell Biol* **7**:523-529.

Hampton RY (2002) ER-associated degradation in protein quality control and cellular regulation. *Curr Opin Cell Biol* **14**:476-482.

Hampton RY, Gardner RG & Rine J (1996) Role of 26S proteasome and *HRD* genes in the degradation of 3-hydroxy-3-methylglutaryl-CoA reductase, an integral endoplasmic reticulum membrane protein. *Mol Biol Cell* **7(12)**:2029-2044.

Hampton RY & Sommer T (2012) Finding the will and the way of ERAD substrate retrotranslocation. *Curr Opin Cell Biol* **24**:460-466.

Hanahan D (1983) Studies on transformation of *Escherichia coli* with plasmids. *J Mol Biol* **166(4)**:557-580.

Hanein D, Matlack KE, Jungnickel B, Plath K, Kalies KU, Miller KR, Rapoport TA & Akey CW (1996) Oligomeric rings of the Sec61p complex induced by ligands required for protein translocation. *Cell* **87(4)**:721-732.

Hann BC & Walter P (1991) The signal recognition particle in *S. cerevisiae*. *Cell* **67(1)**:131-144.

Hanna J & Finley D (2007) A proteasome for all occasions. *FEBS Lett* **581(15)**:2854-2861.

Hansen W, Garcia PD & Walter P (1986) *In vitro* protein translocation across the yeast endoplasmic reticulum: ATP-dependent posttranslational translocation of the prepro-alpha-factor. *Cell* **45**:397-406.

Harada Y, Li H, Wall JS, Li H & Lennarz WJ (2011) Structural studies and the assembly of the heptameric post-translational translocon complex. *J Biol Chem* **286**:2956-2965.

Harding HP & Ron D (2002) Endoplasmic reticulum stress and the development of diabetes: a review. *Diabetes* **51 Supple3**:S455-S461.

Harris JM & Zalipsky S, Eds (1997) Poly(ethylene glycol), Chemistry and Biological Applications. ACS Symposium Series **680**, Washington.

Hartmann E, Sommer T, Prehn S, Görlich D, Jentsch S & Rapoport TA (1994) Evolutionary conservation of components of the protein translocation complex. *Nature* **367**:654-657.

Hartmann-Petersen R & Gordon C (2004) Protein degradation: recognition of ubiquitinylated substrates. *Curr Biol* **14(18)**:R754-R756.

Harty C, Sabine Strahl S & Römisch K (2001) O-mannosylation protects mutant alpha-factor precursor from endoplasmic reticulum-associated degradation. *Mol Biol Cell* **12**:1093-1101.

Heckman KL & Pease LR (2007) Gene splicing and mutagenesis by PCR-driven overlap extension. *Nature Protocols* **2 (4)**:924-932.

Hegde RS & Bernstein HD (2006) The surprising complexity of signal sequences. *Trends Biochem Sci* **31**:563-571.

Hegde NR, Chevalier MS, Wisner TW, Denton MC, Shire K, Frappier L & Johnson DC (2006) The role of BiP in endoplasmic reticulum-associated degradation of major histocompatibility complex class I heavy chain induced by cytomegalovirus proteins. *J Biol Chem* **282(30)**:20910-20919.

Hegde RS, Voigt S & Lingappa VR (1998) Regulation of protein topology by *trans*-acting factors at the endoplasmic reticulum. *Mol Cell* **2**:85-91.

Heinemeyer W, Fischer M, Krimmer T, Stachon U & Wolf DH (1997) The active sites of the eukaryotic 20 S proteasome and their involvement in subunit precursor processing. *J Biol Chem* **272**:25200-25209.

Helenius A (1994) How N-linked oligosaccharides affect glycoprotein folding in the endoplasmic reticulum. *Mol Biol Cell* **5**:253-265.

Helenius A & Aebi M (2004) Roles of N-Linked glycans in the endoplasmic reticulum. *Annu Rev Biochem* **73**:1019-1049.

Helenius A, Trombetta ES, Hebert DN & Simons JF (1997) Calnexin, calreticulin and the folding of glycoproteins. *Trends Cell Biol* **7**:193-200.

Helmers J, Schmidt D, Glavy JS, Blobel G & Schwartz T (2003) The beta-subunit of the protein-conducting channel of the endoplasmic reticulum functions as the guanine nucleotide exchange

factor for the beta-subunit of the signal recognition particle receptor. *J Biol Chem* **28(26)**:23686-23680.

Hendershot LM (2004) The ER function BiP is a master regulator of ER function. *Mt Sinai J Med* **71(5)**:289-297.

Hendershot LM, Wei JY, Gaut JR, Lawson B, Freiden PJ & Murti KG (1995) *In vivo* expression of mammalian BiP ATPase mutants causes disruption of the endoplasmic reticulum. *Mol Biol Cell* **6(3)**:283-296.

Hendershot LM, Wei JY, Gaut J, Melnick J, Aviel S & Argon Y (1996) Inhibition of immunoglobulin folding and secretion by dominant negative BiP ATPase mutants. *Proc Natl Acad Sci USA* **93(11)**:5269-5274.

Hendil KB, Kriegenburg F, Tanaka K, Murata S, Lauridsen AM, Johnsen AH, Hartmann-Petersen (2009) The 20S proteasome as an assembly platform for the 19S regulatory complex. *J Mol Biol* **394**:320-328.

Herrmann JM, Spang A (2008) Freight management in the cell: current aspects of intracellular membrane trafficking. *Methods Mol Biol* **457**:3-12.

Hermanson GT (2008) Bioconjugate techniques. 2nd ed. San Diego, CA: Academic Press.

Hershko A (1983) Ubiquitin: roles in protein modification and breakdown. *Cell* **34(1)**:11-12.

Hershko A & Ciechanover A (1998) The ubiquitin system. *Annu Rev Biochem* **67**:425-479.

Hershko A, Ciechanover A & Varshavsky A (2000) The ubiquitin system. *Nat Med* **10**:1073-1081.

Hershko A, Heller H, Elias S & Ciechanover A (1983) Components of ubiquitin–protein ligase system. Resolution, affinity purification, and role in protein breakdown. *J Biol Chem* **258**:8206-8214.

Hershko A, Leshinsky E, Ganoth D & Heller H (1984) ATP-dependent degradation of ubiquitin–protein conjugates. *Proc Natl Acad Sci* **81**:1619-1623.

Hicke L (2001) Protein regulation by monoubiquitin. *Nat Rev Mol Cell Biol* **2(3)**:195-201.

Higashio H & Kohno K (2002) A genetic link between the unfolded protein response and vesicle formation from the endoplasmic reticulum. *Biochem Biophys Res Commun* **296**:568-574.

Hill K & Cooper AA (2000) Degradation of unassembled Vph1p reveals novel aspects of the yeast ER quality control system. *EMBO J* **19**:550-561.

Hiller MM, Finger A, Schweiger M & Wolf DH (1996) ER degradation of a misfolded luminal protein by the cytosolic ubiquitin–proteasome pathway. *Science* **273**:1725-1728.

Hirano Y, Hayashi H, Iemura S, Hendil KB, Niwa S, Kishimoto T, Kasahara M, Natsume T, Tanaka K & Murata S (2006) Cooperation of multiple chaperones required for the assembly of mammalian 20S proteasomes. *Mol Cell* **24**:977-984.

Hirano Y, Kaneko T, Okamoto K, Bai M, Yashiroda H, Furuyama K, Kato K, Tanaka K & Murata S (2008) Dissecting β-ring assembly pathway oft he mammalian 20S proteasome. *EMBO J* **27**:2204-2213.

Hirao I, Kimoto M, Mitsui T, Fujiwara T, Kawai R, Sato A, Harada Y & Yokoyama S (2006) An unnatural hydrophobic base pair system: site-specific incorporation of nucleotide analogs into DNA and RNA. *Nature Methods* **3**:729–735.

Hitt R & Wolf DH (2004) Der1p, a protein required for degradation of malfolded soluble proteins of the endoplasmic reticulum: topology and Der1-like proteins. *FEMS Yeast Res* **4(7)**:721-729.

Ho SN, Hunt, HD, Horton RM, Pullen JK & Pease LR (1989) Site-directed mutagenesis by overlap extension using the polymerase chain reaction. *Gene* **77**:51-59.

Hoffman CS & Winston F (1987) A ten-minute DNA preparation from yeast efficiently releases autonomous plasmids for transformation of *Escherichia coli*. *Gene* **57(2-3)**:267-72.

Hofmann K, Hofmann K, Titus G, Montibeller JA & Finn FM (1982) Avidin binding of carboxyl-substituted biotin and analogues. *Biochemistry* **21**:978-984.

Hofmann RM & Pickart CM (2001) *In vitro* assembly and recognition of Lys-63 polyubiquitin chains. *J Biol Chem* **276**:27936-27943.

Holtzman JL (1997) The roles of the thiol:protein disulfide oxidoreductases in membrane and secretory protein synthesis within the lumen of the endoplasmic reticulum. *J Investig Med* **45**:28-34.

Hoppe T (2005) Multiubiquitylation by E4 enzymes: 'one size' doesn't fit all. *Trends Biochem Sci* **30(4)**:183-187.

Horn SC, Hanna J, Hirsch C, Volkwein C, Schutz A, Heinemann U, Sommer T & Jarosch E (2009) Usa1 functions as a scaffold of the HRD-ubiquitin ligase. *Mol Cell* **36**:782-793.

Horton RM, Hunt HS, Ho SN, Pullen JK & Pease LR (1989) Engineering hybrid genes without the use of restriction enzymes: gene splicing by overlap extension. *Gene* **77**:61-68.

Horwitz AA, Navon A, Groll M, Smith DM, Reis C & Goldberg AL (2007) ATP-induced structural transitions in PAN, the proteasome-regulatory ATPase complex in archaea. *J Biol Chem* **282**:22921-22929.

Hosokawa N, Kamiya Y & Kato K (2010) The role of MRH domain containing lectins in ERAD. *Glycobiology* **20 (6)**:651-660.

Hosokawa N, Wada I, Hasegawa K, Yorihuzi T, Tremblay LO, Herscovics A & Nagata K (2001) A novel ER alpha-mannosidase-like protein accelerates ER-associated degradation. *EMBO Rep* **2**:415-422.

Hough R, Pratt G & Rechsteiner M (1986) Ubiquitin-lysozyme conjugates. Identification and characterization of an ATP-dependent protease from rabbit reticulocyte lysates. *J Biol Chem* **261(5)**:2400-2408.

Huibregtse JM, Scheffner M, Beaudenon S & Howley PM (1995) A family of proteins structurally and functionally related to the E6-AP ubiquitin-protein ligase. *Proc Natl Acad Sci USA* **92**:2563-2567.

Huppa JB & Ploegh HL (1997) *In Vitro* translation and assembly of a complete T cell receptor–CD3 complex. *J Ex Med* **186**:393-403.

Husnjak K, Elsasser S, Zhang N, Chen X, Randles, Shi Y, Hofmann K, Walters KJ, Finley D &

Dikic I (2008) Proteasome subunit Rpn13 is a novel ubiquitin receptor. *Nature* **453(7194)**:481-488.

Hutagalung AH & Novick PJ (2011) Role of Rab GTPases in membrane traffic and cell physiology. *Physiol Rev* **91(1)**:119-149.

Huyer G, Longsworth GL, Mason DL, Mallampalli MP, McCaffery JM, Wright RL & Michaelis S (2004a) A striking quality control subcompartment in *Saccharomyces cerevisiae*: The Endoplasmic Reticulum-associated compartment. *Mol Biol Cell* **15**:908-921.

Huyer G, Piluek WF, Fansler Z, Kreft SG, Hochstrasser M, Brodsky JL & Michaelis S (2004b) Distinct machinery is required in *Saccharomyces cerevisiae* for the endoplasmic reticulum-associated degradation of a multispanning membrane protein and a soluble luminal protein. *J Biol Chem* **279(37)**:38369-38378.

Ichihara A (2010) Reminiscence of 40-year research on nitrogen metabolism. *Proc Jpn Acad Ser B Phys Biol Sci* **86(7)**:707-716.

Imai J, Hasegawa H, Maruya M, Koyasu S & Yahara I (2005) Exogenous antigens are processed through the endoplasmic reticulum-associated degradation (ERAD) in cross-presentation by dendritic cells. *Int Immunol* **17**:45-53.

Imai Y, Soda M, Inoue H, Hattori N, Mizuno Y & Takahashi R (2001) An unfolded putative transmembrane polypeptide, which can lead to Endoplasmic Reticulum stress, is a substrate of Parkin. *Cell* **105**:891-902.

Isakov E & Stanhill A (2011) Stalled proteasomes are directly relieved by p97 recruitment. *J Biol Chem* **286**:5609-5618.

Jackson MR, Nilsson T & Peterson PA (1990) Indentification of a consensus motif for retention of transmembrane proteins in the endoplasmid reticulum. *EMBO J* **9**:3153-3162.

Jackson MR, Nilsson T & Peterson PA (1993) Retrieval of transmembrane proteins to the endoplasmic reticulum. *J Cell Biol* **121**:317-333.

Jäger R, Bertrand MJ, Gorman AM, Vandenabeele P & Samali A (2012) The unfolded protein response at the crossroads of cellular life and death during endoplasmic reticulum stress. *Biol Cell* **104(5)**:259-270.

Jahn TR & Radford SE (2005) The Yin and Yang of protein folding. *FEBS J* **272(23)**:5962-5970.

Jahn R & Südhof TC (1999) Membrane fusion and exocytosis. *Annu Rev Biochem* **68**:863-911.

Jakob CA, Bodmer P, Spirig U, Battig P, Marcil A, Dignard D, Bergeron JJ, Thomas DY & Aebi M (2001) Htm1p, a mannosidase-like protein, is involved in glycoprotein degradation in yeast. *EMBO Rep* **2(5)**:423-430.

Jakob CA, Burda P, Roth J & Aebi M (1998) Degradation of misfolded endoplasmic reticulum glycoproteins in Saccharomyces cerevisiae is determined by a specific oligosaccharide structure. *J Cell Biol* **142(5)**:1223-1233.

Jensen TJ, Loo MA, Pind S, Williams DB, Goldberg AL & Riordan JR (1995) Multiple proteolytic systems, including the proteasome, contribute to CFTR processing. *Cell* **83**:129-135.

Jentsch S (1992) The ubiquitin-conjugation system. *Annu RevGenet* **26**:179-207.

Jentsch S & Rumpf S (2007) Cdc48 (p97): a "molecular gearbox" in the ubiquitin pathway? *Trends Biochem Sci* **32**:6-11.

Jiang Y, Cheng Z, Mandon EC & Gilmore R (2008) An interaction between the SRP receptor and the translocon is critical during cotranslational protein translocation. *J Cell Biol* **180(6)**:1149-1161.

Jin R, Dobry CJ, McCown PJ & Kumar A (2008) Large-scale analysis of yeast filamentous growth by systematic gene disruption and overexpression. *Mol Biol Cell* **19(1)**:284-296.

Johnson AE & Haigh NG (2000) The ER translocon and retrotranslocation: is the shift into reverse manual or automatic? *Cell* **102**:709-712.

Johnson AE & van Waes MA (1999) The translocon: a dynamic gateway at the ER membrane. *Annu Rev Cell Dev Biol* **15**:799-842.

Jones DT (1999) Protein secondary structure prediction based on position-specific scoring matrices. *J Mol Biol* **292**:195-202.

Julius D, Blair L, Brake A, Sprague G & Thorner J (1983) Yeast a-factor is processed from a larger precursor polypeptide: the essential role of a membrane-bound dipeptidyl aminopeptidase. *Cell* **32**:839-852.

Julius D, Brake A, Blair L, Kunisawa R & Thorner J (1984a) Isolation of the putative structural gene for the lysine-arginine-cleaving endopeptidase required for processing of yeast prepro-α-factor. *Cell* **37**:1075-1089.

Julius D, Schekman R & Thorner J (1984b) Glycosylation and processing of prepro-α-factor through the yeast secretory pathway. *Cell* **36**:309-318.

Jung & Grune T (2008) The proteasome and its role in the degradation of oxidized proteins. *IUBMB Life* **60**:743-752.

Jungnickel B & Rapoport TA (1995) A posttargeting signal sequence recognition event in the endoplasmic reticulum membrane. *Cell* **82**:261-270.

Junne T, Kocik L & Spiess M (2010) The hydrophobic core of the Sec61 translocon defines the hydrophobicity threshold for membrane integration. *Mol Biol Cell* **21**:1662-1670.

Kabani M, Kelley SS, Morrow MW, Montgomery DL, Sivendran R, Rose MD, Gierasch LM & Brodsky JL (2003) Dependence of endoplasmic reticulum-associated degradation on the peptide binding domain and concentration of BiP. *Mol Biol Cell* **14(8)**:3437-3448.

Kaiser C, Michaelis S & Mitchell A (1994) *Methods in Yeast Genetics*. *A Cold Spring Harbor Laboratory Course Manual*. Cold Spring Harbor Laboratory Press, Cold Spring Harbor, NY.

Kajava AV (2002) What curves alpha-solenoids? Evidence for an alpha-helical toroid structure of Rpn1 and Rpn2 proteins of the 26 S proteasome. *J Biol Chem* **277**:49791-49798.

Kalies KU, Allan S, Sergeyenko T, Kroger H & Romisch K (2005) The protein translocation channel binds proteasomes to the endoplasmic reticulum membrane. *EMBO J* **24**:2284-2293.

Kalies KU, Gorlich D, Rapoport TA (1994) Binding of ribosomes to the rough endoplasmic reticulum mediated by the Sec61p-complex. *J Cell Biol* **126**:925-934

Kalies KU & Hartmann E (1998) Protein translocation into the endoplasmic reticulum (ER) - Two similar routes with different modes. *Eur J Biochem* **254(1)**:1-5.

Kalies KU, Rapoport TA & Hartmann E (1998) The beta subunit of the Sec61 complex facilitates cotranslational protein transport and interacts with the signal peptidase during translocation. *J Cell Biol* **141:**887-894.

Kampinga HH & Craig EA (2010) The HSP70 chaperone machinery: J proteins as drivers of functional specificity. *Nat Rev Mol Cell Biol* **11(8)**:579-592.

Kanapin A, Batalov S, Davis MJ, Gough J, Grimmond S, Kawaji H, Magrane M, Matsuda H, Schönbach C, Teasdale RD, RIKEN GER Group and GSL Members & Yuan Z (2003) Mouse proteome analysis. *Genome Res* **13**:1335-1344.

Kanehara K, Kawaguchi S & Ng DT (2007) The EDEM and Yos9p families of lectin-like ERAD factors. *Semin. Cell Dev Biol* **18**:743-750.

Kaneko T, Hamazaki J, Iemura s, Sasaki K, Furuyama K, Natsume T, Tanaka K & Murata (2009) Assembly pathway of the Mammalian proteasome base subcomplex is mediated by multiple specific chaperones. *Cell* 137:914-925.

Katiyar S, Joshi S & Lennarz WJ (2005) The Retrotranslocation Protein Derlin-1 Binds Peptide:*N*-Glycanase to the Endoplasmic Reticulum. *Mol Biol Cell* **16(10)**:4584-4594.

Kawahara T, Yanagi H, Yura T & Mori K (1997) Endoplasmic reticulum stress-induced mRNA splicing permits synthesis of transcription factor Hac1p/Ern4p that activates the unfolded protein response. *Mol Biol Cell* **8**:1845-1862.

Kawahara T, Yanagi H, Yura T & Mori K (1998) Unconventional splicing of *HAC1/ERN4* mRNA required for the unfolded protein response. Sequence-specific and non-sequential cleavage of the splice sites. *J Biol Chem* **273(3)**:1802-1807.

Keenan RJ, Freymann DM, Stroud RM & Walter P (2001) The signal recognition particle. *Annu Rev Biochem* **70**:755-775.

Kerfeld, CA, Sawaya, MR, Tanaka, S, Nguyen, CV, Phillips, M, Beeby, M, Yeates, TO (2005) Protein structures forming the shell of primitive bacterial organelles. *Science* **309(5736)**:936-938.

Kerscher O, Felberbaum R & Hochstrasser M (2006) Modification of proteins by ubiquitin and ubiquitin-like proteins. *Annu Rev Cell Dev Biol* **22**:159-180.

Kim DH & Hwang I (2013) Direct Targeting of Proteins from the Cytosol to Organelles: The ER versus endosymbiotic organelles. *Traffic* **14**: 613-621.

Kim HT, Kim KP, Lledias F, Kisselev AF, Scaglione KM, Skowyra D, Gygi SP & Goldberg AL (2007) Certain pairs of ubiquitin-conjugating enzymes (E2s) and ubiquitin-protein ligases (E3s) synthesize nondegradable forked ubiquitin chains containing all possible isopeptide linkages. *J Biol Chem* **282**:17375-17386.

Kim W, Spear ED & Ng DTW (2005) Yos9p detects and targets misfolded glycoproteins for ER-associated degradation. *Mol Cell* **19**:753-764.

Kimata Y, Kimata YI, Shimizu Y, Abe H, Farcasanu IC, Takeuchi M, Rose MD & Kohno K (2003) Genetic evidence for a role of BiP/Kar2 that regulates Ire1 in response to accumulation of unfolded proteins. *Mol Biol Cell* **14(6)**:2559-2569.

Kimata Y, Oikawa D, Shimizu Y, Ishiwata-Kimata Y & Kohno K (2004) A role for BiP as an adjustor for the endoplasmic reticulum stress-sensing protein Ire1. *J Cell Biol* **167(3)**:445-456.

Kimura T, Hosoda Y, Sato Y, Kitamura Y, Ikeda T, Horibe T & Kikuchi M (2005) Interactions among yeast protein-disulfide isomerase proteins and endoplasmic reticulum chaperone proteins influence their activities. *J Biol Chem* **280(36)**:31438-31441.

Kimura Y, Yahara I & Lindquist S (1995) Role of the protein chaperone YDJ1 in establishing Hsp90-mediated signal transduction pathways. *Science* **268 (5215)**:1362-1365.

Kisselev AF, Akopian TN, Castillo V & Goldberg AL (1999) Proteasome active sites allosterically regulate each other, suggesting a cyclical bite-chew mechanism for protein breakdown. *Mol Cell* **4**:395-402.

Kisselev AF, Callard A & Goldberg AL (2006) Importance of the different proteolytic sites of the proteasome and the efficacy of inhibitors varies with the protein substrate. *J Biol Chem* **281**:8582-8590.

Klionsky DJ (2007) Autophagy: from phenomenology to molecular understanding in less than a decade. *Nat Rev Mol Cell Biol* **8**:931-937.

Klumperman J (2000) Transport between ER and Golgi. *Curr Opin Cell Biol* **12**:445-449.

Knight BC & High S (1998) Membrane integration of Sec61alpha: a core component of the endoplasmic reticulum translocation complex *Biochem J* **331**:161-167.

Knittler MR, Dirks S & Haas IG (1995) Molecular chaperones involved in protein degradation in the endoplasmic reticulum: quantitative interaction of the heat shock cognate BiP with partially folded immunoglobulin light chains that are degraded in the endoplasmic reticulum. *Proc Natl Acad Sci USA* **92**:1764-1768.

Knop M, Finger A, Braun T, Hellmuth K & Wolf DH (1996a) Der1, a novel protein specifically required for endoplasmic reticulum degradation in yeast. *EMBO* **15**:753-763.

Knop M, Hauser N & Wolf DH (1996b) N-Glycosylation affects endoplasmic reticulum degradation of a mutated derivative of carboxypeptidase yscY in yeast. *Yeast* **12(12)**:1229-1238.

Koegl M, Hoppe T, Schlenker S, Ulrich HD, Mayer TU & Jentsch S (1999) A novel ubiquitination factor, E4, is involved in multiubiquitin chain assembly. *Cell* **96(5)**:635-644.

Kölling R & Hollenberg CP (1994) The ABC-transporter Ste6 accumulates in the plasma membrane in a ubiquitinated form in endocytosis mutants. *EMBO J* **13**:3261-3271.

Kölling R & Losko S (1997) The linker region of the ABC transporter Ste6 mediates ubiquitination and fast turnover of the protein. *EMBO J* **16**:225-2261.

Kohno K, Normington K, Sambrook J, Gething MJ & Mori K (1993) The promoter region of the yeast KAR2 (BiP) gene contains a regulatory domain that responds to the presence of unfolded proteins in the endoplasmic reticulum. *Mol Cell Biol* **13(2)**:877-890.

Koivu J, Myllylä R, Helaakoski T, Pihlajaniemi T, Tasanen K & Kivirikko KI (1987) A single polypeptide acts both as the beta subunit of prolyl 4–hydroxylase and as a protein disulfide-isomerase. *J Biol Chem* **262(14)**:6447-6449.

Komitzer D & Ciechanover A (2000) Modes of regulation of ubiquitin-mediated protein degradation. *J Cell Physiol* **182(1)**:1-11.

Korennykh AV, Egea PF, Korostelev AA, Finer-Moore J, Zhang C, Shokat KM, Stroud RM & Walter P (2009) The unfolded protein response signals through high-order assembly of Ire1. *Nature* **457(7230)**:687-693.

Korennykh AV, Korostelev AA, Egea PF, Finer-Moore J, Stroud RM, Zhang C, Shokat KM, & Walter P (2011) Structural and functional basis for RNA cleavage by Ire1. *BMC Biol* **9(1)**:47.

Korennykh A & Walter P (2012) Structural basis of the unfolded protein response. *Annuv Rev Cell Dev Biol* **28**:251-277.

Kostova Z & Wolf DH (2003) For whom the bell tolls: protein quality control of the endoplasmic reticulum and the ubiquitin-proteasome connection. *EMBO J* **22**:2309-2317.

Kostova Z & Wolf DH (2005) Importance of carbohydrate positioning in the recognition of mutated CPY for ER-associated degradation. *J Cell Sci* **118**:1485-1492.

Kozutsumi Y, Segal M, Normington K, Gething MJ & Sambrook J (1988) The presence of malfolded proteins in the endoplasmic reticulum signals the induction of glucose-regulated proteins. *Nature* **332**:462-464.

Kreft SG, Wang L & Hochstrasse M (2006) Membrane topology of the yeast endoplasmic reticulum-localized ubiquitin ligase Doa10 and comparison with its human ortholog TEB4 (MARCH-VI). *J Biol Chem* **281(8)**:4646-4653.

Krick R, Bremer S, Welter E, Schlotterhose P, Muehe Y, Eskelinen EL & Thumm M (2010) Cdc48/p97 and Shp1/p47 regulate autophagosome biogenesis in concert with ubiquitin-likeAtg8. *J Cell Biol* **190**:965-973.

Krieg PA & Melton DA (1987) Functional messenger RNAs are produced by SP6 *in vitro* transcritption of cloned cDNAs. *Nucleic Acids Res* **12**:7057-7070.

Krieg UK, Walter P & Johnson AE (1986) Photocrosslinking of the signal sequence of nascent preprolactin to the 54-kilodalton polypeptide of the signal recognition particle. *Proc Natl Acad Sci USA* **83**:8604-8608.

Kriegenburg F, Seeger M, Saeki Y, Tanaka K, Lauridsen AMB & Hartmann-Petersen R (2008) Mammalian 26S proteasomes remain intact during protein degradation. *Cell* **135(2)**:355-365.

Krogan NJ, Cagney G, Yu H, Zhong G, Guo X, Ignatchenko A, Li J, Pu S, Datta N, Tikuisis AP, Punna T, Peregrín-Alvarez JM, Shales M, Zhang X, Davey M, Robinson MD, Paccanaro A, Bray JE, Sheung A, Beattie B, Richards DP, Canadien V, Lalev A, Mena F, Wong P, Starostine A, Canete MM, Vlasblom J, Wu S, Orsi C, Collins SR, Chandran S, Haw R, Rilstone JJ, Gandi K, Thompson NJ, Musso G, St Onge P, Ghanny S, Lam MHY, Butland G, Altaf-Ul AM, Kanaya S, Shilatifard A, O'Shea E, Weissman JS, Ingles CJ, Hughes TR, Parkinson J, Gerstein M, Wodak SJ, Emili A & Greenblatt JF (2006) Global landscape of protein complexes in the yeast *Saccharomyces cerevisiae*. *Nature* **440**:637-643.

Kruse M, Brunke M, Escher A, Szalay AA, Tropschug M & Zimmermann R (1995) Enzyme assembly after *de novo* synthesis in rabbit reticulocyte lysate involves molecular chaperones and immunophilins. *J Biol Chem* **270**:2588-2594.

Kuchler K, Sterne RE & Thorner J (1989) *Saccharomyces cerevisiae STE6* gene product: a novel

pathway for protein export in eukaryotic cells. *EMBO J* **8**:3973-3984.

Kuglstatter A, Oubridge C & Nagai K (2002) Induced structural changes of 7SL RNA during the assembly of human signal recognition particle. *Nat Struct Biol* **9:**740-744.

Kumar S, Yoshida Y, Noda M (1993) Cloning of a cDNA which encodes a novel ubiquitin-like protein. *Biochem Biophys Res Commun* **195(1)**:393-399.

Kunjappu MJ & Hochstrasser M (2014) Assembly of the 20S proteasome. *Biochim Biophys Acta* **1843(1)**:2-12.

Kunkel TA Roberts JD & Zakour RA (1987) Rapid and efficient site-specific mutagenesis without phenotypic selection. *Methods Enzymol* **154**:367-382.

Kuo SC & Lampen JO (1974) Tunicamycin - an inhibitor of yeast glycoprotein synthesis. *Biochem Biophys Res Commun* **58(1)**:287-295.

Kurjan J & Herskowitz I (1982) Structure of a yeast pheromone gene (MF alpha): A putative alpha-factor precursor contains four tandem copies of mature alpha-factor. *Cell* **30**:933-943.

Kurzchalia TV, Wiedman M, Girshovich AS, Bochkareva ES, Bielka H & Rapoport TA (1986) The signal sequence of nascent preprolactin interacts with the 54K polypeptide of the signal recognition particle. *Nature*, **320**:634-636.

Kusmierczyk AR, Kunjappu MJ, Funakoshi M & Hochstrasser M (2008) A multimeric assembly factor controls the formation of alternative 20S proteasomes. *Nat Struct Biol* **15**:237-244.

Kutay U, Ahnert-Hilger G, Hartmann E, Wiedenmann B & Rapoport TA (1995) Transport route for synaptobrevin via a novel pathway of insertion into the endoplasmic reticulum membrane. *EMBO J* **14**:217-223.

Laboissiere MC, Sturley SL & Raines RT (1995) The essential function of protein-disulfide isomerase is to unscramble non-native disulfide bonds. *J Biol Chem* **270(47)**:28006-28009.

Lacroute F (1968) Regulation of pyrimidine biosynthesis in *Saccharomyces cerevisiae*. *J Bacteriol* **95(3)**:824-832.

Lakkaraju AK, Scherrer MC, Johnson AE & Strub K (2008) SRP keeps polypeptides translocation-competent by slowing translation to match limiting ER-targeting sites. *Cell* **133(3)**:440-451.

Lakkaraju AK, Thankappan R, Mary C, Garrison JL, Taunton J & Strub K (2012) Efficient secretion of small proteins in mammalian cells relies on Sec62-dependent posttranslational translocation. *Mol Biol Cell* **23(14)**: 2712-2722.

Lam YA, Xu W, DeMartino GN & Cohen RE (1997) Editing of ubiquitin conjugates by an isopeptidase in the 26S proteasome. *Nature* **385(6618)**:737-740.

Lander GC, Estrin E, Matyskiela ME, Bashore C, Nogales E & Martin A (2012) Complete subunit architecture of the proteasome regulatory particle. *Nature* **482**:186-191.

Lang S, Benedix J, Fedeles SV, Schorr S, Schirra C, Schäuble N, Jalal C, Greiner M, Haßdenteufel S, Tatzelt J, Kreutzer B, Edelmann L, Krause E, Rettig J, Somlo S, Zimmermann R & Dudek J (2012) Different effects of Sec61α, Sec62 and Sec61 depletion on

transport of polypeptides into the endoplasmic reticulum of mammalian cells. *J Cell Sci* **125(8)**:1958-1969.

Langan TJ & Slater MC (1991) Isoprenoids and astroglial cell cycling: diminished mevalonate availability and inhibition of dolichol-linked glycoprotein synthesis arrest cycling through distinct mechanisms. *J Cell Physiol* **149**:284-292.

Larsen CN & Finley D (1997) Protein translocation channels in the proteasome and other proteases. *Cell* **91(4)**:431-434.

Lasker K, Förster F, Bohn S, Walzthoeni T, Villa E, Unverdorben P, Beck F, Aebersold R, Sali A & Baumeister W (2012) Molecular architecture of the 26S proteasome holocomplex determined by an integrative approach. *Proc Natl Acad Sci USA* **109(5)**:1380-1387.

Lee AS (1987) Coordinated regulation of a set of genes by glucose and calcium ionophores in mammalian cells. *Trends Biochem Sci* **72**:20-23.

Lee RJ, Liu C-W, Harty C, McCracken AA, Latterich M, Römisch K, DeMartino GN, Thomas PJ & Brodsky JL (2004a) Uncoupling retro-translocation and degradation in the ER-associated degradation of a soluble protein. *EMBO J* **23**: 2206-2215.

Lee RJ, Liu C, Harty C, McCracken AA, Romisch K, DeMartino GN, Thomas PJ & Brodsky JL (2004b) The 19S cap of the 26S proteasome is sufficient to retro-translocate and deliver a soluble polypeptide for ER-associated degradation. *EMBO J* **23**:2206-2215.

Lee MC, Miller EA, Goldberg J, Orci L & Schekman R (2004c) Bi-directional protein transport between the ER and Golgi. *Annu Rev Cell Dev Biol* **20**:87-123.

Lee AH, Scapa E, Cohen D & Glimcher L (2008) Regulation of hepatic lipogenesis by the transcription factor XBP1. *Science* **320**:1492-1496.

Lee DH, Sherman MY & Goldberg AL (1996) Involvement of the molecular chaperone Ydj1 in the ubiquitin-dependent degradation of short-lived and abnormal proteins in *Saccharomyces cerevisiae*. *Mol Cell Biol* **16(9)**:4773-4781.

Lee K, Tirasophon W, Shen X, Michalak M, Prywes R, Okada T, Yoshida H, Mori K & Kaufman RJ (2002) IRE1-mediated unconventional mRNA splicing and S2P-mediated ATF6 cleavage merge to regulate XBP1 in signaling the unfolded protein response. *Genes Dev* **16(4)**:452-466.

Legate KR, Falcone D & Andrews DW (2000) Nucleotide-dependent binding of the GTPase domain of the signal recognition particle receptor beta-subunit to the alpha-subunit. *J Biol Chem* **275**:27439-27446.

Leggett DS, Glickman MH & Finley D (2005) Purification of proteasomes, proteasome subcomplexes, and proteasome-associated proteins from budding yeast. *Methods in Molecular Biology* **301**:57-70.

Leggett DS, Hanna J, Borodovsky A, Crosas B, Schmidt M, Baker RT, Walz T, Ploegh H & Finley D (2002) Multiple associated proteins regulate proteasome structure and function. *Mol Cell* **10(3)**:495-507.

Lehle L, Strahl S & Tanner W (2006) Protein glycosylation, conserved from yeast to man: a model organism helps elucidate congenital human diseases. *Angewandte Chemie* (International Ed.) **45(41)**:6802-6818.

Lemmon SK (2001) Clathrin uncoating: Auxilin comes to life. *Curr Biol* **11**:R49-R52.

Letunic I, Doerks T & Bork P (2009) SMART 6: recent updates and new developments. *Nucleic Acids Res* **37**:D229-D232.

Levy R, Wiedmann M & Kreibich G (2001) *In vitro* binding of ribosomes to the beta subunit of the Sec61p protein translocation complex. *J Biol Chem* **276**:2340-2346.

Li W, Schulman S, Boyd D, Erlandson K, Beckwith J & Rapoport TA (2007) The plug domain of the SecY protein stabilizes the closed state of the translocation channel and maintains a membrane seal. *Mol Cell* **26**:511-521.

Li W, Tu D, Brunger AT & Ye Y (2007) A ubiquitin ligase transfers preformed polyubiquitin chains from a conjugating enzyme to a substrate. *Nature* **446**:333-337.

Lilley BN, Gilbert JM, Ploegh HL & Benjamin TL (2006) Murine polyomavirus requires the endoplasmic reticulum protein Derlin-2 to initiate infection. *J Virol* **80**:8739-8744.

Lilley BN & Ploegh HL (2004) A membrane protein required for dislocation of misfolded proteins from the ER. *Nature* **429(6994)**:834-840.

Lilley BN & Ploegh HL (2005) Ploegh Multiprotein complexes that link dislocation, ubiquitination, and extraction of misfolded proteins from the endoplasmic reticulum membrane. *Proc Natl Acad Sci USA* **102**:14296-14301.

Lippincott-Schwartz J, Bonifacino JS Yuan IC & Klausner RD (1998) Degradation from the endoplasmic reticulum: disposing of newly synthesized proteins. *Cell* **54**:209-220.

Liu Y, Choudhury P, Cabral CM & Sifers RN (1997) Intracellular disposal of incompletely folded human α1-antitrypsin involves release from calnexin and post-translational trimming of asparagine-linked oligosaccharides. *J Biol Chem* **272**:7946-7951.

Liu YP, Choudhury P, Cabral CM & Sifers RN (1999) Oligosaccharide modification in the early secretory pathway directs the selection of a misfolded glycoprotein for degradation by the proteasome. *J Biol Chem* **274**:5861-5867.

Liu CW, Corboy MJ, DeMartino GN & Thomas PJ (2003) Endopoteolytic activity of the proteasome. *Science* **299**:408-411.

Liu CW, Millen L, Roman TB, Xiong H, Gilbert HF, Noiva R, DeMartino GN & Thomas PJ (2002) Conformational remodeling of proteasomal substrates by PA700, the 19S regulatory complex of the 26S proteasome. *J Biol Chem* **277**:26815-26820.

Lloyd DJ, Wheeler MC & Gekakis N (2010) A point mutation in Sec61a1 leads to diabetes and hepatosteatosis in mice. *Diabetes* **59**:460-470.

Loayza D & Michaelis S (1998) Role for the ubiquitin-proteasome system in the vacuolar degradation of Ste6p, the a-factor transporter in *Saccharomyces cerevisiae*. *Mol Cell Biol* **18**:779-789.

Loayza D, Tam A, Schmidt WK & Michaelis S (1998) Ste6p mutants defective in exit from the endoplasmic reticulum (ER) reveal aspects of an ER Quality Control pathway in *Saccharomyces cerevisiae*. *Mol Biol Cell* **9**:2767-22784.

Lodder AL, Lee TK & Ballester R (1999) Characterization of the Wsc1 protein, a putative receptor in the stress response of *Saccharomyces cerevisiae*. *Genetics* **152**:1487-1499.

Lorick KL, Jensen JP, Fang S, Ong AM, Hatakeyama S & Weissman AM (1999) RING fingers mediate ubiquitin-conjugating enzyme (E2)-dependent ubiquitination. *Proc Natl Acad Sci USA* **96**:11364-11369.

Losev E, Reinke CA, Jellen J, Strongin DE, Bevis BJ & Glick BS (2006) Golgi maturation visualized in living yeast. *Nature* **441**:1002-1006.

Lowe J, Stock D, Jap B, Zwickl P, Baumeister W & Huber R (1995) Crystal structure of the 20S proteasome from the archaeon *T. acidophilum* at 3.4 A resolution. *Science* **268**:533-539.

Lucero HA, Chojnicki EW, Mandiyan S, Nelson H & Nelson N (1995) Cloning and expression of a yeast gene encoding a protein with ATPase activity and high identity to the subunit 4 of the human 26 S protease. *J Biol Chem* **270(16)**:9178-9184.

Lütcke H, High S, Römisch K, Ashford AJ & Dobberstein B (1992) The methionine-rich domain of the 54 kDa subunit of signal recognition particle is sufficient for the interaction with signal sequences. *EMBO J* **11:**1543-1551.

Lukacs GL & Verkman AS (2012) CFTR: folding, misfolding and correcting the ΔF508 conformational defect. *Trends Mol Med* **18(2)**:81-91.

Lupas A, Baumeister W & Hofmann K (1997a) A repetitive sequence in subunits of the 26S proteasome and 20S cyclosome (anaphase-promoting complex). *Trends Biochem Sci* **22**:195-196.

Lupas A, Flanagan JM, Tamura T & Baumeister W (1997b) Self-compartmentalizing proteases. *Trends Biochem Sci* **22**:399-404.

Lyman SK & Schekman R (1995) Interaction between BiP and Sec63p is required for the completion of protein translocation into the ER of *Saccharomyces cerevisiae. J Cell Biol* **131**:1163-1171.

Lyman SK & Schekman R (1997) Binding of secretory precursor polypeptides to a translocon subcomplex is regulated by BiP. *Cell* **88(1)**:85-96.

Ma W & Goldberg J (2013) Rules for the recognition of dilysine retrieval motifs by coatomer. *EMBO J* **32(7)**:926-937.

Ma YJ & Hendershot LM (2001) The unfolding tale of the unfolded protein response. *Cell* **107**:827-830.

Maccecchini ML, Rudin Y, Blobel G & Schatz G (1979) Import of proteins into mitochondria: precursor forms of the extramitochondrially made F1-ATPase subunits in yeast. *Proc Natl Acad Sci USA* **76**:343-347.

Mades A, Gotthardt K, Awe K, Stieler J, Doring T, Fuser S & Prange R (2012) Role of human sec63 in modulating the steady-state levels of multi-spanning membrane proteins. *PLoS One* **7(11)**:e49243.

Madsen L, Seeger M, Semple CA & Hartmann-Petersen R (2009) New ATPase regulators - p97 goes to the PUB. *Int J Biochem Cell Biol* **41**:2380-2388.

Määttänen P, Gehring K, Bergeron JJ & Thomas DY (2010) Protein quality control in the ER: the recognition of misfolded proteins. *Sem Cell Dev Biol* **21**:500-511.

Manting EH, van Der Does C, Remigy H, Engel A & Driessen AJ (2000) SecYEG assembles into a tetramer to form the active protein translocation channel. *EMBO J* **19**:852-861.

Martin W (2010) Evolutionary origins of metabolic compartmentalization in eukaryotes. *Philos Trans R Soc Lond B Biol Sci* **365(1541)**:847-855.

Martoglio B & Dobberstein B (1998) Signal sequences: More than just greasy peptides. *Trends Cell Biol* **8(10)**:410-415.

Mason N, Ciufo LF & Brown JD (2000) Elongation arrest is a physiologically important function of signal recognition particle. *EMBO J* **19**:4164-4174.

Mast SW, Diekman K, Karaveg K, Davis A, Sifers RN & Moremen KW (2005) Human EDEM2, a novel homolog of family 47 glycosidases, is involved in ER-associated degradation of glycoproteins. *Glycobiology* **15**:421-436.

Matlack KE, Misselwitz B, Plath K & Rapoport TA (1999) BiP acts as amolecular ratchet during posttranslational transport of prepro-alpha factor across the ERmembrane. *Cell* **97**:553-564.

Matlack KE, Mothes W & Rapoport TA (1998) Protein translocation: tunnel vision. *Cell* **92(3)**:381-390.

Matlack KE, Plath K, Misselwitz B & Rapoport TA (1997) Protein transport by purified yeast Sec complex and Kar2p without membranes. *Science* **277**:938-941.

Mayer A (1999) Intracellular membrane fusion: SNAREs only? *Curr Opin Cell Biol* **11(4)**:447-452.

Mayer T, Braun T & Jentsch S (1998) Role of the proteasome in membrane extraction of a short-lived ER-transmembrane protein. *EMBO J* **17**:3251-3257.

Mayinger, P & Meyer, DI (1993). An ATP transporter is required for protein translocation into the yeast endoplasmic reticulum. *EMBO J* **12(2)**:659-666.

McClellan AJ, Tam S, Kaganovich D & Frydman J (2005) Protein quality control: chaperones culling corrupt conformations. *Nat Cell Biol* **7**:736-741.

McCracken AA & Brodsky JL (1996) Assembly of ER-associated protein degradation *in vitro*: dependence on cytosol, calnexin, and ATP. *J Cell Biol* **132**:291-298.

McGeoch DJ (1985) On the predictive recognition of signal peptide sequences. *Virus Res* **3**:271-286.

Medicherla B, Kostova Z, Schaefer A & Wolf DH (2004) A genomic screen identifies Dsk2p and Rad23p as essential components of ER-associated degradation. *EMBO Rep* **5(7)**:692-697.

Mehnert M, Sommer T & Jarosch E (2010) ERAD ubiquitin ligases: multifunctional tools for protein quality control and waste disposal in the endoplasmic reticulum. *Bioessays* 32:905-913.

Mehnert M, Sommer T & Jarosch E (2014) Der1 promotes movement of misfolded proteins through the endoplasmic reticulum membrane. *Nat Cell Biol* **16**:77-86.

Meldolesi J & Pozzan T (1998) The endoplasmic reticulum $Ca2^{+}$ store: a view from the lumen. *Trends Biochem Sci* **23(1)**:10-14.

Mellman I & Warren G (2000) The road taken: the past and future foundations of membrane traffic. *Cell* **100**:99-112.

Mendoza JL, Schmidt A, Li Q, Nuvaga E, Barrett T, Bridges RJ, Feranchak AP, Brautigam CA & Thomas PJ (2012) Requirements for efficient correction of DeltaF508 CFTR revealed by analyses of evolved sequences. *Cell* **148**:164-174.

Menetret JF, Neuhof A, Morgan DG, Plath K, Radermacher M, Rapoport TA & Akey CW (2000) The structure of ribosome-channel compexes engaged in protein translocation. *Mol Cell* **6**:1219-1232.

Menzel R, Vogel F, Kargel E & Schunck WH (1997) Inducible membranes in yeast: relation to the unfolded-protein-response pathway. *Yeast* **13**:1211-1229.

Merksamer PI, Trusina A & Papa FR (2008) Real-time redox measurements during endoplasmic reticulum stress reveal interlinked protein folding functions. *Cell* **135**:933-947.

Meusser B, Hirsch C, Jarosch E & Thomas Sommer (2005) ERAD: the long road to destruction. *Nature Cell Biol* **7(8):**766-772.

Meyer HA, Grau H, Kraft R, Kostka S, Prehn S, Kalies KU & Hartmann E (2000) Mammalian Sec61 is associated with Sec62 and Sec63. *J Biol Chem* **275**:14550-14557.

Meyer DI, Kranse E & Dobberstein B (1982) Secretory protein translocation across membranes - the role of the "docking protein. *Nature* **297**:503-508.

Meyer, H. & Popp, O (2008) Role(s) of Cdc48/p97 in mitosis. *Biochem Soc Trans* **36**:126-130.

Michaelis S (1993) STE6, the yeast a-factor transporter. *Semin Cell Biol* **4(1)**:17-27.

Miller, JH (1972) *Experiments in Molecular Genetics* (Cold Spring Harbor Laboratory, Cold Spring Harbor, NY).

Miller S & Krijnse-Locker J (2008) Modification of intracellular membrane structures for virus replication. *Nat Rev Microbiol* **6(5)**:363-374.

Miller JD, Tajima S, Lauffer L & Walter P (1995) The beta subunit of the signal recognition particle receptor is a transmembrane GTPase that anchors the alpha subunit, a peripheral membrane GTPase, to the endoplasmic reticulum membrane. *J Cell Biol* **128(3)**:273-282.

Milstein C, Brownlee GG, Harrison TM & Mathews MB (1972) A possible precursor of immunoglobulin light chains. *Nature New Biol* **239**:117-120.

Misselwitz B, Staeck O, Matlack KE & Rapoport TA (1999) Interaction of BiP with the J-domain of the Sec63p component of the endoplasmic reticulum protein translocation complex. *J Biol Chem* **274(29)**:20110-20115.

Moelleken J, Malsam J, Betts MJ, Movafeghi A, Reckmann I, Meissner I, Hellwig A, Russell RB, Söllner T, Brügger B & Wieland FT (2007) Differential localization of coatomer complex isoforms within the Golgi apparatus. *Proc Natl Acad Sci USA* **104(11):**4425-4430.

Moir D, Stewart SE, Osmond BC & Botstein D (1982) Cold-sensitive cell-division cycle mutants of yeast: isolation, properties, and pseudoreversion studies. *Genetics* **100**:547-563.

Molinari M (2007) N-glycan structure dictates extension of protein folding or onset of disposal. *Nat Chem Biol* 3:313-320.

Morar AS, Schrimsher JL, Chavez MD (2006) PEGylation of proteins: A structural approach. *BioPharm Int* **19(4)**:34-46.

Moremen KW (2002) Golgi alpha-mannosidase II deficiency in vertebrate systems: implications for asparagine-linked oligosaccharide processing in mammals. *Biochim Biophys Acta* **1573**:225-235.

Moremen KW & Molinari M (2006) N-linked glycan recognition and processing: the molecular basis of endoplasmic reticulum quality control. *Curr Opin Struct Biol* **16**:592-599.

Morgan DG, Menetret JF, Neuhof A, Rapoport TA & Akey CW (2002) Structure of the mammalian ribosome-channel complex at 17A resolution. *J Mol Biol* **324**:871-886.

Mori K, Kawahara T, Yoshida H, Yanagi H & Yura T (1996) Signalling from endoplasmic reticulum to nucleus: transcription factor with a basic-leucine zipper motif is required for the unfolded protein-response pathway. *Genes Cells* **1(9)**:803-817.

Mori K, Ma W, Gething MJ & Sambrook J (1993) A transmembrane protein with a cdc21/CDC28-related kinase activity is required for signaling from the ER to the nucleus. *Cell* **74**:743-756.

Mori K, Ogawa N, Kawahara T, Yanagi H & Yura T (1998) Palindrome with spacer of one nucleotide is characteristic of the *cis*-acting unfolded protein response element in *Saccharomyces cerevisiae*. *J Biol Chem* **273(16)**:9912-9920.

Mori K, Sant A, Kohno K, Normington K, Gething MJ & Sambrook JF (1992) A 22 bp *cis*-acting element is necessary and sufficient for the induction of the yeast *KAR2* (BiP) gene by unfolded proteins. *EMBO J* **17**:2583-2593.

Mori H, Tsukazaki T, Masui R, Kuramitsu S, Yokoyama S, Johnson AE, Kimura Y, Akiyama Y & Ito K (2003) Fluorescence resonance energy transfer analysis of protein translocase. SecYE from *Thermus thermophilus* HB8 forms a constitutive oligomer in membranes. *J Biol Chem* **278**:14257-14264.

Morris LL, Hartman IZ, Jun DJ, Seemann J & DeBose-Boyd RA (2014) Sequential actions of the AAA-ATPase VCP/p97 and the proteasome 19S regulatory particle in sterol-accelerated ER-associated degradation of 3-hydroxy-3-methylglutaryl coenzyme A reductase. *J Biol Chem* **289**:19053-19066.

Mothes W, Prehn S & Rapoport TA (1994) Systematic probing of the environment of a translocating secretory protein during translocation through the ER membrane. *EMBO J* **13**:3937-3982.

Müller L, de Escauriaza MD, Lajoie P, Theis M, Jung M, Müller A, Burgard C, Greiner M, Snapp EL, Dudek J & Zimmermann R (2010) Evolutionary gain of function for the ER membrane protein Sec62 from yeast to humans. *Mol Biol Cell* **21(5)**:691-703.

Mumberg, D, Müller, R & Funk, M (1994) Regulatable promoters of *Saccharomyces cerevisiae*: comparison of transcriptional activity and their use for heterologous expression. *Nucleic Acids Res* **22 (25)**:5767-5768.

Munro A & Nichols BJ (1999) The GRIP domain – a novel Golgi-targeting domain found inseveral coiled-coil proteins. *Curr Biol* **9**:377-380

Munro S & Pelham HRB (1986) An Hsp70-like protein in the ER: Identity with the 78 kd glucose-regulated protein and immunoglobulin heavy chain binding protein. *Cell* **46**:291-300.

Munro S & Pelham HR (1987) A C-terminal signal prevents secretion of luminal ER proteins. *Cell* **48 (5)**:899-907.

Murata S, Yashiroda H & Tanaka K (2009) Molecular mechanisms of proteasome assembly. *Nat Rev Mol Cell Biol* **10(2)**:104-115.

Murphy CK & Beckwith J (1994) Residues essential for the function of SecE, a membrane component of the *Escherichia coli* secretion apparatus, are located in a conserved cytoplasmic region. *Proc Natl Acad Sci USA* **91**:2557-2561.

Mutka SC & Walter P (2001) Multifaceted physiological response allows yeast to adapt to the loss of the signal recognition particle-dependent protein-targeting pathway. *Mol Biol Cell* **12(3)**:577-588.

Nagai K, Oubridge C, Kuglstatter A, Menichelli E, Isel C & Jovine L (2003) New *EMBO* member's review: structure, function and evolution of the signal recognition particle. *EMBO J* **22**:3479-3485.

Nakatsukasa K & Brodsky JL (2008) The recognition and retrotranslocation of misfolded proteins from the endoplasmic reticulum. *Traffic* **9**:861-870.

Nandi D, Tahiliani P, Kumar A & Chandu D (2006) The ubiquitin-proteasome system. *J Biosci* **31(1)**:137-155.

Neuhof A, Rolls MM, Jungnickel B, Kalies KU & Rapoport (1998) Binding of signal recognition particle gives ribosome/nascent chain complexes a competitive advantage in endoplasmic reticulum membrane interction. *Mol Biol Cell* **9**:103-115.

Ng DT, Brown JD, Walter P (1996) Signal sequences specify the targeting route to the endoplasmic reticulum membrane. *J Cell Biol* **134**: 269-278

Ng DTW, Randall RE & Lamb RA (1989) Intracellular maturation and transport of the SV5 type II glycoprotein hemagglutinin-neuraminidase: specific and transient association with GRP78-BiP in the endoplasmic reticulum and extensive internalization from the cell surface. *J Cell Biol* **109**:3273-3289.

Ng W, Sergeyenko T, Zeng N, Brown JD & Römisch K (2007) Characterization of the proteasome interaction with the Sec61 channel in the endoplasmic reticulum. *J Cell Sci* **120**:682-692.

Ng DTW, Spear ED & Walter P (2000) The unfolded protein response regulates multiple aspects of secretory and membrane protein biogenesis and endoplasmic reticulum quality control. *J Cell Biol* **150 (1)**:77-88.

Ng DTW, Watowich SS & Lamb RA (1992) Analysis *in vivo* of GRP78-BiP/substrate interactions and their role in induction of the GRP78-BiP gene. *Mol Biol Cell* **3**:143-155.

Nijman SM, Luna-Vargas MP, Velds A, Brummelkamp TR, Dirac AM, Sixma TK & Bernards R (2005) A genomic and functional inventory of deubiquitinating enzymes. *Cell* **123(5)**:773-786.

Nikawa JI, Akiyoshi M, Hirata S & Fukuda T (1996) *Saccharomyces cerevisiae IRE2/HAC1* is involved in *IRE1*-mediated *KAR2* expression. *Nucleic Acids Res* **24**:4222-4226.

Nikawa JI & Yamashita S (1992) *IRE1* encodes a putative protein kinase containing a membrane-spanning domain and is required for inositol prototrophy in *Saccharomyces cerevisiae*. *Mol Microbiol* **6**:1441-1446.

Nishikawa SI, Brodsky JL & Nakatsukasa K (2005) Roles of molecular chaperones in endoplasmic reticulum (ER) quality control and ER-associated degradation (ERAD). *J Biochem* **137**:551-555.

Nishikawa SI, Fewell SW, Kato Y & Brodsky JL (2001) Molecular chaperones in the yeast endoplasmic reticulum maintain the solubility of proteins for retrotranslocation and degradation. *J Cell Biol* **153**:1061-1070.

Niwa M, Sidrauski C, Kaufman RJ & Walter P (1999) A role for presenilin-1 in nuclear accumulation of Ire1 fragments and induction of the mammalian unfolded protein response. *Cell* **99**:691-702.

Norgaard P, Westphal V, Tachibana C, Alsoe L, Holst B, Winther JR (2001) Functional differences in yeast protein disulfide isomerases. *J Cell Biol* 152(3):553-562.

Novick P & Brennwald P (1993) Friends and family: the role of Rab GTPases in vesicular traffic. *Cell* **75**:597-601.

Ogg SC, Barz WP & Walter P (1998) A functional GTPase domain, but not its transmembrane domain, is required for function of the SRP receptor β-subunit. *J Cell Biol* **142**:341-354.

Ohya T, Miaczynska M, Coskun Ü, Lommer B, Runge A, Drechsel D, Kalaidzidis Y & Zerial M (2009) Reconstitution of Rab- and SNARE-dependent membrane fusion by synthetic endosomes. *Nature* **459**:1091-1097.

Oikawa D1, Kimata Y & Kohno K (2007) Self-association and BiP dissociation are not sufficient for activation of the ER stress sensor Ire1. *J Cell Sci* **120(9)**:1681-1688.

Okuda-Shimizu Y & Hendershot LM (2007) Characterization of an ERAD pathway for non-glycosylated BiP substrates which requires Herp. *Mol Cell* **28(4)**:544-554.

Olivari S, Cali T, Salo KE, Paganetti P, Ruddock LW & Molinari M (2006) EDEM1 regulates ER-associated degradation by accelerating de-mannosylation of folding-defective polypeptides and by inhibiting their covalent aggregation. *Biochem Biophys Res Commun* **349**:1278-1284.

Olivari S & Molinari M (2007) Glycoprotein folding and the role of EDEM1, EDEM2 and EDEM3 in degradation of folding-defective glycoproteins. *FEBS Lett* **581**:3658-3664.

Orci L, Ravazzola M, Volchuk A, Engel T, Gmachl M, Amherdt M, Perrelet A, Sollner TH & Rothman JE (2000) Anterograde flow of cargo across the Golgi stack potentially mediated via bidirectional “percolating” COPI vesicles. *Proc Natl Acad Sci USA* **97**:10400-10405.

Osborne AR & Rapoport TA (2007) Protein translocation is mediated by oligomers of the SecY complex with one SecY copy forming the channel. *Cell* **129(1)**:97-110.

Osborne AR, Rapoport TA & van den Berg (2005) Protein translocation by the Sec61/SecY channel. *Annu Rev Cell Dev Biol* **21**:529-550.

Otto H, Hanson PI & Jahn R (1997) Assembly and disassembly of a ternary complex of synaptobrevin, syntaxin, and SNAP-25 in the membrane of synaptic vesicles. *Proc Natl Acad Sci*

USA **94**:6197-6201.

Oubridge C, Kuglstatter A, Jovine L & Nagai K (2002) Crystal structure of SRP19 in complex with the S domain of SRP RNA and its implication for the assembly of the signal recognition particle. *Mol Cell* **9:**1251-1261.

Oyadomari S, Yun C, Fisher EA, Kreglinger N, Kreibich G, Oyadomari M, Harding HP, Goodman AG, Harant H, Garrison JL, Taunton J, Katze MG & Ron D (2006) Cotranslocational degradation protects the stressed endoplasmic reticulum from protein overload. *Cell* **126(4)**:727-739.

Paetzel M, Dalbey RE & Strynadka NC (1998) Crystal structure of a bacterial signal peptidase in complex with a beta-lactam inhibitor. *Nature* **396 (6707)**:186-190.

Palade G (1975) Intracellular aspects of the process of protein synthesis. *Science* **189**:347-358.

Panzner S, Dreier L, Hartmann E, Kostka S & Rapoport TA (1995) Posttranslational protein transport in yeast reconstituted with a purified complex of Sec proteins and Kar2p. *Cell* **81**:561-570.

Papa FR (2012) Endoplasmic reticulum stress, pancreatic β-cell degeneration, and diabetes. *Cold Spring Harb Perspect Med* **2**:a007666.

Papa FR, Zhang C, Shokat K & Walter P (2003) Bypassing a kinase activity with an ATP competitive drug. *Science* **302(5650)**:1533-1537.

Pariyarath R, Wang H, Aitchison JD, Ginsberg HN, Welch WJ, Johnson AE & Fisher EA (2001) Co-translational interactions of apoprotein B with the ribosome and translocon during lipoprotein assembly or targeting to the proteasome. *J Biol Chem* **276**:541-550.

Park Y, Hwang YP, Lee JS, Seo SH, Yoon SK & Yoon JB (2005) Proteasomal ATPase-associated factor 1 negatively regulates proteasome activity by interacting with proteasomal ATPases. *Mol Cell Biol* **25**:3842-3853.

Park E & Rapoport TA (2011) Preserving the membrane barrier for small molecules during bacterial protein translocation. *Nature* **473**:239-242.

Park E & Rapoport TA (2012) Mechanisms of Sec61/SecY-mediated protein translocation across membranes. *Annu Rev Biophys* **41**:21-40.

Parlati F, Dignard, D, Bergeron JJM & Thomas DY (1995) The calnexin homologue *cnx1*$^{+}$ in *Schizosaccharomyces pombe*, is an essential gene which can be complemented by its soluble ER domain. *EMBO J* **14**:3064-3072.

Parlati F, Dominguez M, Bergeron JJ & Thomas DY (1995) *Saccharomyces cerevisiae CNE1* encodes an endoplasmic reticulum (ER) membrane protein with sequence similarity to calnexin and calreticulin and functions as a constituent of the ER quality control apparatus*. J Biol Chem* **270**:244-253.

Park E, Ménétret J-F, Gumbart JC, Ludtke SL, Li W, Whynot A, Rapoport TA & Akey CW (2014) Structure of the SecY channel during initiation of protein translocation. *Nature* **506(7486)**:102-106.

Patel S & Latterich M (1998) The AAA team: related ATPases with diverse functions. *Trends Cell Biol* **8(2)**:65-71.

Pathare GR, Nagy I, Bohn S, Unverdorben P, Hubert A, Körner R, Nickell S, Lasker K, Sali A, Tamura T, Nishioka T, Förster F, Baumeister W & Bracher A (2011) The proteasomal subunit Rpn6 is a molecular clamp holding the core and regulatory subcomplexes together. *Proc Natl Acad Sci USA* **109**:149-154.

Patil C & Walter P (2001) Intracellular signaling from the endoplasmic reticulum to the nucleus: the unfolded protein response in yeast and mammals. *Curr Opin Cell Biol* **13(3)**:349-355.

Pearse BR & Hebert DN (2010) Lectin chaperones help direct the maturation of glycoproteins in the endoplasmic reticulum. *Biochim Biophys Acta* **1803(6)**:684–693.

Pelham HR (1995) Sorting and retrieval between the endoplasmic reticulum and Golgi apparatus. *Curr Opin Cell Biol* **7**:530-535.

Pelham HR (2000) Using sorting signals to retain proteins in the endoplasmic reticulum. *Methods Enzymol* **327**:279-283.

Pelham HR & Rothman JE (2000) The debate about transport in the Golgi—two sides of the same coin? *Cell* **102**:713-719.

Pereira C, Ferreiro E, Cardoso SM & de Oliveira CR (2004) Cell degeneration induced by amyloid-beta peptides: implications for Alzheimer's disease. *J Mol Neurosci* **23**:97-104.

Perham RN (2000) Swinging arms and swinging domains in multifunctional enzymes: catalytic machines for multistep reactions. *Annu Rev Biochem* **69**:961-1004.

Pestka S (1971) Inhibitors of ribosome functions. *Annu Rev Microbiol* **25**:487-562.

Peters JM, Cejka Z, Harris JR , Kleinschmidt JA & Baumeister W (1993) Structural features of the 26 S proteasome complex. *J Mol Biol* **234(4)**:932-937.

Peth A, Uchiki T & Goldberg AL (2010) ATP-dependent steps in the binding of ubiquitin conjugates to the 26S proteasome that commit to degradation. *Mol Cell* **40**:671-681.

Petroski MD (2008) The ubiquitin system, disease, and drug discovery. *BMC Biochem* **9 (Suppl 1)**:S7.

Pfeffer SR (1994) Rab GTPases: master regulators of membrane trafficking. *Curr Biol* **6**:522-526.

Pfeffer S & Aivazian D (2004) Targeting Rab GTPases to distinct membrane compartments. *Nat Rev Mol Cell Biol* **5**:886-896.

Pickart CM (2000) Ubiquitin in chains. *Trends Biochem Sci* **25(11)**:544-548.

Pickart CM (2001) Mechanisms underlying ubiquitination. *Annu Rev Biochem* **70**:503-533.

Pickart CM (2004) Back to the future with ubiquitin. *Cell* **116**:181-190.

Pickart CM & Cohen RE (2004) Proteasomes and their kin: proteases in the machine age. *Nat Rev Mol Cell Biol* **5**:177-187.

Pickart CM & Eddins MJ (2004) Ubiquitin: structures, functions, mechanisms. *Biochim Biophys Acta* **1695(1-3)**:55-72.

Pickart Cm & Fushman D (2004) Polyubiquitin chains: polymeric protein signals. *Curr Opin Chem Biol* **8(6)**:610-616.

Pierce NW, Kleiger G, Shan S & Deshaies RJ (2009) Detection of sequential polyubiquitylation on a millisecond timescale *Nature* **462**:615-619**.**

Pilon M, Römisch K, Quach D & Schekman R (1998) Sec61p serves multiple roles in secretory precursor binding and translocation into the endoplasmic reticulum membrane. *Mol Biol Cell* **9**:3455-3473.

Pilon M, Schekman R & Romisch K (1997) Sec61p mediates export of a misfolded secretory protein from the endoplasmic reticulum to the cytosol for degradation. *EMBO J* **16**:4540-4548.

Pincus D, Chevalier MW, Aragon, van Anken E, Vidal SE, El-Samad H & Walter P (2010) BiP binding to the ER-stress sensor Ire1 tunes the homeostatic behavior of the unfolded protein response. *PLoS Biol* **8(7)**:e1000415

Piotrowski J, Beal R, Hoffman L, Wilkinson KD, Cohen RE & Pickart CM (1997) Inhibition of the 26S proteasome by polyubiquitin chains synthesized to have defined lengths. *J Biol Chem* **272**:23712-23721.

Plath K, Mothes W, Wilkinson BM, Stirling CJ & Rapoport TA (1998) Signal sequence recognition in posttranslational protein transport across the yeast ER membrane. *Cell* **94**:795-807.

Plath K & Rapoport TA (2000) Spontaneous release of cytosolic proteins from posttranslational substrates before their transport into the endoplasmic reticulum. *J Cell Biol* **151**:167-178.

Plemper RK, Bohmler S, Bordallo J, Sommer T & Wolf DH (1997) Mutant analysis links the translocon and BiP to retrograde protein transport for ER degradation. *Nature* **388**:891-895.

Plemper RK, Bordallo J, Deak PM, Taxis C, Hitt R & Wolf DH (1999a) Genetic interactions of Hrd3p and Der3p/Hrd1p with Sec61p suggest a retrotranslocation complex mediating protein transport for ERdegradation. *J Cell Sci* **112**:4123-4134.

Plemper RK, Deak PM, Otto RT & Wolf DH (1999b) Re-entering the translocon from the lumenal side of the endoplasmic reticulum. Studies on mutated carboxypeptidase yscY species. *FEBS Lett* **443(3)**:241-245.

Plemper RK, Egner R, Kuchler K & Wolf DH (1998) Endoplasmic reticulum degradation of a mutated ATP-binding cassette transporter Pdr5 proceeds in a concerted action of Sec61 and the proteasome. *J Biol Chem* **273(49)**:32848-32856.

Plemper RK & Wolf DH (1999) Retrograde protein translocation: ERADication of secretory proteins in health and disease. *Trends Biochem Sci* **24**:266-270.

Pool MR, Stumm J, Fulga TA, Sinning I & Dobberstein B (2002) Distinct modes of signal recognition particle interaction with the ribosome. *Science* **297(5585)**:1345-1348.

Potter MD & Nicchitta CV (2000) Regulation of ribosome detachment from the mammalian endoplasmic reticulum membrane. *J Biol Chem* **275**:33828-33835.

Potter MD & Nicchitta CV (2002) Endoplasmic reticulum-bound ribosomes reside in stable association with the translocon following termination of protein synthesis. *J Biol Chem* **277**:23314-23320.

Powell KS & Latterich M (2000) The making and breaking of the endoplasmic reticulum. *Traffic* **1**:689-694.

Prajapati RS, Das M, Sreeramulu S, Sirajuddin M, Srinivasan S, Krishnamurthy V, Ranjani R, Ramakrishnan C & Varadarajan R (2007) Thermodynamic effects of proline introduction on protein stability. *Proteins* **66(2)**:480-491.

Prinz A, Behrens C, Rapoport TA, Hartmann E & Kalies KU (2000) Evolutionarily conserved binding of ribosomes to the translocation channel via the large ribosomal RNA. *EMBO J* **19**:1900-1906.

Pryer NK, Wuestehube LJ & Schekman R (1992) Vesicle-mediated protein sorting. *Annu Rev Biochem* **61**:471-516.

Pye VE, Dreveny I, Briggs LC, Sands C, Beuron F, Zhang X & Freemont PS (2006) Going through the motions: the ATPase cycle of p97. *J Struct Biol* **156**:12-28.

Qu D, Teckman J, Omura S & Perlmutter D (1996) Degradation of a mutant secretory protein, alpha1-antitrypsin Z, in the endoplasmic reticulum requires proteasome activity. *J Biol Chem* **271**:22791-22795.

Quan EM, Kamiya Y, Kamiya D, Denic V, Weibezahn J, Kato K & Weissman JS (2008) Defining the glycan destruction signal for endoplasmic reticulum-associated degradation. *Mol Cell* **32(6)**:870-877.

Rabeh WM, Bossard F, Xu H, Okiyoneda T, Bagdany M, Mulvihill CM, Du K, di Bernardo S, Liu Y, Konermann L, Roldan A & Lukacs GL (2012) Correction of both NBD1 energetics and domain interface is required to restore DeltaF508 CFTR folding and function. *Cell* **148**:150-163.

Rabinovich E, Kerem A, Fröhlich KU, Diamant N & Bar-Nun S (2002) AAA-ATPase p97/Cdc48p, a cytosolic chaperone required for endoplasmic reticulum-associated protein degradation. *Mol Cell Biol* **22(2)**:626-634.

Rabu C, Wipf P, Brodsky JL & High S (2008) A precursor-specific role for Hsp40/Hsc70 during tail-anchored protein integration at the endoplasmic reticulum. *J Biol Chem* **283**:27504-27513.

Raden D, Song W & Gilmore R (2000) Role of the cytoplasmic segments of Sec61alpha in the ribosome-binding and translocation-promoting activity of the Sec61 complex. *J Cell Biol* **150(1)**:53-64.

Rao H & Sastry A (2002) Recognition of specific ubiquitin conjugates is important for the proteolytic functions of the ubiquitin-associated domain proteins Dsk2 and Rad23. *J Biol Chem* **277**:11691-11695.

Rao-Naik C, dela Cruz W, Laplaza JM, Tan S, Callis J, Fisher AJ (1998) The rub family of ubiquitin-like proteins. Crystal structure of *Arabidopsis* rub1 and expression of multiple rubs in *Arabidopsis*. *J Biol Chem* **273**:34976-34982.

Rape M, Hoppe T, Gorr I, Kalocay M, Richly H & Jentsch S (2001) Mobilization of processed, membrane-tethered SPT23 transcription factor by CDC48(UFD1/NPL4), a ubiquitin-selective chaperone. *Cell* **107**:667-677.

Rapiejko PJ & Gilmore R (1992) Protein translocation across the ER requires a functional GTP binding site in the α subunit of the signal recognition particle receptor. *J Cell Biol* **117**:493-503.

Rapiejko PJ & Gilmore R (1997) Empty site forms of the SRP54 and SRα GTPases mediate targeting of ribosome-nascent chain complexes to the endoplasmic reticulum. *Cell* **89**:703-713.

Rapoport TA (2007) Protein translocation across the eukaryotic endoplasmic reticulum and bacterial plasma membranes. *Nature* **450**:663-669.

Rapoport TA, Jungnickel B & Kutay U (1996) Protein transport across the eukaryotic endoplasmic reticulum and bacterial inner membranes. *Annu Rev Biochem* **65**:271-303.

Rapoport TA, Matlack KE, Plath K, Misselwitz B & Staeck O (1999) Posttranslational protein translocation across the membrane of the endoplasmic reticulum. *Biol Chem* **380**:1143-1150.

Ravid T & Hochstrasser M (2007) Autoregulation of an E2 enzyme by ubiquitin-chain assembly on its catalytic residue. *Nat Cell Biol* **9**:422-427.

Ravid T, Kreft SG & Hochstrasser M (2006) Membrane and soluble substrates of the Doa10 ubiquitin ligase are degraded by distinct pathways. *EMBO J* **25(3)**:533-543.

Reyes-Turcu FE, Ventii KH & Wilkinson KD (2009) Regulation and cellular roles of ubiquitin-specific deubiquitinating enzymes. *Annu Rev Biochem* **78**:363-397.

Rock KL & Goldberg AL (1999) Degradation of cell proteins and the generation of MHC class I-presented peptides. *Annu Rev Immunol* **17**:739-779.

Rock KL, Gramm C, Rothstein L, Clark K, Stein R, Dick L, Hwang D, Goldberg AL (1994) Inhibitors of the proteasome block the degradation of most cell proteins and the generation of peptides presented on MHC class 1 molecules. *Cell* **78**:761-771.

Roelofs J, Park S, Haas W, Tian G, McAllister FE, Huo Y, Lee BH, Zhang F, Shi Y, Gygi SP & Finley D (2009) Chaperone-mediated pathway of proteasome regulatory particle assembly. *Nature* **459**:861-865.

Römisch K (2004) A cure for traffic jams: small molecule chaperones in the endoplasmic reticulum. *Traffic* **5**:815-820.

Römisch K (2005) Endoplasmic reticulum-associated degradation. *Annu Rev Cell Dev Biol* **21**:435-456.

Römisch K, Collie N, Soto N, Logue J, Lindsay M, Scheper W & Cheng CH (2003) Protein translocation across the endoplasmic reticulum membrane in cold-adapted organisms. *Cell Sci* **116**:2875-2883.

Römisch K, Webb J, Herz J, Prehn S, Frank R, Vingron M & Dobberstein B (1989) Homology of 54K protein of signal recognition particle, docking protein and two *E. coli* proteins with putative GTP-binding domains. *Nature* **340**:478-482.

Ron D & Walter P (2007) Signal integration in the endoplasmic reticulum unfolded protein response. *Nat Rev Mol Cell Biol* **8**:519-529.

Rossanese OW, Soderholm J, Bevis BJ, Sears IB, O'Connor J, Williamson EK, & Glick BS (1999) Golgi structure correlates with transitional endoplasmic reticulum organization in *Pichia pastoris* and *Saccharomyces cerevisiae*. *J Cell Biol* **145(1)**:69-81.

Rothblatt J & Meyer D (1986) Secretion in yeast: translocation and glycosylation of prepro-α-factor *in vitro* can occur via an ATP-dependent posttranslational mechanism. *Cell* **44**:619-628.

Rothman JE (1994) Mechanisms of intracellular protein transport, *Nature* **372**:55-63.

Rothman JE & Wieland FT (1996) Protein sorting by transport vesicles. *Science* **272**:227-234.

Rubenstein EM, Kreft SG, Greenblatt W, Swanson R & Hochstrasser M (2012) Aberrant substrate engagement of the ER translocon triggers degradation by the Hrd1 ubiquitin ligase. *J Cell Biol* **197(6)**:761-773.

Rubin DM, Glickman MH, Larsen CN, Dhruvakamar S & Finley D (1998) Active site mutants in the six regulatory particle ATPases reveal multiple roles for ATP in the proteasome. *EMBO J* **17**:4909-4919.

Rubio C, Pincus D, Korennykh A, Schuck S, El-Samad H & Walter P (2011) Homeostatic adaptation to endoplasmic reticulum stress depends on Ire1 kinase activity. *J Cell Biol* **193(1)**:171-184.

Rüegsegger U, Leber JH & Walter P (2001) Block of HAC1 mRNA translation by long-range base pairing is released by cytoplasmic splicing upon induction of the unfolded protein response. *Cell* **107**:103-114.

Ruggiano A, Foresti O & Carvalho P (2014) ER-associated degradation: Protein quality control and beyond. *J Cell Biol* **6**:869-879.

Rumpf S & Jentsch S (2005) Functional division of substrate processing cofactors of the ubiquitin-selective Cdc48 chaperone. *Mol Cell* **21(2)**:261-269.

Russell SJ, Steger KA, Johnston SA (1999) Subcellular localization, stoichiometry, and protein levels of the 26S proteasome subunits in yeast. *J Biol Chem* **274**:21943-52.

Saeki Y, Kudo T, Sone T, Kikuchi Y, Yokosawa H, Toh-e A & Tanaka K (2009) Lysine 63-linked polyubiquitin chain may serve as a targeting signal for the 26S proteasome. *EMBO J* **28**:359-371.

Saeki Y, Toh-E A, Kudo T, Kawamura H & Tanaka K (**2009)** Multiple proteasome-interacting proteins assist the assembly of the yeast 19S regulatory particle. *Cell* **137**:900-913.

Sakata E, Stengel F, Fukunaga K, Zhou M, Saeki Y, Förster F, Baumeister W, Tanaka K & Robinson CV (2011) The catalytic activity of Ubp6 enhances maturation of the proteasomal regulatory particle. *Mol Cell* **42(5)**:637-649.

Sanders SL, Whitfield KM, Vogel JP, Rose MD & Schekman (1992) Sec61p and BiP directly facilitate polypeptide translocation into the ER. *Cell* **69(2)**:353-365.

Sanger F, Nicklen S, Coulson AR (1977) DNA sequencing with chain-terminating inhibitors. *Proc Natl Acad Sci USA* **74**:5463-5467.

Saparov SM, Erlandson K, Cannon K, Schaletzky J, Schulman S, Rapoport TA & Pohl P (2007) Determining the conductance of the SecY protein translocation channel for small molecules. *Mol Cell* **26**:501-509.

Sato BK & Hampton RY (2006) Yeast Derlin Dfm1 interacts with Cdc48 and functions in ER homeostasis. *Yeast* **23**:1053-1064.

Sato BK, Schulz D, Do PH & Hampton RY (2009) Misfolded membrane proteins are specifically recognized by the transmembrane domain of the Hrd1p ubiquitin ligase. *Mol Cell* **34**:212-222.

Satoh Y, Mori H & Ito K (2003) Nearest neighbor analysis of the SecYEG complex. 2. Identification of a SecY-SecE cytosolic interface. *Biochemistry* **42**:7442-7447.

Sayeed A & Ng DTW (2005) Search and destroy: ER quality control and ER-associated protein degradation. *Crit Rev Biochem Mol Biol* **40**:75-91.

Schäfer A & Wolf DH (2009) Sec61p is part of the endoplasmic reticulum-associated degradation machinery. *EMBO J* **28**:2874-2884.

Schäuble N, Lang S, Jung M, Cappel S, Schorr S, Ulucan Ö, Linxweiler J, Dudek J, Blum R, Helms V, Paton AW, Paton JC, Cavalié A & Zimmermann R (2012) BiP-mediated closing of the Sec61 channel limits Ca^{2+} leakage from the ER. *EMBO J* **31(15)**:3282-3296.

Schatz PJ & Beckwith J (1990) Genetic analysis of protein export in *Escherichia Coli*. *Annual Review of Genetics* **24**:215-248.

Schatz G & Dobberstein B (1996) Common principles of protein translocation across membranes. *Science* **271(5255)**:1519-1526.

Schechter I, McKean DJ, Guyer R & Terry W (1975) Partial amino acid sequence of the precursor of immunoglobulin light chain programmed by messenger RNA *in vitro*. *Science* **188**:160-162.

Scheffner M, Nuber U & Huibregtse JM (1995) Protein ubiquitination involving an E1-E2-E3 enzyme ubiquitin thioester cascade. *Nature* **373**: 81-83.

Schekman R & Orci L (1996) Coat proteins and vesicle budding. *Science* **271(5255)**:1526-1533.

Scheper W, Thaminy S, Kais S, Staglar I & Römisch K (2003) Coordination of N-glycosylation and protein translocation across the endoplasmic reticulum membrane by Sss1 protein. *J Biol Chem* **278(39)**:37998-38003.

Schmid FX (1995) Prolyl isomerases join the fold. *Curr Biol* **5**:993-994.

Schmid SL (1997) Clathrin-coated vesicle formation and protein sorting: an integrated process. *Annu Rev Biochem* **66**:511-548.

Schmitz A, Herrgen H, Winkeler A & Herzog V (2000) Cholera toxin is exported from microsomes by the Sec61p complex. *J. Cell. Biol*. **148**:1203-1212.

Schmitz A, Maintz M, Kehle T & Herzog V (1995) *In vivo* iodination of a misfolded proinsulin reveals co-localized signals for BiP binding and for degradation in the ER. *EMBO J* **14(6)**:1091-1098.

Schmitz A, Schneider A, Kummer MP & Herzog V (2004) Endoplasmic reticulum-localized amyloid beta-peptide is degraded in the cytosol by two distinct degradation pathways. *Traffic* **5**:89-101.

Schröder M & Kaufman RJ (2005) The mammalian unfolded protein response. *Annu Rev Biochem* **74**:739-789.

Schubert U, Anton LC, Gibbs J, Norbury CC, Yewdell JW & Bennink JR (2000) Rapid degradation of a large fraction of newly synthesized proteins by proteasomes. *Nature* **404**:770-774.

Schuberth C, Richly H, Rumpf S & Buchberger A (2004) Shp1 and Ubx2 are adaptors of Cdc48 involved in ubiquitin-dependent protein degradation. *EMBO Rep* **5(8)**:818-824.

Schultz J, Milpelz F, Bork P & Ponting C (1998) SMART, a simple modular architecture research tool: identification of signaling domains. *Proc Natl Acad Sci USA* **95**:5857-5864.

Schulze A, Standera S, Buerger E, Kikkert M, van Voorden S, Wiertz E, Koning F, Kloetzel PM & Seeger M (2005) The ubiquitin-domain protein HERP forms a complex with components of the endoplasmic reticulum associated degradation pathway. *J Mol Biol* **354(5)**:1021-1027.

Schutze MP, Peterson PA & Jackson MR (1994) An N-terminal double-arginine motif maintains type II membrane proteins in the endoplasmic reticulum. *EMBO J* **13**:1696-1705.

Schwartz T & Blobel G (2003) Structural basis for the function of the beta subunit of the eukaryotic signal recognition particle receptor. *Cell* **112**:793-803.

Scidmore MA, Okamura HH & Rose MD (1993) Genetic interactions between *KAR2* and *SEC63*, encoding eukaryotic homologues of DnaK and DnaJ in the endoplasmic reticulum. *Mol Biol Cell* **4**:1145-1159.

Scott DC & Schekman R (2008) Role of Sec61p in the ER-associated degradation of short-lived transmembrane proteins. *J Cell Biol* **181 (7)**:1095-1105.

Seeger M, Hartmann-Petersen R, Wilkinson CRM, Wallace M, Samejima I, Taylor MS & Gordon C (2003) Interaction of the anaphase-promoting complex/cyclosome and proteasome protein complexes with multiubiquitin chain-binding proteins. *J Biol Chem* **278**:16791-16796.

Servas C & Römisch K (2013) The Sec63p J-domain is required for ER-associated degradation of soluble proteins in yeast. *PLoS ONE* **8(12)**:e82058.

Shamu CE, Story CM, Rapoport TA & Ploegh HL (1999) The pathway of US11-dependent degradation of MHC class I heavy chains involves a ubiquitin-conjugated intermediate. *J Cell Biol* **147**:45-58.

Shamu CE & Walter P (1996) Oligomerization and phosphorylation of the Ire1p kinase during intracellular signaling from the endoplasmic reticulum to the nucleus. *EMBO J* **15**:3028-3039.

Sharon M, Witt S, Felderer K, Rockel B, Baumester W & Robinson CV 2006) 20S proteasomes have the potential to keep substrates in store for continual degradation. *J Biol Chem* **281(14)**:9569-9575.

Shen SH, Chrétien P, Bastien L & Slilaty SN (1991) Primary sequence of the glucanase gene from *Oerskovia xanthineolytica*. Expression and purification of the enzyme from *Escherichia coli*. *J Biol Chem* **266**:1058-1063.

Sidrauski C, Cox JS & Walter P (1996) tRNA ligase is required for regulated mRNA splicing in the unfolded protein response. *Cell* **87(3)**:405-413.

Sidrauski C & Walter P (1997) The transmembrane kinase Ire1p is a site-specific endonuclease that initiates mRNA splicing in the unfolded protein response. *Cell* **90(6)**:1031-1039.

Siegel V & Walter P (1985) Elongation arrest is not a prerequisite for secretory protein translocation across the microsomal membrane. *J Cell Biol* **100(6)**:1913-1921.

Siegel V & Walter P (1986) Removal of the Alu structural domain from signal recognition particle leaves its protein translocation activity intact. *Nature* **320:**81-84.

Siegel V & Walter P (1988) Each of the activities of signal recognition particle (SRP) is contained within a distinct domain: analysis of biochemical mutants of SRP. *Cell* **52(1)**:39-49.

Sikorski RS, Hieter P (1989) A system of shuttle vectors and yeast host strains designed for efficient manipulation of DNA in *Saccharomyces cerevisiae*. *Genetics* **122**:19-27.

Simon M, Binder M, Adam G, Hartig A & Ruis H (1992) Control of peroxisome proliferation in *Saccharomyces cerevisiae* by *ADR1*, *SNF1* (*CAT1*, *CCR1*) and *SNF4* (*CAT3*). *Yeast* **8(4)**:303-309.

Singh A, Chen EY, Lugovoy JM, Chang CN, Hitzman RA & Seeburg PH (1983) *Saccaromyces cerevisiae* contains two discrete genes coding for the α-factor pheromone. *Nucleic Acids Res* **11**:4049-4063.

Sitia R & Braakman I (2003) Quality control in the endoplasmic reticulum protein factory. *Nature* **426**:891-894.

Smith DM, Chang SC, Finley D, Cheng Y & Goldberg AL (2007) Docking of the proteasomal ATPases' carboxyl termini in the 20S proteasome's alpha ring opens the gate for substrate entry. *Mol Cell* **27(5)**:731-744.

Smith DM, Fraga H, Reis C, Kafri G, Goldberg AL (2011) ATP binds to proteasomal ATPases in pairs with distinct functional effects, implying an ordered reaction cycle. *Cell* **144**:526-538.

Snapp EL, Reinhart GA, Bogert BA, Lippincott-Schwartz J & Hegde RS (2004) The organization of engaged and quiescent translocons in the endo-plasmic reticulum of mammalian cells. *J Cell Biol* **164**:997-1007.

Sommer T & Jentsch S (1993) A protein translocation defect linked to ubiquitin conjugation at the endoplasmic reticulum. *Nature* **365**:176-179.

Sommer T & Wolf DH (1997) Endoplasmic reticulum degradation: reverse protein flow of no return. *FASEB J* **11**:1227-1233.

Sone T, Saeki Y, Toh-e A & Yokosawa H (2004) Sem1p is a novel subunit of the 26S proteasome from *Saccharomyces cerevisiae*. *J Biol Chem* **279**:28,807-28,816.

Song W, Raden D, Mandon EC & Gilmore R (2000) Role of Sec61alpha in the regulated transfer of the ribosome-nascent chain complex from the signal recognition particle to the translocation channel. *Cell* **100**:333-343.

Sorger PK & Pelham HRB (1987) Purification and characterization of a heat shock element binding protein from yeast. *EMBO J* **6**:3035-3041.

Sousa R & Lafer EM (2006) Keep the traffic moving: mechanism of the Hsp70 motor. *Traffic* **7**:1596-1603.

Spear E & Ng DTW (2001) The unfolded protein response: No longer just a special teams player. *Traffic* **2**:515-523.

Spear E & Ng DTW (2003) Stress tolerance of misfolded carboxypeptidase Y requires maintenance of protein trafficking and degradative pathways. *Mol Biol Cell* **14(7)**:2756-2767.

Spiller MP & Stirling CJ (2011) Preferential targeting of a signal recognition particle-dependent precursor to the Ssh1p translocon in yeast. *J Biol Chem* **286**:21953-21960.

Sprague Jr GF, Jensen R & Herskowitz I (1983) Control of yeast cell type by the mating type locus: Positive regulation of the α-specific *STE3* gene by the *MAT*α 1 product. *Cell* **32(2)**:409-415.

Spurway TD, Dalley JA, High S & Bulleid NJ (2001) Early events in glycosylphosphatidylinositol anchor addition. substrate proteins associate with the transamidase subunit gpi8p. *J Biol Chem* **276(19)**:15975-15982.

Stagljar I, Korostensky C, Nils J & te Heesen S (1998) A genetic system based on split-ubiquitin for the analysis of interactions between membrane proteins in vivo. *Proc Natl Acad Sci USA* **95**:5187-5192.

Stanley AM, Carvalho P & Rapoport T (2011) Recognition of an ERAD-L substrate analyzed by site-specific *in vivo* photocrosslinking. *FEBS Lett* **585**:1281-1286.

Steel GJ, Brownsword J & Stirling CJ (2002) Tail-anchored protein insertion into yeast ER requires a novel posttranslational mechanism which is independent of the SEC machinery. *Biochemistry* **41**:11914-11920.

Stefanovic S & Hegde RS (2007) Identification of a targeting factor for posttranslational membrane protein insertion into the ER. *Cell* **128**:1147-1159.

Stennicke HR, Mortensen UH & Breddam K (1996) Studies on the hydrolytic properties of (serine) carboxypeptidase Y. *Biochemistry* **35**:7131-7141.

Stevens T, Esmon B & Schekman R (1982) Early stages in the yeast secretory pathway are required for transport of carboxypeptidase Y to the vacuole. *Cell* **30**:439-448.

Stirling CJ (1993) Similarities between *S. cerevisiae* Sec61p and *E. coli* SecY suggest a common origin for protein translocases of the eukaryotic ER and the bacterial plasmamembrane. *Protein Synthesis and Targeting in Yeast* (NATO ASI series) **H71**:293-306.

Stirling CJ & Hewitt EW (1992) The *S. cerevisiae SEC65* gene encodes a component of yeast signal recognition particle with homology to human SRP19. *Nature* **356**:534-537.

Stirling CJ, Rothblatt J, Hosobuchi M, Deshaies R & Schekman R (1992) Protein translocation mutants defective in the insertion of integral membrane proteins into the endoplasmic reticulum. *Mol Biol Cell* **3**:129-142.

Stötzler D, Kiltz H & Duntze W (1976) Primary structure of α-factor peptides from *Saccharomyces cerevisiae*. *Eur J Biochem* **69**:397-400.

Stolz A & Wolf DH (2010) Endoplasmic reticulum associated protein degradation: a chaperone assisted journey to hell. *Biochim. Biophys. Acta* **1803 (6)**:694-705.

Strub K Fornallaz M & Bui N (1999) The Alu domain homolog of the yeast signal recognition particle consists of an Srp14p homodimer and a yeast-specific RNA structure. *RNA* **5:**1333-1347.

Su K, Stoller T, Rocco J, Zemsky J & Green R (1993) Pre-Golgi degradation of yeast prepro-

alpha-factor expressed in a mammalian cell. Influence of cell type-specific oligosaccharide processing on intracellular fate. *J Biol Chem* **268**:14301-14309.

Suzuki T, Yan Q & Lennarz WJ (1998) Complex, two-way traffic of molecules across the membrane of the endoplasmic reticulum. *J Biol Chem* **273(17)**:10083-10086.

Swanson R, Locher M & Hochstrasser M (2001) A conserved ubiquitin ligase of the nuclear envelope/endoplasmic reticulum that functions in both ER-associated and Matalpha2 repressor degradation. *Genes Dev* **15**:2660-2674.

Swanton E, Bishop N, Sheehan J, High S & Woodman P (2000) Disassembly of membrane-associated NSF 20S complexes is slow relative to vesicle fusion and is Ca^{2+}-independent. *J Cell Sci* **113**:1783-1791.

Tajima S, Lauffer L, Rath VL & Walter P (1986) The signal recognition particle receptor is a complex that contains two distinct polypeptide chains. *J Cell Biol* **103(4)**:1167-1178.

Tatu U, Braakman I & Helenius A (1993) Membrane glycoprotein folding, oligomerization and intracellular transport: effects of dithiothreitul in living cells. *Eur Mol Biol Org J* **12**:2151-2157.

Taxis C, Hitt R, Park, SH, Deak PM, Kostova Z & Wolf DH (2003) Use of modular substrates demonstrates mechanistic diversity and reveals differences in chaperone requirement of ERAD. *J Biol Chem* **278**:35903-35913.

Taxis C, Vogel F & Wolf DH (2002) ER-Golgi traffic is a prerequisite for efficient ER degradation. *Mol Biol Cell* **13**:1806-1818.

Taylor SC, Thibault P, Tessier DC, Bergeron JJ & Thomas DY (2003) Glycopeptide specificity of the secretory protein folding sensor UDP-glucose glycoprotein:glucosyltransferase. *EMBO Rep* **4**:405-411.

Thomas Y, Bui N & Strüb K (1997) A truncation in the 14 kDa protein of the signal recognition particle leads to tertiary structure changes in the RNA and abolishes the elongation arrest activity of the particle. *Nucleic Acids Res* **25**:1920-1929.

Thompson D, Hakala K & DeMartino GN (2009) Subcomplexes of PA700, the 19S regulator of the 26 S proteasome, reveal relative roles of AAA subunits in 26 S proteasome assembly and activation and ATPase activity. *J Biol Chem* **284**:24891-24903.

Thrower JS, Hoffman L, Rechsteiner M & Pickart CM (2000) Recognition of the polyubiquitin proteolytic signal. *Embo J* **19**:94-102.

Tian G, Park S, Lee MJ, Huck B, McAllister F, Hill CP, Gygi SP & Finley D (2011) An asymmetric interface between the regulatory and core particles of the proteasome. *Nat Struct Mol Biol* **18**:1259-67.

Toikkanen J, Gatti E, Takei K, Saloheimo M, Olkkonen VM, Soderlund H, De Camilli P & Keranen S (1996) *Yeast* protein translocation complex: isolation of two genes *SEB1* and *SEB2* encoding proteins homologous to the Sec61 beta subunit. *Yeast* **12(5)**:425-438.

Tomko RJ Jr & Hochstrasser M (2011) Incorporation of the Rpn12 subunit couples completion of proteasome regulatory particle lid assembly to lid-base joining. *Mol Cell* **44(6)**:907-917.

Tomko RJ Jr, Funakoshi M, Schneider K, Wang J & Hochstrasser M (2010) Heterohexameric ring arrangement of the eukaryotic proteasomal ATPases: implications for proteasome structure and assembly. *Mol Cell* **38(3)**:393-403.

Torres-Quiroz F, García-Marqués S, Coria R, Randez-Gil F & Prieto JA (2010) The activity of yeast Hog1 MAPK is required during endoplasmic reticulum stress induced by tunicamycin exposure. *J Biol Chem* **285(26)**:20088-20096.

Tran J, Tomsic L & Brodsky J (2011) A Cdc48p-associated factor modulates endoplasmic reticulum-associated degradation, cell stress, and ubiquitinated protein homeostasis. *J Biol Chem* **286**:5744-5755.

Travers KJ, Patil CK, Wodicka L, Lockhart DJ, Weissman JS & Walter P (2000) Functional and genomic analysis reveal essential coordination between the unfolded protein response and endoplasmic reticulum-associated degradation. *Cell* **101**:249-258.

Tretter T, Pereira FP, Ulucan O, Helms V, Allan S, Kalies K-U & Römisch K (2013) ERAD and protein import defects in a *sec61* mutant lacking ER-lumenal loop 7. *BMC Cell Biol* **14**:56.

Trombetta ES & Parodi AJ (2003) Quality control and protein folding in the secretory pathway. *Annu Rev Cell Dev Biol* **19**:649-676.

Trueman SF, Mandon EC & Gilmore R (2011) Translocation channel gating kinetics balances protein translocation efficiency with signal sequence recognition fidelity. *Mol Biol Cell* **22(17)**:2983-2993.

Tsai B, Ye Y & Rapoport TA (2002) Retro-translocation of proteins from the endoplasmic reticulum into the cytosol. *Nat Rev Mol Cell Biol* **3**:246-255.

Tyedmers J, Lerner M, Wiedmann M, Volkmer J & Zimmermann R (2003) Polypeptide-binding proteins mediate completion of co-translational protein translocation into the mammalian endoplasmic reticulum. *EMBO Rep* **4(5)**:505-510.

Tyedmers J, Mogk A & Bukau B (2010) Cellular strategies for controlling protein aggregation. *Nat Rev Mol Cell Biol* **11**:777-788.

Tsukazaki T, Mori H, Fukai S, Ishitani R, Mori T, Dohmae N, Perederina A, Sugita Y, Vassylyev DG, Ito K & Nureki O (2008) Conformational transition of Sec machinery inferred from bacterial SecYE structures. *Nature* **455**:988-991.

Tu B & Weissman JS (2004) Oxidative protein folding in eukaryotes - mechanisms and consequences. *J Cell Biol* **164(3)**:341-346.

Unger C (2000) Analyse funktioneller Domänen von SEC71 und SEC72 im posttranslationalen Translokationsprozeß Saccharomyces cerevisiae. Dissertation, Hunmboldt-Universität Berlin.

Unno M, Mizushima T, Morimoto Y, Tomisugi Y, Tanaka K, Yasuoka N & Tsukihara T (2002) The structure of the mammalian 20S proteasome at 2.75 Å resolution. *Structure* **10**:609-618.

Ullu E, Murphy S & Melli M (1982) Human 7SL RNA consists of a 140 nucleotide middle-repetitive sequence inserted in an Alu sequence. *Cell* **29:**195-202.

van Anken E & Braakman I (2005) Versatility of the endoplasmic reticulum protein folding factory. *Crit Rev Biochem Mol Biol* **40**:191-228.

van den Berg B, Clemons WM, van Collinson I, Modis Y, Hartmann E, Harrison SC & Rapoport TA (2004) X-ray structure of a protein-conducting channel. *Nature* **427**:36-44.

van den Hazel HB, Kielland-Brandt MC & Winther JR (1996) Review: biosynthesis and function of yeast vacuolar proteases. *Yeast* **12(1)**:1-16.

van Nocker S, Sadis S, Rubin DM, Glickman M, Fu H, Coux O, Wefes I, Finley D & Vierstra RD (1996) The multiubiquitin-chain-binding protein Mcb1 is a component of the 26S proteasome in *Saccharomyces cerevisiae* and plays a nonessential, substrate-specific role in protein turnover. *Mol Cell Biol* **16**:6020-6028.

van Nues RW & Brown JD (2004) *Saccharomyces* SRP RNA secondary structures: A conserved S-domain and extended Alu-domain. *RNA* **10(1):**75-89.

Varki A (1993) Biological roles of oligosaccharides: all of the theories are correct. *Glycobiology* **3**:97-130.

Varshavsky A (2005) Regulated protein degradation. *Trends Biochem Sci* **30**:283-286.

Vashist S, Kim W, Belden WJ, Spear ED, Barlowe C, Ng DTW (2001) Distinct retrieval and retention mechanisms are required for the quality control of endoplasmic reticulum protein folding. *J Cell Biol* **155(3)**:355-367.

Vashist S & Ng DTW (2004) Misfolded proteins are sorted by a sequential checkpoint mechanism of ER quality control. *J Cell Biol* **165**:41-52.

Vazquez-Martinez R, Diaz-Ruiz A, Almabouada F, Rabanal-Ruiz Y, Gracia-Navarro F & Malagon MM (2012) Revisiting the regulated secretory pathway: From frogs to human. *Gen Comp Endocrinol* **175 (1)**:1-9.

Veenendaal AKJ, van der Does C & Driessen AJM (2004) The protein-conducting channel SecYEG. *Biochim Biophys Acta* **1694**:81-95.

Velichutina I, Connerly PL, Arendt CS, Li X & Hochstrasser M (2004) Plasticity in eucaryotic 20S proteasome ring assembly revealed by a subunit deletion in yeast. *EMBO J* **23(3)**:500-510.

Vembar SS & Brodsky JL (2008) One step at a time: endoplasmic reticulum-associated degradation. *Nat Rev Mol Cell Biol* **9**:944-957.

Verma R, Aravind L, Oania R, McDonald WH, Yates JR, Koonin EV & Deshaies RJ (2002) Role of Rpn11 metalloprotease in deubiquitination and degradation by the 26S proteasome. *Science* **298**:611-615.

Verma R, Chen S, Feldman R, Schieltz D, Yates J, Dohmen J & Deshaies RJ (2000). Proteasomal proteomics: identification of nucleotide-sensitive proteasome-interacting proteins by mass spectrometic analysi of affinity-purified proteasomes. *Mol Biol Cell* **11**:3425-3439.

Verma R, Oania R, Fang R, Smith GT & Deshaies RJ (2011) Cdc48/p97 mediates UV-dependent turnover of RNA Pol II. *Mol Cell* **41**:82-92.

Verma R, Oania R, Graumann J & Deshaies RJ (2004) Multiubiquitin chain receptors define a layer of substrate selectivity in the ubiquitin proteasome system. *Cell* **118**:99-110.

Veronese F & Harris JM, Eds (2002) Peptide and protein PEGylation. *Advanced Drug Delivery Review* **54(4)**:453-609.

Vilardi F, Lorenz H & Dobberstein B (2011) WRB is the receptor for TRC40/Asna1-mediated insertion of tail-anchored proteins into the ER membrane. *J Cell Sci* **124(8)**:1301-1307.

Vogel JP, Misra LM & Rose MD (1990) Loss of BiP/GRP78 unction blocks translocation of secretory proteins in yeast. *J Cell Biol* **110**:1885-1895.

Voges D, Zwickl P & Baumeister W (1999) The 26S proteasome: a molecular machine designed for controlled proteolysis. *Annu Rev Biochem* **68**:1015-1068.

von Heijne G (1983) Patterns of amino acids near signal-sequence cleavage sites. *Eur J Biochem* **133(1)**:17-21.

von Heijne G (1984) Analysis of the distribution of charged residues in the N-terminal region of signal sequences: implications for protein export in prokaryotic and eukaryotic cells. *EMBO J* **3**:2315-2318.

von Heijne G (1985) Signal sequences. The limits of variation. *J Mol Biol* **184**:99-105.

von Heijne G (1986) A new method for predicting signal sequence cleavage sites. *Nucleic Acids Res* **14**:4683-4690.

von Heijne G (1989) The structure of signal peptides from bacterial lipoproteins. *Protein Eng* **2**:531-534.

von Heijne G (1990) Protein targeting signals. *Curr Opin Cell Biol* **2**:604-608.

von Heijne G & Abrahmsén L (1989) Species-specific variation in signal peptide design: implications for proteins secretion in foreign hosts. *FEBS Lett* **244**:439-446.

Voorhees RM, Fernandez IS, Scheres SHW & Hegde RS (2014) Structure of the mammalian ribosome-Sec61 complex to 3.4 Å resolution. *Cell* **157**:1632-1643.

Wada I, Rindress D, Cameron PH, Ou WJ, Doherty JJ 2nd, Louvard D, Bell AW, Dignard D, Thomas DY & Bergeron JJ (1991) SSR alpha and associated calnexin are major calcium binding proteins of the endoplasmic reticulum membrane. *J Biol Chem* **266(29)**:19599-19610.

Wahlman J, DeMartino GN, Skach WR, Bulleid NJ, Brodsky JL & Johnson AE (2007) Real-time fluorescence detection of ERAD substrate retro-translocation in a mammalian in vitro system. *Cell* **129**:943-955.

Walker JE, Saraste M, Runswick MJ & Gay NJ (1982) Distantly related sequences in the a- and b-subunits of ATP synthase, myosin, kinases and other ATP-requiring enzymes and a common nucleotide binding fold. *EMBO J* **1**:945-951.

Walter P & Blobel G (1980) Purification of a membrane-associated protein complex required for protein translocation across the endoplasmic reticulum. *Proc Natl Acad Sci USA* **77(12)**:7112-7116.

Walter P & Blobel G (1981a) Translocation of proteins across the endoplasmic reticulum. II. Signal recognition protein (SRP) mediates the selective binding to microsomal membranes of *in-vitro*-assembled polysomes synthesizing secretory protein. *J Cell Biol* **91(2)**:551-556.

Walter P & Blobel G (1981b) Translocation of proteins across the endoplasmic reticulum. III. Signal recognition protein causes signal sequence-dependent and site-specific arrest of chain elongation that is released by microsomal membranes. *J Cell Biol* **91**:557-561.

Walter P & Blobel G (1982) Signal recognition particle contains a 7S RNA essential for protein translocation across the endoplasmic reticulum. *Nature* **299**:691-698.

Walter P, Ibrahimi I & Blobel G. (1981) Translocation of proteins across the endoplasmic reticulum. I. Signal recognition protein (SRP) binds to *in-vitro*-assembled polysomes synthesizing secretory protein. *J Cell Biol* **91(2)**:545-550.

Walter P & Johnson AE (1994) Signal sequence recognition and protein targeting to the endoplasmic reticulum membrane. *Annu Rev Cell Biol* **10**:87-119.

Walter P & Lingappa VR (1986) Mechanism of protein translocation across the endoplasmic reticulum membrane. *Annu Rev Cell Biol* **2**:499-516.

Walter J, Urban J, Volkwein C & Sommer T (2001) Sec61p-independent degradation of the tail-anchored membrane protein Ubc6p. *EMBO J*. **20**:3124-3131.

Wang J & Maldonado MA (2006) The Ubiquitin-Proteasome System and its role in inflammatory and autoimmune diseases. *Cell Mol Immunol* **3(4)**:255-261.

Wang M & Pickart CM (2005) Different HECT domain ubiquitin ligases employ distinct mechanisms of polyubiquitin chain synthesis. *EMBO J* **24**:4324–4333.

Wang S, Xin F, Liu X, Wang Y, An Z, Qi Q & Wang PG (2009) N-terminal deletion of Peptide:N-glycanase results in enhanced deglycosylation activity. *PLoS One* **4(12)**:e8335.

Ward CL, Omura S & Kopito RR (1995) Degradation of CFTR by the ubiquitin-proteasome pathway. *Cell* **83**:121-127.

Warren G & Mellman I (1999) Bulk flow redux? *Cell* **98**:125-127.

Warren W & Schekman R (2005) Protein translocation across biological membranes. *Science* **310**:1452-1456.

Warren G & Wickner W (1996) Organelle inheritance. *Cell* **84(3)**:395-400.

Waters MG & Blobel G (1986) Secretory protein translocation in a yeast cell-free system can occur posttranslationally and requires ATP hydrolysis. *J Cell Biol* **102**:1543-1550.

Waters MG, Evans EA & Blobel G (1988) Prepro-alpha factor has a cleavable signal sequence. *J Biol Chem* **263**:6209-6214.

Weber PC (1989) Structural origins of high-affinity biotin binding to Streptavidin. *Science* **243 (4887)**: 85-88.

Weeden, NF (1981) Genetic and biochemical implications of the endosymbiotic origin of the chloroplast. *J Mol Evol* **17**:133-139.

Weihofen A, Binns K, Lemberg MK, Ashman K & Martoglio B (2002) Identification of signal peptide peptidase, a presenilin-type aspartic protease. *Science* **296**:2215-2218.

Weissman AM (2001) Themes and variations on ubiquitylation. *Nat Rev Mol Cell Biol* **2(3)**:169-178.

Welihinda AA & Kaufman RJ (1996) The unfolded protein response pathway in *Saccharomyces cerevisiae*. Oligomerization and trans-phosphorylation of Ire1p (Ern1p) are required for kinase activation. *J Biol Chem* **271(30)**:18181-18187.

Werner ED, Brodsky JL, & McCracken AA (1996) Proteasome-dependent endoplasmic reticulum-associated protein degradation: an unconventional route to a familiar fate. *Proc Natl Acad Sci USA* **93**:13797-13801.

Wheeler MC & Gekakis N (2012) Defective ER associated degradation of a model luminal substrate in yeast carrying a mutation in the 4th ER luminal loop of Sec61p. *Biochem Biophys Res Commun* **427**:768-773.

Whitby FG, Xia G, Pickart CM & Hill CP (1998) Crystal structure of the human ubiquitin-like protein NEDD8 and interactions with ubiquitin pathway enzymes, *J Biol Chem* **273:**34893-34991.

Wickliffe K, Williamson A, Jin L & Rape M (2009) The multiple layers of ubiquitin-dependent cell cycle control. *Chem Rev* **109**:1537-1548.

Wiertz EJ, Jones TR, Sun L, Bogyo M, Geuze HJ & Ploegh HL (1996a) The human cytomegalovirus US11 gene product dislocates MHC class I heavy chains from the endoplasmic reticulum to the cytosol. *Cell* **84**:769-779.

Wiertz EJ, Tortorella D, Bogyo M, Yu J, Mothes W, Jones TR, Rapoport TA & Ploegh HL (1996b) Sec61-mediated transfer of a membrane protein from the endoplasmic reticulum to the proteasome for destruction. *Nature* **384**:432-438.

Wilcox AJ & Laney JD (2009) A ubiquitin-selective AAA-ATPase mediates transcriptional switching by remodelling a repressor-promoter DNA complex. *Nat Cell Biol* **11**:1481-1486.

Wilkinson BM, Brownsword JK, Mousley CJ & Stirling CJ (2010) Sss1p is required to complete protein translocon activation. *J Biol Chem* **285(42)**:32671-326777.

Wilkinson BM, Critchley AJ & Stirling CJ (1996) Determination of the transmembrane topology of yeast Sec61p, an essential component of the endoplasmic reticulum translocation complex. *J Biol Chem* **271(41)**:25590-25597.

Wilkinson BM, Esnault Y, Craven RA, Skiba F, Fieschi J, Képès F & Stirling CJ (1997) Molecular architecture of the ER translocase probed by chemical crosslinking of Sss1p to complementary fragments of Sec61p. *EMBO J* **16(15)**:4549-4559.

Wilkinson CR, Seeger M, Hartmann-Petersen R, Stone M, Wallace M, Semple C & Gordon C (2001) Proteins containing the UBA domain are able to bind to multi-ubiquitin chains. *Nat Cell Biol* **3**:939-943.

Wilkinson BM, Tyson JR, Reid PJ & Stirling CJ (2000) Distinct domains within yeast Sec61p involved in post-translational translocation and protein dislocation. *J Biol Chem* **275**:521-529.

Wilkinson KD, Urban MK & Haas AL (1980) Ubiquitin is the ATP-dependent proteolytic factor of rabbit reticulocytes. *J Biol Chem* 255**:**7529-7532.

Willer M, Forte GMA & Stirling CJ (2008) Sec61p is required for ERAD-L. *J Biol Chem* **283**:33883-33888.

Wilson R, Lees FJ & Bulleid NJ (1998) Protein disulphide isomerase acts as a chaperone during the assembly of procollagen. *J Biol Chem* **273**:9637-9643.

Windheim M, Stafford M, Peggie M & Cohen P (2008) Interleukin-1 (IL-1) induces the Lys63-linked polyubiquitination of IL-1 receptor-associated kinase 1 to facilitate NEMO binding and the activation of IkappaBalpha kinase. *Mol Cell Biol* **28(5)**:1783-1791.

Wirth A, Jung M, Bies C, Frien M, Tyedmers J, Zimmermann R & Wagner R (2003). The Sec61p complex is a dynamic precursoractivated channel. *Mol Cell* **12**:261-268.

Wittke S, Dunnwald M, Albertsen M & Johnsson N (2002) Recognition of a subset of signal sequences by Ssh1p, a Sec61p-related protein in the membrane of endoplasmic reticulum of yeast Saccharomyces cerevisiae. *Mol Biol Cell* **13(7)**:2223-2232.

Wittke S, Lewke N, Müller S & Johnsson N (1999) Probing the molecular environment of membrane proteins *in vivo*. *Mol Biol Cell* **10**:2519-2530.

Wolf DH (2011) The ubiquitin clan: A protein family essential for life. *FEBS Lett* **585**:2769-2771.

Wolf DH & Hilt W (2004) The proteasome: a proteolytic nanomachine of cell regulation and waste disposal. *Biochim Biophys Acta* **1695(1-3)**:19-31.

Wolf DH & Stolz A (2011) The Cdc48 machine in endoplasmic reticulum associated protein degradation. *Biochim Biophys Acta* **1823 (1)**:117-124.

Woodman PG (2003) p97, a protein coping with multiple identities. *J Cell Sci* **116**:4283-4290.

Xu X, Azakami H & Kato A (2004a) P-domain and lectin site are involved in the chaperone function of *Saccharomyces cerevisiae* calnexin homologue. *FEBS Lett* **570**:155-160.

Xu X, Kanbara K, Azakami H & Kato A (2004b) Expression and characterization of *Saccharomyces cerevisiae* Cne1p, a calnexin homologue. *J Biochem* **135**:615-618.

Yabal M, Brambillasca S, Soffientini P, Pedrazzini E, Borgese N & Makarow M (2003) Translocation of the C terminus of a tail-anchored protein across the endoplasmic reticulum membrane in yeast mutants defective in signal peptide-driven translocation. *J Biol Chem* **278**:3489-3496.

Yachdav G, Kloppmann E, Kajan L, Hecht M, Goldberg T, Hamp T, Honigschmid P, Schafferhans A, Roos M, Bernhofer M, Richter L, Ashkenazy H, Punta M, Schlessinger A, Bromberg Y, Schneider R, Vriend G, Sander C, Ben-Tal N & Rost B (2014) PredictProtein - an open resource for online prediction of protein structural and functional features. *Nucleic Acids Res* **42**:W337-W343.

Yang M, Omura S, Bonifacino JS & Weissman A (1998) Novel aspects of degradation of T cell receptor subunits from the endoplasmic reticulum (ER) in T cells: importance of oligosaccharide processing, ubiquitination, and proteasome-dependent removal from ER membranes. *J Exp Med* **187**:835-846.

Yahr TL & Wickner WT (2000) Evaluating the oligomeric state of SecYEG in preprotein translocase. *EMBO J.* **19**:4393-4401.

Yao T & Cohen RE (2002) A cryptic protease couples deubiquitination and degradation by the proteasome. *Nature* **419**:403-407.

Yashiroda H, Mizushima T, Okamoto K, Kameyama T, Hayashi H, Kishimoto T, Niwa S, Kasahara M, Kurimoto E, Sakata E, Takagi K, Suzuki A, Hirano Y, Murata S, Kato K,

Yamane T & Tanaka K (2008). Crystal structure of a chaperone complex that contributes to theassembly of yeast20S proteasomes. *Nat Struct Biol* **15**:228-236.

Ye Y, Meyer HH & Rapoport TA (2001) The AAA ATPase Cdc48/p97 and its partners transport proteins from the ER to the cytosol. *Nature* **414**:652-656.

Ye Y, Meyer HH & Rapoport TA (2003) Function of the p97-Ufd1-Npl4 complex in retrotranslocation from the ER to the cytosol: dual recognition of non-ubiquitinated polypeptide segments and polyubiquitin chains. *J Cell Biol* **162**:71-84.

Ye Y, Shibata Y, Kikkert M, van Voorden S, Wiertz E & Rapoport TA (2005) Inaugural article: recruitment of the p97 ATPase and ubiquitin ligases to the site of retrotranslocation at the endoplasmic reticulum membrane. *Proc Natl Acad Sci USA* **102**:14132-14138.

Ye Y, Shibata Y, Yun C, Ron D & Rapoport TA (2004) A membrane protein complex mediates retro-translocation from the ER lumen into the cytosol. *Nature* **429**:841-847.

Youker RT, Walsh P, Beilharz T, Lithgow T & Brodsky JL (2004) Distinct roles for the Hsp40 and Hsp90 molecular chaperones during cystic fibrosis transmembrane conductance regulator degradation in yeast. *Mol Biol Cell* **15(11)**:4787-4797.

Young BP, Craven RA, Reid PJ, Willer M & Stirling CJ (2001) Sec63p and Kar2p are required for the translocation of SRP-dependent precursors into the yeast endoplasmic reticulum *in vivo*. *EMBO J* **20(1-2)**:262-271.

Young JC, Ursini J, Legate KR, Miller JD, Walter P & Andrews DW (1995) An amino-terminal domain containing hydrophobic and hydrophilic sequences binds the signal recognition particle receptor alpha subunit to the beta subunit on the endoplasmic reticulum. *J Biol Chem* **270**:15650-15657

Younger JM, Chen L, Ren H-Y, Rosser MFN, Turnbull EL, Fan C-Y, Patterson C & Cyr DM (2006) Sequential Quality-Control Checkpoints Triage Misfolded Cystic Fibrosis Transmembrane Conductance Regulator. *Cell* **126(3)**:571-582.

Zapun A, Jakob CA, Thomas DY & Bergeron JJ (1999) Protein folding in a specialized compartment: the endoplasmic reticulum. *Structure* **7(8)**:R173-R182.

Zerial M & McBride H (2001) Rab proteins as membrane organizers. *Nat Rev Mol Cell Biol* **2(2)**:107-117.

Zhang H, He J, Ji Y, Kato A & Song Y (2008a) The effect of calnexin deletion on the expression level of PDI in Saccharomyces cerevisiae under heat stress conditions. *Cell Mol Biol Lett* **13:**38-48.

Zhang H, Hu B, Ji Y, Kato A & Song Y (2008b) The effect of calnexin deletion on the expression level of binding protein (BiP) under heat stress conditions in *Saccharomyces cerevisiae*. *Cell Mol Biol Lett* **13**:621-631.

Zhang F, Hu M, Tian G, Zhang P, Finley D, Jeffrey PD & Shi Y (2009) Structural insights into the regulatory particle of the proteasome from Methanocaldococcus jannaschii. *Mol Cell* **34(4)**:473-484.

Zhang Y, Nijbroek G, Sullivan ML, McCracken AA, Watkins SC,Michaelis S & Brodsky JL (2001) The Hsp70 molecular chaperone facilitates the ER associated degradation of the cystic fibrosis transmembrane conductance regulator in yeast. *Mol Biol Cell* **12**:1303-1314.

Zhou Y, Aebersold R & Zhang H (2007) Isolation of N-linked glycopeptides from plasma. *Anal Chem* **79**:5826-5837.

Zhou J, Liu CY, Back SH, Clark RL & Peisach D (2006) The crystal structure of human *IRE1* luminal domain reveals a conserved dimerization interface required for activation of the unfolded protein response. *Proc Natl Acad Sci USA* **103(39)**:14343-14348.

Zhou M & Schekman R (1999) The engagement of Sec61p in the ER dislocation process. *Molecular Cell* **4**:925-934.

Zimmer C (2009) On the origin of eukaryotes. *Science* **325**:666-668.

Zimmer J, Nam Y & Rapoport TA (2008) Structure of a complex of the ATPase SecA and the protein-translocation channel. *Nature* **455**:936-943.

Zimmermann R, Eyrisch S, Ahmad M & Helms V (2011) Protein translocation across the ER membrane. *Biochim Biohys Acta* **1808(3)**:912-924.

Zopf D, Bernstein HD, Johnson AE & Walter P (1990) The methionine-rich domain of the 54 kd protein subunit of the signal recognition particle contains an RNA binding site and can be crosslinked to a signal sequence. *EMBO J* **9(13)**:4511-4517.

6 ABBREVIATIONS

Δgpαf	Signal-cleaved form of pΔgpαf (ERAD substrate)
3gpαf	Triply N-glycosylated, signal-cleaved form of wild-type alpha factor precursor (ppαf)
5-FOA	5-Fluoroorotic acid
Å	Angstrom
AA	Amino acid
AAA	ATPase associated with various cellular actvities
AAA-ATPase	ATPases associated with different cellular activities
Ab	Antibody
ABC	ATP-binding cassette
ACT1	Actin 1
ADP	Adenosine diphosphate
AEBSF	4-(2-Aminoethyl)benzenesulfonyl fluoride
AMC	7-Amido-4-methylcoumarin
Amp	Ampicillin
AP-1/3	Activator protein 1/3
APS	Ammonium persulfate
ARS	Autonomously replicating sequence; ATP regenerating sytem
ATF6	Activating transcription factor-6 (PKR)-like ER kinase
ATP	Adenosine triphosphate
BiP	Binding immunoglobulin protein
BOF	BODIPY FL
bp	base pair
BSA	Bovine serum albumin
C. elegans	*Caenorhabditis elegans*
CAA	Casamino acids
CaAc	Calcium acetate
Cdc48p	Cell Division Cycle
CDK2-like	Cyclin-dependent kinase 2-like
cDNA	Complementary DNA
CEN	Centromere
CGN	*cis* Golgi network
CI	Chloroform-isoamyl alcohol
CJD	Creutzfeld-Jakob disease
CMV	Cytomegalovirus
CNX	Calnexin
COP9	Constitutive photo-morphogenesis 9
COPI/II	Coat protein complex I/II
CP	Core particle, 20S CP of the proteasome
CPY	Carboxypeptidase Y
CPY*	Mutant carboxypeptidase Y (ERAD substrate in yeast)
CRT	Calreticulin
C-terminus	Carboxy-terminus
Cue1p	Coupling of ubiquitin conjugation to ER degradation
D	Aspartic acid
Da	Dalton
dATP	2’ Deoxyadenosine 5’-triphosphate
dCTP	2’ Deoxycytidine 5’-triphosphate
DEPC	Diethylpyrocarbonate
dGTP	2’ Deoxyguanosine 5’-triphosphate
Deoxy BigCHAP	N,N-Bis[3-(D-gluconamido)propyl]deoxycholamide

Der1p	Degradation in the ER
DMSO	Dimethylsulfoxide
DNA	Deoxyribonucleic acid
dNTP	Deoxyribonucleotide triphosphate (dATP, dCTP, dGTP, dTTp)
d/o	Drop-out
Doa10p	Degradation of alpha 2 protein 10
DPAP-B	Dipeptidyl aminopeptidase B
DPY	CPY* where the targeting sequence was replaced with that of DPAP-B
ds	Double-stranded
Dsk2	Dominant suppressor of kar1 protein 2
DTT	Dithiothreitol
DUB	Deubiquitinating enzymes
E	Glutamic acid
E1	Ubiquitin-activating enzyme
E2	Ubiquitin-conjugating enzyme
E3	Ubiquitin-protein ligase
E4	Enzymes involved in polyubiquitination of substrates
ECL	Enhanced chemiluminescence
E. coli	*Escherichia coli*
EDEM	ER degradation-enhancing α-mannosidase-like protein
EDTA	Ethylenediamine tetraacetic acid
EGTA	Ethylene glycol tetraacetic acid
eIF3	Eukaryotic translation initiation factor 3
EM	Electron microscopy
Eq	Equal (unit definition for ER membranes)
ER	Endoplasmic reticulum
ERAC	ER-associated compartment
ERAD	ER-associated degradation
ERGIC	ER-Golgi intermediate compartment
ERQC	ER quality control
ERSE	ER stress response element
EtBr	Ethidium bromide
EtOH	Ethanol
F	Phenylalanine
Flag-tag	A polypeptide protein tag (N-DYKDDDDK-C) for affinity purification
G	Glycine
Gal	Galactose
GEF	Guanine nucleotide exchange factor
GET	Guided entry of TA proteins
GFP	Green fluorescent protein
$GlcNAc_2Man_9Glc_3$	$N\text{-acetylglucosamine}_2\text{Mannose}_9\text{Glucose}_3$
GPI-anchor	Glycosylphophatidylinositol anchor
GRP-78	78 kDa Glucose-regulated protein
GTP	Guanosine triphosphate
H_2O dest.	Distilled water
Hac1p	Homologous to Atf/Creb1
HbYX	Hydrophobic-tyrosine-X
HC	Heavy chain
HCl	Hydrochloric acid
HCMV	Human cytomegalovirus
HECT	Homologous to the E6-AP carboxy-terminus
Hepes	4-(2-Hydroxyethyl)-1-piperazineethanesulfonic acid
His	Histidine
HIV	Human immunodeficiency virus
Hlj1p	Homologous to *E. coli* DnaJ protein 1

Hmg1p	3-Hydroxy-3-methylglutaryl-coenzyme A reductase
HMG-CoA	Hydroxymethylglutaryl-CoA reductase
Hr	Hour(s)
Hrd1p	HMG-CoA reductase degradation protein 1
HRP	Horseradish peroxidase
Hsm3	Enhanced spontaneous mutability
Hsp	Heat shock protein (e.g. Hsp70: heat shock protein of about 70 kDa)
Htm1	Homologous to mannosidase 1
Ig	Immunoglobulin
IP	Immunoprecipitation
IPTG	Isopropyl-β-D-thio-galactopyranoside
Ire1p	Inositol-requiring protein 1
Jem1p	DnaJ-like protein of the ER membrane
K	Lysin
KAc	Potassium acetate
Kan	Kanamycin
kanr	Kanamycin resistence
Kar2p	Karyogamy 2 protein
kb	Kilobase
kbp	Kilobase pair
KCl	Potassium chloride
kDa	Kilodalton
KOAc	Potassium acetate
KOH	Potassium hydroxide
KWW	KHN lumenal domain/Wsc1p TMD/Wsc1p cytosolic domain
L	Loop; Leucine
LB	Lysogeny broth
Leu	Leucine
LiAc	Lithium acetate
LRR	Leucine-rich repeat
M. jannaschii	*Methanocaldococcus* jannaschii
MCS	Multiple cloning site
Met	Methionine
$MgCl_2$	Magnesium chloride
$Mg(OAc)_2$	Magnesium acetate
$MgSO_4$	Magnesium sulfate
MHC	Major histocompatibility complex
min	Minute(s)
Mnl1	Mannosidase-like protein 1
MOPS	3-(N-morpholino)propanesulfonic acid
MPN domain	Mpr1-Pad1-N-terminal domain
MRH	Mannose 6-phosphate receptor homology
mRNA	Messenger RNA
$MS(PEG)_8$	Methyl-PEG_8-N-Hydroxysuccinimide-ester
NaAc	Sodium acetate
NaCl	Sodium chloride
NaOH	Sodium hydroxide
NaH_2PO_4	Sodium dihydrogen phosphate
Na_2HPO_4	Disodium hydrogen phosphate
NaN_3	Sodium Azide
Nas	Non-ATPase Subunit
NC	Nitrocellulose
NEDD8	Neuronal-precursor-cell-expressed developmentally down-regulated protein-8
NEF	Nucleotide exchange factors

NH_4OAc	Ammonium acetate
NHS	N-hydroxysuccinimide
Npl4p	Nuclear protein localization
NLS	Nuclear localization signals
N-Terminus	Amino-termimus
OD	Optical density
OMP	Orotidine-5'-phosphate
ONPG	2-Ortho-nitrophenyl-β-D-galactopyranoside
OPY*	CPY* where the targeting sequence was replced with that of Ost1p
ORF	Open reading frame
OST	Oligosaccharyl-transferase
Otu1p	Ovarian tumor
P	Proline
pΔgpαf	Mutant alpha factor precursor (ERAD substrate)
PAAF1	Proteasomal ATPase-associated factor 1
PAGE	Polyacrylamide gel electrophoresis
PC	Phosphatidylcholine
PCI	Phenol-chloroform-isoamyl alcohol
PCI complex	Proteasome/COP9/eIF3 complex
PCI domain	Proteasome-COP9-eIF3 domain
PCR	Polymerase chain reaction
PC repeat	Proteasome cyclosome repeat
PDI/Pdi1p	Protein disulfide isomerase
Pdr5p	Pleiotropic drug resistance
PE	Phosphatidylethanolamine
PEG	Polythylene glycol
PERK	Protein kinase RNA (PKR)-like ER kinase
PK-RM	Puromycin and high-salt (potassium acetate) stripped rough microsomes derived from ER membranes
Png1p	Peptide N-glycanase
PMSF	Phenylmethanesulfonyl fluoride
ppαf	Prepro-alpha factor (wild-type alpha factor precursor)
PPIases	Peptidyl prolyl isomerases
PrA*	Proteinase A (mutant form)
Rab	Ras-related in brain
Rad23p	Radiation sensitive protein 23
Ras	Rat sarcoma
RNC	Ribosome nascent chain
RNP	Ribonucleoprotein particle
RING	Really interesting new gene
RM	Rough microsomes (rough ER membranes)
RNA	Ribonucleic acid
RNAi	RNA interference
RNase	Ribonuclease
RNC	Ribosome-nascent chain
RNP	Ribonucleoprotein particle
RP	Regulatory particle, 19S RP of the proteasome
rpm	Rounds per minute
Rpn	Regulatory Particle Non-AAA-ATPase
Rpt	Regulatory Particle AAA-ATPase
RT	Room temperature (in 3.6.2. Reverse transcription)
Rub1	Related to ubiquitin
S	Serine
Sbh1p	Sec61 beta homologue 1
S. cerevisia	*Saccharomyces cerevisiae*

SC	Synthetic complete
Scj1	*S. cerevisiae* DnaJ
SD	Synthetic defined
SDS	Sodium dodecyl sulfate (Sodium lauryl sulfate)
SDS-PAGE	SDS-polyacrylamide gel electrophoresis
Sec61p	Secretory
SNARE	Soluble N-ethylmaleimide-sensitive-factor attachment receptor
SOC	Super optimal broth with catabolite repression
SOE	Splicing by overlapping extension
SP	Signal peptidase
S. pombe	*Schizosaccharomyces pombe*
SR	Sigal recognition particle receptor
SRP	Sigal recognition particle
ss	Single-stranded
S-S	Disulfide bonds
Ssa1p	Stress-seventy subfamily A protein 1
Ssh1p	Sec sixty-one homologue
Sss1p	Sec sixty-one suppressor
Ste6	Sterile
Suc-LLVY-AMC	N-succinyl-Leu-Leu-Val-Tyr-7-amido-4-methylcourmarin
SUMO	Small ubiquitin-like modifier
SV5 HN	Simian virus 5 hemagglutinin-neuraminidase
$t_{1/2}$	Half-life
TA	Tail-anchored
TAE	Tris, acetate, EDTA
Taq	*Therminus aquaticus*
TBE	Tris, borate, EDTA
TBS	Tris-buffered saline
TBS(T)	TBS + 0.1 % Tween
TCA	Trichloroacetic acid
TE	Tris-EDTA
TEMED	N,N,N',N'-Tetramethylethan-1.2-diamine
TES	Tris-HCl, EDTA, SDS
TF	Transcription factor
Tm	Tunicamycin (also melting temperature)
TM	Transmembrane
TMD	Transmembrane domain
TGN	*trans* Golgi network
TRAM	Translocation-associated membrane protein
TRAP	Translocon-associated protein
Tris-HCl	Tris(hydroxymethyl)aminomethane hydrochloride
TRC	Transmembrane recognition complex
Trp	Tryptophan
Tris	Tris(hydroxymethyl)aminomethane
t-SNARE	target-SNARE
U	Unit
Ub	Ubiquitin
UBA	Ubiquitin-associated domain
Ubc6p	Ubiquitin conjugating protein 6
UBL	Ubiquitin-like
Ubp6	Ubiquitin-specific protease 6
Ubx2p	Ubiquitin regulatory X
UDP	Uridine diphosphate
Ufd1p	Ubiquitin fusion degradation protein
UGGT	UDP-glucose:glycoprotein glucosyltransferase

UPR	Unfolded protein response
UPRE	Unfolded protein response element
UPS	Ubiquitin-proteasome-system
Ura	Uracil
US2, 11	Unique short region protein 2, 11
Usa1p	U1-Snp1 Associating
UTP	Uridine 5′-triphosphate
UTR	Untranslated region
UV	Ultra violet
VCP	Valosin-containing protein
v-SNARE	vesicle-SNARE
VSP	Vacuolar protein sorting
v/v	Volume per volume
vWF-A	von Willebrand factor A domain
W/O	Without
wt	Wild-type
w/v	Weight per volume
X-Gal	5-Brom-4-chloro-3-indoxyl-ß-D-galactopyranosid
Ydj1p	Yeast DnaJ protein 1
VIMP	VCP-interacting membrane protein
YNB	Yeast nitrogen base
Yos9p	Yeast OS-9 homologue
YP	Yeast peptone
YPD	Yeast peptone dextrose
YPG	Yeast peptone galactose

7 PUBLICATIONS

Kaiser ML & Römisch K (2015) A mutation in ER lumenal loop 7 of Sec61p interferes with proteasome binding to the Sec61 channel and ERAD. *PLoS ONE* **10(2)**:e0117260.

Kaiser ML & Römisch K

Mutations in *SEC61* that affect proteasome binding

American Society For Cell Biology 50th Annual Metting 2010, Phildelphhia (USA)

(Poster)

Kaiser ML & Römisch K

Mutations in *SEC61* that affect proteasome binding

EMBO | EMBL Symposium 2012: Quality Control – From Molecules to Organelles, EMBL Heidelberg (GERMANY)

(Poster)

8 ACKNOWLEDGEMENTS

An erster Stelle möchte ich meiner Doktormutter Prof. Dr. Karin Römisch für die freundliche Überlassung des hochinteressanten, herausfordernden Themas und die wissenschaftliche Begleitung danken. Besonders bedanken möchte ich mich für die Freiheit, die sie mir während des gesamten Projektes gewährte und ihre Geduld und Unterstützung vor allem in der Endphase meiner Arbeit. Auch für viele Denkanstöße während der Entstehung dieser Arbeit, die für mich sehr wertvolle Hilfestellungen waren, möchte ich meinen Dank aussprechen. Diese machten meine Arbeit nicht nur besser, sondern regten mich auch dazu an viele Sachverhalte aus verschiedenen Blickwinkeln zu betrachten.

Prof. Dr. Manfred Schmitt danke ich sehr für die Übernahme des Koreferats, und auch für seine Freundlichkeit und sein Interesse and meiner Arbeit.

Ein großer Dank geht an die AG Schmitt. Hier v.a. Dr. Julia Dausend, die mir vor allem am Anfang mit Rat und Tat zur Seite stand und Dr. Frank Breinig für Ratschläge und Motivation. Roswitha Schepp, die immer Zeit hatte, danke ich für ihre große Hilfsbereitschaft. Ein Dank für ihre herzliche Art geht an Dr. Esther Gießelmann, Dr. Björn Becker, Dr. Björn Diehl, Dr. Thorsten Hoffmann und Nicole Jundel. Besonders herzlich bedanken möchte ich mich bei der lieben Nina Müller, die immer da war wenn ich Hilfe brauchte, für ihre Warmherzigkeit, fürs Zuhören und für die schöne Zeit im “Iso-lab”.

Des Weiteren danke ich der gesamten Arbeitsgruppe Giffhorn, im Besonderen Dr. Sabrina Gemperlein und Dr. Martina Pitz für die Hilfe und die großartige Stimmung in Labor und Büro. Sabrina möchte ich für ihre fröhliche, offene Art und dafür danken, dass sie mich oft zum Lachen gebracht hat.

Ein besonderer Dank gilt der gesamten Arbeitgsgruppe Römisch: Carmen Clemens, Juncal Gonzales, Birgit Hasper, Marie-Christine Klein, Prof. Dr. Gert Kohring, Michael Lafontaine, Dr. Christina Servas, Nina Tran, Dr. Thomas Tretter und Klaus Witte:

Juncal danke ich für ihre Hilfe bei allen Verwaltungsfragen und dafür, dass sie mich mit ihrem spanischen Temperament aufgeheitert hat.

Bei Gert Kohring möchte ich mich herzlich für seine Hilfe rund um Forschung und Labortechnik, vor allem aber auch während der Praktika, und Motivation während der gesamten Zeit bedanken.

Ein besonderes Dankeschön gilt Klaus und Veronika Witte für ihre Hilfe und Aufmunterungen, wenn einmal etwas nicht klappen wollte, und viele schöne Gespräche im Labor und darüber hinaus.

Der lieben Christina danke ich dafür, dass sie mir durch vier Jahre “Laborwahnsinn” geholfen hat. Danke auch für eine schöne Zeit im Labor und besonders abseits der Arbeit, die freundschaftliche Atmosphäre und viele lustige Momente.

Mein großer Dank gilt vor allem den beiden Menschen, die mich täglich ertragen haben: Birgit und Carmen danke ich von ganzem Herzen für vier Jahre fachmännische und menschliche Unterstützung. An dieser Stelle möchte ich mich auch dafür bedanken, dass sie mir während der gesamten Zeit, weit über das Selbstverständliche hinaus, viele Aufgaben abgenommen haben. Birgit bin ich unendlich dankbar für ihre Hilfe bei einfach allem, besonders während der Praktika, die mir mit ihr sehr viel Spaß gemacht haben. Meiner lieben Carmen danke ich dafür, dass sie mich jeden Tag in jeder Hinsicht unterstützt und motiviert hat, und mein Ruhepool war. Danke für viele schöne und humorvolle Momente. Die Zeit mit euch wird mir unvergesslich bleiben.

Meinen Mädels Nina Tran und Marie-Christine Klein danke ich für ihre Herzlichkeit, ihren Humor und viele schöne Erlebnisse ... (die Liste ist lang) … Nina, danke, dass du mich so immer zum Lachen gebracht hast und es nie übel genommen hast, wenn ich mich länger nicht gemeldet habe (und danke für dein traumhaftes Curry). Tina, danke, dass du dich mit meiner Einleitung geplagt hast und mich während der gesamten Zeit sehr geduldig unterstützt hast. xoxo

Meiner großartigen Freundin Martina Pitz danke ich von Herzen für einfach alles. You are the cat’s meow. Ich danke dir dafür, dass du für mich da warst, es irgendwie immer wieder geschafft hast mich zu motivieren und für die unsagbar große Hilfe beim Lesen meiner Arbeit. Danke, dass du meine Freundin bist.

Mein innigster Dank gilt meiner lieben Famile, die mir bei allem unterstützend und liebevoll zur Seite stand. Danke.